UNIVERSIDADE DE STUTTGART
UNIVERSIDADE FEDERAL DO PARANÁ

ANDRÉ RAZENTE

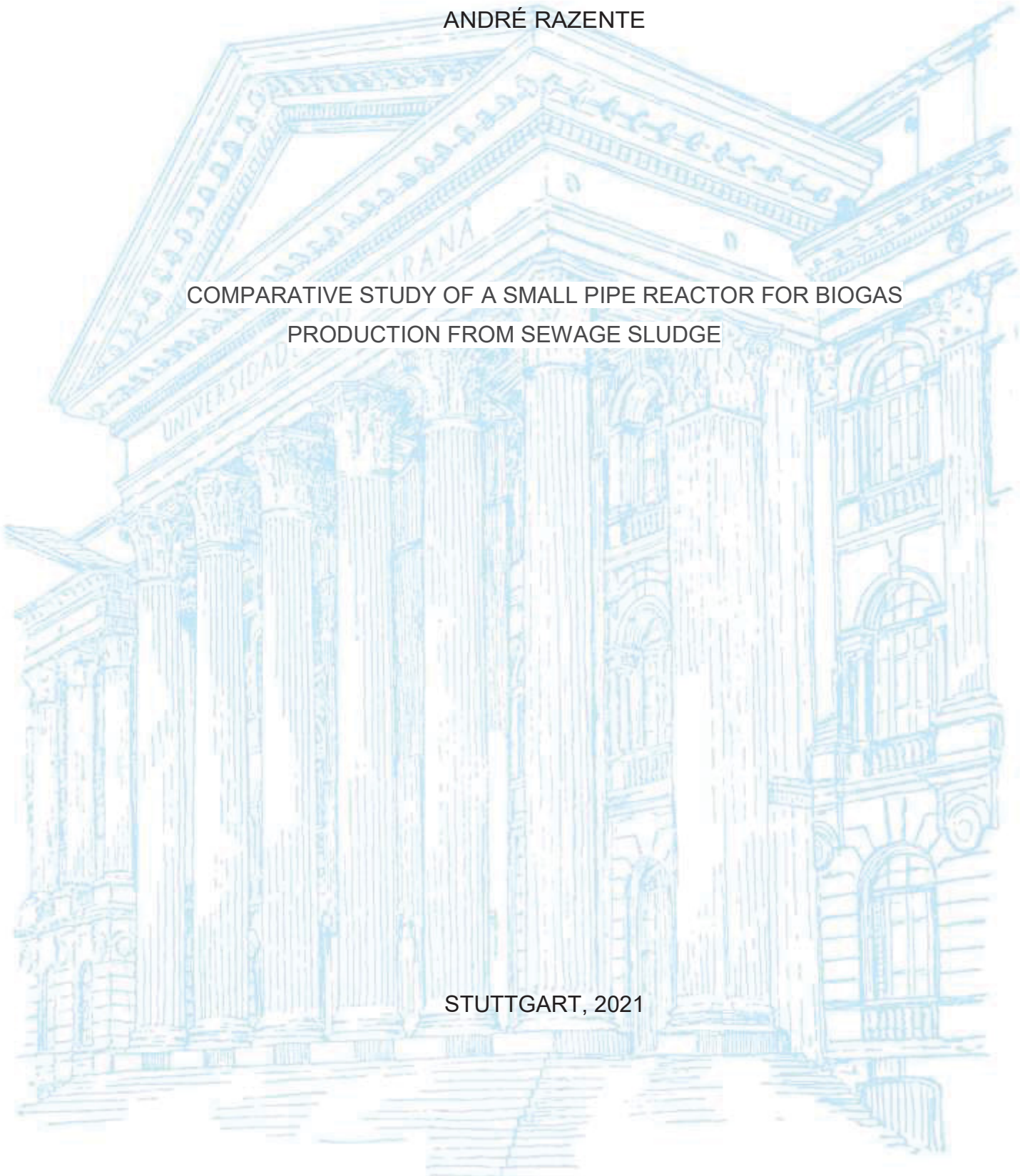

COMPARATIVE STUDY OF A SMALL PIPE REACTOR FOR BIOGAS PRODUCTION FROM SEWAGE SLUDGE

STUTTGART, 2021

ANDRÉ RAZENTE

COMPARATIVE STUDY OF A SMALL PIPE REACTOR FOR BIOGAS PRODUCTION FROM SEWAGE SLUDGE

Dissertação apresentada ao curso de Pós-Graduação em Meio Ambiente Urbano e Industrial, Setor de Tecnologia, Universidade Federal do Paraná, como requisito parcial à obtenção do título de Mestre em Meio Ambiente Urbano e Industrial.

Orientador: Prof. Dr. Arion Zandoná Filho

Coorientador: Prof. Dr. Harald Schönberger

STUTTGART

2021

DADOS INTERNACIONAIS DE CATALOGAÇÃO NA PUBLICAÇÃO (CIP)
UNIVERSIDADE FEDERAL DO PARANÁ
SISTEMA DE BIBLIOTECAS – BIBLIOTECA CIÊNCIA E TECNOLOGIA

Razente, André.
Comparative study of a small pipe reactor for biogas production from sewage slude. / André Razente. – Curitiba, 2022.
1 recurso on-line : PDF.

Dissertação (Mestrado) – Universidade Federal do Paraná, Setor de Tecnologia, Programa de Pós-Graduação em Meio Ambiente Urbano e Industrial; Universidade de Stuttgart e SENAI-PR.
Orientador: Prof. Dr. Arion Zandoná Filho.

1. Meio ambiente. 2. Biogás. 3. Lodo de esgoto. 4. Digestão anaeróbica. I. Zandoná Filho, Arion. II. Universidade Federal do Paraná. Programa de Pós-Graduação em Meio Ambiente Urbano e Industrial. IV. Universidade de Stuttgart. V. SENAI-PR. VI. Título.

Bibliotecário: Nilson Carlos Vieira Júnior CRB-9/1797

TERMO DE APROVAÇÃO

Os membros da Banca Examinadora designada pelo Colegiado do Programa de Pós-Graduação MEIO AMBIENTE URBANO E INDUSTRIAL da Universidade Federal do Paraná foram convocados para realizar a arguição da Dissertação de Mestrado de **ANDRÉ RAZENTE** intitulada: **COMPARATIVE STUDY OF A SMALL PIPE REACTOR FOR BIOGAS PRODUCTION FROM SEWAGE SLUDE**, sob orientação do Prof. Dr. ARION ZANDONÁ FILHO, que após terem inquirido o aluno e realizada a avaliação do trabalho, são de parecer pela sua APROVAÇÃO no rito de defesa.

A outorga do título de mestre está sujeita à homologação pelo colegiado, ao atendimento de todas as indicações e correções solicitadas pela banca e ao pleno atendimento das demandas regimentais do Programa de Pós-Graduação.

CURITIBA, 04 de Maio de 2022.

Assinatura Eletrônica
04/05/2022 17:38:55.0
ARION ZANDONÁ FILHO
Presidente da Banca Examinadora

Assinatura Eletrônica
11/05/2022 16:01:22.0
SÉRGIO HENRIQUE BERNARDO DE FARIA
Avaliador Externo (UNIVERSIDADE ESTADUAL DE MARINGÁ)

Assinatura Eletrônica
04/05/2022 18:09:00.0
ARISLETE DANTAS DE AQUINO
Avaliador Interno (UNIVERSIDADE FEDERAL DO PARANÁ)

DECLARATION OF AUTHORSHIP

I hereby certify that the thesis I am submitting is totally my own original work except where otherwise indicated. I am aware of the University's regulations concerning plagiarism, including those regulations concerning disciplinary actions that may result from plagiarism. Any use of the works of any other author, in any form, is properly acknowledged at their point of use.

Stuttgart, 20.12.2021

André Razente

Dissertação apresentada ao Programa de Mestrado Profissional em Meio Ambiente Urbano e Industrial, Setor de Tecnologia da Universidade Federal do Paraná (UFPR), em parceria com a Universidade de Stuttgart e o Sistema Nacional de Aprendizagem Industrial do Paraná (SENAI), como requisito parcial à obtenção do título de Mestre em Meio Ambiente Urbano e Industrial.

Supervisor (UniStutt): Herr Dipl.-Ing Maurer
Supervisor (UFPR): Prof. Dr. Arion Zandoná Filho
Examiner: Herr PD Dr.-Ing. habil. Harald Schönberger

I wish to dedicate this work to all of my friends, Family and professor who helped me during my time in Germany and before.

AGRADECIMENTOS

Quero agradecer a todos que ajudaram durante todo esse tempo, todos vocês me deram forças para seguir em frente e nunca olhar para trás. Por isso, obrigado a todos.

“Some believe uncertainty is an evil that should be dispelled through divination. Others claim it's change that is evil. But that isn't true either. Every minute of every day, we each become someone new. We shouldn't fear change itself, but only who we might change into. Knowing one's path is the most important.” (Olszewski, Misty, 2017)

RESUMO

Este trabalho comparou o desempenho de um biodigestor anaeróbio de fluxo contínuo alimentado com lodo primário e lodo em excesso em condições mesofílicas com processos equivalentes em reatores tipo tanque. A estabilidade operacional foi analisada em relação ao controle de temperatura, combinado com a eficiência do sistema de bombeamento para manter o fluxo constante sem controle automatizado. O desempenho da digestão foi avaliado pela capacidade de retenção de partículas e demanda química de oxigênio reduzida, além dos rendimentos e qualidade do biogás. Os resultados mostraram grande resiliência a mudanças na carga orgânica e na composição da entrada, com rendimentos e retenção de sólidos não sendo impactados. Também foi observado que reduções no tempo de retenção hidráulica não afetaram significativamente o desempenho do processo. Por fim, o controle de temperatura e o sistema de bombeamento mostraram uma operação estável, mas sinais de desgaste foram verificados.

Palavras chaves: Meio ambiente, Biogás, Lodo de esgoto, Digestão anaeróbica, Protótipo.

ABSTRACT

This work compared the performance of a plug flow anaerobic digester fed with primary sludge and excess sludge at mesophilic conditions to equivalent processes in tank-like reactors. Operational stability was analyzed regarding temperature control in combination with the efficiency of the pumping system in keeping flow constant without automated control. The digestion performance was evaluated by its capacity to retain particles and reduced chemical oxygen demand in addition to biogas yields and quality. Results showed great resilience to changes in organic load and input composition, being yields and solids retention not impacted. It was also observed that hydraulic retention time reductions did not greatly impact the process performance. At last, the temperature control and pumping system showed a stable operation, but signs of it being worn out were verified.

Keywords: Environment, Biogas, Sewage sludge, Anaerobic Digestion, Prototype

ZUSAMMENFASSUNG

Diese Arbeit verglich die Leistung eines plug-flow-anaeroben Vergärers, der mit primärem Klärschlamm und Überschussschlamm unter mesophilen Bedingungen versorgt wurde, mit äquivalenten Prozessen in tankähnlichen Reaktoren. Die operationelle Stabilität wurde hinsichtlich der Temperaturkontrolle in Kombination mit der Effizienz des Pumpensystems analysiert, um den konstanten Fluss ohne automatische Steuerung aufrechtzuerhalten. Die Verdauungsleistung wurde anhand der Fähigkeit zur Rückhaltung von Partikeln und reduziertem chemischen Sauerstoffbedarf sowie der Biogaserträge und -qualität bewertet. Die Ergebnisse zeigten eine hohe Widerstandsfähigkeit gegenüber Veränderungen in der organischen Belastung und Zusammensetzung der Zufuhr, wobei Erträge und Rückhaltung von Feststoffen nicht beeinträchtigt wurden. Es wurde auch beobachtet, dass Reduzierungen der hydraulischen Verweilzeit das Prozessleistungsverhalten nicht stark beeinflussten. Schließlich zeigten die Temperaturkontrolle und das Pumpensystem eine stabile Betriebsweise, aber Anzeichen von Abnutzung wurden verifiziert.

Schlüsselwörter: Umwelt, Biogas, Klärschlamm, anaerobe Vergärung, Prototyp

LIST OF FIGURES

LIST OF TABLES

LIST OF ABBREVIATIONS AND ACRONYMS

PFR	- Plug Flow Reactor
HOL	- High Organic Load
LOL	- Low Organic Load
CSTR	- Continuously Stirred Tank Reactor
HHRT	- High Hydraulic Retention Periods
LHRP	- Low Hydraulic Retention Periods
TOC	- Total Organic Carbon
OL	- Organic Load
VS	- Volatile Solids
TS	- Total Solids
COD	- Chemical Oxygen Demand
HRT	- Hydraulic Retention Time
ODM	- Organic Dry Matter

LIST OF SYMBOLS

π - Constant pi

$\int$ - Integration operator

Σ - Summation operator

Π - Multiplication operator

SUMMARY

1. INTRODUCTION

Sewage treatment in big cities is a challenge faced by humankind since cities have become the heart of modern society. After cities' population started to become larger and larger, direct discharge of sewage started not to viable any longer, treatment came as the only solution. The first concepts were based on the idea that pollution could be handled by dilution, leading to early treatment being dealt with by rain water dilution and direct disposal (NATHANSON; AMBULKAR, 2021).

Due to the increasing population and the dawn of environmental thinking, only diluting the sewage was not more accepted, creating a necessity to develop the modern concept of a wastewater treatment plant (WWTP). As reported by the European Commission of Urban waste water, just in Germany there were almost 3800 WWTP in operation in 2021 (ECUWW, 2021). As a result of this wide WWTP application, products of the sewage treatment started also to be a problem, such as sludge.

According to DE Statis, in 2019 over 3,48 million tons of WWTP sludge were treated and disposed of, being almost 220 thousand tons only in the state of Baden-Württemberg (BUNDESAMT, 2019). Treatment of this amount of waste has been indeed one of the challenges brought by the treatment of sewage, demanding to development of techniques that can efficiently deal with it. One of the available techniques for treatment is anaerobic digestion (AD), which is one of the most widespread methods to help treat this kind of residue.

There are many options to conduct anaerobic digestion of WWTP sludge, but most processes follow the same logic. Firstly, sludge is concentrated and may undergo or not a pretreatment before being sent to a digester, where the anaerobic digestion takes place. During this process, a mixture of methane, carbon dioxide, and other trace gases called biogas is produced and the solids material left is dewatered and disposed of (APPELS et al., 2008). The main reason AD is commonly used for sludge treatment is the production of biogas, which can be used as a by-product for energy production (ACHINAS; ACHINAS; EUVERINK, 2017).

With that, the main goal of AD of WWTP sludge became the gas production and not the treatment itself. Therefore, the heart of the process is the digesters, which in most cases consists of a tank reactor or a combination of several, being operated continuously, semi-continuously, or in batches, but being tank-like reactor nevertheless.

This type of approach has several advantages, but also several disadvantages, which make tank reactor not the best option for all cases. This work, however, shows an alternative of this type of reactor, a plug flow reactor (PFR) with phase separation, that can prove itself the best option for dealing with WWTP organic residue. For that, this project aims: verify if the experimental setup can be successfully operated, how the system will respond in different load regimes, and how it would be the response upon a dwindling of the hydraulic retention time, both regarding gas production and solid matter removal.

2. Theoretical Background

2.1. Anaerobic Digestion

Anaerobic digestion (AD) is a biological process chain in which microorganisms break down biodegradable macro molecules into non-degradable substances in no-oxygen conditions (WAHONO; MARYANA; KISMURTONO, 2009). The process is divided into four major steps: hydrolysis, acidosis or acidogenesis, acetogenesis, and methanogenesis, as shown by Figure 1, which only occur in strictly anaerobic conditions (GERARDI, 2003).

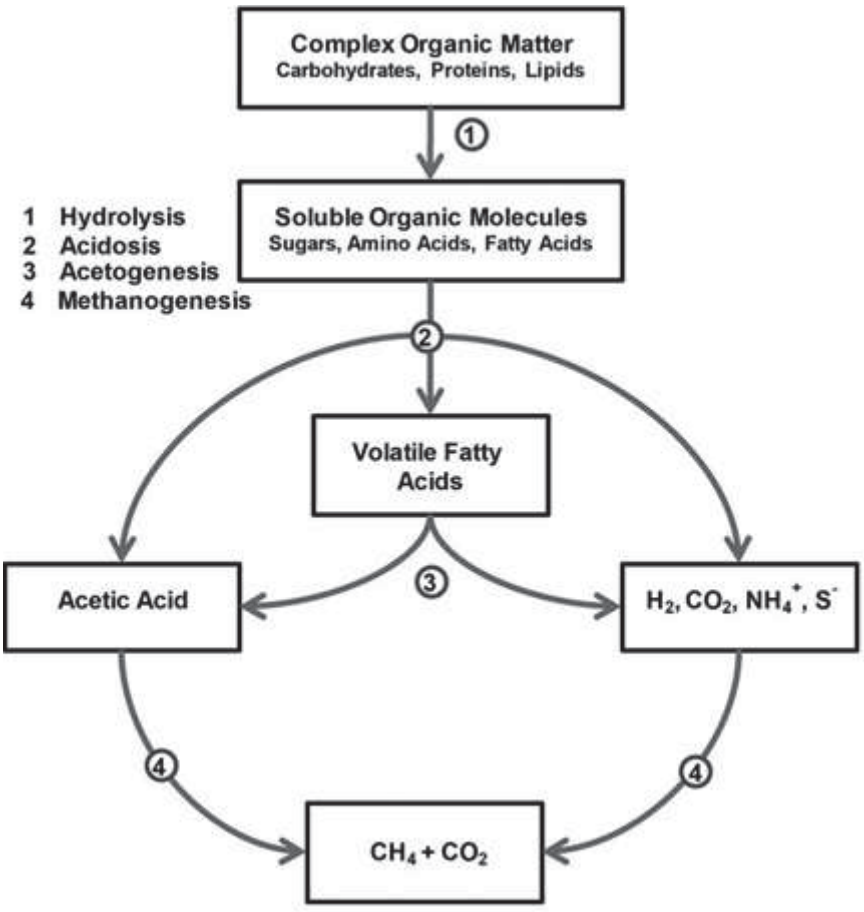

Figure 1 – Anaerobic digestion simplified scheme (adapted from *(HAMILTON, 2016)*).

AS the first step of the process, hydrolysis is often denoted as the limiting step of the process due to its overall lower kinetics (GUO et al., 2021a). It is

responsible for breaking the majority of macro organic molecules in the medium, such as lipids and proteins, into small their respectively monomers: amino acids, sugars, and fatty acids. This process is slow in comparison to the next steps, as the complexity range of molecules degraded during this stage is wider than the next ones.

Afterward, products of hydrolysis are used during the fermentation process, leading to the production of a wide range of volatile fatty acids (VFA), in a process called acidogenesis (APPELS et al., 2008). During this process, mainly acetic acids are produced in comparison to longer carbon chain acids, like propionic and butyric acids in addition to several other by-products, like alcohols and sulfidic compounds (HAMILTON, 2016).

Longer organic molecules produced during the acidogenesis process are further degraded in smaller compounds in the third process of AD, acetogenesis. This process is responsible for the production of the majority of H_2 used in the following steps of AD and its partial pressure dictates the speed at which the macromolecules were degraded. This process results in the production of also acetic acid and carbon dioxide as well as ammonium and sulfidic ions, which lead to H_2S and ammonia formation during other simultaneous processes (APPELS et al., 2008; CÓRDOVA; CHAMY, 2020).

After acetic acid, carbon dioxide, and hydrogen are produced during previous steps of AD, the methanogenesis steps start to take place. This step is when methane is produced and it is conducted mainly in three different pathways: hydrogenotrophic, methylotrophic, and acetoclastic (BERGHUIS et al., 2019; CONRAD, 2009). Hydrogenotrophic and methylotrophic methanogenesis contemplate the majority of the methane produced, with a ratio of 30% and 70% respectively (LUQUE et al., 2016).

During the Hydrogenotrophic pathway, hydrogen and carbon dioxide are consumed by archaea, producing methane and water during the process. Methylotrophic, however, is conducted mainly by methanogenic bacteria and uses acetic acid as its main raw material for methane production, but also produces carbon dioxide (WELLINGER; MURPHY; BAXTER, 2013). Methane production via

acetoclastic and other processes can be neglected because they happen only in very specific conditions and small quantities in comparison with the other two pathways (THAUER, 1998).

Moreover, as the process is conducted in several steps by different organisms, development times for each type of colony are exclusive, greatly varying between them. Microorganisms responsible for hydrolysis, such as ones from the Clostridium family take up to 36h to double their population, as acetogenic bacteria can take up to 90h to accomplish that. In addition, methanogenic bacteria from the genus *Methanosarcina,* which act during the methylotrophic pathway, can take between five to fifteen days to double in numbers. Hydrogenotrophic archaea and bacteria usually take more than 10 days (ZEIG, 2014).

2.2. Process influences

AD can be influenced by several parameters, however, in this section, only the ones which were actively relevant for the process are discussed. Influences due to non-measured or controlled parameters are not discussed, such as pH, micronutrients, volatile fatty acids, ammonia, and phosphorus concentrations.

2.2.1. Organic load

Organic load (OL) is defined as the total amount of organic matter fed in a system in a given time, it is usually shown with the units' g VS or kg VS, which means grams or kilograms of volatile solids.

Studies showed that OL is directly related to gas production, is it is the main source of degradable substances necessary to start AD. Even though gas production increases with an increase of OL, production per quantity of organic matter fed may not. After a certain limit yields do not increase anymore, this can be shown in the example researched by Song *et al.*, 2021, as shown in Figure 2.

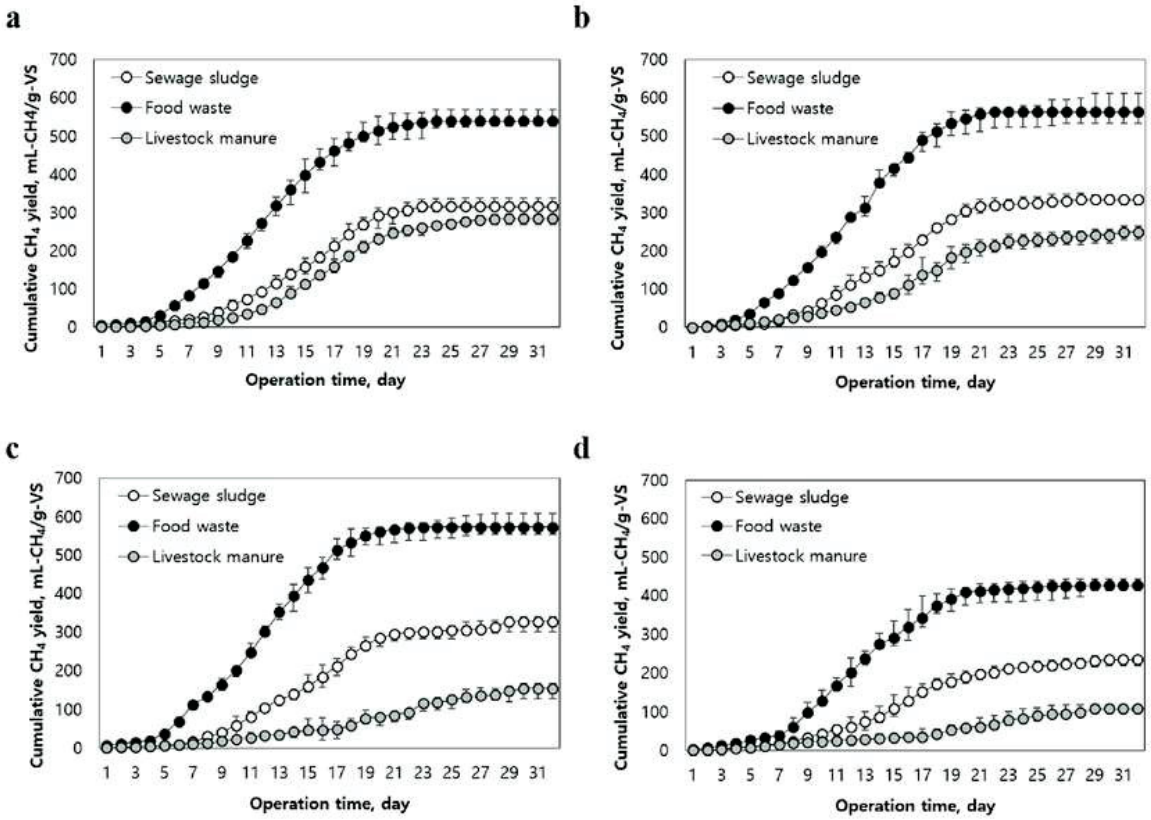

Figure 2 – Cumulative methane yields of sewage sludge, food waste, and livestock manure under various organic loading rates of (a) 2 kg VS, (b) 4 kg VS, (c) 6 kg VS, and (d) 8 kg VS (adapted from Song *et al.*, 2021).

Moreover, studies found that OL above 0,30 kg VS/L.d cannot maintain stable production in mesophilic semi-continuous tank reactors for food waste, with increasing efficiency losses as the load reach this limit (BLASIUS et al., 2020). When this point is reached, it is said the reactor has overloaded. In addition, quick changes also showed an impact, doubling the OL faster than one hydraulic retention time showed that yields can be reduced by 40% with methane content reaching 30% (BRAZ et al., 2018b).

As a consequence of an overload, VFAs concentration increases and pH decreases, which can create secondary inhibitory effects by themselves (FRANKE-WHITTLE et al., 2014). The maximum reactor capacity may vary with the type of feed and with the operation of the system, however, overloading can be detected using VFA concentration, which response to overfeeding simultaneously (LI et al., 2014). To relate VFA only with the amount prevenient from organic matter, the rate

between VFA and total inorganic carbon (TIC) is used (LOSSIE; PÜTZ, 2019). An example of these effects can be seen in Figure 3

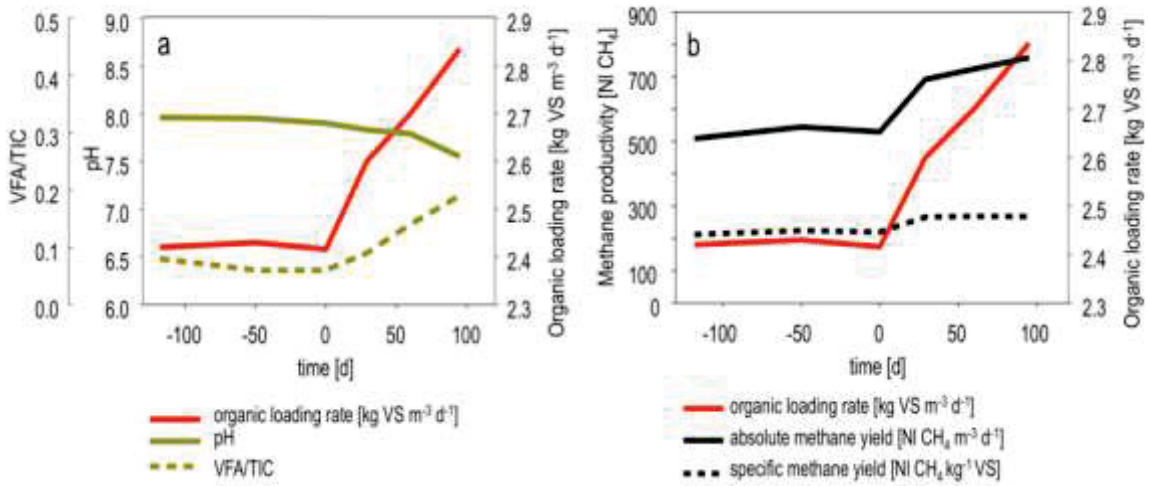

Figure 3 – Example of effects of increasing the organic load upon volatiles fatty acids concentration, pH, gas production, and methane content (adapted from *(R. BENGELSDORF et al., 2015)*).

In addition to the effects observed in several types of feed, in WWTP sludge digestion, high OLs contribute to organic formation. Loads above 2,5 kg/m³ d can cause consistent foam formation in the reactor, with values above 5 kg/m³d causing foam to persist during the operation (GANIDI; TYRREL; CARTMELL, 2011). This effect is not exclusive to WWTP sludge, OL can form with other types of feed, but they tend to be associated with to presence of inorganic contaminants and nitrogen compounds (MOELLER et al., 2015)

2.2.2. Temperature

AD is sensitive to temperature, being overall more efficient as temperature increases. AD is categorized into three classes regarding temperature: thermophilic, mesophilic, psychrophilic. By definition, the thermophilic condition is above 45°C up to 80°C, mesophilic is when organisms are adapted to temperatures between 15 and 45°C, and below that operation is considered psychrophilic. Some authors disagree with the limit of these classifications, but operation regimes commonly used for each regime are far from each other. Therefore, the terms thermophilic are referred to

when temperatures between 50°C and 60°C are used, mesophilic between 30-40°C, and psychrophilic when no temperature control or isolation is used.

Overall thermophilic conditions lead to higher yields in a lower time, but at high thermophilic regimes (>58°C) performance starts to drop, as shown by the example of Figure 4. Several studies showed a 20-30% increase in yields when the regime was changed from mesophilic to thermophilic (BRAGUGLIA et al., 2015; ZÁBRANSKÁ et al., 2000). Differences in operation regime regarding temperatures also lead to changes in micronutrients requirements for gas production as well as the concentration of trace gases in the output, as the microbial community differs greatly between them (DU; PARKER, 2012; HENDRIKS; VAN LIER; DE KREUK, 2018; MOSET et al., 2015). T

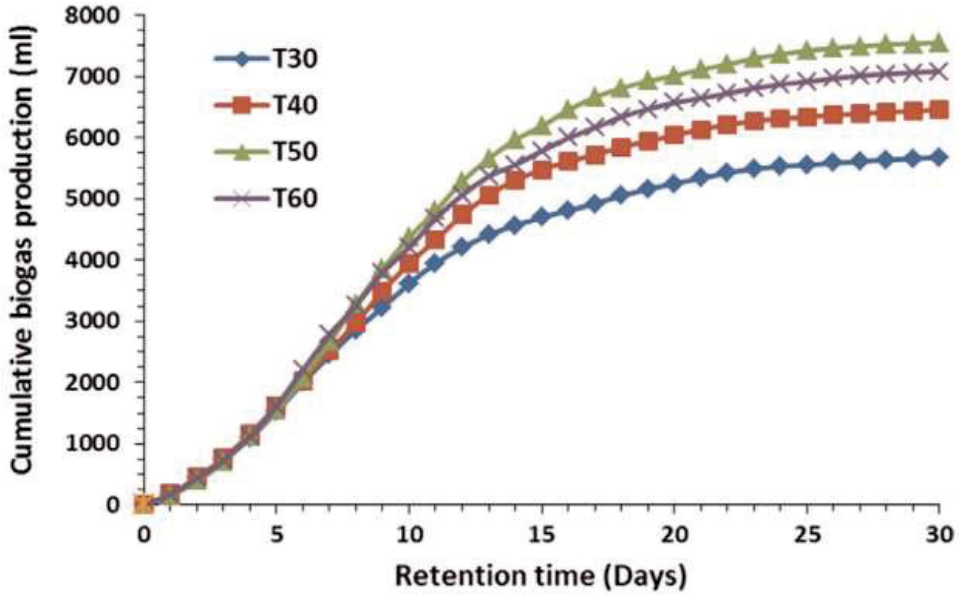

Figure 4 – Example of gas production profile at 30°C, 40°C, 50°C, and 60°C in a batch anaerobic digester (adapted from Deepanraj, Sivasubramanian, and Jayaraj, 2015).

Greater effects are also seen between mesophilic and psychrophilic conditions. On average, yields drop approximately 15% for each 5°C of reduction in temperature after 30°C. For the same retention, time yields can drop 90% from a temperature of 35°C to 10°C, being close almost null when closing to 0°C. This is exemplified in Figure 5, which shows the study conducted by Sebola, Tesfagiorgis,

and Muzenda, 2014, of the response of methane production to changes in temperatures in storage tanks with food waste.

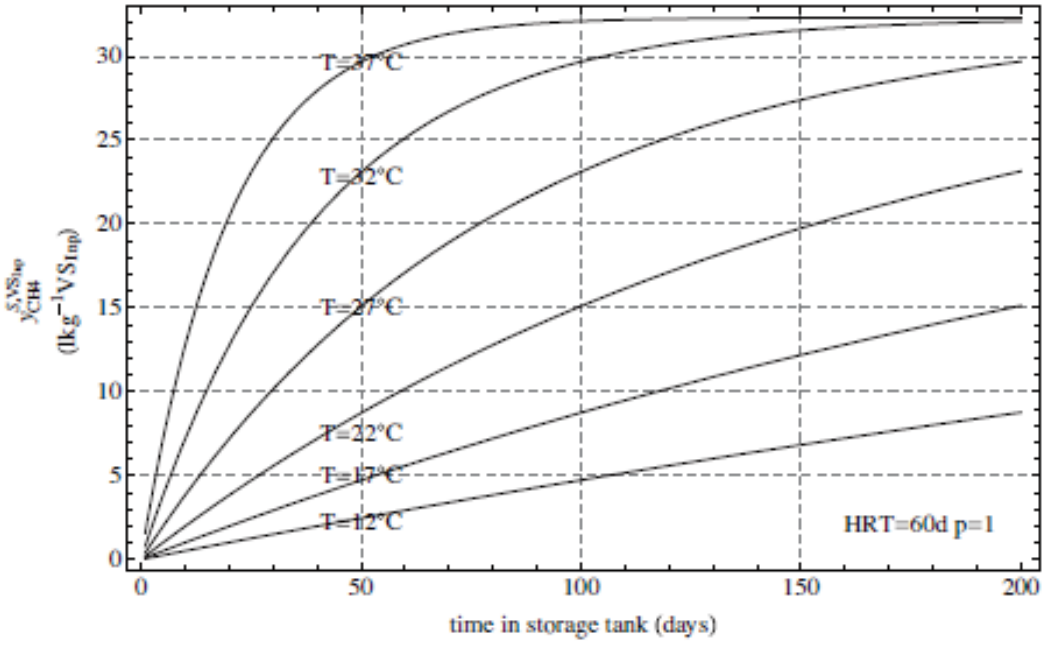

Figure 5 – Example of methane yields as a function of retention time in storage tank for the temperatures for six temperatures between 12 and 37°C at a constant pressure of 1 atm (adapted from Sebola, Tesfagiorgis, and Muzenda, 2014).

2.2.3. Retention time

The concept of hydraulic retention time (HRT) is often confused with the term retention time. HRT is the average time required from a control volume to travel from the input to the output of a reactor, for example. Retention time only refers to the period that an element is retained in a given space or volume before leaving. Therefore, for batch operation, the retention time should be used, as the HRT makes only sense for continuous and semi-continuous operations

As shown by examples of Figure 4 and Figure 5, total gas production increases with the increase of retention time, as biogas is produced over time. However, as shown by the exponential profile of the gas production curves, the production rate decreases over time being closer to 0 as time passes. Production rates in these cases are often modeled using first order, but studies suggested that

other models can be used for better approximations, such as a modified Gompertz, as shown by Figure 6 (PRAMANIK et al., 2019; WEALKENS, 2020).

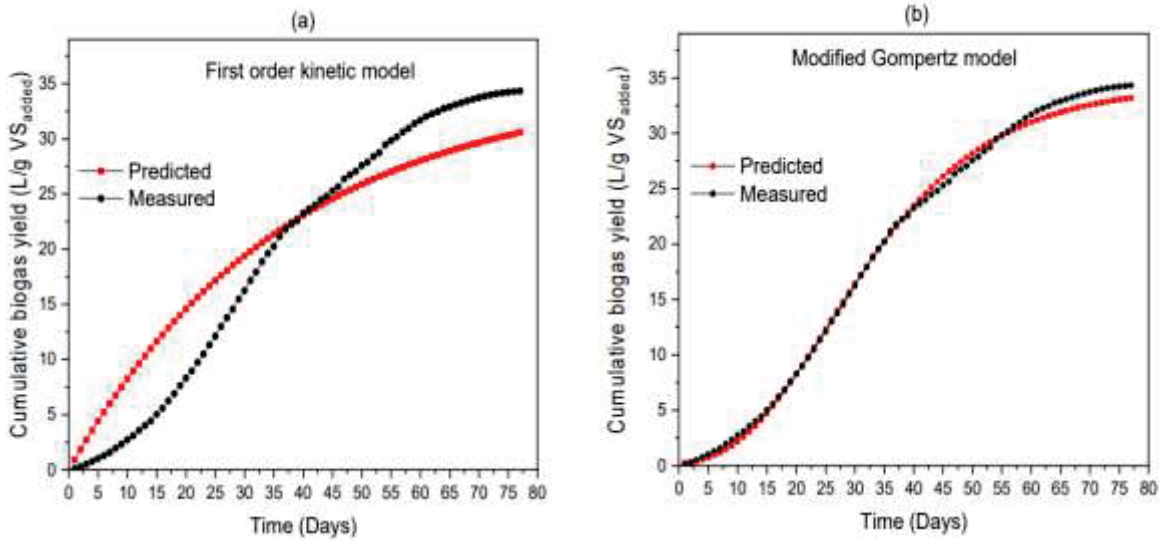

Figure 6 – Cumulative biogas yield from the (a) first-order kinetic model, (b) modified Gompertz model *(PRAMANIK et al., 2019)*

In a continuous or semi-continuous operation, a low HRT not only leads to lower yields but also production instabilities and reduction in gas quality. Studies showed that an HRT reduction from 20 to 5 days can result in efficiency drops of up 40% in production, with even more intense drops in methane content (TORECI; KENNEDY; DROSTE, 2009). Reduction to HRT around 10 days showed lesser losses in efficiencies, but a dwindle of methane content from averages of 70% to 50-55%

This difference is associated with organisms being often flushed out of the reactors with the output. Therefore, in low HRT regimes when volume inside reactors is replaced faster, the replenishment rates of bacteria are not high enough to sustain losses.

2.2.4. Recirculation rate and mixing efficiency

Mixing is required to allow a homogenous distribution of nutrients along with the reactors, reducing accumulation spots and dead zones. For conventional digesters, mixing can be made by rotors with impales or my recirculating material

between different spots. A moderate mixing was found to increase yields and production stability in tank reactors (ZHAI; KARIYAMA; WU, 2018). This is related to the fact that with a moderate mixing, particle size and its concentration in the reactor volume decreases, improving the performance of enzymes involved in the AD. At a higher mixing rate, the risk of cell wall and membrane of microorganism increases, which diminishes AD kinetics (MA et al., 2019).

For the case of the plug flow, mixing in the axial direction is negligible, therefore the role of the recirculation is not to perfectly mix the reactor, but to transport nutrients along the length. Therefore, observations in the literature do not apply to this case. With that, recirculation in a plug flow reactor was only used to transport and not to mix.

2.3. Plug flow reactors

Most conventional anaerobic digesters are based on tank-like reactors with different shapes and designs, but with the same principle of operation, they operate with the well-mixed assumption. This assumption considers that the properties gradients in the whole volume of the reactor is zero, which means, that every point of the volume have the same concentration, temperature, etc. (SCOTT FOGLER, 1987)

On the other hand, a plug flow reactor (PFR) design was used during this work, which operates with low axial mixing. However, if one considers a reactor to be a PFR, radial mixing is considered perfect. With that, a PFR can be understood as a combination of several thin slices with the same concentration in the whole slice volume (SCOTT FOGLER, 1987).

This difference of behavior leads also to differences in the distribution of residence time. If a pulse of tracer is applied in a PFR, all the volume injected tends to leave the reactor all at once after one HRT. In a tank reactor, however, the tracer would leave slowly the system, retaining volumes for several HRT. These differences in mixing can be seen in Figure 7, where $E(t)$ is the tracer concentration in the

output, $F(t)$ the accumulated mount of tracer that left, V reactor volume, v_0 flow rate and τ the hydraulic retention time.

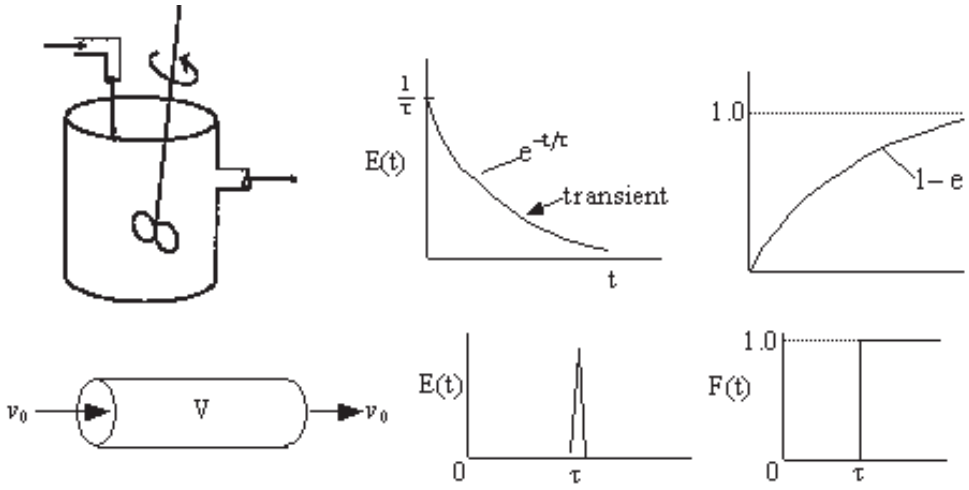

Figure 7 – Distribution of residence time for ideal plug flow and well-stirred reactors during a pulse test *(SCOTT FOGLER, 1987)*.

As the mixing profile is different from tank reactors, concentration along with the reactor changes, allowing a higher concentration of reactants to be achieved at the input. With that, PFRs are suitable for studying rapid reactions and allow a larger load to be used, as the feed does not affect the rest of the reactor at the moment of feed. Moreover, as no moving parts are required for mixing, maintenance of the reactor end is cheaper, but they are harder to be controlled. Due to axial variations of concentration, several measurements points must be installed, as for tank reactors, one measurement point is already sufficient due to perfect mixing assumptions.

2.4. Sewage sludge

During the treatment of wastewater from residential water, sewage is submitted to several physical and biological processes of purification. As a result, a solid residue rich in organic substances is produced, which is called sludge.

Sludge can be produced in several steps of a conventional WWTP, having different properties and being named after the order of its production in the process chain. The first type is the primary sludge, which is produced during primary

purification steps, such as chemical precipitation and sedimentation. Secondary sludge is obtained during biological treatment, consisting of most of the activated organic biological mass of the treatment process. In most cases, these two residues are mixed for further treatment and disposal (GROBELAK; CZERWIŃSKA; MURTAŚ, 2019; SCHOLZ, 2016).

This combination leads to a mixture with high organic matter content and the presence of innumerous contaminants, with composition varying region to region. According to the DWA (Deutsche Vereinigung für Wasserwirtschaft, Abwasser und Abfall), sewage sludge in Germany had a concentration of approximately 30% of volatile solids (wet base), ranging between 45 to 90% of the total dry matter in the mixture. Even most of the organic matter being consisted of carbon, hydrogen, and oxygen, up to 2% of the total dry mass is sulfur, which led to hydrogen sulfide during treatment steps (SCHOLZ, 2016).

Tertiary sludge can be also produced in some processes which have further specialized treatment or nutrient recovery, such as phosphorus. In some cases, this type of residue can be denominated as excess sludge (ES). The destination of this type of residue may vary with the post-treatment in place, which would dictate if it could be mixed with primary and secondary sludge for a combined treatment. Usually, this combination increases the number of macronutrients in the final mixture, as ES often has a high concentration of nitrogen and phosphorus (WIECHMANN et al., 2013).

Treatment of sludge may vary with legislative characteristics of the country and amount produced, but most followed the following steps (WIECHMANN et al., 2013):

1. Thickening: sedimentation process which aims to reduce water from the sludge. Sludge is sent directly to tanks and heavier particles are removed as they reach the bottom;
2. Hygienization: aim to reduce the pathogen and harmful organisms from the sludge according to local regulations. There are many possible options of which most are thermal or pH treatments;

3. Biological stabilization: used to neutralize biological activity and reduce the production of gases and odors. This step is conducted mainly in anaerobic digesters, which are used to produce methane as a by-product of the treatment;
4. Dewatering: used to remove water from the output of the anaerobic digester mechanically. This is mainly conducted in centrifuges, or in belt or chamber type filter presses, which can concentrate the final product up to 50% of total dry matter;
5. Drying: reduces the water level to minimum values required for the final disposition. There are many options to conduct this process, but the main ones are related to flue gas utilization in drum or fluidized bed dryers;

After being treated, sludge can be used in the agricultural sector as a fertilizer or it can be disposed of in a landfill or incinerated, according to regional regulations.

2.5. Mathematical background and calculation samples

2.5.1. Internal liquid and gas volume

The reactor is not filled by the liquid phase, a portion of it is filled by the gas and may vary along with the operation. With that, the volume of both phases must be calculated as a function of the filling level height, which can be controlled. These considerations are shown in the scheme of Figure 8:

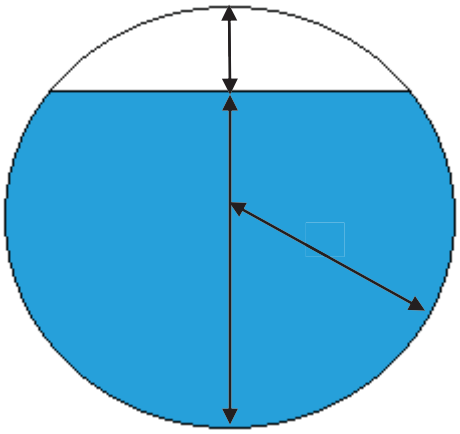

Figure 8 – Reactor`s transversal cut scheme.

Where q is the high of the liquid phase, r the internal radius, and a the distance between the top of the internal wall and the interface.

Therefore, the volume of the liquid phase (V_l) can be written as the transversal area of the liquid phase (A_l) times the length of the reactor (L), as shown by equation 1:

$$V_l = A_l . L \tag{1}$$

Since only A_l is a function of the filling level, $A_l(a)$ must be determined. To accomplish it, a Cartesian plan is centered at the center of the transversal section of the reactor. With that, the area of the section can be determined by the integration of the circle equation (2).

$$r^2 = x^2 + y^2 \tag{2}$$

As the control parameter a varies on the y-axis, the integration must be carried out along the y-axis. Due to symmetry, the total area of the liquid phase will be two times the area of half of the circle integration. Therefore, the area $A_l(a)$ can be defined as:

$$A_l(a) = 2 \int_{-r}^{r-a} \sqrt{r^2 - y^2} dy \tag{3}$$

This integral can be easily solved by trigonometric substitution, as follows:

$$y = r\sin(u) \rightarrow u = \arcsin\left(\frac{y}{r}\right), dy = r\cos(u) \tag{4}$$

Which results in the expression 5:

$$r\int cos^2(u)du = r\left(\frac{\cos(u)\sin(U) + u}{2}\right) + C \tag{5}$$

Undoing the substitution and simplifying the expression, the following is obtained:

$$\frac{r}{2}\left(\arcsin\left(\frac{y}{r}\right) + \frac{y\left(\sqrt{r^2 - y^2}\right)}{r}\right) + C \tag{6}$$

The transversal area is given by equation 7 when applying the integration limits:

$$A_l(a) = r^2\left[\frac{\pi}{2} + \arcsin\left(1 - \frac{a}{r}\right)\right] + (r - a)\sqrt{2ar - a^2} \tag{7}$$

The volume of the liquid phase is obtained when one substitutes equation 7 on equation 1:

$$V_l(a) = L\left\{r^2\left[\frac{\pi}{2} + \arcsin\left(1 - \frac{a}{r}\right)\right] + (r - a)\sqrt{2ar - a^2}\right\} \tag{8}$$

The gas-phase volume ($V_g(a)$) is the difference between the total internal volume and the liquid phase volume, which can be written as follows:

$$V_g(a) = L\left\{r^2\left[\frac{\pi}{2} - \arcsin\left(1 - \frac{a}{r}\right)\right] - (r - a)\sqrt{2ar - a^2}\right\} \tag{9}$$

Considering equations 8 and 9, the volume of the liquid phase at normal operation, $a = 2\,cm$, internal radius of 12,5 cm and reactor length of 500 cm is calculated as follows:

$$V_l(a) = 500\ cm\left\{(12{,}5\ cm)^2\left[\frac{\pi}{2} + \arcsin\left(1 - \frac{2\ cm}{12{,}5\ cm}\right)\right]\right.$$
$$\left. + (12{,}5\ cm - 2\ cm)\sqrt{2(12{,}5\ cm\ .\ 2\ cm) - (2\ cm)^2}\right\} \quad (10)$$
$$= 233699\ cm^3 = 233{,}70\ L$$

And the gas phase:

$$V_g(a) = 500\ cm\left\{(12{,}5\ cm)^2\left[\frac{\pi}{2} - \arcsin\left(1 - \frac{2\ cm}{12{,}5\ cm}\right)\right]\right.$$
$$\left. - (12{,}5\ cm - 2\ cm)\sqrt{2(12{,}5\ cm\ .\ 2\ cm) - (2\ cm)^2}\right\} \quad (11)$$
$$= 11738\ cm^3 = 11{,}74\ L$$

2.5.2. Mass Balances

Mass balances were necessary to find the accumulation and the real digestion of organic matter inside the reactor. For that, mass flows within the system are identified in the scheme of Figure 9:

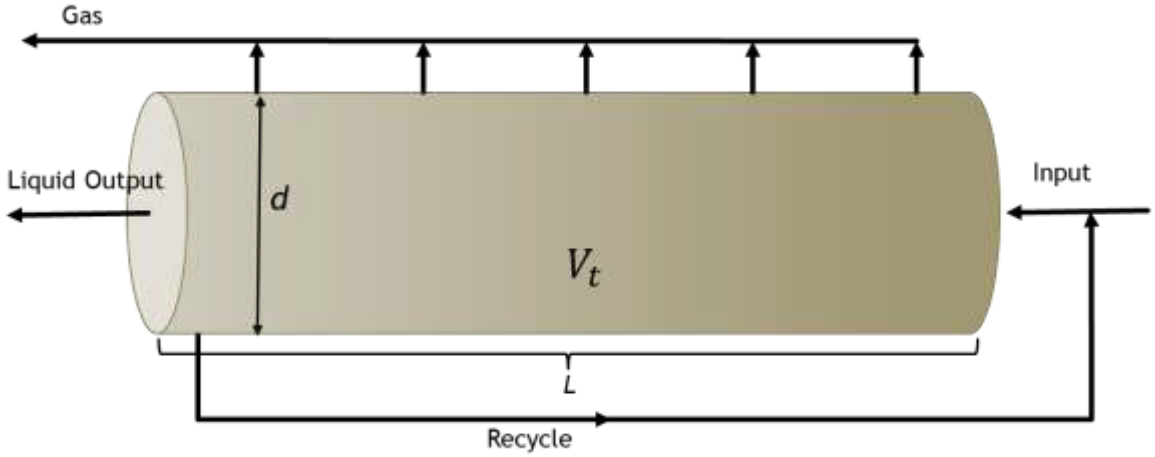

Figure 9 – Pipe reactor simplified current scheme.

Therefore, by the principle of mass conservation, the followed relation is obtained:

$$m_{out,l} + m_{out,g} = m_{in} + m_{ret} \quad (12)$$

Where $m_{out,l}$ is the mass flow of the liquid output, $m_{out,g}$ is the mass flow of the gaseous output, m_{in} is the mass flow of the input and m_{ret} is the retention rate, all with M.t^{-1} dimensions.

If one considers that the liquid input and output, as well as the retention rate, can be described as a function of organic and inorganic matter, equation 12 can be rewritten as follows:

$$(m_{out,org} + m_{out,ino}) + m_{out,g} = (m_{in,org} + m_{in,ino}) + (m_{ret,org} + m_{ret,ino}) \quad (13)$$

Where $m_{i,org}$ are the organic fractions of the mass fluxes, $m_{i,ino}$ are the inorganic fractions and the index i indicates input or output.

In addition, the global balance equation 13 can be expanded in two mass balances if the following is considered:

- The digestion only produces a gaseous mixture of CO_2 and CH_4;
- Only the organic fraction is converted to gas;
- Reactions between organic and inorganic matter result in a negligible change of both fractions.

$$m_{out,org} + m_{out,g} = m_{in,org} + m_{ret,org} \quad (14)$$

$$m_{out,ino} = m_{in,ino} + m_{ret,ino} \quad (15)$$

Inorganic and organic mass flow can be calculated in terms of load and mass fractions considering negligible water accumulation in the system. This can be applied to equations 14 and 15 to obtain the following relations:

$$m_{ret,org} = vx_{in,org} - (vx_{out,org} + m_{out,g}) \quad (16)$$

$$m_{ret,ino} = v(x_{in,ino} - x_{out,ino}) \quad (17)$$

Where v is the total amount of feeding, which was kept equal with the total mass that was removed from the reactor, and $x_{i,j}$ the mass fractions.

Considering the gas produced to be an ideal gas, the gas mass flow can be calculated as follows:

$$m_{out,g} = m_{out,CO_2} + m_{out,CH_4} = \frac{PV_g}{R\overline{\overline{T}}}\left(\frac{y_{CO_2}}{mm_{CO_2}} + \frac{y_{CH_4}}{mm_{CH_4}}\right)^{-1} \quad (18)$$

Where V_g is the volume of gas produced in a given period, P is the reactor operation pressure, $\overline{T}$ is the average pressure of the reactor during the period, R is the gas constant, y_i is the gas molar fractions and mm_i is the molar masses.

Combining equations 16 and 18, the mass balance equation for organic matter is achieved:

$$m_{ret,org} = v(x_{in,org} - x_{out,org}) - \frac{PV_g}{R\overline{\overline{T}}}\left(\frac{y_{CO_2}}{mm_{CO_2}} + \frac{y_{CH_4}}{mm_{CH_4}}\right)^{-1} \quad (19)$$

Equation 19 must be further modified to adjust to operational data and the feeding schedule. Both molar fraction and gas production rate was as well measured through averages over 10 min. In addition, composition and quantity of feeding also vary over time, but daily, being also necessary to adjust the equations for them. Therefore, the accumulation of organic matter was calculated as sums of different indexes using the following equation:

$$m_{ret,org} = \sum_{j=1}^{t}\left[v_j(x_{in,org,j} - x_{out,org,j})\right] - \frac{P}{R}\sum_{i=1}^{n}\frac{V_{g,i}}{\overline{\overline{T}}_i}\left(\frac{y_{CO_2,i}}{mm_{CO_2}} + \frac{y_{CH_4.i}}{mm_{CH_4}}\right)^{-1} \quad (20)$$

$$m_{ret,ino} = \sum_{j=1}^{t} v_j(x_{in,ino,j} - x_{out,ino,j}) \quad (21)$$

Where t is the total number of days within the period and n the total number of 10 min averages measured during the period. Due to the raw number of values

for the gas term during a given day, it is not feasible to give an example of a real calculation using equation 20.

2.5.3. Hydraulic retention time (HRT)

The hydraulic retention time can be defined as the average time for volume elements to be transported along the whole length of the reactor. Mathematically, HRT can be written as the ratio between the useful volume, in this case, the liquid phase volume V_l, and the flow rate $\dot{V}$ as follows:

$$HRT = \frac{V_l}{\dot{V}} \tag{22}$$

To calculate HRT, $\dot{V}$ must be considered a function of time ($\dot{V}(t)$) due to variations of flow rate over time. With that, the retention time must be calculated as a function of the volume transported (V_{Tr}) during a given time using the following definition of flow rate:

$$\dot{V} = \frac{dV_{Tr}}{dt} \rightarrow V_{Tr}(t) = \int_{t_0}^{t_f} \dot{V} dt \tag{23}$$

Where t_0 and t_f are the boundaries in time. This integral must be solved numerically to be adjusted to experimental data, for this the trapezoidal rule for a constant time step Δt is used:

$$V_{Tr}(t) = \int_{t_0}^{t_f} \dot{V} dt \approx \Delta t \sum_{i}^{n} \frac{\dot{V}_{i-1} + \dot{V}_i}{2} \tag{24}$$

Considering a time step Δt = 10 min, the volume transported in 1 h can be calculated as follows:

$$V_{Tr}(1h) = \frac{1}{6} \sum_{i}^{6} \frac{\dot{V}_{i-1} + \dot{V}_i}{2} \tag{25}$$

Adjusting for the experimental data, which the residence time of a value i is calculated from the current and previous measurements only, the residence time can be calculated with a ten minutes resolution as follows:

$$HRT_i = \frac{12\ V_l}{\sum_i^6 (\dot{V}_{i-6} + \dot{V}_{i-5})} \tag{26}$$

For the calculation example, a sample of measured experimental data is shown in Table 1:

Table 1 – Examples of flow rates values for calculation's sample.

i	*Date/Time*	*Flow Rate (L/h)*
1	01/11/2021 12:00	241
2	01/11/2021 12:10	220
3	01/11/2021 12:20	211
4	01/11/2021 12:30	198
5	01/11/2021 12:40	157
6	01/11/2021 12:50	131
7	01/11/2021 13:00	266

Therefore, the calculation of HRT for $i = 7$ and useful volume $V_l = 233{,}70\ L$

$$HRT_7 = \frac{12 * 233{,}70\ L}{[220 + 2(211 + 198 + 157 + 131) + 266]L/h} = 1{,}20\ h = 1h12min \tag{27}$$

For the five first measured values of flow rate, the HRT was not calculated.

For the residence time based on input and output, the same principle was used, but the time step used was 1 day and a period of 5 days was used as the basis, due to the feeding schedule used. Periods with an average flow rate below 30 L/h were skipped.

2.5.4. Chemical oxygen demand and solids removal

The removal/reduction of chemical oxygen demand and solids from the feeding stream were calculated using values of samples from input and output

collected on the same feeding batch and day. Removal was calculated for the following parameters: TDM, ODM, and COD all by the following generic equation:

$$R_i = \frac{x_{i,in} - x_{i,out}}{x_{i,in}} * 100\% \quad (28)$$

Where R_i is the reduction in percentage, $x_{i,in}$ is the parameter measured at the input and $x_{i,out}$ at the output.

2.5.5. Specific gas production

During this work, specific gas production was calculated based on volatile solids (m_{VS}) and chemical oxygen demand (m_{COD}), both in kilograms. For specific production based on feed-to-feed intervals, values were set also on time, being necessary to average by day. With that, daily specific production ($\dot{g}_{day}$) was calculated using the following equations:

$$\dot{g}_{day}(L\ kgVS^{-1}\ d^{-1}) = \frac{g_{ftf}}{t * m_{VS}} \quad (29)$$

$$\dot{g}_{day}(L\ kgCOD^{-1}\ d^{-1}) = \frac{g_{ftf}}{t * m_{COD}} \quad (30)$$

Where g_{ftf} is the accumulated feed-to-feed gas production in liters and t is the time in between feeds in days. A calculation example for August 23rd is shown as follows:

$$\dot{g}_{day}(L\ kgVS^{-1}\ d^{-1}) = \frac{23{,}51\ L}{1{,}104\ d * 0{,}135\ kgVS} = 265{,}56\ L/kgVSd \quad (31)$$

$$\dot{g}_{day}(L\ kgCOD^{-1}\ d^{-1}) = \frac{23{,}51\ L}{1{,}104\ d * 0{,}187\ kgCOD} = 113{,}88\ L/kgCODd \quad (32)$$

For specific production over a week, values were not adjusted with time as week length differences were negligible, therefore the following equations were used for the calculation of specific products over a week:

$$\dot{g}_{day}(L\ kgVS^{-1}) = \frac{g_{wtw}}{m_{VS}} \quad (33)$$

$$\dot{g}_{day}(L\ kgCOD^{-1}) = \frac{g_{wtw}}{m_{COD}} \quad (34)$$

Where g_{wtw} is the total gas production over a week. An example of this equation application is shown for week 14 as follows:

$$\dot{g}_{day}(L\ kgVS^{-1}) = \frac{323{,}65\ L}{0{,}682\ kgVS} = 474{,}33\ L/kgVS \quad (35)$$

$$\dot{g}_{day}(L\ kgCOD^{-1}) = \frac{323{,}65\ L}{0{,}910\ kgCOD} = 355{,}78\ L/kgCOD \quad (36)$$

2.5.6. Sludge age

Sludge age (S_{age}) is the average time a particle of suspended solids remains in the activated sludge system and it can be calculated by the ratio of the total inorganic matter in the reactor and the rate at which inorganic matter is removed from it. The total inorganic matter inside the reactor was obtained during the mass balances, being the difference between the total and organic matter.

With that, sludge age was calculated using the following equation:

$$S_{age} = \frac{m_{a,ino}}{(TDM_{out} - ODM_{out}) * v * d} \quad (37)$$

Where TDM_{out} is the total dry matter in the output in m/m%, ODM_{out} the organic dry matter in the output in m/m%, v is the output flow rate in L/d, d the output density (1 kg/L), and $m_{a,ino}$ the accumulated inorganic matter in the reactor in kg at the moment of the feeding. An example of calculation for September 13th is shown:

$$S_{age} = \frac{1{,}455\ kg}{(0{,}10\% - 0{,}06\%) * 10\ L/d * 1\ kg/L} = 113{,}04\ days \quad (38)$$

3. Experimental Setup

During this work, the experimental setup was consisted of: an anaerobic pipe reactor (digester), pump, heating system, 150 L storage tank, measurement system, and data log, all installed at the research hall of Büsnau wastewater treatment plant. The scheme of the installation and disposition of valves and connections is shown in Figure 10.

The reactor consists of five tubular sections with 1 m of length, 273 mm, and 250 mm of external and internal diameter respectively. The sections were built-in stainless steel (DIN 1.4571) and are separated by perforated plates with 250 mm of diameter opening and 50 mm of rectangular blockade from the top of the perforation. The connection between sections and plates was done by bolts and nuts, which allowed the separators to be built into the reactor`s support. In addition, each section has three small connections installed at 0°, 90°, and 180° centered at the length of 50 cm (except valve 16, located at 25 cm). Ten valves were installed in these connections as follows: valves 6 to 10 regulate the gas collection and valves 12 to 16 for sampling. Design details of the reactor are shown in annex 1.

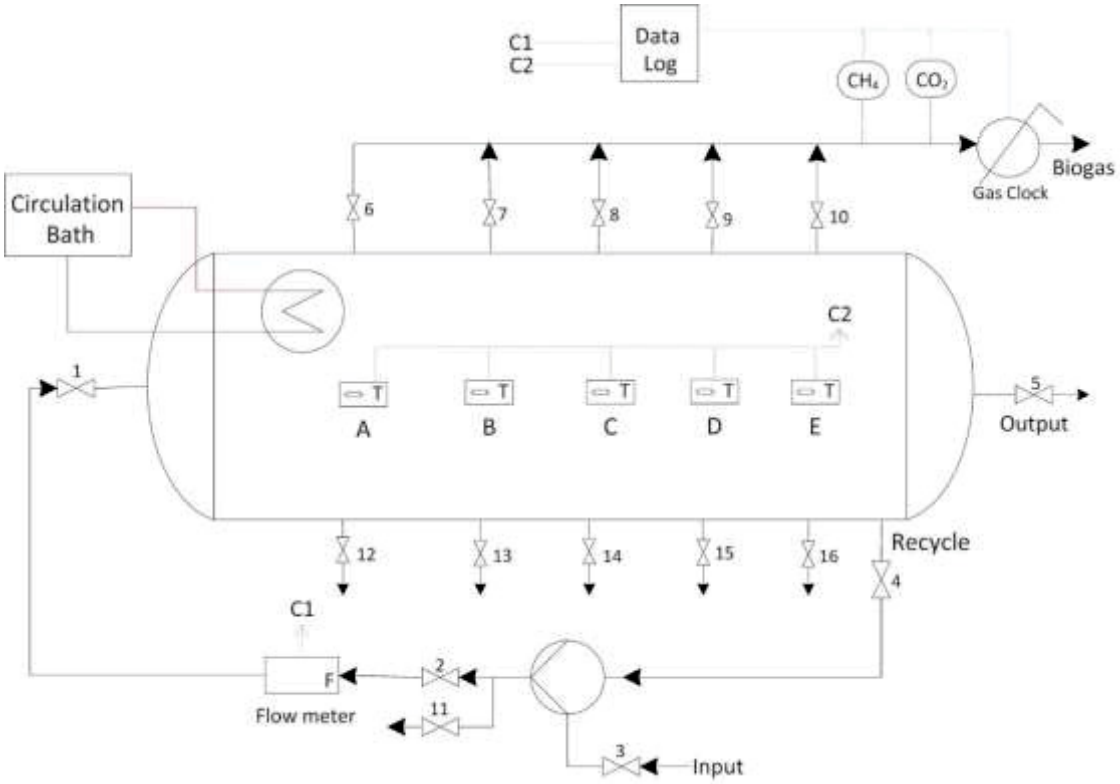

Figure 10 – Experimental setup equipment and valves scheme

Moreover, the filling level was controlled by an external arm installed close to the output. With an angle of 30° perpendicular to the digester, being connected to the end wall of the last section, as shown by the picture in Figure 11. The connection is centered at the same height (36.5 mm above the digester's center) as the pipe connected to the end wall of the first section. This arrangement of elbows and pipes kept the water level under 2 cm from the top of the internal wall as an effect of the hydrostatic pressure. The reactor also has a perpendicular smaller pipe (external diameter 114.3 mm) connected by a smooth reducer on the bottom of the last section (recycle). All these features are sealed to the main body of the digester with a meld finish and allow the output to be easily collected by a tank.

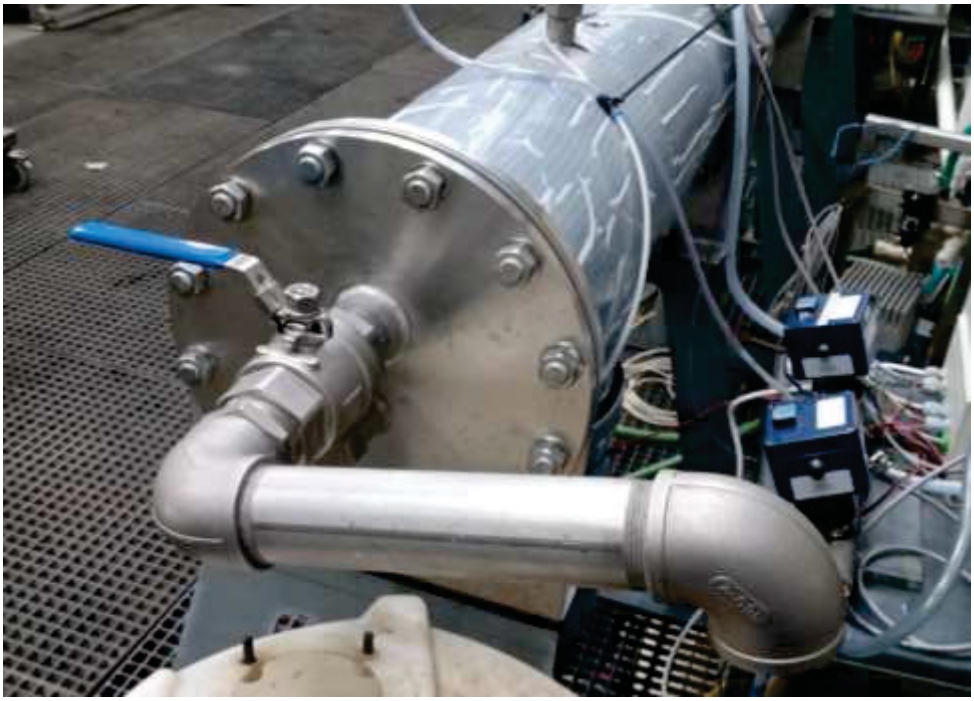

Figure 11 – Filling level control arm.

At last, feed and recirculation are controlled by the valves 1 to 4. Valves 3 and 2 are installed directly to the pump and are not part of the reactor, but are required to adjust the flow rate to switch between feeding and recirculation regime. The connection between these valves was done by plastic hoses. There is also one valve installed to the pump that allows the collection of the recycling material without interrupting the operation. All of the valves installed both in the pump and reactor are of ball type. A screw pump from the manufacturer NETZSCH Pumpen & Systeme used to recirculate material in the system has 16 Nm of power and a maximum flow rate of 1600 L/h.

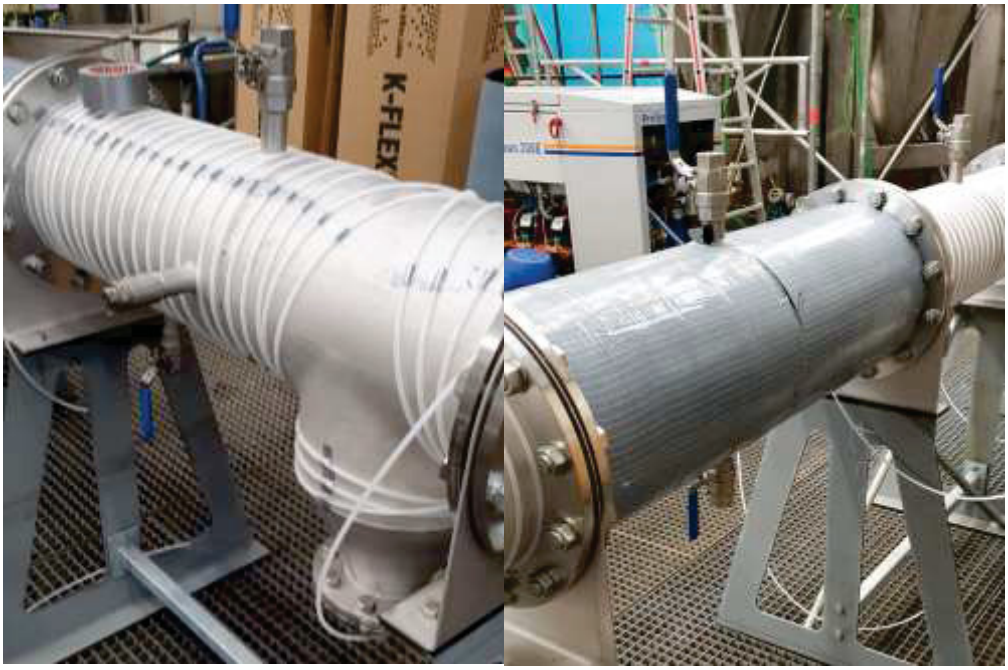

Figure 12 – Installed thermal isolation and heating hoses

The temperature was controlled by a combination of isolation, hoses, and a thermal bath. Hoses were installed in direct contact with the reactor external wall, circulating each section similarly, as shown in Figure 12. This arrangement was covered by thermal isolation, which was not sufficiently thick to cover the area of the connection between sections. With that, the hoses were connected to a heating circulator CD-BC12 from Julabo GmbH, which has a maximum flow rate of 15 L/min (0.35 of maximum pumping pressure) and 2 kW of heating capacity. In addition, each section has its control valve for flow rate control. This system has a maximum operating temperature of 75°C in the bath.

In addition, five thermometers were installed, one in each section, at the points A to E, as shown by Figure 10. Each of them measures the temperature of the liquid phase at a height of 125 mm and 75 mm from the sidewall. The instruments have a precision of 0.1°C.

Other four measurement instruments were installed: gas clock (Figure 13 left), flow meter (Figure 13 middle), methane, and carbon dioxide analyzers (Figure 13 right). The gas clock installed was a type TG05 from Dr.-Ing. RITTER Apparatebau GmbH & Co. KG, which can measure flow between 1 and 60 L/h of

gas (standardized at 20°C). The flow meter is from the provider Endress+Hauser GmbH+Co.KG. Both CH_4 and CO_2 are measured by the infra-red (dual wave) principle by two BCP type analyzers, BCP-CH4 and BCP-CO2 respectively, which are both manufactured by BlueSens GmbH. In addition, these analyzers are capable to measure concentrations from 0 to 100% of methane and up to 50% of carbon dioxide with a minimum accuracy of 0,2% plus 0.02 times the current measured value.

Figure 13 – Gas clock (left), flow meter (middle), gas analyzers (right)

All measurement instruments are connected to an RSG10 data log from Endress+Hauser GmbH+Co.KG. It displays the current value of temperature, flow rate, and gas concentrations as well the accumulated gas production. Measurements are saved and stored in an internal database every two minutes, except the gas production which is saved each 10 min. If a diskette unit is inserted into the equipment, the system saves data also on the diskette unit in addition to its database. All stored data can be accessed by the software ReadWin 2000 from the same provider.

During the period, the experimental setup was submitted to the following changes:

- 02/06/2021: the filling level control arm was installed;
- 30/07/2021: the pump stator was replaced;
- 27/09/2021: gas analyzers were installed;
- 26/10/2021: the hose connecting valve 4 to the pump was replaced.

4. Feed

The reactor was only fed with primary, excess sludge, water, or a mixture of them during the experiments. Both primary and excess sludge were gathered from the local wastewater treatment plant from a bypass for sampling. Water used during experiments was collected from a local source located at the research hall. Figure 14 shows a comparative picture between the feeding mixture (right), substrate (middle), and output (left).

Figure 14 – Example of feeding mixture (right), substrate (middle), and output (left) collected on November 1st.

From July 23rd to August 23rd, sludge was fetched daily during the morning, being used and disposed of during the same day. From the 24th of August and forward, collect sludge was stored up to four days at a 6°C in a fridge because the daily collection led to an unstable quality of the excess sludge. To obtain an overall concentrate sludge, during September and October, primary sludge was fetched between 13:00 and 14:30h, due to the operation schedule of the WWTP. During no collection days, an amount greater than 50 L of either sludge was collected and stored. Stored primary sludge was collected majority on Mondays and Thursdays, no sludge was collected during weekends.

5. Methodology

5.1. Analytics

5.1.1. Total dry matter, organic dry matter, inorganic dry matter

Total dry matter (TDM) is a measurement of total dry matter after all water is evaporated from a given sample. Inorganic dry matter (IDM), however, is the total remaining matter after ignition losses, usually done at temperatures above 450°C (TELLIARD, 2001). The difference between TDM and ODM is the organic dry matter (ODM), which can be associated with the total organic matter.

For these methods the following equipment was used:

- Small beakers Duran® (for total solids only);
- Small ceramic crucibles;
- Analytic scale (Precisa gravimetric® LX220A scs);
- Semi-analytic scale (Sartorius ED62025);
- Drying oven;
- Muffle oven.

Firstly, all beakers and crucibles are weighted before sampling. Afterward, an approximated amount of 100 ml for the beakers and 50 ml for the crucibles were collected and transferred to the corresponding recipients. Next, all recipients with the material were weighed once again and put into the drying oven at 105°C, where crucibles stay for a minimum of 18h and beakers for 44h[1]. After this period, samples were cooled to ambient temperature and weighted. These steps of the procedure were sufficient when only total solids values were required.

For the volatile and fixed solids, however, the samples contained in the ceramic crucibles were placed into the muffle oven at 600°C for 2h. After they were cooled on a thermal resistant surface for 2-3 min and then placed in a desiccator

[1] During experiments, it was found that 20h were not sufficient to completely dry samples in beakers, therefore it was decided to keep them inside the drying oven for one extra day.

until they reached ambient temperature when they were weighted. With the mass values from each step, the total, fixed, and volatiles solids were calculated using the equations 39, 40 and 41 respectively:

$$TDM(\%) = \frac{m_{do} - m_c}{m_0 - m_c} \quad (39)$$

$$IDM(\%) = \frac{m_{mo} - m_c}{m_0 - m_c} \quad (40)$$

$$ODM(\%) = TDM - TFM \quad (41)$$

Where m_{mo} is the mass of crucible with the sample after the muffle oven, m_{do} the mass of the crucible with the sample after the drying oven, m_0 the mass of the crucible with the sample after collection, m_c the mass of the crucible, ODM the organic dry matter, TDM the total dry matter, and IDM the inorganic dry matter.

5.1.2. Total dissolved solids

Total dissolved matter (TdiM) is a measurement of the dissolved matter of a given sample after all water has evaporated. To obtain it, the following equipment was used:

- Filter funnel;
- Filter funnel support;
- Filter paper (MN 615 ¼ Ø 320 mm);
- Drying oven;
- Graduated cylinder of at least 100 ml;
- Analytic scale;
- Wash bottle with distilled water;

Before starting the analysis, the filter papers were numbered and drought at the drying oven for at least two hours (in most cases they stayed overnight in preparation for the next day) to remove any residual moisture. After the period, all

filters were placed into a desiccator to cool until ambient temperature, when they were weighted in an analytic scale.

Afterward, the filter funnels were attached to the support and the filters papers were placed onto the funnels. Then, the papers were watered with 30-50 ml of distilled water, allowing them to stick to the walls of the funnel. Next, an aliquot of 100 ml was transferred to the filters, until no water could be seen or 2h had passed. After this period, filters were sealed and placed into the drying oven for 20h at 105°C, when they were placed into a desiccator and weighted after reaching ambient temperature. TdiM can be calculated as follows:

$$TdiM\ (g/l) = \frac{m_{fdo} - m_f}{V} \quad (42)$$

Where m_{fdo} is the mass of the sample with the filter after the drying oven, m_f the mass of the dry filter (both in g) and V the sample aliquot in L. Su

spended solids were assumed to be the positive difference between TdiM with TDM.

5.1.3. Chemical Oxygen Demand (COD)

Chemical oxygen demand is the measurement of the oxygen required to be present in water to oxidize all chemical compounds present in a given sample. This analysis was done by the laboratory staff following the method DIN 34809-41 of samples collected in a plastic 500 ml sealed vessel. These samples were delivered on the same day when collected, but when it was not possible to do so, they were stored at 6°C inside a fridge until delivery. No samples were stored for more than 72 hours under these conditions.

5.2. Feeding procedure and sample collection

The following items were used during feeding:

- Three 15 L graduated buckets;
- Plastic stick for mixing;

- Large beaker;
- Stickers for labels;
- Cleaning brush;

Firstly, values of accumulated gas production, flow rate, methane, and carbon dioxide composition displayed on the data log were verified and noted as well as accumulated gas production was shown on the gas clock. If the flow rate was below 100 L/h, the rate was increased to 200-250 L and, then, verified after 30-45 min before starting the feeding procedure. This step was done until the stabilization of the flow rate at the set value.

The procedure started by collecting samples from the recirculation. For that, a bucket was placed under the exit after valve 11 to collect the recirculation liquid. Then, valve 11 was opened and the sample was collected after 20-30s, closing valve 11 afterward. Before starting the next procedure, the excess liquid was disposed of and the bucket cleaned.

In sequence, a second bucket is filled with 5-7 L of water and placed close to the pump to help wash sampling vessels and other items. After the feed mixture was prepared using the third bucket. If the amount of material was greater than the bucket capacity, one bucket was prepared with the final rate sludge/water and a second bucket was filled with the remaining sludge only. When this happened, the cleaning bucket was used to collect and transfer water. This was made because the place of handling of sludge and experiments were different.

After the feed preparation, the sample was collected using a large beaker and transferred to final vessels. Then, the feeding hose was dived into the bucket, and valves 6 to 10 closed. Afterward, the pump was shut while closing valve 2 followed by the closure of valve 4. After these valves were closed, the pump was set to reverse while valve 3 was opened. This was done to remove air from the feeding hose. When any bubbles could be seen, the pump was switched to the normal direction and the flow rate adjusted to 150 L/h. After two to three liters of feed had been pumped in, valve 5 was slowly opened and the flowrate adjusted to 200 L/h.

Once the output had stabilized, a sample was collected, which usually happened after 2 min after the feeding had begun for low amounts (≤ 10 L) and 5-8

min for higher amounts. If a change of state of output was visually verified, multiple samples were collected and mixture together at similar rates.

The pump was shut after almost all of the material was fed, only leaving a small quantity in the bucket (≤ 300 mL) to avoid air going into the digester. After turning the pump off, valves 3 and 5 were closed, opening valve 2 immediately after. Then, valves 6 to 10 were opened and the pump restarted at a flow rate of 200-250 L/h. After the procedure was done, all items used were cleaned.

One hour after feeding, values of flow rate, accumulated gas production, methane, and carbon dioxide were checked and the flow rate was adjusted when a reduction was verified. In most cases, the pump was set to operate above 250 L/h before leaving, once constant decay in flow speed was verified several times during operation.

6. Results

In this and the following sections, the measurement points for temperature follow the scheme of Figure 10. Also, the number of samples from the reactor's bed where it indicates for which valve they were taken. If the sample is named by 12 it was collected from valve 12, as indicated in Figure 10. All values of gas production shown in the following sections were adjusted for normal conditions of pressure and temperature.

Problems with measurements and other errors or interferences are explained when describing results on the date it had happened and for the outcome, it had interfered. For graphs with two units involved in the y-axis, units are described in the graph description/title, which is located under every figure, in addition, to being already represented in the axes.

For the sake of calculations, a week is considered to be between the first feeding on Monday until the feeding on the next following Monday. However, the normal operation period is considered to start on August 2nd at 00:00h.

6.1. Operation Schedule

The operation of the reactor started by evaluating the performance of the equipment installed, which consisted of evaluating pumping and temperature stability. For that, between 01th and 23rd of June (week 1 to 3), the reactor was filled with water and the recirculation pump was set to operate at a flow rate of 200 L/h.

After the 20 days, the reactor was loaded with approximated 70 L of concentrate primary sludge on the 23rd of June and set to operate without feeding during the period until the 1st of July (week 4 to 5). The flow rate during this period was set to be 100 L/h and the heating system was adjusted to maintain the same temperatures conditions as before. After ten days of observations, a daily fed started to be conducted.

To verify the initial response of the system to the feeding and to set the ideal feeding procedure for the rest of the work, an initial 10 L of excess sludge was daily fed for 5 days. The initial feeding period was from the 1st to 27th of July (week 5 to 9) and feeding proceeded daily on workdays (five times a week). No measurements or analyses from the input and output were done during this step.

In the subsequent period, the reactor response to a measured amount of solids fed was evaluated for mixtures of excess and primary sludge fetch daily and stored at 6°C. From the 27th of July to the 10th of September (week 9 to 15), the digester was fed also once a day, 5 days a week. After this period, the reactor was fed 27 days straight with 10 L of PS until the 9th of October (week 16 to 19).

The last stage consisted of feeding with increasing volumes, but with similar amounts of PS. During the three last weeks of the experiment (week 20 to 22), an amount of 20, 30, and 60 L of a mixture of water and primary sludge were fed daily for 6 days a week, one week each. The feeding schedule is displayed in Table 2.

Table 2 – Feeding schedule, feeding mixture fractions, and composition.

Week	*Period*	*Volume (L)*	*PS (L)*	*ES (L)*	*Water (L)*	*Days Fed*	*Daily Fetched*
5	01/07/2021 – 04/07/2021	10	0	10	0	2	Yes
6	05/07/2021 – 11/07/2021	10	5	5	0	3	Yes
7	12/07/2021 – 18/07/2021	10	5	5	0	5	Yes
8	19/07/2021 – 25/07/2021	10	5	5	0	5	Yes
9	26/07/2021 – 01/08/2021	10	5	5	0	5	Yes
10	02/08/2021 – 08/08/2021	10	5	5	0	5	Yes
11	09/08/2021 – 15/08/2021	10	5	5	0	5	Yes
12	16/08/2021 – 22/08/2021	10	8	2	0	5	Yes
13	23/08/2021 – 29/08/2021	10	5	5	0	5	No
14	30/08/2021 – 05/09/2021	10	10	0	0	5	No
15	06/09/2021 – 12/09/2021	10	10	0	0	5	No
16	13/09/2021 – 19/09/2021	10	10	0	0	7	No
17	20/09/2021 – 26/09/2021	10	10	0	0	7	No
18	27/09/2021 – 03/10/2021	10	10	0	0	7	No
19	04/10/2021 – 10/10/2021	10	10	0	0	6	No
20	11/10/2021 – 17/10/2021	20	10	0	10	6	No
21	18/10/2021 – 24/10/2021	30	12	0	18	6	No
22	25/10/2021 – 31/10/2021	60	12	0	48	6	No

Besides temperature and flow rate, not all parameters were analyzed during the whole period. Gas production could only be measured after the 1st of July due to the misconfiguration of the data log. Total solids and COD of the input and output, however, were only required to be measured after both a stable operation and adequate feeding procedure were achieved, which led to analyzes being done after the 27th of July. On the other hand, total solids started to be conducted on the 28th of June.

Due to human failure, organic dry matter (ODM) analyzes were only done after the 26th of August, however, unknown values could be calculated with reasonable precision. Methane and carbon dioxide concentration in the biogas started to be measured on the 27th of September when gas analyzers were installed. Filtrate matter of the output was first conducted on the 18th of October after floatable solids had been detected at the output,

6.2. Startup and Initial Operation

During this step, only the equipment stability and the initial response of the reactor were evaluated. After filling it with water and setting the pump to operate at 200 L/h on the 1st of June, the system developed a stable operation for two weeks, regarding temperature and flow rate.

Without any adjustments, the flow rate decayed from 1st until 19th of June, when a sudden stop was observed due to a power failure. Temperatures behaved equally stable during this first period, only dropping due to the heating system being mistakenly disconnected from a power source on June 17th. Besides that, temperatures oscillated between 35,4°C and 38,0°C, being the point D the lowest, approximately 0,4°C below the average, as shown by Figure 15.

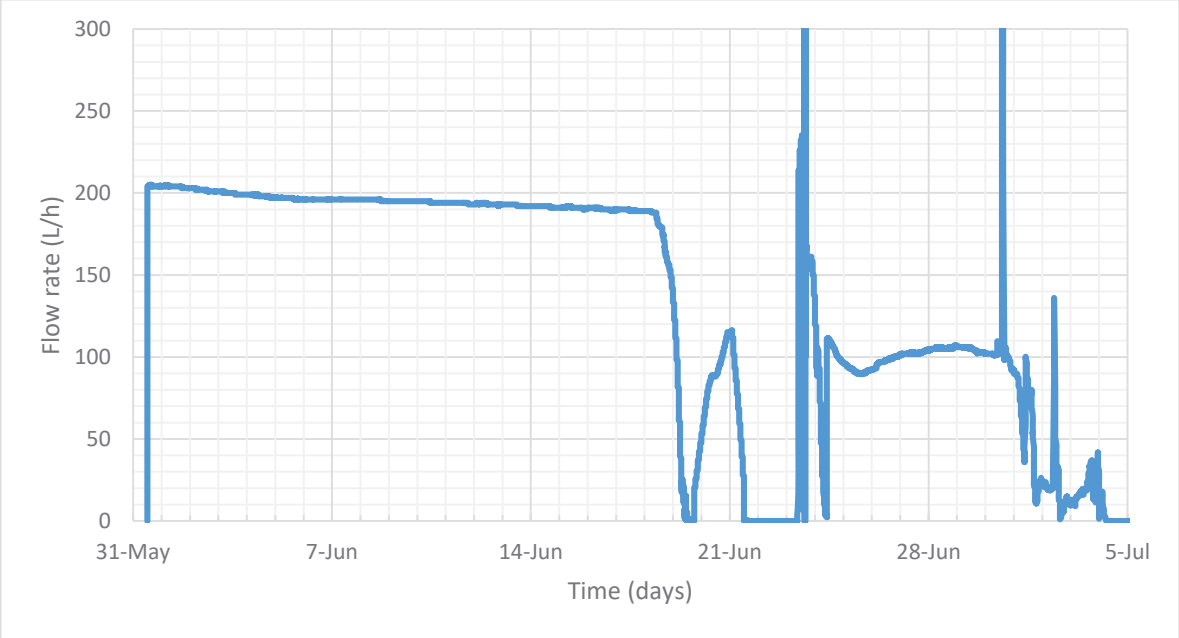

Figure 15 – Circulation flow rate between May 31st and July 7th.

The reactor took 7 hours to cool down to ambient temperatures after being disconnected, decaying 1,8°C/h until the reestablishment of temperatures 16h after reconnection. Afterward, temperatures were stable and kept around 35°C, with points A and B registering consistently temperatures 0,7°C lower on average.

Even with this problem, the reactor was filled with approximately 70 L of concentrated PS at a high flow rate, which resulted in a flow rate spike on the 23rd of June. After finishing the procedure, the pump was set to operate at 200 L/h but failed to maintain the flow. After resetting it to 100 L/h on the following day, the pump operation happened without any major issues until the 1st of July.

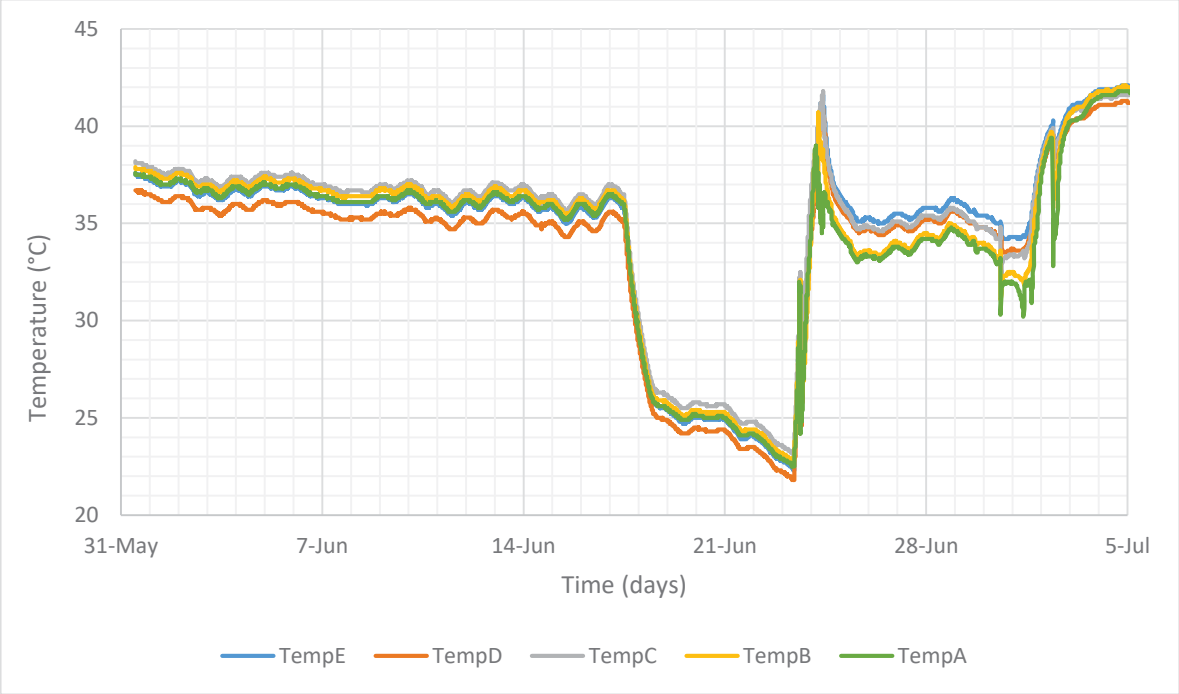

Figure 16 – Temperature profile between May 31st and July 7th.

On the 30th of June, the pump operated close to the maximum capacity for 30 min, leading to a second spike, as shown in Figure 16. This resulted in a temperature drop of approximately 3°C at all measurement points, which suggested a considerable heat loss in the hoses connecting the pump to the reactor.

After a week of stabilization, the digester was first fed on the 1st of July, every workday, once a day During the first two days of feeding, the pump showed great instabilities, with several flow rate drops and a total of five failures in July. Drops were greater on the two first days of feeding when two failures took place. Due to these observations, feeding on the 5th and 6th of June was canceled, which led to a stable flow rate during these days.

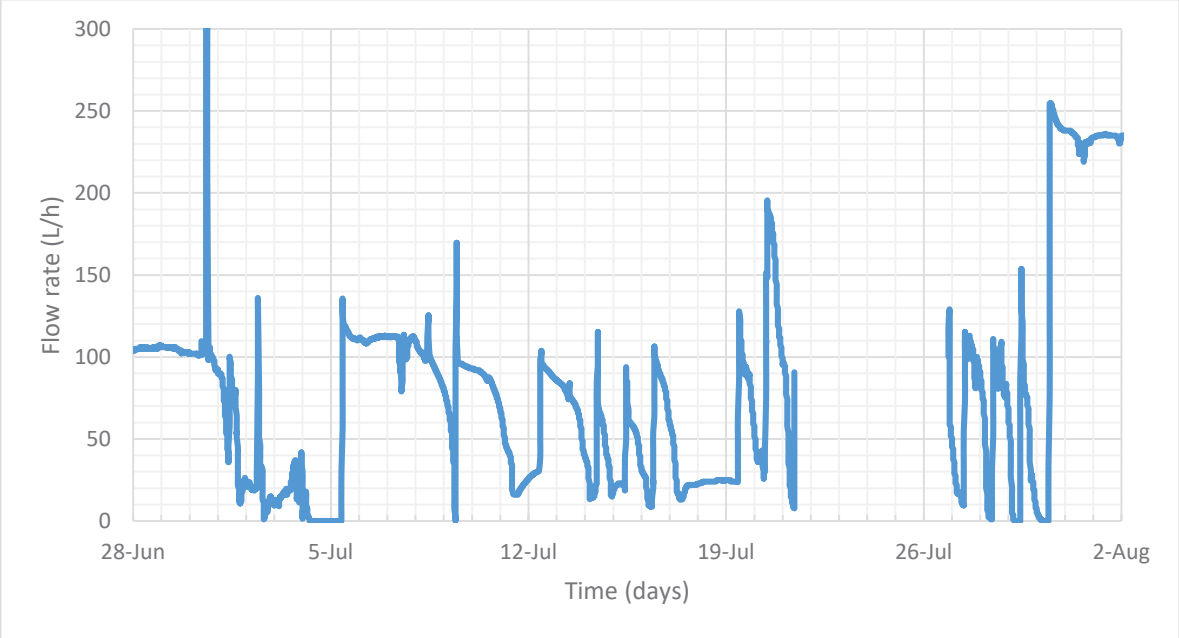

Figure 17 – Circulation flow rate between June 28th and August 2nd.

Drops were verified every day after feeding the digester, even when the pump was set to operate at 200 L/h. Tests with higher rates were conducted between the 20th and 23rd of July, which showed similar results to what was observed previously[2]. After this period, the pump was set to operate at 100 L/h, which resulted in the same flow pattern, as shown by Figure 17. Following this, as the problem with the pump persisted, the pump stator was replaced on the 30th of July.

As shown by Figure 18, flow oscillations were also followed by an equivalent temperature instability. Averages temperatures slowly increased as the flow rate decreased, repeating the pattern on every day of the period. When the flow was reestablished to 100 L/h, temperatures decreased on average by 1,5°C in 30 minutes, going back to the previous value while the flow rate decayed.

In addition, temperatures were higher than 40°C at all measurement points between the 1st and 5th of July during a pump failure episode. However, on the 18th and 19th of July, these temperature levels were reached only at C, D, and E, as points A and B had lower values. These differences were also verified in the rate at

[2] Data from the period between 21st and 27th of July are unavailable due to problems with the data log.

which temperatures decay after an increase in flow rate. Points A and B dropped faster as others only felt these disturbances later.

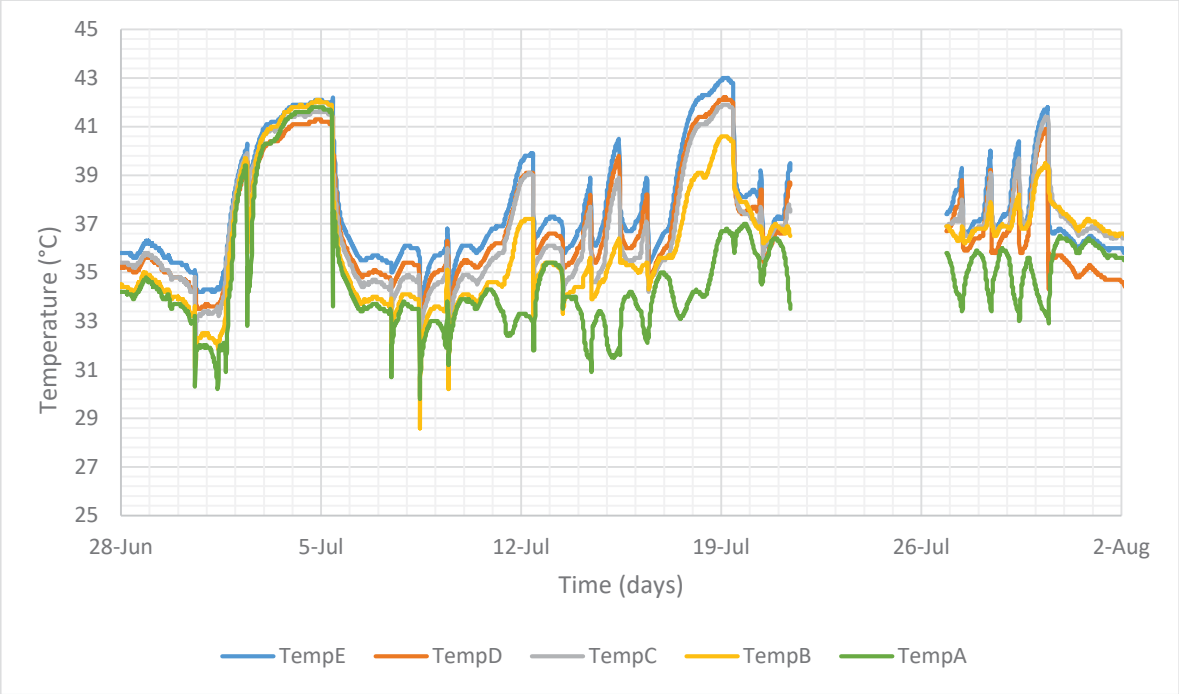

Figure 18 – Temperature profile between June 28th and August 2nd.

To evaluate solids transport inside the reactor, an experiment with control particles was conducted. A 50 g pulse of particles with a density between 1,1 and 1,3 kg/L was injected into the reactor during the water recirculation. This showed that the majority of particles were deposited in the bottom of the reactor near the input and stuck on the reactor's floor. This made it impossible to detect particles on the output and, then, plot the residence time distribution. Hence, the transport was evaluated after filling the reactor with sludge by measuring total solids from points 12 to 16 (see Figure 10).

Starting from one week after filling the digester, each sampling point was measured weekly. During the first measurements, points closer to the input (12,13, and 14) had a considerably higher TDM than further ones (15 and 16). TDM values were below 2,00% at 16 until 29th of July, reaching a level close to early points only on 11th of August, being similar to 12, which reached to other points on 11th August. The TDM profile for the period between 28th of June and 26th of October is shown in Figure 19.

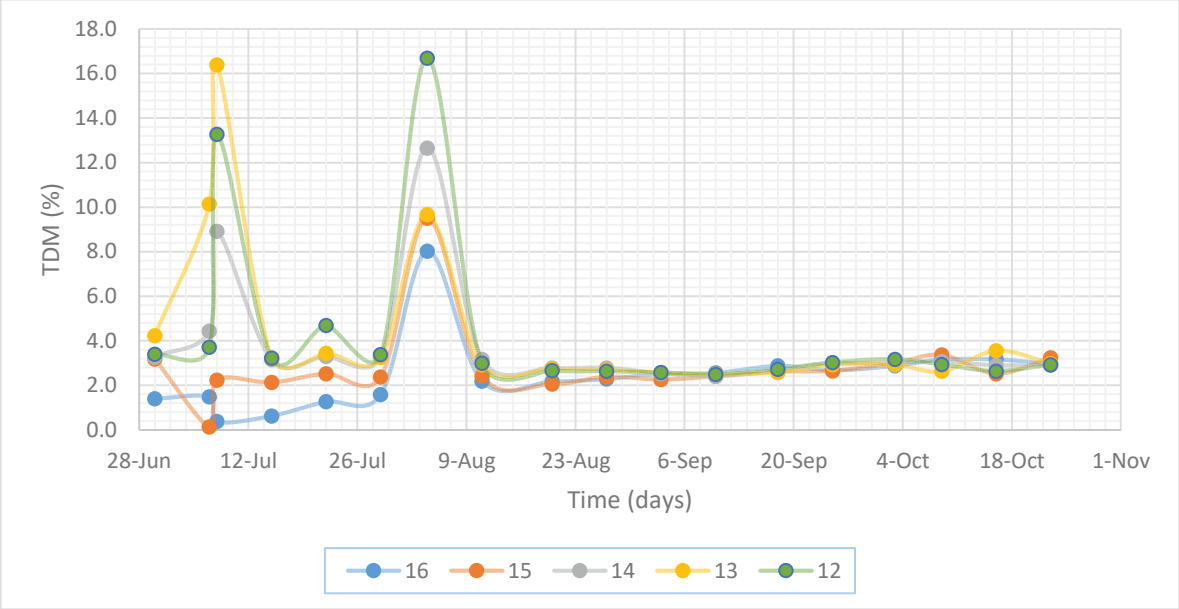

Figure 19 – Total dry matter at substrate`s collection points

TDM spikes were observed twice during experiments and were due to insufficient time in the drying oven. Even though the original method consisted of keeping samples 24h in the drying oven, it was found that this time was not sufficient for reliably drying them. Samples collected on the 11th of August were weighted three times on three consecutive days. With that, it was concluded that after 48h the final sample mass was constant. Therefore, samples were drought in the drying oven over the weekend for the following measurements.

TDM in the recycle current was also measured during the period. Except for the two first measurements, on the 30th of June and 7th of July, the total dry matter was 0,50%, as shown by Figure 20. Higher values observed during the two first measurements were associated with the sampling method. Sample collection was conducted after reestablishing the pump from a failure episode, which could have allowed elements blocking the pump to be collected, increasing the TDM. This fact is outside of normal operation conditions, so this measurement should not be considered in further discussion.

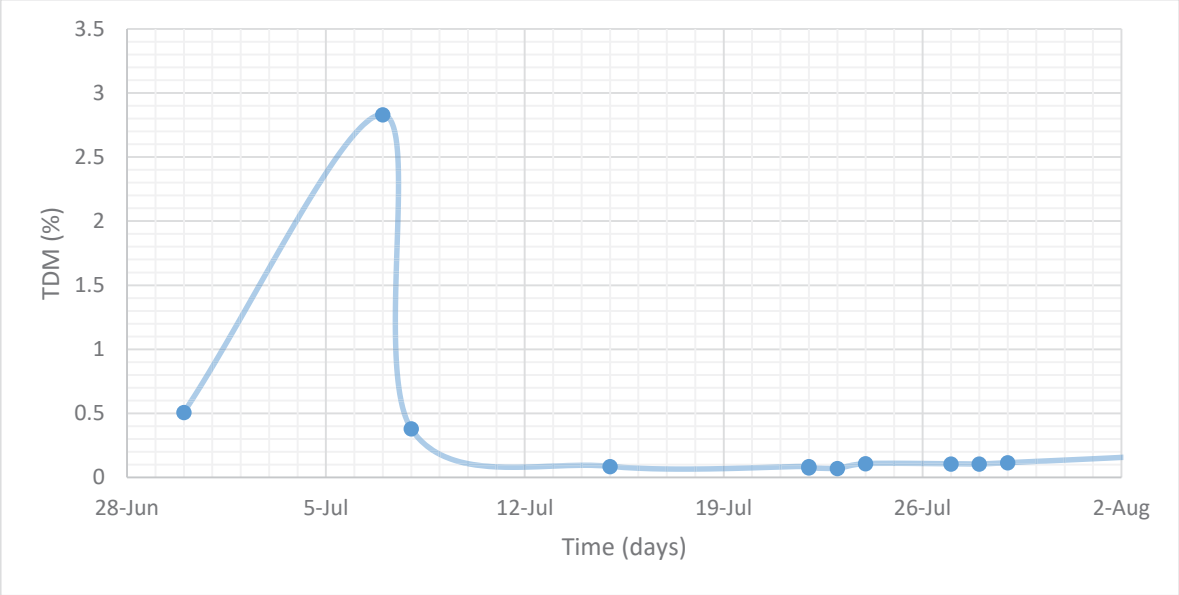

Figure 20 – Organic dry matter in the recirculation between June 28th and August 2nd.

Moreover, relatively small gas production was also verified during the period. After the gas clock had been correctly set for measurements, a gas production below 1 L/h started to be detected, as shown by Figure 21. However, due to the equipment specifications, variations during this period cannot be fully trusted. The used gas clock is designed to measure a gas flow within 1 and 60 L/h. making the measurements for this period not trustworthy. Even not being possible to accurately quantify values below 1 L/h, it was possible to detect if gas had been being produced.

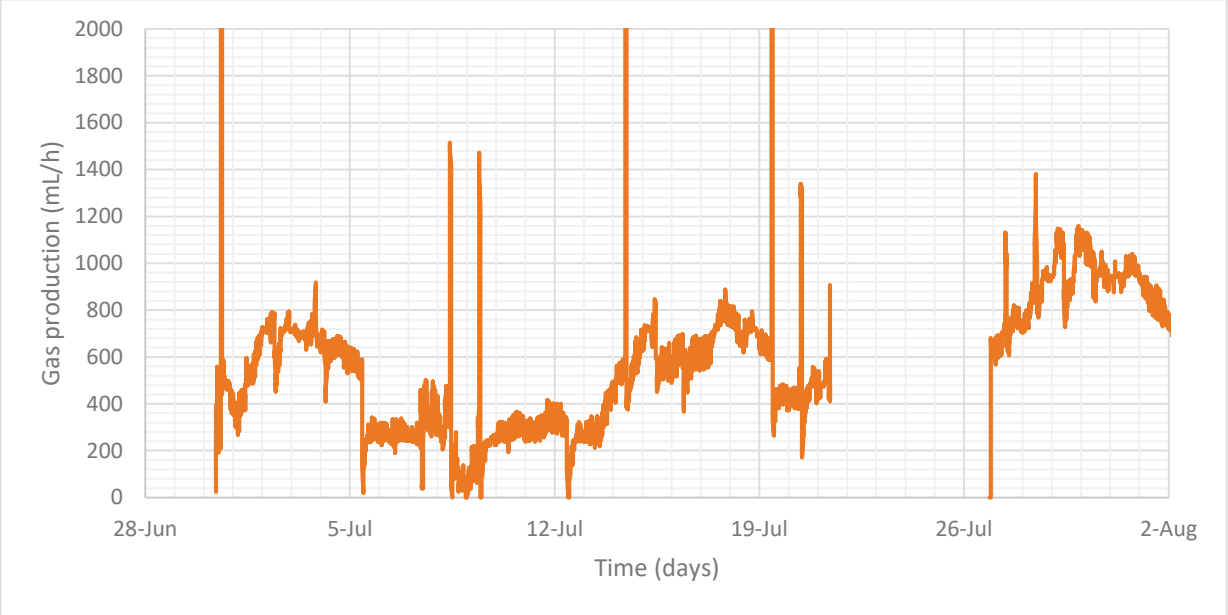

Figure 21 – Gas production profile between June 28th and August 2nd.

Spikes in data production were observed eight times in July during feeding procedures. Those spikes were caused by air infiltrating into the reactor by the feeding hose, resulting in bubbles being pumped into the system with the sludge. With that, measurements of an extra amount of gas in addition to the gas produced were observed. This effect was seen during the following periods and it can be also noticed in measurements of methane and carbon dioxide concentration in October.

6.3. Normal Operation

In this section, the results of the reactor operation between the 27th of July and the 1st of November, 2021, are shown.

6.3.1. Flow rate, temperature, and recirculation control

The temperature was controlled to be operating around 35°C. Due to the design of the heating system, a homogenous temperature could not be achieved. In addition, equipment failed twice during operation, both between the 10th and 12th of August, as shown by Figure 22. Following these failures, temperature levels dropped

to ambient conditions, down to 23°C on both days, with an average rate of 1,8°C/h. This failure was a product of mismanagement of the equipment, which lead the water in the thermal bath to be insufficient, causing the equipment to shut down automatically.

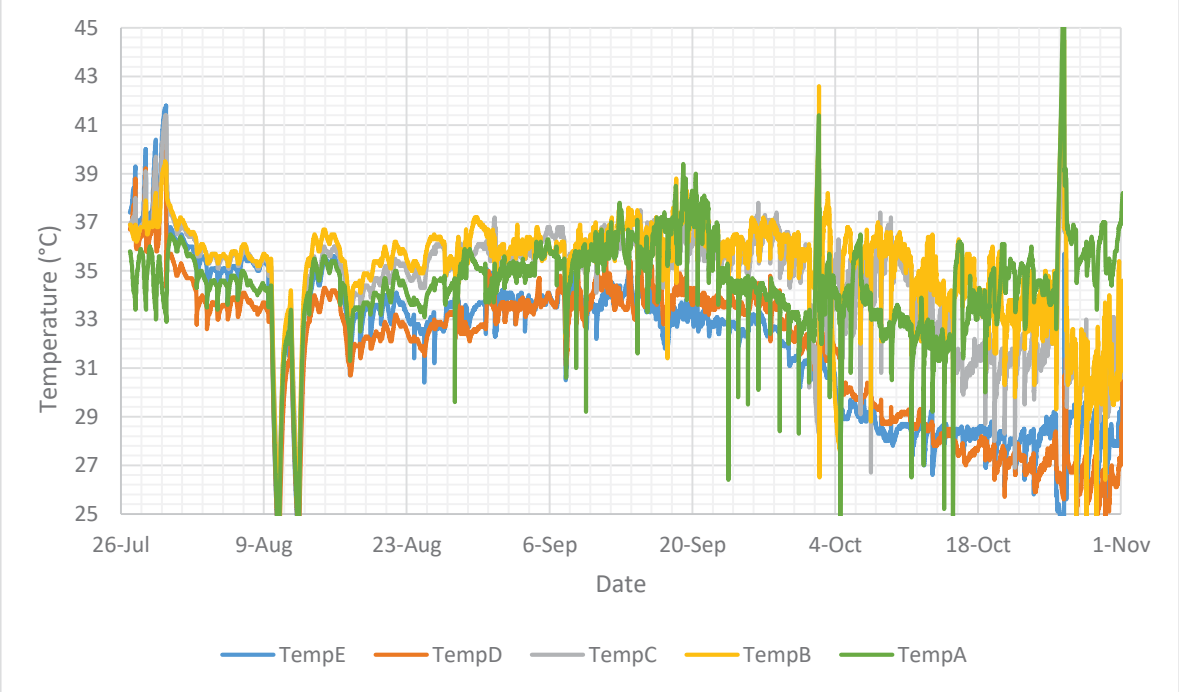

Figure 22 – Temperature profile between July 26th and November 1st.

Between the 13th of August and the 22nd of September, the average temperature in the reactor was kept stable at an average of 34,7°C with a standard deviation between measurement points of 1,3°C. During this period, temperatures measured at B and C were higher than other points, but differences to other points did not differ more than 3%. After September 22nd, temperatures at E and D started to drop continuously from an average of 33,6°C and 33,3°C to 28,2°C and 27,8°C at the end of October. Points C and B had a smaller drop in temperature during the period, with an average temperature decay of 2,2°C from September until the last week of October, as shown by Figure 24.

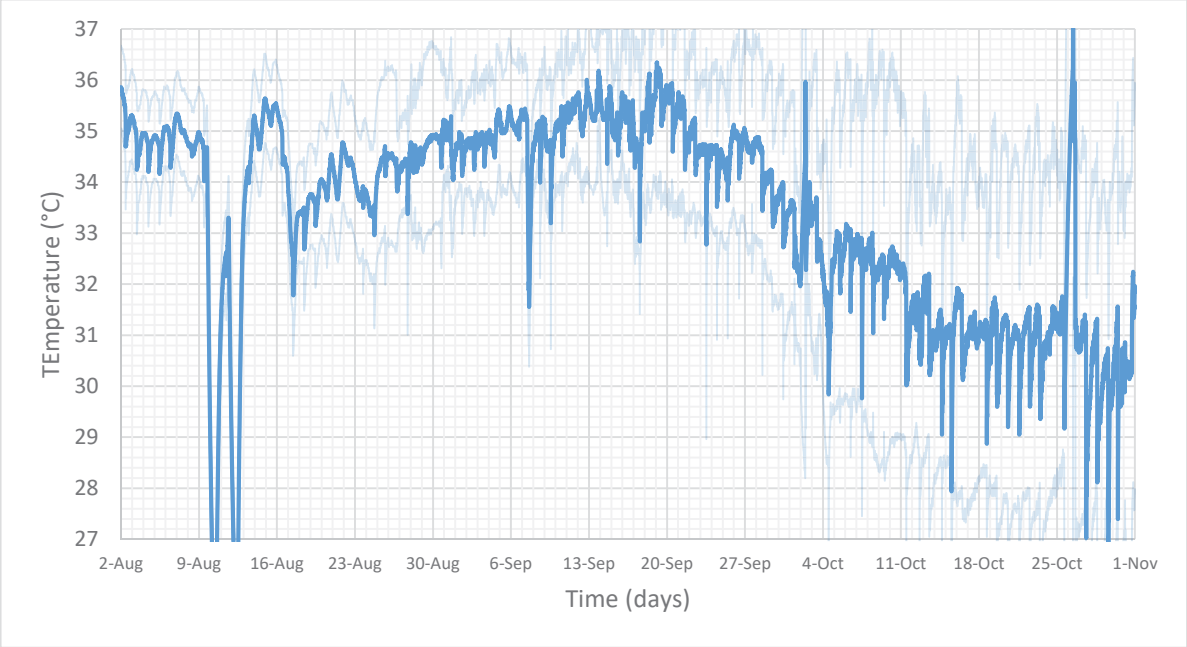

Figure 23 - Average reactor temperature and standard deviation between August 2nd and November 1st.

Great variations at B and C in the second half of October were also observed. Those were due to adjustments in the heating system to balance the heat exchange inefficiency in the last two sections of the reactor. For that, the hot water flow in the first section was reduced to increase its availability in other ones. However, this did not increase the flow rate at D and E, but only at B and C, leading to a sudden increase in temperature in these sections. After applying several configurations of valve openings, no effective one could be found. Moreover, the spike in temperature on the 26th of October (48°C for 30 min), was due to one of the tested configurations of the heating system.

Daily drops in temperatures observed at A and, to a certain extent, at B happened during the feeding procedure. After the 23rd of August, sludge started to be fetched and cooled down for storage twice a week. This made the feeding mixture have a low temperature, around 5-7°C, which, when fed, greatly reduced the temperature in the first section. However, the impact was not propagated to other ones, as cooled volumes were heated along the course. In addition, it was found that the time required for the mixture to achieve ambient temperatures was too long.

Moreover, the addition of water into the mixture did not act to mitigate this effect, as the water available in loco was as cold as the stored sludge.

The temperature reduction after the feeding can be seen in Figure 24, which displays the average temperature profile during days without any failures in the heating or pumping system. On average, temperatures drop 1,5°C during feeding at A through C, but only 0,5°C on D and E. The recovery of temperatures took on average 12 h to be fully achieved in all points, being constant afterward. The reduction observed towards the end of the 24 h is due to statistical error, as some days had an interval between feeding below 24h.

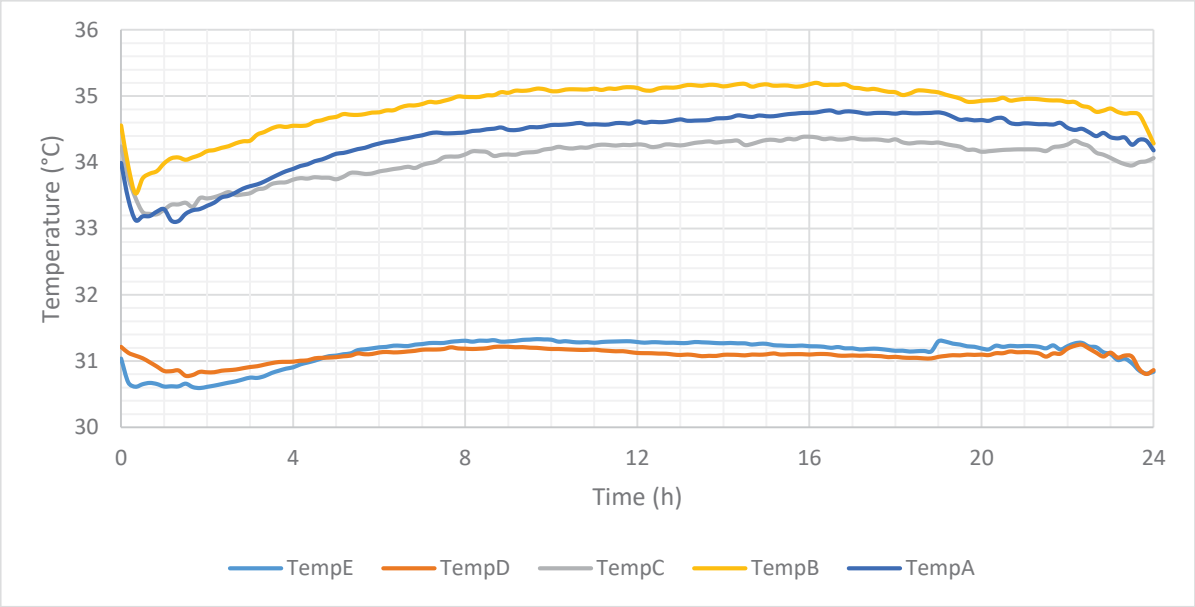

Figure 24 – 24h average temperature profile after feeding between August 2nd and November 1st.

The recirculation during the period was set to operate at 220 L/h, but it showed an average of 197,8 L/h, as seen in Figure 25. Due to the configuration of the data log, only positive values of flow rate are shown for week 14, although the flow direction was reversed. During the period, only one failure episode was observed in the pumping system, on October 25th, which was caused by the presence of leaves mixed in the primary sludge. Besides that, drops in flow rate happened daily due to the feeding procedure required to be done at a low flow rate for safety and practical reasons. Then, after reestablishing the flow rate to 200 L/h,

a continuous decrease was observed for 2h, forcing the pump to be adjusted a second time after 2h of the procedure.

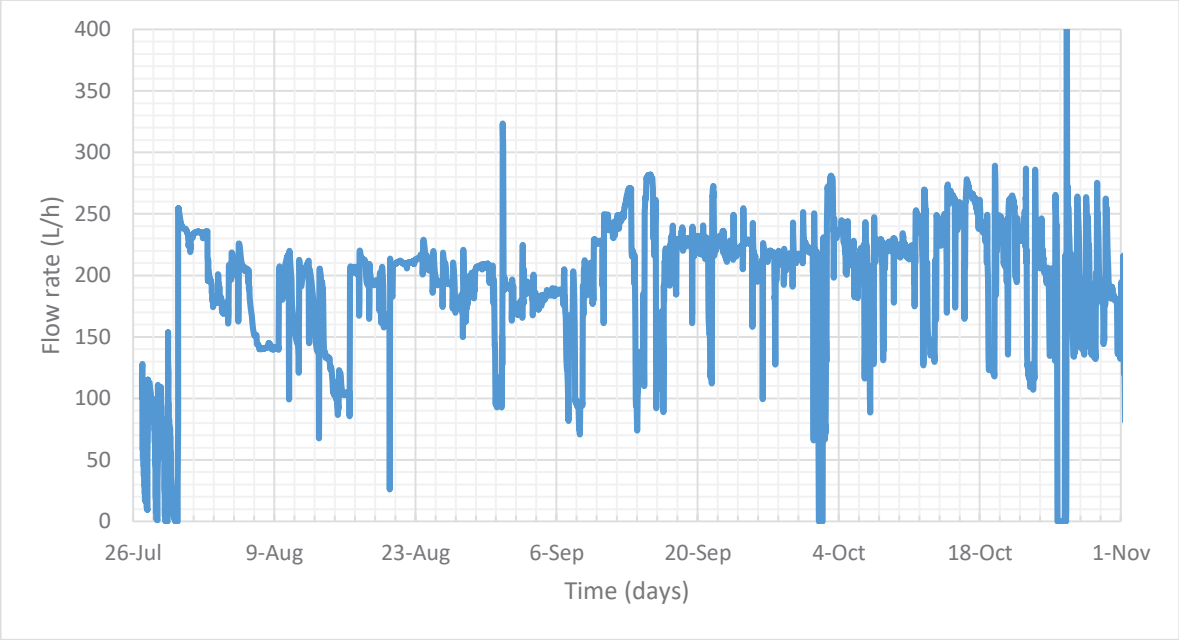

Figure 25 – Circulation flow rate between July 26th and November 1st.

Moreover, higher flow rates were a result of experiments that aimed to set the pumping system to 200 L/h without the need to readjust the pump. The adjustment was done by setting the initial flow rate to a higher level to induce the velocity decay to a stable one around the desired value. Steep drops during the period were all related to the necessity for reduction and, often, interruption of the flow while feeding. These effects were more noticeable during the last three weeks of experiments, between October 11th and 31st when the feeding procedure took longer than other periods and stoppages were more often.

On days which no pumping failures happened, the average flow rate behaved without any major drops, as shown by the examples in Figure 26. On average, flow rate developed within a 50 L/h range around the set value, with a tendency of slightly reducing over time. Besides drops, flow recoveries without any intervention occurred often, but in most cases, it was only observed after manual adjustment of the pump. In the case of October 30th, shown in Figure 26, two automatic recoveries of flow drop happened as a result of more dense matter being

flushed out of the hoses, reducing friction and pressure drops and, thus, increasing the flow rate.

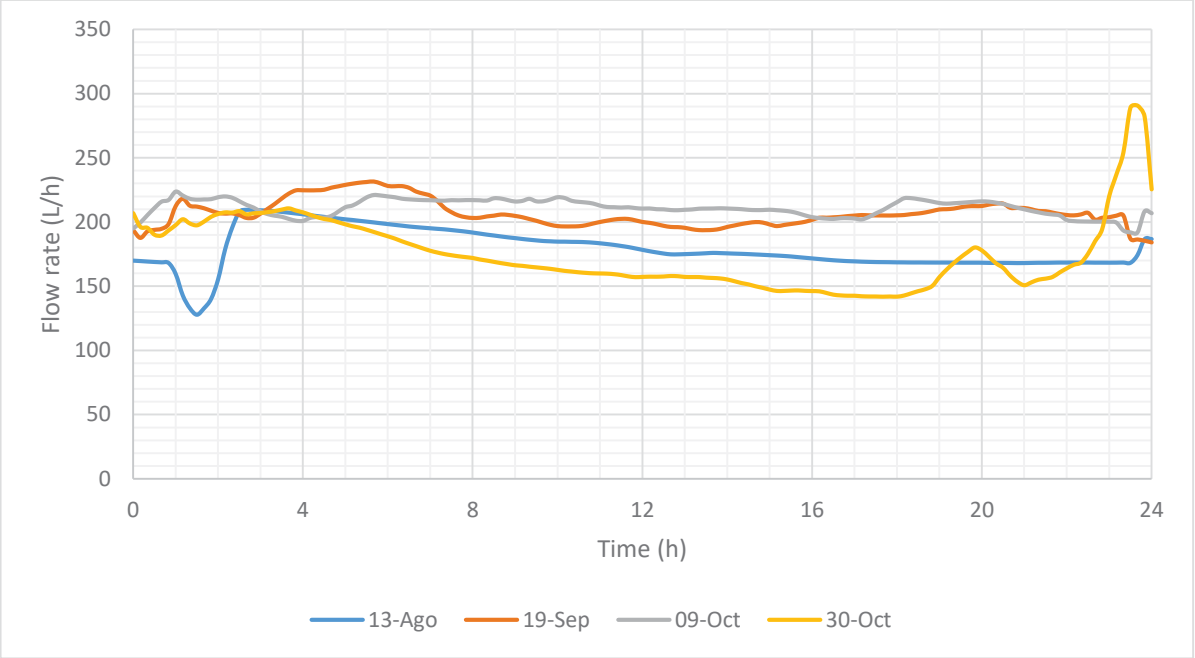

Figure 26 – 24h flow rate profile after feeding on August 13th, September 19th, and October 9th and 30th.

With that, HRT could only be accurately defined after the 2nd of August. As shown by Figure 27, HRT had variations above 3h between July 26th and August 2nd, which were solo related to the instability of the pumping system. After this period, HRT was more stable, having an average of 1h and 15min (1,25h) with a standard deviation of 23min (0,38h). Moreover, HRT was higher than 8h for less than 20h and was lower than 30 min for less than 2h.

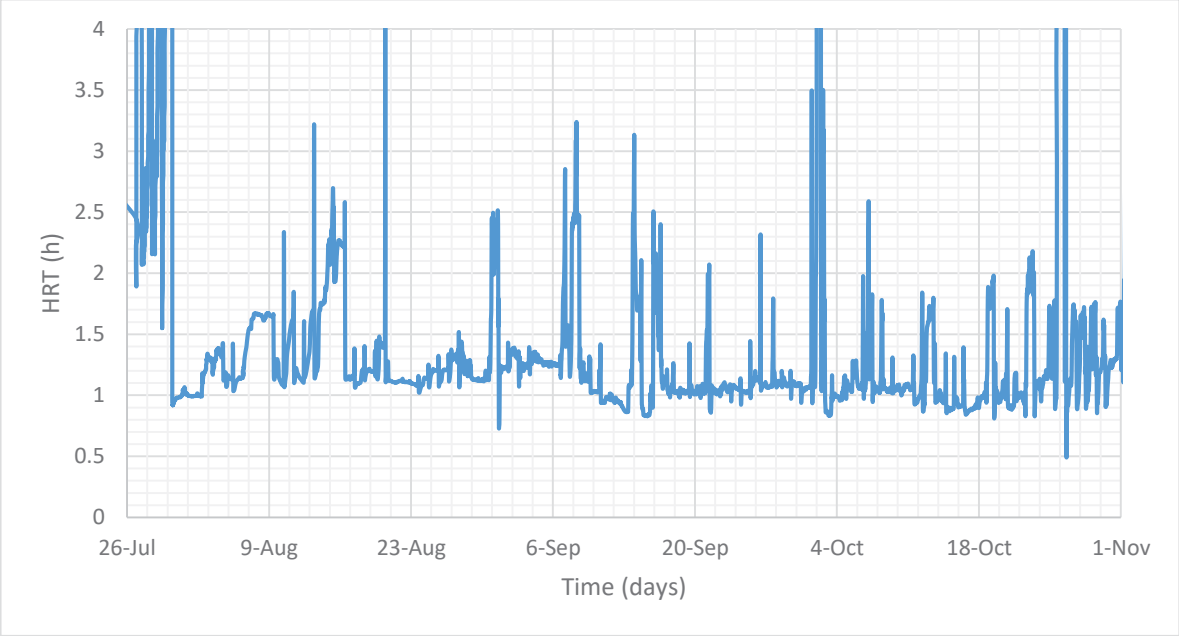

Figure 27 – Hydraulic retention time between July 26th and November 1st.

As shown by Figure 19, TDM in the substrate was virtually constant during normal operation, even with a higher flow rate and organic loads. However, it was observed an overall higher solids concentration in the recycle current, as seen in Figure 28. ODM was measured weekly during the first four weeks of normal operation, showing increasing values over time, from a minimum of 0,18% on August 4th to 0,81% on August 20th.

Starting on September 1st and onwards, samples were taken daily approximately an hour after the feeding procedure was complete. Different from weekly sampling, daily samples showed an unstable behavior in TDM. Values greatly oscillated between days, which is shown by the relative standard deviation of 53,5% between the 1st and 23rd of September. Then, to check if the sampling method was inadequate, recycled samples started to be taken before the feeding procedure.

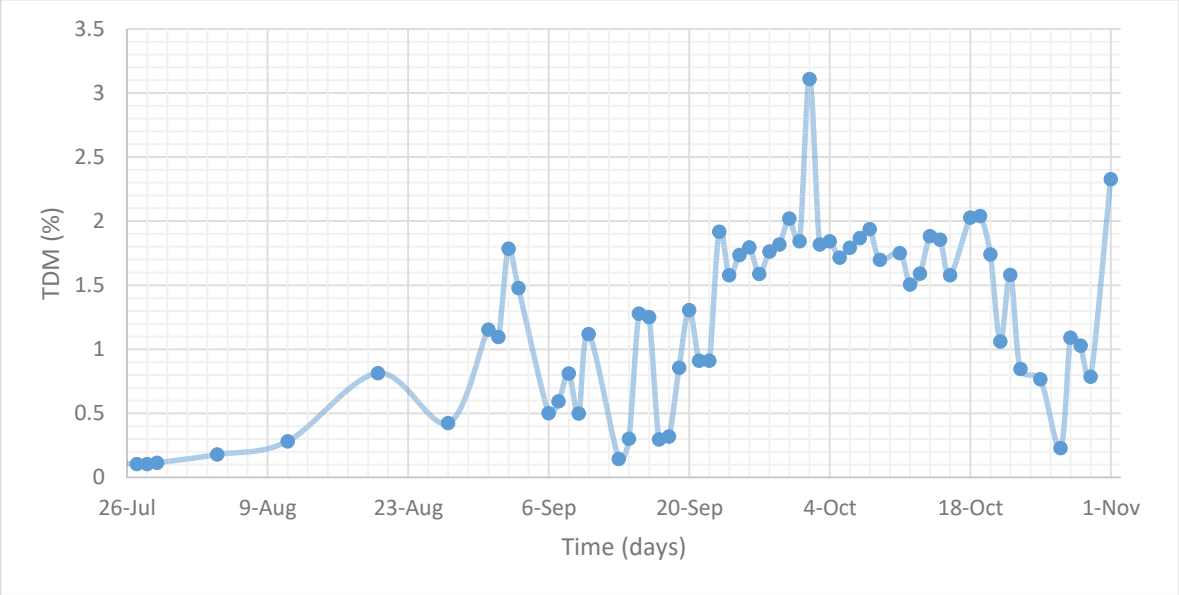

Figure 28 – Total dry matter in the recirculation between July 26th and November 1st.

With changes in the sampling procedure on September 23rd, recirculation samples showed higher and more stable TDM overall. Between September 23rd and October 19th, the average TDM value in the recycle current was 1,84±0,30%, which was 115% higher in comparison to the previous 15 days (0,86±0,46%). The spike in TDM observed on October 2nd was due to sampling immediately after the reestablishment of the flow rate, which was necessary because of a pump failure. Therefore, the failure observed on that day could be associated with a sudden increase in solids in the recirculation, causing a blockade inside the pump.

The period after the 19th of October showed significant TDM drops in the recirculation, which were followed by quick recoveries. Values dropped from 2,04% on October 19th to 0,23% on October 27th, increasing on the following days, when it reached 2,33% on November 1st. This was related to the presence of leaves mixed within the feeding material, which led to random drops in flow rates, affecting the transport of particles. The minimum on October 27th, however, was also related to great disturbances as a result of the replacement of the hose connecting valve 4 to the pump for a larger one on the 26th of October. With a larger hose and after the leaves were degraded inside the reactor, the amount of solids in the recycle increased to a similar level than what was observed previously.

6.3.2. COD, total and organic dry matter relationship

Between the 2nd and 25th of August, ODM was not measured both in the output and input, but only TDM. For that reason, values of ODM were estimated by developing a relationship between those parameters when both were measured.

Firstly, TDM and ODM for the input and output were plotted in two different graphs regardless of the measurement period, this is shown in Figure 29 and Figure 30. In both cases, a linear correlation can be observed, which could be confirmed by adjusting the data by a polynomial of the first order. With that, ODM could be written as a function of TDM by a linear expression, as the values of R^2 were 0,9932 for the input and 0,8959 for the output. The expressions adjusted to the data can be seen in Figure 29 and Figure 30, in all following figures ODM and TDM are expressed in fraction and not in percentage.

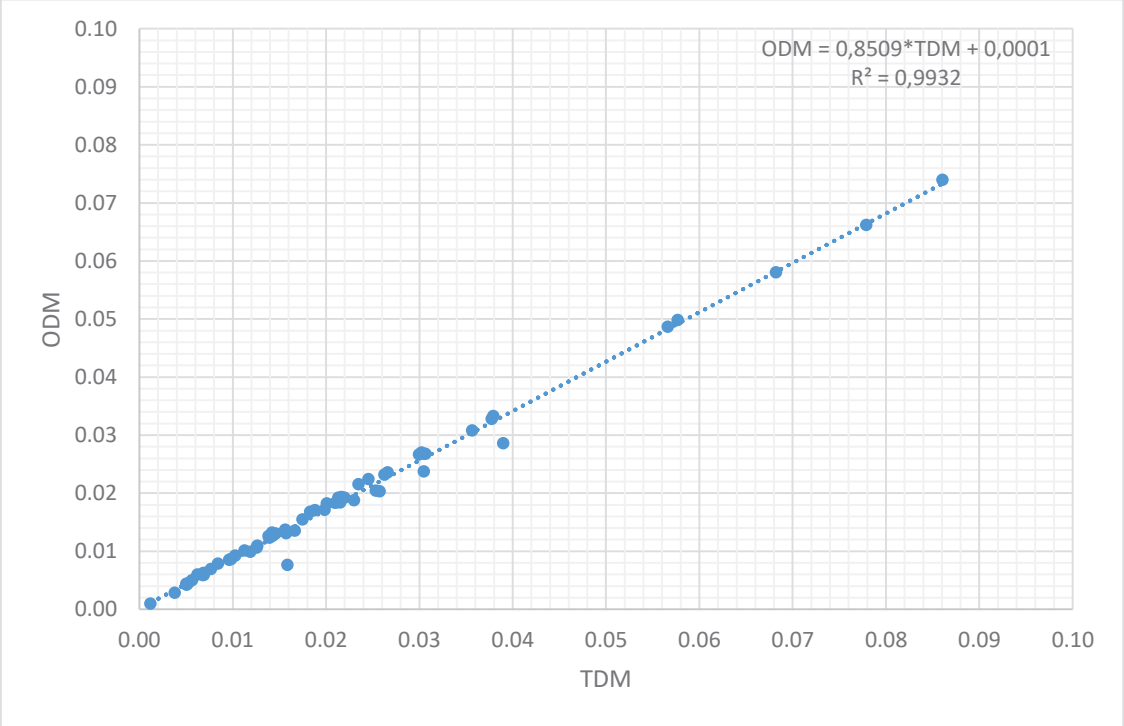

Figure 29 – Organic dry matter as a function of total dry matter in the input.

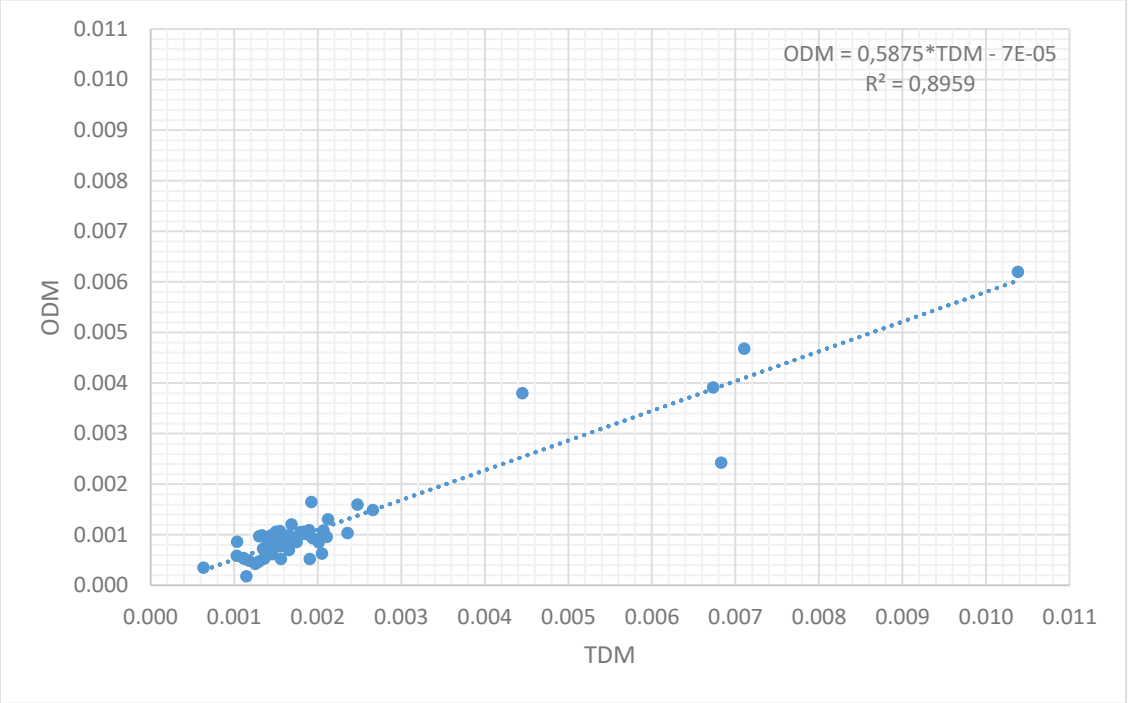

Figure 30 – Organic dry matter as a function of total dry matter in the output.

Due to the high values of R^2, an individualized analysis for the ODM/TDM relationship for a period was found to be unnecessary. At the output, only higher values of TDM/ODM distanced themselves from the linear approximation, which did not impact the estimation, once all estimated values were below 0,1%.

COD in the input showed a linear relationship to TDM during the whole period with an R^2 of 0,9552, as shown in Figure 31. However, the linear relation showed an intersection to the y-axis at the point (0; -2130) and the x-axis at (0,0015;0). This means that estimated COD for mixtures with TDM below 0,15% would have negative values. If the intersection at (0;0) is set, R^2 value decreases to 0,9517.

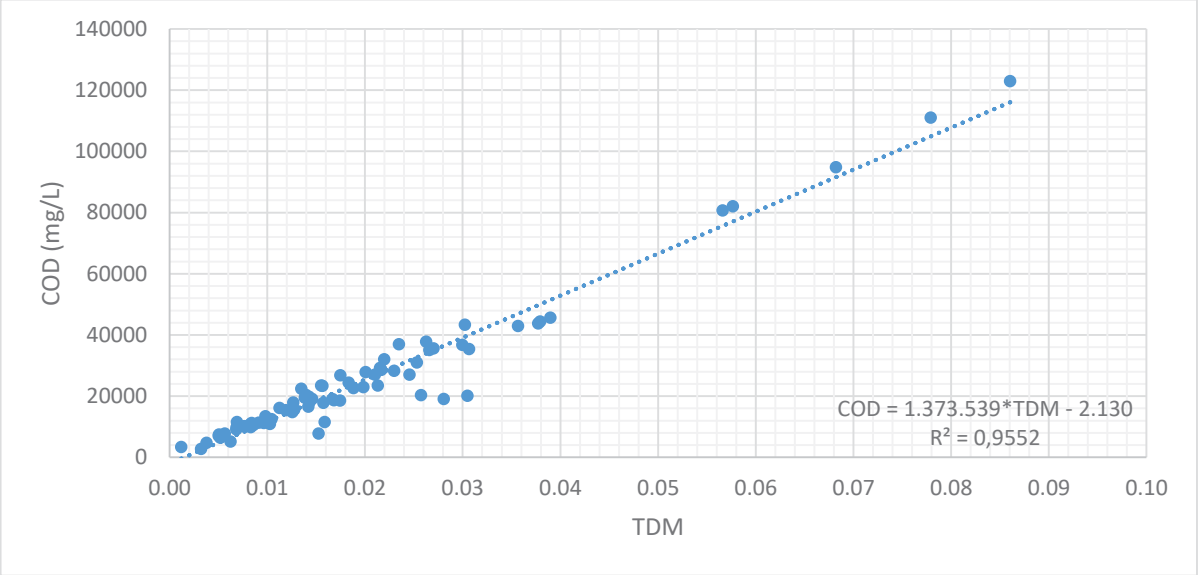

Figure 31 – Chemical oxygen demand as a function of total dry matter in the input

In contradiction to what was observed in the input, a generic relationship between COD and TDM with an R^2 above 0,5 could not be found for the output. This is associated with the presence of outliers, which showed values of COD above 2500 mg/L and/or TDM above 0,40%. Removing outliers improved R^2 values, but the value achieved was 0,4093, but an increasing trend could be identified, as shown by Figure 32. Analyzing different feeding schedules individually did yield a better result.

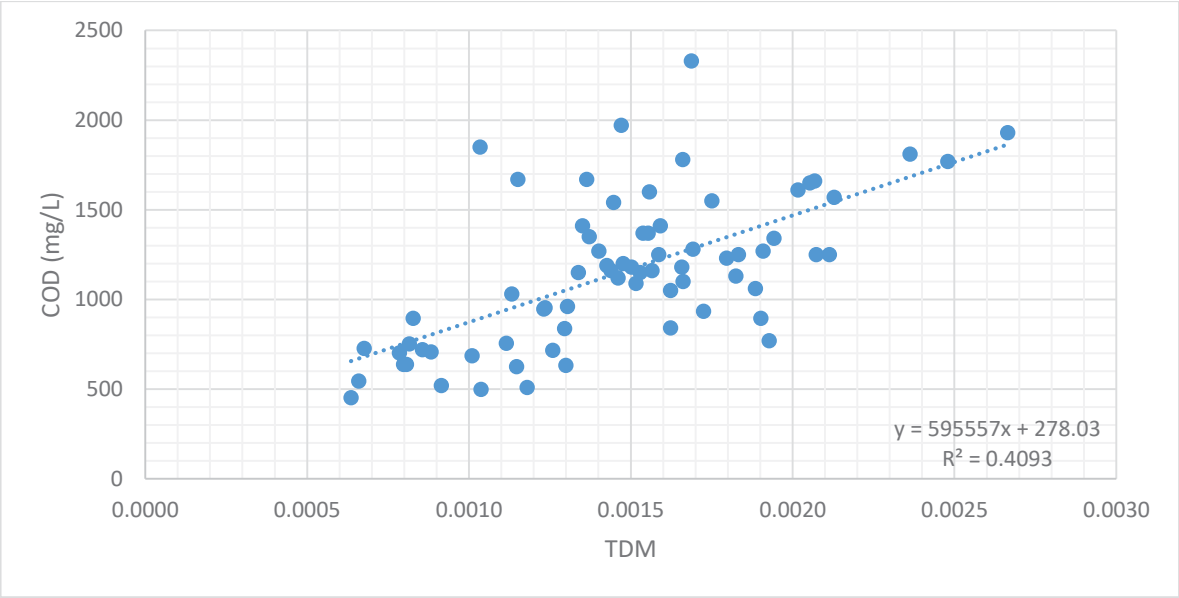

Figure 32 – Chemical oxygen demand as a function of total dry matter in the output

6.3.3. Five-days feed regime

During the period between the 28th of July until 13th of September (weeks 9 to 15), sludge was fed into the reactor once a day five times a week. Rates of water, primary, and excess sludge used during the period are shown in Table 2.

Even with a controllable volume of primary and excess sludge in the feed, the composition of the feeding mixture did vary along the period. Especially between August 2nd and 23rd (weeks 10 to 12), when sludge was fetched daily during mornings, measurements of TDM, ODM, and COD oscillated outside the range of 50% of the average. Values for all parameters vary up to 60% between days, leading to high standard deviations as shown by Table 3. As a result, average TDM, ODM, and COD were at the lowest in week 12, when it was fed 8 L of primary sludge. This was in contradiction to weeks 11 and 13, when only 5 L were fed and had higher values overall.

Table 3 – Total dry matter, Organic dry matter, Chemical oxygen demand in the input and output during weeks 10 through 15.

Week	Input			Output		
	TDM (%)	ODM (%)	COD (mg/L)	TDM (%)	ODM (%)	COD (mg/L)
10	1,09 ± 0,57	0,93 ± 0,48	10306 ± 5843	0,12 ± 0,04	0,07 ± 0,02	888 ± 194
11	1,51 ± 0,75	1,28 ± 0,64	16606 ± 4526	0,10 ± 0,02	0,06 ± 0,02	780 ± 135
12	1,22 ± 0,83	1,04 ± 0,70	15700 ± 11133	0,10 ± 0,02	0,06 ± 0,01	766 ± 169
13	1,67 ± 0,21	1,53 ± 0,25	20440 ± 2607	0,08 ± 0,02	0,04 ± 0,01	598 ± 132
14	1,52 ± 0,55	1,36 ± 0,51	18194 ± 5752	0,16 ± 0,03	0,08 ± 0,02	949 ± 304
15	1,89 ± 0,74	1,72 ± 0,66	24428 ± 11770	0,15 ± 0,03	0,10 ± 0,03	1016 ± 358
Period	1,48 ± 0,64	1,31 ± 0,53	17612 ± 8288	0,12 ± 0,04	0,08 ± 0,03	833 ± 252

Therefore, to reduce the variability of the input, after week 13, a higher amount of sludge was collected on one day and, then, stored for later use. This change greatly reduced the variability as well as consistency in the final mixture concentration, as shown by a lower standard deviation during weeks 13 to 15 and higher average TDM and ODM. TDM's Relative standard deviation in weeks 10 and

11 were 51,7% and 49,9%, respectively, as during weeks 14 and 15 the values were 36,4% and 39,4%, respectively.

ODM followed the same pattern as TDM, in which standard deviations were lower during weeks 13 through 15 in comparison to weeks 10 through 12. In addition, week 13 showed the smallest variability in input for TDM and ODM. During this week, the relative standard deviation for TDM was 12,4% and for ODM 16,5%, which is 33% of what was observed during weeks 14 and 15. Concentration values were also higher than week 14, despite week 14 having a 10 L of PS feed and week 13 only 5 L, which is reflected by a higher quality sludge as shown in Table 4.

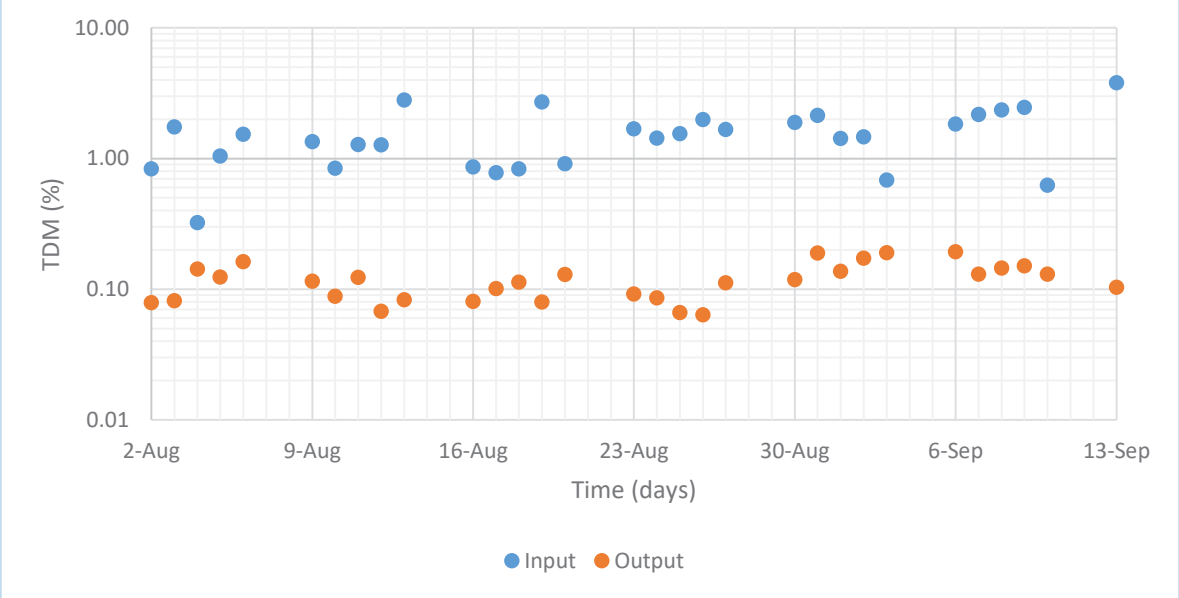

Figure 33 – Total dry matter in the input and output between August 2nd and September 13th.

It is important to point that ODM values between August 2nd and 25th were calculated by the average input and output TDM/ODM relationship calculated in section 6.3.2. Due to a linear correlation was used, the trend observed in both Figure 33 and Figure 34 are the same, but ODM values are on average 85,9% lower than TDM's during the period. Nevertheless, this similar trend was also verified during the following weeks, which supports the high R^2 for input and output relationship.

Moreover, TDM and ODM during week 14 had two sequences of two days with constant values as sludge was collected on Friday of the previous week and Wednesday. As PS was not sufficient for the feed on Friday, PS was also fetched

on that day, which led to a lower quality sludge with a TDM of 0,68%. This was similar to what was done during week 13 when sludge was collected on Monday and used until Thursday with higher TDM and ODM, but fetching on Friday led to a bad quality input, as shown by Figure 33 and Figure 34.

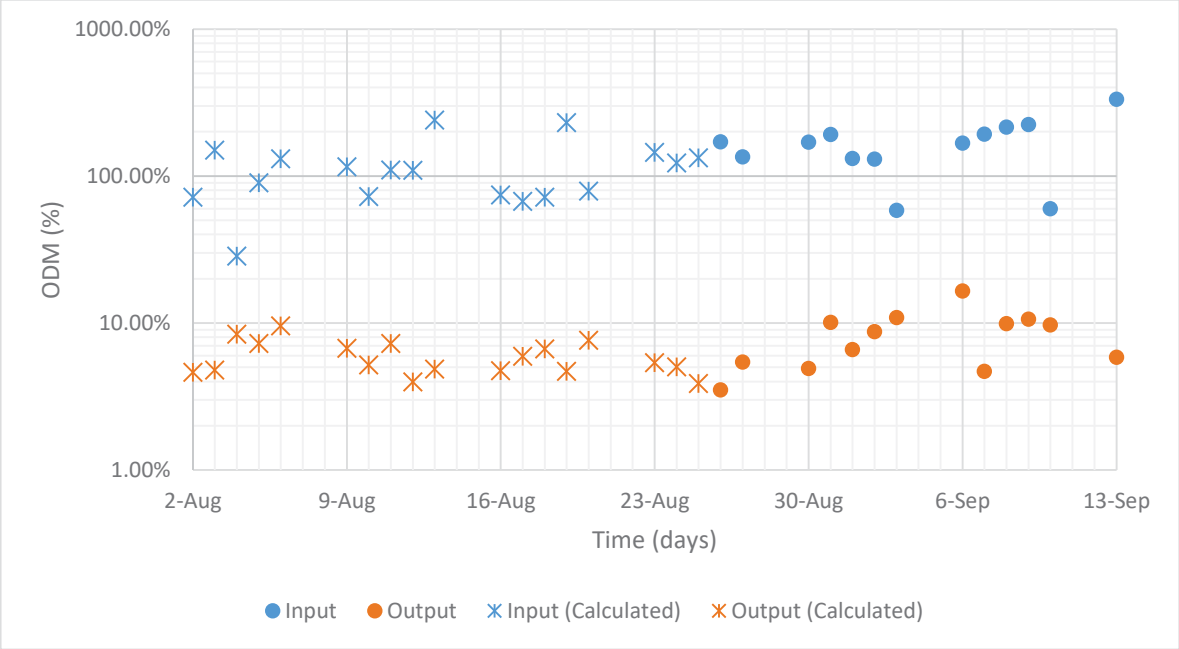

Figure 34 – Organic dry matter in the input and output between August 2nd and September 13th.

With an exception of week 10, the weekly COD averages of the input were above 15000 mg/L, being at highest when 10 L of primary were feed, reaching an average of 24428 mg/L during week 15. Values for week 13 were the highest registered per amount of PS, as seen by the average PS quality in Table 4. This increase in average is an effect of the high-quality PS collected on August 23rd which could be used for four days in that week. In addition, sludge fetched on Friday had similar properties to what was used on the previous days, with a TDM, ODM, and COD of 1,68%, 1,35 %, and 19100 mg/L, respectively.

In addition, during two days in weeks 11 and 12 (August 13th and 18th) a high concentrate sludge was fetched, which led to a final mixture in terms of ODM of 2,39% and 2,31%, respectively. However, COD did not show the same rate of increase as observed in ODM of August 13th, as 19100 mg/L was measured, instead of 35600 mg/L on August 18th, as shown in Figure 35. Besides this difference, no

other similar divergences in COD and ODM relationship behavior in the input were verified during the period.

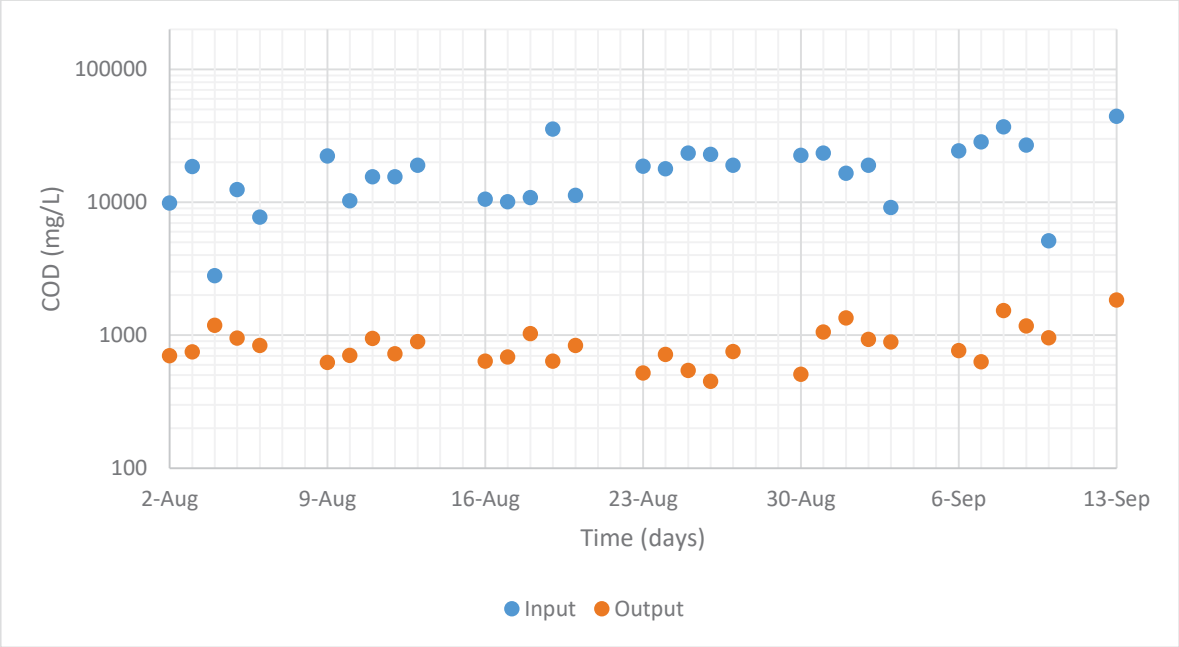

Figure 35 – Chemical oxygen demand in the input and output between August 2nd and September 13th.

The measured input quality was naturally reflected on the loads, which both COD and organic loads did oscillate daily, as shown by Figure 38. Average OL went from 402 g/m³d during week 10 to 735 g/m³d in week 15, not following linearly the amount of PS fed. However, OL increased consecutively after week 12, but with an overall decrease in week 14 in comparison to week 13, as average OL dropped from 605 g/m³d to 583 g/m³d, representing a nominal reduction of 3%. Total COD, OL, and PS quality are shown in Table 4.

Organic load during weeks 10 and 11 were below 600 g/m³d during 8 of the 10 days with feed, as S was mixed with ES during the week, as shown by Figure 37. PS quality during these weeks was slightly higher than was observed in weeks 14 and 15, averaging 22,35 g VS/L. COD load during the period was on average 13% higher than the OL, only being lower on August 6th. Week 12 had similar behavior to weeks 10 and 11, with OL under 600 g/m³d on four of five days, only surpassing this level on August 19th, when 1,151 kg/m³d was reached, as shown by Figure 38.

OL in week 13 was higher than the previous one, as values ranged between 600 and 1000 g/m³d during all days, as PS started to be collected in a day and stored for later uses. The difference between maximum and minimum values was within 15% of the average, as shown by Figure 38. In the following weeks, 14 and 15, organic and COD loads were kept above 600 g/m³d, being above 1 kg/m³d during the four days in week 15, as illustrated in Figure 39. The load was reduced on both Fridays due to the collection of PS low quality, as TDM values of the feeding mixture on August 20th and 27th were below 0,70%

The liquid output showed values of ODM, TDM, and COD around ten times lower than what was observed in the input. TDM and ODM were both below 0,2% between August 2nd and September 12th, reaching a minimum of respectively 0,06% and 0,04% on August 26th. As shown by Table 3, ODM weekly averages ranged between 0,04% and 0,10% with a relative standard deviation below 30%. This represented an average daily reduction of 89,65±8,21% in ODM in comparison to the feed.

Moreover, days of higher TDM and ODM in the input did show the same increases in the output. As shown by Figure 33 and Figure 34, ODM and TDM did not increase after a higher concentrate mixture had been fed. However, weeks 14 and 15, when only PS was fed, showed higher TDM and ODM overall, as average values during weeks 10 through 12 were below 0,07% as weeks 14 and 15 had values above 0,08%. Week 13 showed the lowest average in all three parameters, being respectively 0,08%, 0,04%, and 598 mg/L for TDM, ODM, and COD, as shown in Table 3.

In addition, the inorganic matter content in the input ranged between 0,11% and 0,32% and the output 0,03% to 0,09%. The average for the period was calculated to be 0,21% in the input and 0,06% in the output, which consists of a dry content of 10,88% and 41,85%. This lead to an average reduction of 71,48% from the input and output.

Table 4 – Average organic and chemical oxygen demand loads, primary sludge quality during weeks 10 through 15.

Week	OL (kg/m³d)	COD load (kg/m³d)	PS (L)	ODM/PS (g/L)	COD/PS (g/L)
10	0,402	0,441	5	18,80	20,61
11	0,554	0,710	5	25,91	33,21
12	0,447	0,672	8	13,06	19,63
13	0,605	0,874	5	28,29	40,88
14	0,583	0,778	10	13,65	18,19
15	0,735	1,045	10	17,19	24,43
Period	0,554	0,754	7,17	19,48	26,16

COD, on the other hand, only surpassed 1000 mg/L on six days during the period, with all values within 492 and 1540 mg/L. In a similar way to TDM and ODM, values were constantly low even with variations in load and composition of the input, as shown by Figure 35. Week averages ranged from 598 mg/L in week 13 to 1016 mg/L in week 15 with a relative standard deviation below 35% in all cases. In addition, it was noticed that weekly peaks occurred on Wednesdays in 5 of the 6 weeks, but differences to the averages in all cases were less than 20%. At last, the highest COD values were observed also during weeks 14 and 15.

As shown by Figure 36, overall TDM and COD reduction/retention stayed above 70% during the whole period. Besides August 4th when the reduction was 55,81%, during weeks 10 and 11, TDM and COD retention/reduction stayed consistently above 85%, being at highest at 97,05% on August 13th for TDM and at 97,21% on August 9th for COD. In addition, the reduction ratio did not show any well-defined trend over this week, having an oscillatory behavior within the range of 85% and 97% for both COD and TDM.

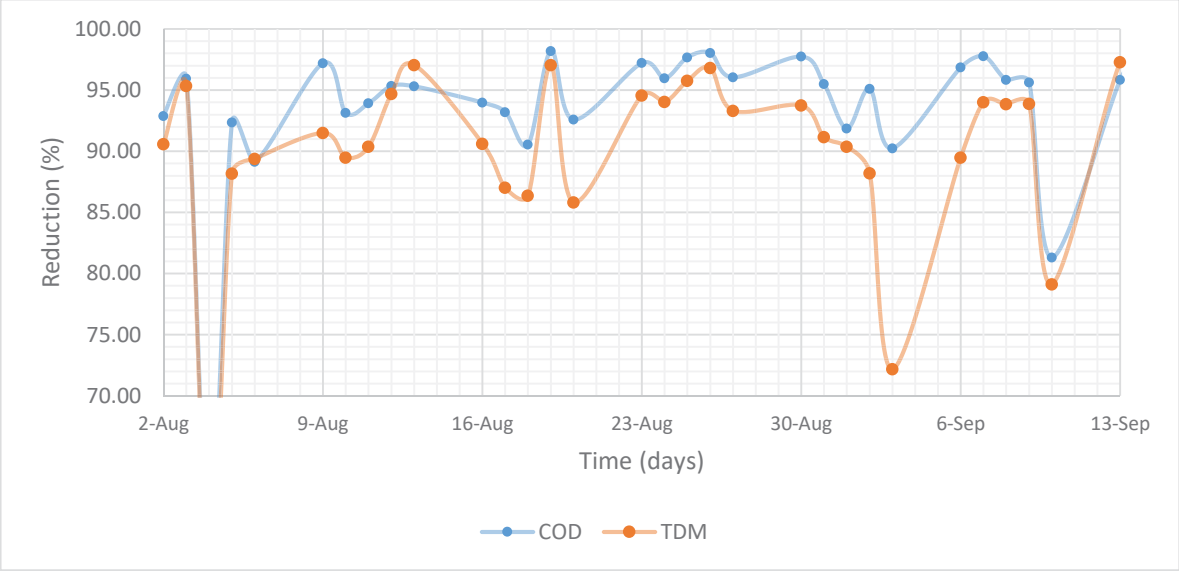

Figure 36 – Chemical oxygen demand and total dry matter reduction between August 2nd and September 13th.

Weeks 12 and 13 showed had a retention rate above 85%, with a minimum retention of TDM at 85,81% on August 22nd and for COD, the minimum value during these weeks was 90,55% on August 18th. In addition, week 12 had an overall lower retention rate than week 13, as TDM retention was below 91% during 4 of 5 measurements, as week 13 was above 94% during the whole week. Similar variations were also verified for the COD, as shown by Figure 36.

On the other hand, weeks 14 and 15 had each one day, which TDM retention was below 80%, on September 3rd and 10th respectively, but a lower COD retention was verified only on September 10th when it reached 81,31%. Besides these observations, values for TDM retention were above 88,19% and COD 90,25%, with maximum removal rates of 93,88% and 97,79 respectively. Overall retention during week 15 was higher than during week 14, as shown by Figure 36.

As shown by Table 5, gas production increased over the period, from a total production of 130,74 L of biogas in week 10 to 329,10 L in week 15. It was observed that the gas production in week 12 was higher than in week 11, even with a higher OL being used during week 11. Moreover, if one compares the production between weeks 11 and 13, one can verify that the production increased 43% for an increase of 12% in ODM and 23% in COD. A similar effect was also observed between weeks 13 and 14 when a 6% ODM increase led to a 36% increase in yields. Contrariwise,

a greater increase in ODM (27%) in week 15 resulted in a minor increase (12%) in total gas production.

Table 5 – Total biogas production and yields for the amount of feed during weeks 10 through 15.

Week	Biogas (L)	Biogas/OL (L/kg)	Biogas/COD (L/kg)	Biogas/PS (L/L)
10	130,74	278,71	253,71	5,230
11	165,98	256,26	197,82	6,639
12	199,61	382,14	254,19	4,990
13	238,17	336,80	233,04	9,527
14	323,65	474,33	355,78	6,473
15	329,10	382,95	269,44	6,582
Period	1387,25	356,64	262,55	6,452

These observations were reflected in the relative production concerning ODM, COD load, and PS. The average production for OL during the period was 356,064 L/kg per week, which is 28% higher than the calculated for the lowest week in the period. If consecutive weeks are compared, an oscillatory behavior can be observed, which for every decrease in production per OL, a subsequent increase happened. Moreover, it was also observed that each oscillation led to slightly higher base values than the previous one, from 382,14 L/kg VS in week 12 to 474,33 L/kg VS in week 14. This behavior was also verified regarding COD load, but with overall lower increments, and could not be verified regarding the amount of PS fed.

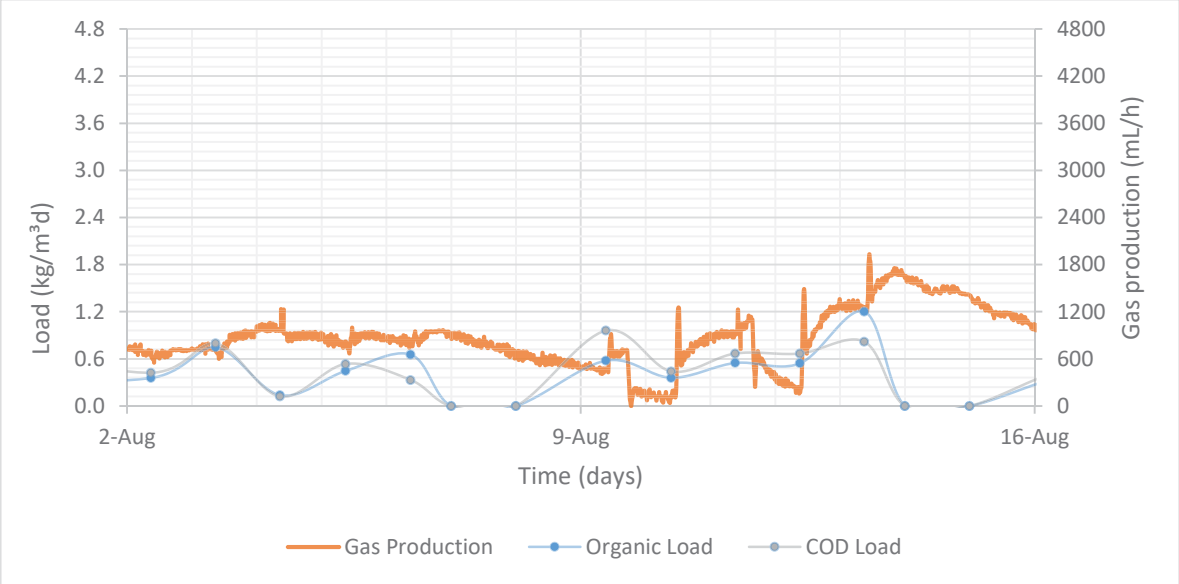

Figure 37 – Gas production (mL/h), organic load (kg/m³d), and chemical oxygen demand load (kg/m³d) between August 2nd and 16th.

During weeks 10 and 11, production stayed mostly under 1000 mL/h, under the quantification limit of the gas clock. As a result, variations under this limit are not reliable, but for values above 500 mL/h, it is possible to say that gas is being produced in the system. However, on August 5th, 10th, and after August 12th, production could be quantified at levels close to 1000 mL/h, with a maximum on August 13th at 1721 mL/h. As shown by Figure 37, production after August 12th had a stepwise increase, reaching a stable value and increasing after the next feed, with a 300 mL/h increment a day.

Weeks 12 and 13 showed similar behavior to the final days of week 11, but with different intensities, as the production rate profile assumed also a stepwise shape, as illustrated in Figure 38. After feeding, production rapidly increased until reaching a plateau starting from 830 mL/h in week 12 and 1000 mL/h in week 15. Then, it increased at constant increments, 300 mL/h and 75 mL/h per day, with both Tuesdays and Thursdays having a small increment of 75 mL/h approximately. S

This behavior was observed during the whole week 12, but in week 13 higher production rates increments on Friday led to a peak at 2669 mL/h on August 28th. In addition, the production profile shape was different from week 12, being more similar to what was observed in weeks 16 to 19 (see section 6.3.4). Production rates

increased to a well-defined peak after decreasing continuously during the weekend until the next feed on Monday. In addition, a small bump in production was registered on August 28th. Nevertheless, both weeks had a final baseline production below 800 mL/h, as shown by Figure 38 and Figure 40.

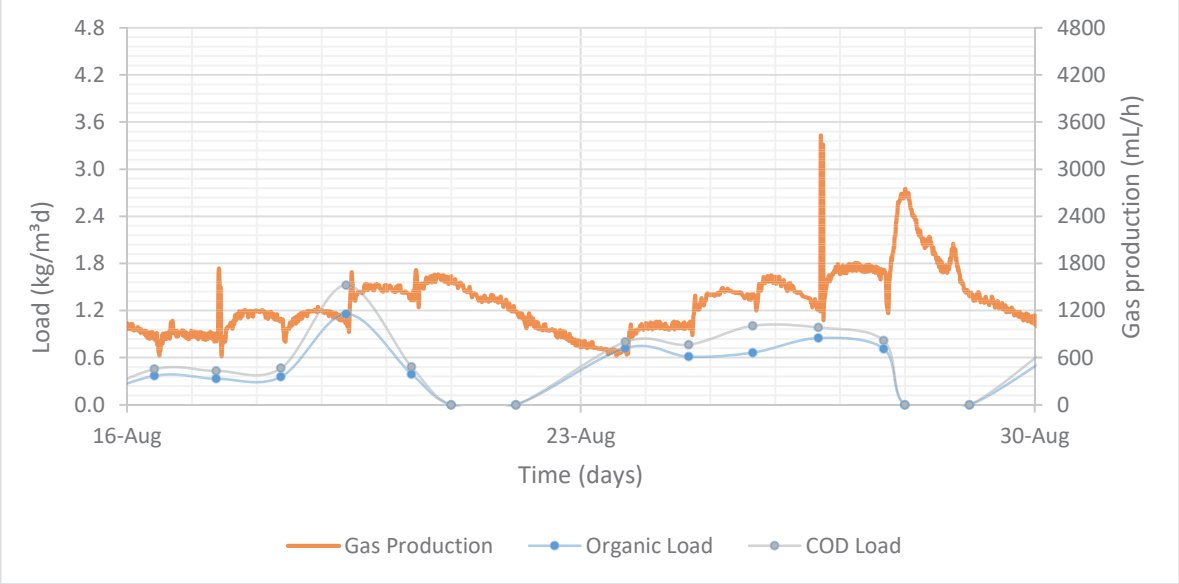

Figure 38 – Gas production (mL/h), organic load (kg/m³d), and chemical oxygen demand load (kg/m³d) between August 16th and 30th.

Moreover, the production profile had a similar shape between weeks 14 and 15, showing a maximum production over the week followed by a continuous decrease during weekends, as shown in Figure 38. During the first three weeks of the period, the increase of production during the week was small, being negligible in week 10. In week 11 the production increased from a baseline of 460 mL/h on Monday to 1500 mL/h on Thursday, returning to a lower state over the weekend. This happened also in week 12, but the starting baseline was higher, 1000 mL/h.

Gas yields and OL were higher on Wednesday and Thursday in week 15 compared to the same weekdays in week 14. However, the higher load did not change the time for the production to decay over the weekend, but it led to a higher baseline. However, baseline production was lower in week 14 in comparison to 13, as bottom production rates were 461 mL/h 790 mL/h respectively. In addition, week 13 had a shorter period between the last feeding on Friday to the first of the following week on Monday than week 14, which had 78 h instead of 69 h of week 13.

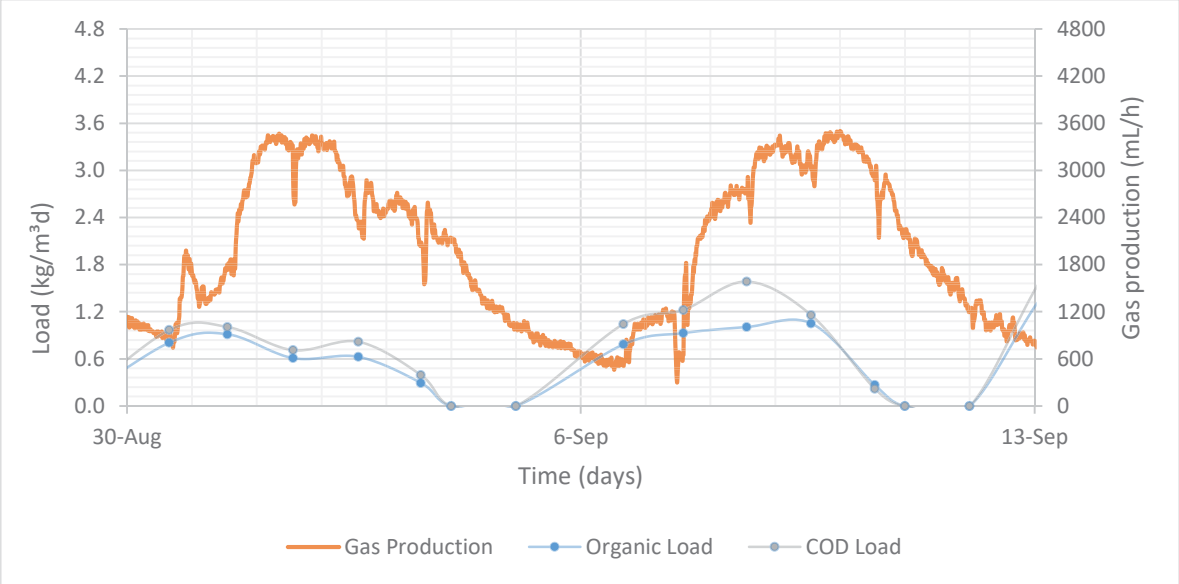

Figure 39 – Gas production (mL/h), organic load (kg/m³d), and chemical oxygen demand load (kg/m³d) between August 30th and September 13th.

Besides the air infiltration event registered on August 26th, production peaked at 3451 mL/h on September 9th, but top production in week 14 had a similar value at 3391 mL/h on September 1st. Even though production peaks happened on different days of the week, top production on adjacent days was similar, when rates reached 3360 mL/h on Wednesday in week 14 and 3387 mL/h on Tuesday in week 15. Dropping rates occurred with similar rates after top production, but in week 14 the drop was not steady, when production between Thursday and Friday was stable for 18h, as on week 15 production dropped continuously from Thursday night until Monday next week.

However, the production profile on Mondays was different, being overall lower on September 6th than on August 30th. Production on August 30th increased from an 800 mL/h baseline to well-defined peak production of 1768 mL/h 4 hours after the feeding, decreasing to a local minimum at 1308 mL/h before starting increasing once again without feed. On the other hand, on September 6th production increased until 1100 mL/h rapidly, reducing the increasing speed afterward, until reaching a maximum of 1212 mL/h, just before the feeding procedure started. This was reflected in peaks during different days of the weeks, as a stepwise increase was observed during week 15 and not during week 14.

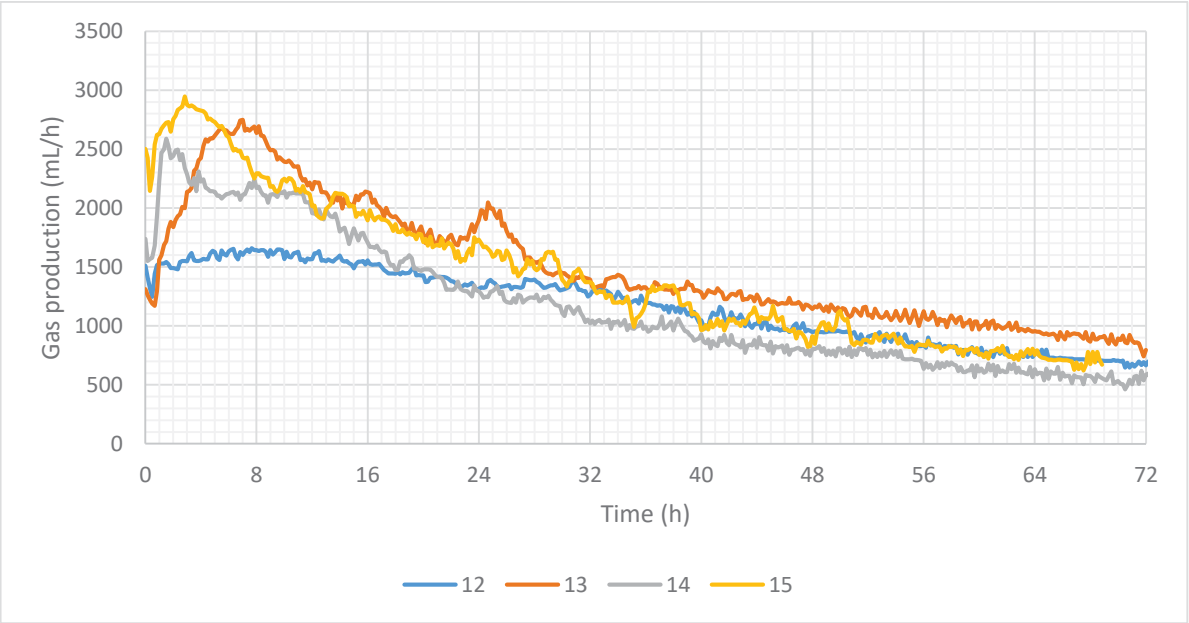

Figure 40 – 72h gas production profile after feeding on weekends from weeks 12 through 15.

As shown by Figure 40, the production decay over the weekend was smooth for weeks 12 to 15. Besides week 12, which showed a negligible increase in gas production, weeks 13 to 15 had maximum rates over 2500 mL/h, being achieved faster in week 14 (2h) and slower in week 13 (8h). In addition, week 12 reached half of the maximum production in 22h and 30h the minimum quantifiable value of 1000 mL/h. This was also observable in weeks 14 and 15, which both achieved the half-maximum production after 22h of the peak, but they took more than 50 to achieve 1000 mL/h. At the end of 72h, all weeks showed similar end production around 750 mL/h, but small differences at this low production rates cannot be discussed as the gas clock quantification limit is 1000 mL/h.

With that, accumulated feed-to-feed production was lower during weeks 10 through 12 in comparison to weeks 13 through 15. Accumulated production on weekdays during weeks 10 and 11 were below 25 L on 9 of 10 days, which the exception of August 12th when 27,13 L of gas were produced, as shown by Figure 41. In addition, only 50,91 L of gas was produced over the weekend during week 10, however, production during week 11 was comparable to what was observed on the following weekends at 99,31 L.

Production on weekdays during weeks 12 and 13 increased similarly as the days passed, but week 13 had a higher starter point, as shown by Figure 41. On August 16th, accumulated production was 20,86 L increasing over the week up to 35,69 L on August 19th, as during week 13, production increased from 23,81 L on August 23rd to 39,14 on August 26th. Production over the weekend was slightly higher during week 13, with a value of 108,69 L instead of 89,27 L of week 12. Weekend production during week 13 was the highest for the 5-days feed regime.

Moreover, accumulated feed-to-feed production increased during week 14, from 33,19 L on August 30th to 73,61 L on September 1st, oscillating down to 54,88 L on September 2nd. Similarly, production during week 15 increased from 23,06 L on September 6th to 73,50 on September 9th, but without any oscillations, as shown in Figure 41. Production over the weekend was higher during week 15 than 14, with a production of 98,46 L instead of 87,07 L.

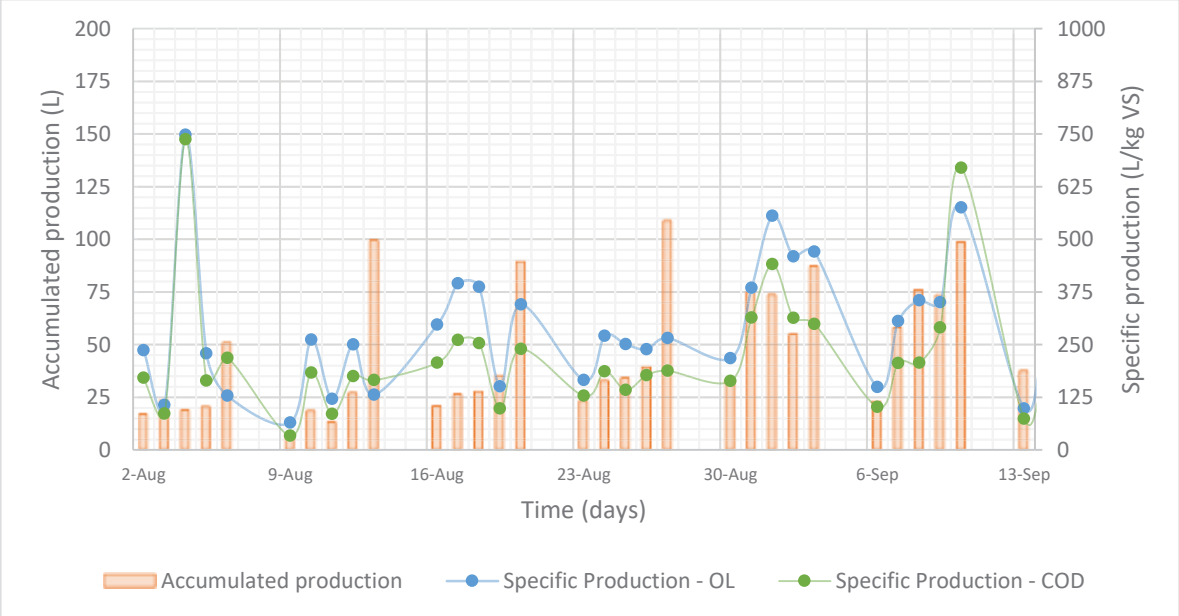

Figure 41 – Accumulated production (L), specific gas production based on the organic load (L/kg VS d), and specific gas production based on the chemical oxygen demand (L/kg COD d)between August 2nd and September 13th.

As OL used over the experiments could not be kept constant, variations of specific production differed from the accumulated production during most of the period. As shown by Figure 41, specific production oscillated between 64,32 and 261,34 L/kg VS d during most of the weeks 10 and 11, being above 750 L/kg VS d

on August 4th when OL was 0,123 kg/m³d. Even with this variability, values of yields over the weekend were similar, as 128,51 L/kg VS d was verified during week 10 and 131,02 L/kg VS d during week 11.

During week 12, specific production increased over the first three days of the week, from 297,13 L/kg VS d on August 16th to 386,32 L/kg VS d on August 18th, oscillating to 151,26 L/kg VS d and 345,23 L/kg VS d on the following days. This was different from week 13 which, after an initial increase, kept the specific production above 235 L/kg VS d, as shown by Figure 41. Values increased from 166,25 L/kg VS d on August 23rd to 270,21 L/kg VS d on August 24th, being kept around this value until August 27th when specific production was 265,45 L/kg VS d.

Specific production profile during weeks 14 and 15 was similar to the accumulated feed-to-feed production, as seen in Figure 41. On the first three days of week 14, specific production increased from 217,66 on August 30th to 555,26 on September 1st, oscillating down on the following two days reaching a value of 473 L/kg VS d on September 3rd. Week 15, however, slowly increased from 149,23 L/kg VS d on September 6th to 350,98 L/kg VS d on September 9th, increasing once again to 575,23 L/kg VS d over the weekend.

Moreover, specific production regarding COD was at its highest on August 4th when a value of 737,04 L/ kg COD d was observed. Besides this high value, yields were below 250 L/ kg COD d during weeks 10 and 11, oscillating between 86,12 L/ kg COD d, on August 3rd, and 183,29 L/ kg COD d, on August 10th, during other days. As shown by Figure 41, values overcame the 250 L/ kg COD d' mark on two days during week 12, but between 239,51 L/ kg COD d, measured on August 20th, and 98,42 L/ kg COD d until the end of week 13. Values during week 13 were very similar, ranging between 124,01 and 183,24 L/ kg COD d with three total days above the 175 L/ kg COD d' mark. Weeks 14 and 15 had their lowest values on Monday, measuring 163,68 and 102,36 L/ kg COD d respectively. However, their highest values were measured on different weekdays, on Wednesday at 440,24 L/ kg COD d in week 14 and on Friday at 669,84 L/ kg COD d in week 15.

Steep drops in production rates were observed during the period, all happening after feeding the reactor. This effect was directly related to the feeding

procedures, which closed the valves where the gas was collected, briefly blocking the gas passage to the measurement device. At last, two unusual peaks were observed on August 18th and 26th, of which all were related to air coming inside the reactor. No other anomalies could be identified in the period, as no other steep variations could be identified in the production rate during the days.

6.3.4. Seven-days feed regime

After six weeks of excluding weekends from the feeding schedule, feeding started to be done every day for 27 days. During this period, however, the feed was overall two times more concentrated than what was prepared during the previous period. TDM and ODM showed an average value of 125% higher and COD 150% higher, as shown in Table 6. However, the composition of the feeding mixture was less constant than the previous period, leading to a higher standard deviation for all three controlled parameters.

Table 6 – Total dry matter, Organic dry matter, Chemical oxygen demand in the input and output during weeks 16 through 19.

Week	Input			Output		
	TDM (%)	ODM (%)	COD (mg/L)	TDM (%)	ODM (%)	COD (mg/L)
16	3,15 ± 0,59	2,66 ± 0,59	35329 ± 9252	0,14 ± 0,02	0,07 ± 0,02	1564 ± 551
17	1,79 ± 0,55	1,52 ± 0,45	21786 ± 6143	0,16 ± 0,03	0,09 ± 0,01	1230 ± 120
18	4,36 ± 2,46	3,68 ± 2,08	60829 ± 34539	0,17 ± 0,03	0,07 ± 0,03	1539 ± 203
19	4,16 ± 2,53	3,61 ± 2,15	57567 ± 37213	0,44 ± 0,35	0,22 ± 0,21	1997 ± 854
Period	3,36 ± 1,96	2,87 ± 1,67	43877 ± 29008	0,23 ± 0,19	0,11 ± 0,11	1582 ± 545

Average TDM and ODM in the input during this period were respectively 3,36% and 2,87%, which was 127% and 119% higher than the previous period. In addition, overall standard deviations were above 1,5%, representing 58,3% and 58,2% for TDM and ODM respectively, which is was higher than the 43,4% and 40,4% registered between weeks 10 and 15. Overall COD followed the same trend,

with an overall average of 43877 mg/L, but higher with a relative standard deviation of 66,1%, as shown by Table 6.

Overall, the input during the period had a TDM above 3% on 15 days, being above 7% between October 1st and 5th, as seen in Figure 42. A 4-days stable feeding mixture quality was observed during the most period, being the period between October 1st and 5th being kept within 20% range from the average for five days straight. Outliners of this pattern were registered on three days, September 23rd, 27th, and 28th, when TDM and ODM were 50% higher than the adjacent days. This difference was also verified in COD, but the difference was 30%, as shown by Figure 44.

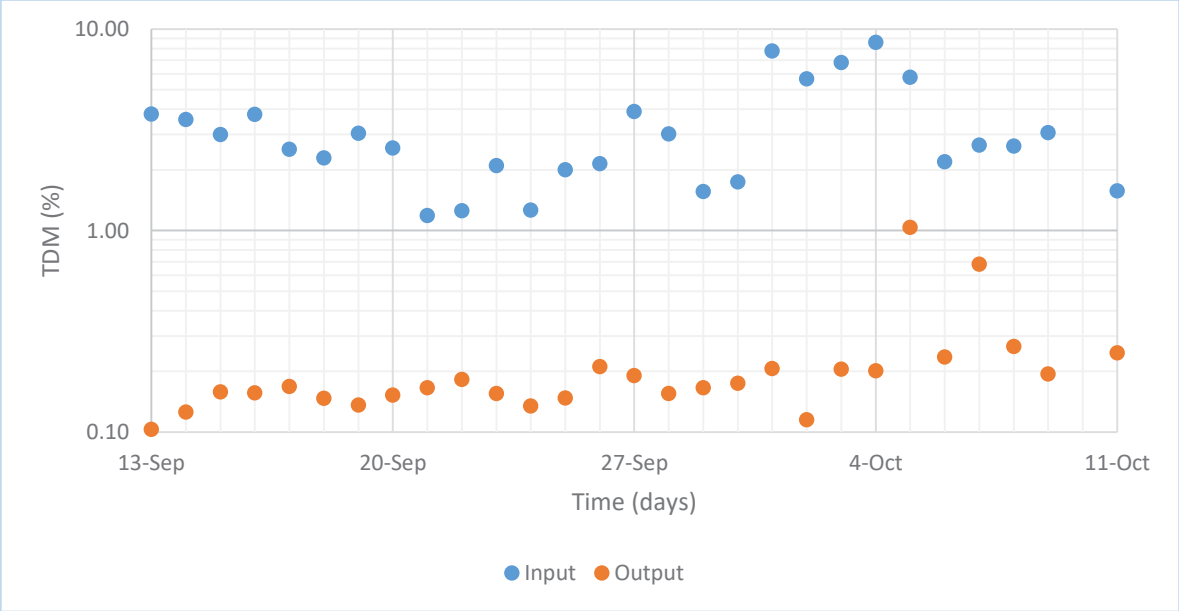

Figure 42 – Total dry matter in the input and output between September 13th and October 11th.

Moreover, TDM and ODM of the input showed higher variation in regular intervals and not weekly, leading to high standard deviations in weeks 18 and 19. As shown by Table 6, the standard deviation in the input was 2,06% and 2,15% in weeks 18 and 19, respectively, which represents a relative standard deviation of 56,2% and 59,6%. During these weeks, the input had an ODM of around 1,7% on two days, increasing to values above 5% on the following four and dropping to 2-3% on the final four days, as shown by Figure 43.

During week 17, values were overall lower than other weeks due to bad quality PS collected on September 20th and mishandling of the sample container on September 24th. During September 21st and 22nd, ODM values were 0,99% and 1,05%, respectively, which are on average 25% lower than the lowest value from other weeks, 1,36% on September 29th. After collecting a new batch of sludge on Wednesday, an ODM of 1,83% was achieved. However, due to not properly agitating the storage containers before preparing the feeding mixture, ODM in the input was 60% lower, 1,09%.

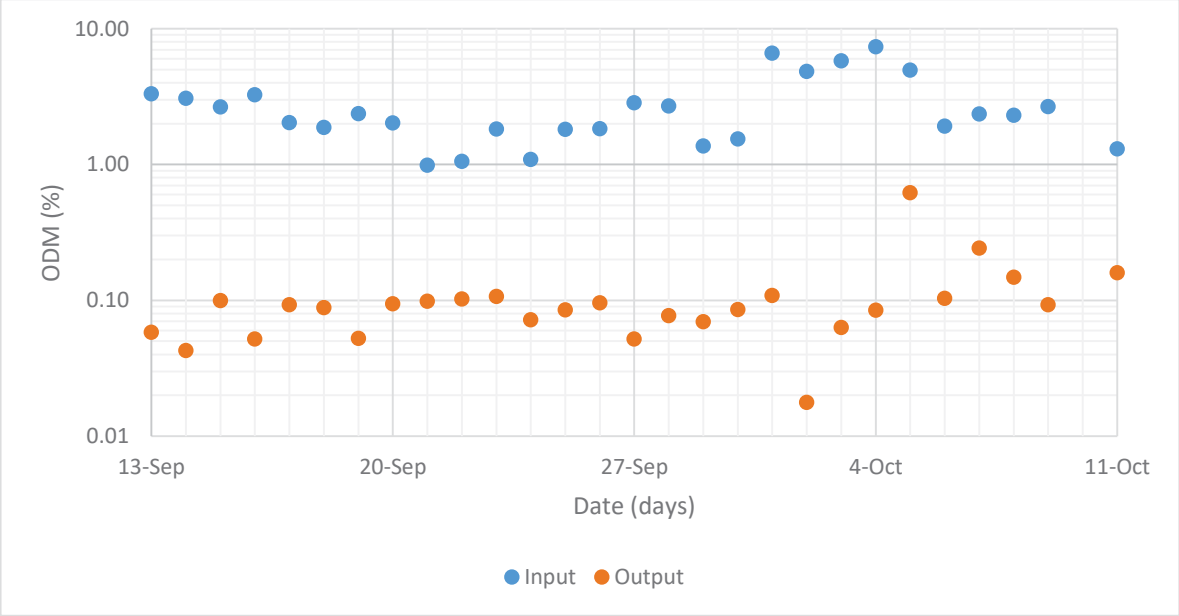

Figure 43 – Organic dry matter in the input and output between September 13th and October 11th.

In addition, between October 1st and 5th, the aspect of the input also changed to a pastier liquid on days with ODM above 5%. Because of that, a large quantity of water was required to drag the PS out of the storage containers, as the mixture had solidified. Even with water being added, the mixture behaved like a crumbly pizza dough, which made pumping the material not feasible. To mitigate this effect, 5 liters of the recirculation was used to dilute the input and make it possible for the feeding procedure to happen. Because of the extracted liquid being reintroduced to the reactor, the residence time and amount of input did not change. Samples were taken before mixing the input to the recycle.

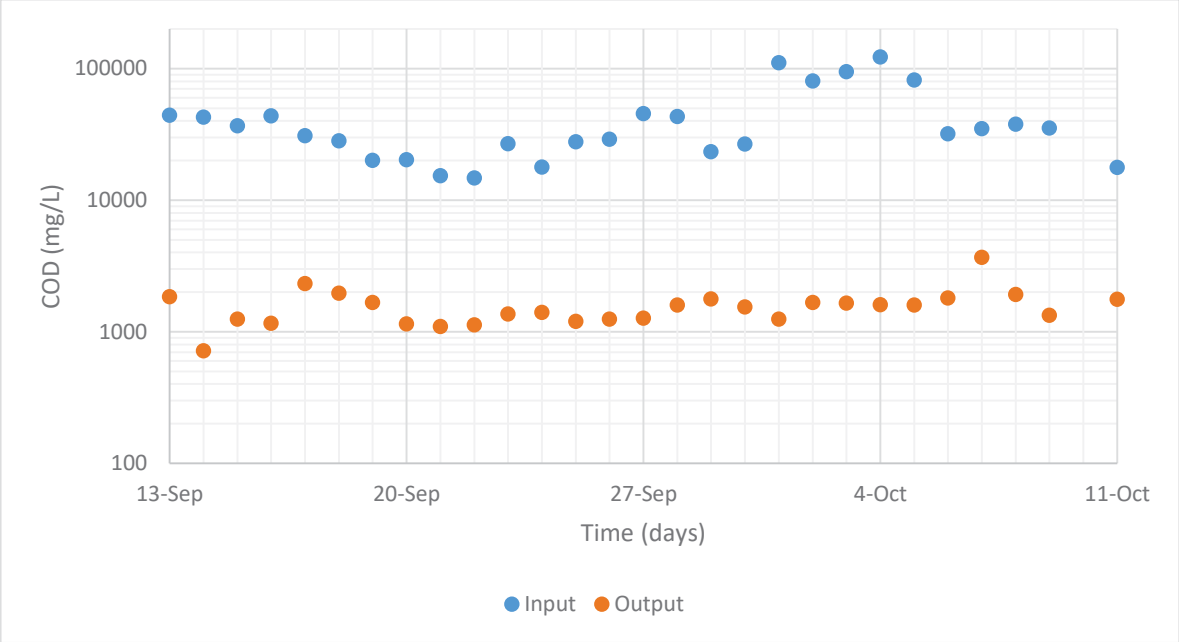

Figure 44 – Chemical oxygen demand in the input and output between September 13th and October 11th.

COD in the input was higher than 20000 mg/L in weeks 16, 18, and 19, but during week 17 values were often below this mark. COD in the input varied as the ODM and TDM did, reaching extremely high values above 100000 mg/L between October 1st and 5th. COD analyses from these days gave results in mg/kg due to the solid aspect of the samples, requiring to be converted afterward to mg/L. For that reason, COD values for the period may be overestimated, due to the density of 1,05 g/L being used for the calculation. COD measurements for the period can be seen in Figure 44.

With the high concentrate PS collected, the organic load was also 120% higher on average than what was used in the previous period. As shown by Table 7, the total organic load for these 4 weeks was higher than what was used on the six previous weeks combined. The average OL in the input was 1,201 kg/m³d and COD 1,877 kg/m³d, which represented an average concentration of 28,07 g and 43,37 g for a liter of PS respectively. COD and Organic load are shown in Figure 46 and Figure 47.

On September 20th and 21st, OL was higher than COD load, as values of 1,353 and 1,107 kg/m³d for OL and 0,861 and 0,866 kg/m³d for COD were calculated

respectively. Besides these two days, COD load was overall 20% higher than OL and was higher than 0,650 kg/m³d during the whole period. This reflected on the weekly average COD and organic loads being above 1 kg/m³d during weeks 16, 18, and 19, but not in week 17, when lower quality sludge (<1,2%) was fetched on three days.

Table 7 – Average organic and chemical oxygen demand loads, primary sludge quality during weeks 16 through 19.

Week	OL (kg/m³d)	COD load (kg/m³d)	PS (L)	ODM/PS (g/L)	COD/PS (g/L)
16	1,139	1,512	10	26,62	35,33
17	0,651	0,932	10	15,22	21,79
18	1,574	2,603	10	36,79	60,83
19	1,440	2,463	10	33,66	57,57
Period	1,201	1,877	10	28,07	43,37

Liquid output had overall stable values of TDM, ODM, and COD during the period. Values of TDM were consistently under 0,2%, being on average 0,18% between September 13th and October 11th, showing no outliner during this time. Weeks 16 to 18 also showed a stable ODM with weekly averages below 0,1% and low standard deviations, as shown by Table 6. In addition, on October 19th, ODM showed an unusually low value when taken into consideration TDM for the day. An ODM of 0,02% was observed, while a TDM of 0,12% was measured. This resulted in a ratio of 0,153 between ODM and TDM in the output, three times lower than the average of 0,582 observed.

Different from other weeks, output in week 19 did not show a stable behavior nor consistent low concentrations. On October 5th and 7th, ODM reached 0,62% and 0,24% respectively, with an ODM of 0,10% on the day in-between. This made the average and standard deviation for the week jump to 0,22%±0,21%, which was the highest for the period. Both spikes were also observed for TDM, but only the October 7th spike was observed for COD (3690 mg/L), values from October 5th were virtually the same as the previous days, 1600 mg/L.

These spikes on TDM and ODM occurred as the foam was observed during the high concentrate PS between October 1st and 5th. Foam presence was confirmed by visually analyzing the output storage tank before emptying it. It was verified that water on the bottom of the tank had an aspect cleaner than the liquid on the top. Furtherly, it was confirmed by filtrate analysis, that this foam was composed mainly of solids in suspension.

If one does not consider measurements on October 5th and 7th, TDM and ODM for the period were slightly higher than what was observed between weeks 10 and 15, but within the standard deviation range. COD, however, had an overall increase of 70% in comparison he the previous period, which is seen in the COD range of both periods. Between weeks 16 and 19, most values ranged between 1000 and 1800 mg/L, while COD between weeks 10 and 15 ranged mostly from 500 to 1300 mg/L. Moreover, only on September 14th, a measurement was below 1000 mg/L.

With that, retention of TDM and COD were above 95% during the beginning of week 16, decreasing to an average of 92,6% for COD and 94,1% for TDM of the three last days. In addition, retention was not lower than 92% during week 16, both for COD and TDM, as shown in Figure 45. On the other hand, week 17 showed an overall lower TDM retention as COD retention was virtually the same. On September 21st and 22nd, TDM retention was on average 85,8% as COD was 92,6%, being 5 percentage points lower than what was measured in the same period of the previous week. In addition, TDM retention oscillated twice between 90 and 92% as COD did it only once.

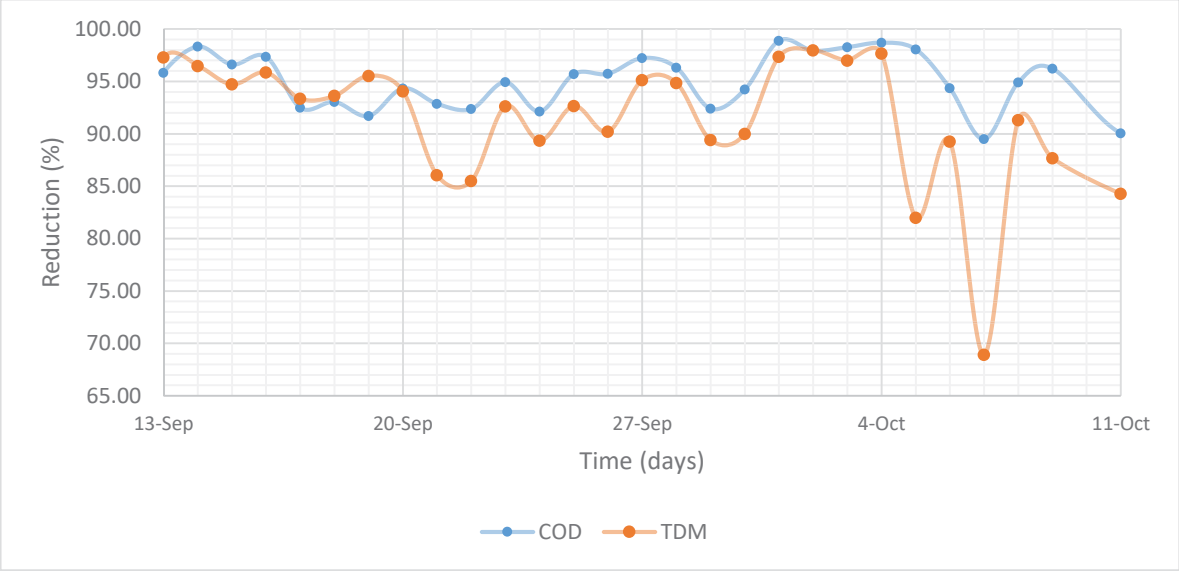

Figure 45 – Chemical oxygen demand and total dry matter reduction between September 13th and October 11th.

On the other hand, weeks 18 showed two days of lower TDM retention during the beginning of the week, at 89,39% and 89,98% on September 29th and 30th respectively, being followed by COD, but to a lesser extent, as shown by Figure 45. After these days, TDM retention increased to 97,33% on October 1st, being kept at this level for four days straight both regarding TDM and COD. After this period, TDM retention dropped to 81,51% and oscillated downwards to 68,91% two days after. Efficiency was restored during the followed two days, but retention could not reach the same levels that were observed between October 1st and 4th.

In contraction to TDM and ODM in the liquid output, gas production and its profile were different from what was observed in previous weeks. Starting with a day of continuous increase in gas production, the period registered yields between 500 and 600 L/week for four weeks, as shown by Table 8. Total production was similar in the first three weeks, but it increased 20% in week 19, with a total of 592,86 L. This increase happened even though the number of feeding days was 6 instead of 7 from previous weeks. This was despite the most concentrated PS being fed in between the end of week 18 and the beginning of 19.

Table 8 – Total biogas production and yields for the amount of feed during weeks 16 through 19.

Week	Biogas (L)	Biogas /OL (L/kg)	Biogas/COD (L/kg)	Biogas/PS (L/L)
16	544,45	292,14	220,16	7,778
17	515,25	483,55	337,87	7,361
18	507,72	197,16	119,11	7,253
19	592,86	293,53	171,64	9,981
Period	2160,07	287,16	184,27	8,008

Different from the last period, with daily feeding, it was not possible to calculate the real gas production for the amount of feed. This happens because there was not enough time for the gas production rate to reach low levels. As shown by Figure 46 and Figure 47, rates had a wave format along the week, quickly increasing after feeding and gradually decaying until the next feed. Production peaked on average 4000 mL/h in weeks 16, 18, and 19, but it was lower in week 17 when peaks were most under 3500 mL/h. In addition, most days showed an increase of approximately 600 mL/h in production rate immediately after opening the gas collection valves, which started the production increase until the top production.

In consonance with weeks 10 to 15, specific production oscillated between weeks, but instead of small positive increments, a negative one was observed from weeks. Overall, values were below what was observed during previous weeks, as the average observed for the period was 287,16 L/kg of OL, which was a reduction of 16%. However, calculations of yields for weeks 10 through 15 considered days without feeding, giving more time for production to happen in comparison to weeks 16 through 19.

Table 9 – Total biogas production, average organic load, and yields for the amount of feed during periods of similar organic load during weeks 16 through 19

Period	Biogas (L)	Average Load (kg VS/m³d)	Biogas /OL (L/kg d)	Biogas/COD (L/kg d)	Biogas/PS (L/L d)
13/09 - 16/09	296,06	1,512	209,38	176,33	7,402

Period	Biogas (L)	Average Load (kg VS/m³d)	Biogas /OL (L/kg d)	Biogas/COD (L/kg d)	Biogas/PS (L/L d)
17/09 - 20/09	333,25	1,190	318,59	334,25	8,331
21/09 - 26/09	430,39	0,712	431,25	325,56	7,173
27/09 - 30/09	264,35	1,095	219,56	189,77	5,287
01/10 - 05/10	404,25	2,966	116,63	82,23	10,106
06/10 - 10/10	431,97	0,967	382,27	246,31	8,639

Table 9 shows the total feed-to-feed and specific gas production regarding OL, COD, and PS for the period in which OL was similar between days. Specific production was higher between September 17th and 20th if one analyzes regarding COD, 334,25 L/ kg COD d, and, if one analyzes in regard of OL, it was higher between September 21st and 26th, 431,25 L/kg VS d. The period between October 1st and 5th showed the highest average OL at 2,966 kg VS/m³d and the lowest specific production regarding COD and OL at 116,63 L/kg VS d and 82,23 L/kg COD d, respectively. Specific production related to PS was at the highest during the period between October 1st and 5th and October with 10,106 L/L PS d and the lowest between September 27th and 30th when only 5,207 L/L PS d was produced.

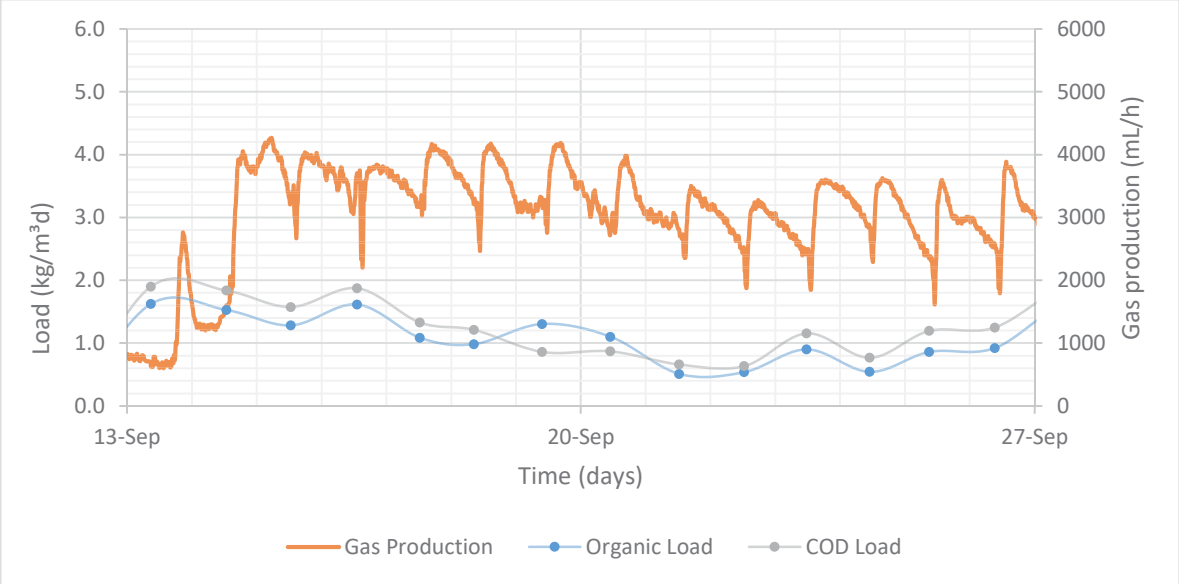

Figure 46 – Gas production (mL/h), organic load (kg/m³d), and chemical oxygen demand load (kg/m³d) between September 13th and September 27th.

As shown by Figure 46, production rates during this time did not go down under 3000 mL/h (excluding feeding times when the gas collection valves were closed). In week 17, however, the baseline for production reduced to an average of 2640 mL/h, following the reduction of the maximum production during the day. Week 18 had a similar minimum production rate as week 17, but the maxima were higher than the previous week. At last, the baseline and maximum rates were similar in week 19 in comparison to week 16, if one does not consider the first two days of feeding in week 16 when production was stable at 1230 mL/h after a spike of production, the gas production profile for weeks 18 and 19 is displayed in Figure 47.

One can observe in Figure 46, that the first two days of feeding, September 13th, and 14th, yields behaved similarly to what was observed in week 14 (see Figure 39). After the feeding had been completed, production achieved a well-defined peak at 2621 L/h after a 6 hours' delay, rapidly decreasing to a local minimum around 1200 mL/h, starting to increase once again just after the had feeding began. The time length of the production spike was approximately 6 hours and production was kept around the local minimum for 14 h.

The behavior between September 14th and 15th showed a different pattern than the standard observed in other instances. As shown by Figure 46, after 2h that

the feeding procedure had been completed, the production rate increased towards a local well-defined maximum at 4051 mL/h, decreasing at a rate of 50 mL/h² afterward. When a local minimum at 3850 mL/h was achieved, production rates started to increase once again, until a well-defined maximum production rate at 4289 mL/h was achieved. This oscillation occurred for 12 hours until it decreased down to 3223 mL/h when the next feeding procedure started.

The following days, the production profile showed a wave-like shape, but on September 16th and 17th, the wave base was wider and the maximum value was not well-defined. On both days, global maxima, 4021 mL/h, and 3700 mL/h respectively, were observed 3h hours after feeding, with a slower decay rate than following days would have shown. Moreover, production on September 16th oscillated greatly during the decay, with gas being measured in pulses, if bigger effects were felt 2 h before the feeding on September 17th, as shown by Figure 46. September 18th showed a similar shape, but the maximum was better defined than the two previous days.

Between September 19th and 22nd, the production profile showed three different phases in chronological order: production increase, decrease, and a stable baseline production. The production increase occurred soon after the feeding was concluded until a maximum above 4000 mL/h was achieved, which took on average 3h. Following this period, gas production decreased slower down to a baseline above around 3000 mL/h, a process that took 9h. After the baseline was achieved, production was kept constant until the next feeding on the following day. This behavior slightly between September 19th and 20th, as the production greatly oscillated similarly to what was observed on September 18th.

Starting from September 22nd and finishing on 26th, the production profile did not show a third continuous production phase, as shown by Figure 46. During this period, production had a proper wave-like shape, with the maximum being achieved on average 4 h after feeding and production reducing until the next feeding on the following day. As mentioned before, baseline production during this period was below the 3000 mL/h' mark and maximum values were at the lowest, being at 3272 mL/h on September 23rd. The stable production phase could be verified on

September 27th, which made the production baseline be above 3000 mL/h once again. However, top daily production did not surpass the 4000 mL/h until week 18.

Besides September 28th, production peaks during the first four days of week 18 did not reach 4000 mL, topping values at 3840 mL/h, 3679 mL/h, and 3497 mL/h on September 27th, 29th, and 30th respectively. Between September 27th and 29th, no constant gas production phase was verified, however, on September 28th a slower production rate decay was observed, when production dropped from 4000 mL/h to 3000 mL/h in 5h, but the following reduction to 2750 mL/h took 12 h to be accomplished. On September 30th, production rates slightly increased after reaching the local minimum, from 2385 mL/h to 3533 mL/h, as shown by Figure 47.

.

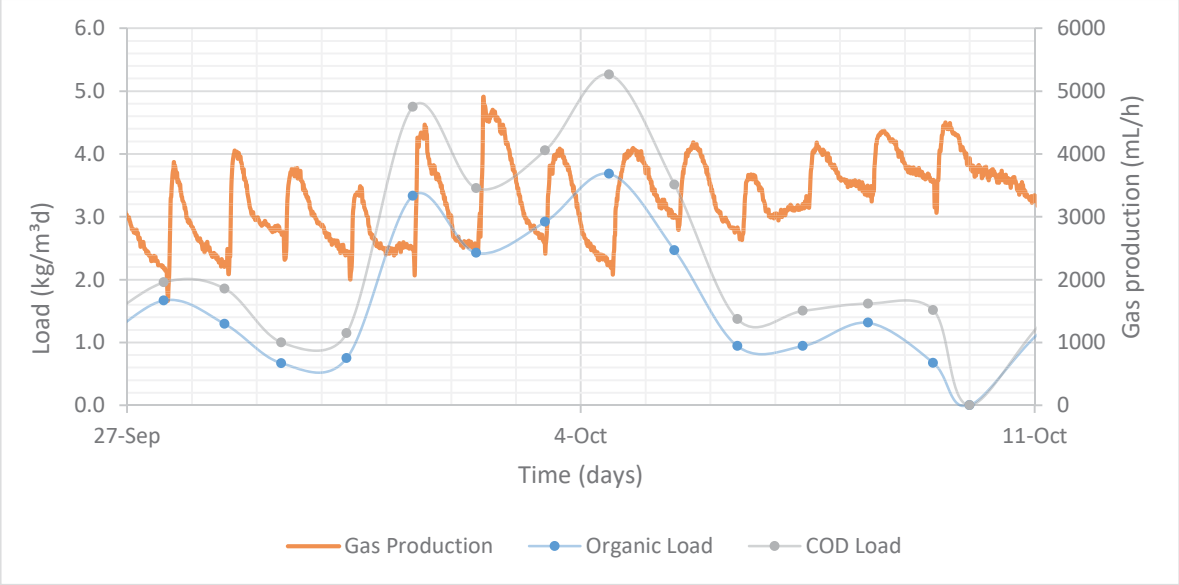

Figure 47 – Gas production (mL/h), organic load (kg/m³d), and chemical oxygen demand load (kg/m³d) between September 27th and October 11th.

Between October 1st and 5th, when OL was above 2,4 kg/m³d, production peaks were at their highest, showing the maximum production at 4701 mL/h on October 2nd. Top production rates on other days ranged between 4452 and 4041 mL/h, on October 1st and 4th, as shown by Figure 47. In addition, after reopening the gas collection valves on October 2nd, production jumped from 3065 mL/h to 4902 mL/h in 60 min, stabilizing at 4520 mL/h after the accumulated production while the

valves where closed did not interfere in measurements anymore. This was the higher jump registered during the whole experiment period.

Profile during the high load period was also similar to what was observed in previous days, production increased immediately after feeding with a following decay until the next feed. The steady production period was only verified on October 1st and slow decay, similar to what was described for September 28th, was verified on October 5th. End production rates ranged between 2350 mL/h and 2662 mL/h between October 1st and 4th, being higher than 3000 mL/h on October 5th. No post-reduction increase in production rates was observed during this period.

On the following days, October 6th through 11th, the production profile showed the same three well-defined phases of production observed between September 18th and 20th, as illustrated in Figure 47. On October 6th production topped at 3674 mL/h, decaying to a local minimum of 2997 mL/h after 7 h, but rates increased over the next 12 hours until the next feeding was conducted, reaching 3313 mL/h. This behavior was not verified on the following three days, as rates deaccelerated after reaching the production baseline, with an average reduction of 176 mL/h over 12 hours.

Moreover, top production rates increased over this period, topping at 4179 mL/h, 4367 mL/h, and 4501 mL/h, on October 7th through 9th respectively. This represented an increment of 505 mL/f on the first day and approximately 150 mL/h on the following two. Time for achieving maxima was similar between then, averaging 2,5 h. Baseline production after an average of 7 h of the maximum rate had been reached increased from 2997 mL/h on October 6th to 3731 on October 9th, as shown by Figure 47.

Overall, the average production profile during the first 24h after the feeding for weeks 16, 17, and 19 was very similar in shape. During these weeks, after an initial drop, production increased for four hours on average, decreasing slowly in the following hours. The decay rate was more or less constant towards the end, leading to a value after 24h slightly higher than the initial one. In week 18, maximum production was achieved faster than other weeks, 3 hours on average, being sustained for 2 hours. However, the production rate decreased at a quicker pace

than other weeks, dropping on average 1400 mL/h in 12 hours, 500 mL/h more than the average of weeks 16 and 19, but achieved the same baseline as week 17. The average 24h gas production profile after feeding can be seen in Figure 48.

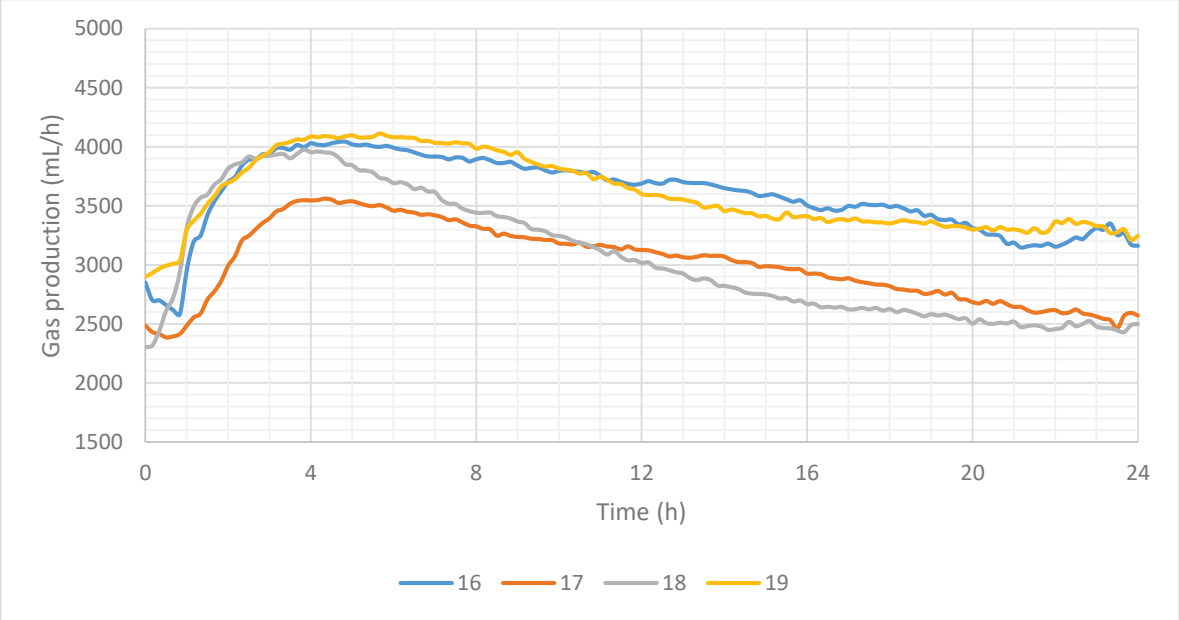

Figure 48 – 24h average gas production profile after feeding during weeks 16 through 19.

A similar shape and production profile along the weeks can be observed on the accumulated gas production between feeds, which are displayed in Figure 49. Besides September 13th when the accumulated production was 37,19 L, yields ranged between 76,67 and 90,07 L during week 16, which resulted in an average of 84,65 L for each feed-to-feed period. On the other hand, accumulated production did not surpass 85 L during week 17, ranging between 83,67 L, measured on September 21st, and 65,89 L, measured on September 22nd. This represented an overall 13% reduction in feed-to-feed production in comparison to week 16.

During week 18, accumulated production ranged from the minimum 62,38 L on September 27th to the maximum of 88,13 L on October 2nd. An accumulated production below 65 L was also verified on September 28th and 30th, when only 62,49 L and 64,29 L were produced respectively, contrariwise to other days, when production was above 75 L, as shown by Figure 49. On the other hand, week 19 showed an accumulated feed-to-feed production above 75 L during the whole week, with a maximum of 90,99 L on October 8th and a minimum of 76,00 L on October 5th.

The accumulated production on October 9th of 170,65 L is related to feed-to-feed interval being 48h instead of the average 24h.

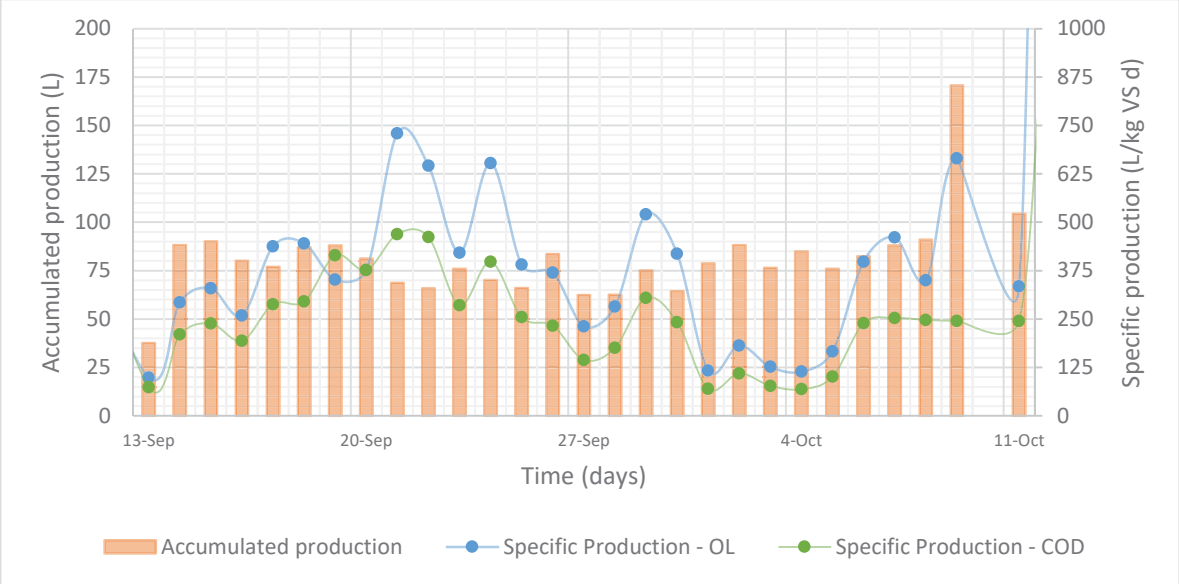

Figure 49 – Accumulated production (L) specific gas production based on the organic load (L/kg VS d), and specific gas production based on the chemical oxygen demand (L/kg COD d) between September 13th and October 11th.

Besides September 13th, which registered a value of 98,66 L/kg VS d, specific gas production during week 16 oscillated from 259,49 L/kg VS d on September 16th to 445,26 L/kg VS d on September 18th. As shown by Figure 49, values on Friday and Saturday were similar, decreasing approximately 100 L/kg VS d on Sunday. This same behavior was observed between Tuesday and Thursday, but with an overall 100 L/kg VS lower.

Week 17 showed higher oscillations than the previous one in addition to a wider range, down from 376,54 L/kg VS d on September 20th to 729,18 L/kg VS d on September 21st. Specific production increased during September 20th, decreasing to 420,19 L/kg VS during the following two days, when it increased once again reaching 652 L/kg VS on September 24th. On the last two days of this week, yields were constant around 375 L/kg VS.

During week 18, specific production increased between September 27th and 29th, from 231,12 L/kg VS to 520,29 L/kg VS. This was followed by two days of decreasing values, down to the minimum value for weeks 16 through 19 at 116,21

L/kg VS on October 1st. Afterward, specific production slightly increased but stayed below 185 L/kg VS until October 6th, when a value of 398,28 L/kg VS was registered. The last three days of week 19 showed an oscillation between 460,83 L/kg VS and 349,96 L/kg VS before increasing to 664,91 L/kg VS on October 9th, as shown by Figure 49.

As shown by Figure 49, specific gas production regarding COD increased during week 16, from a value of 73,94 L/ kg COD d on Monday to 414,42 L/ kg COD d on Sunday. After slightly decreasing on September 20th, 376,46 L/ kg COD d, yields increased to 361,74 L/ kg COD d on the following two days, falling to 232,35 L/ kg COD d towards the end of the week. Values oscillated between 142,38 and 308,21 L/ kg COD d between September 27th and 30th, before decreasing to a range of 69,56 and 109,26 L/ kg COD d between October 1st and 5th. The final four days of the 7-days feed regime had a constant specific production regarding COD of 252 L/ kg COD d.

Different from the last period, methane concentration was measured, but only between September 27th and October 11. As shown by Figure 50, methane concentration dropped during the first days of measurements, from 64,4% on September 27th down to 60,6% on September 29th. This reduction of methane content occurred after air infiltration was detected during the feeding procedure However, only during one day between September 27th and October 11th, October 1st, air infiltration could be confirmed in the system.

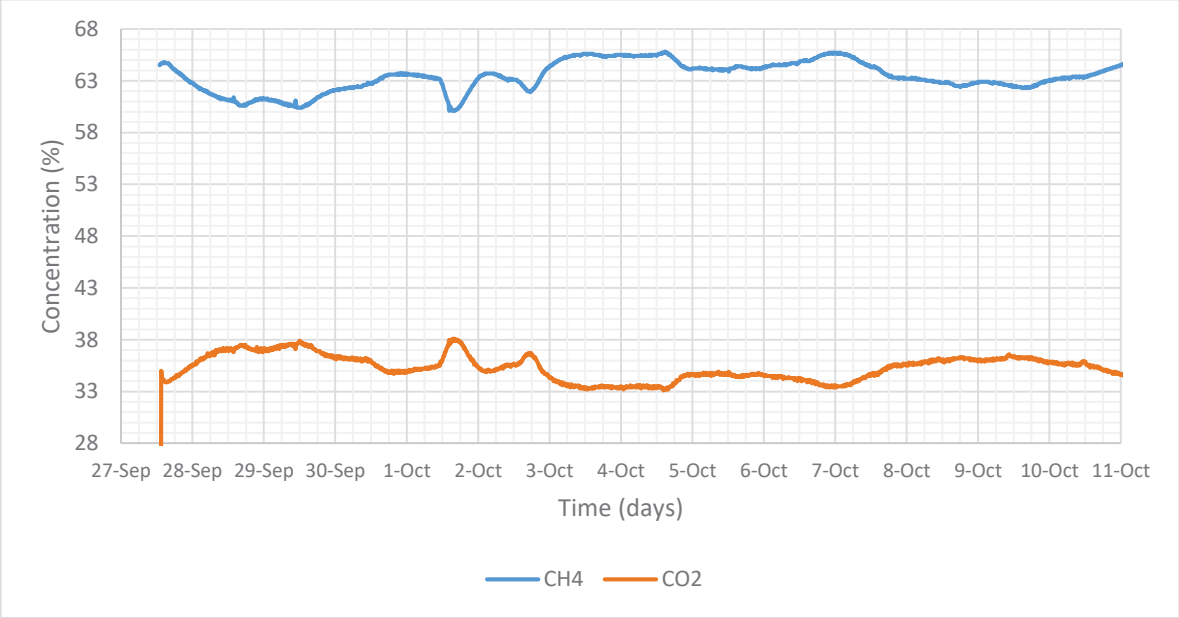

Figure 50 – Methane and carbon dioxide concentration in the biogas between September 27th and October 11th.

Moreover, methane concentration also dropped after the feeding with the highest ODM mixture of the period on October 1st. Concentration went from 63% to 60% in 12 hours, but it went back to 63,5% on the October 2nd morning. A similar drop was also observed on October 3rd, but with a lesser intensity. After these events, concentrations stabilized above 65,5% for 2 days, oscillating down to 64% afterward. Through the end of week 19, methane content operated below the 63% mark. With that, the average methane concentration was 63,5% during this measurement period, ranging from 60% to 65,8%.

Carbon dioxide concentration varies in opposition to methane. The CO_2 content in the gas ranged between 33,2% and 38,1% between weeks 18 and 19, as shown by Figure 50. This made the combined concentration with methane being above 98% during the whole period, only being below this value during 2 hours at the beginning of week 18, as shown by Figure 51. The combined concentration increase after the gas analyzers' installation increased to 99% on average toward the end of week 19, reaching 99,3% on October 10th.

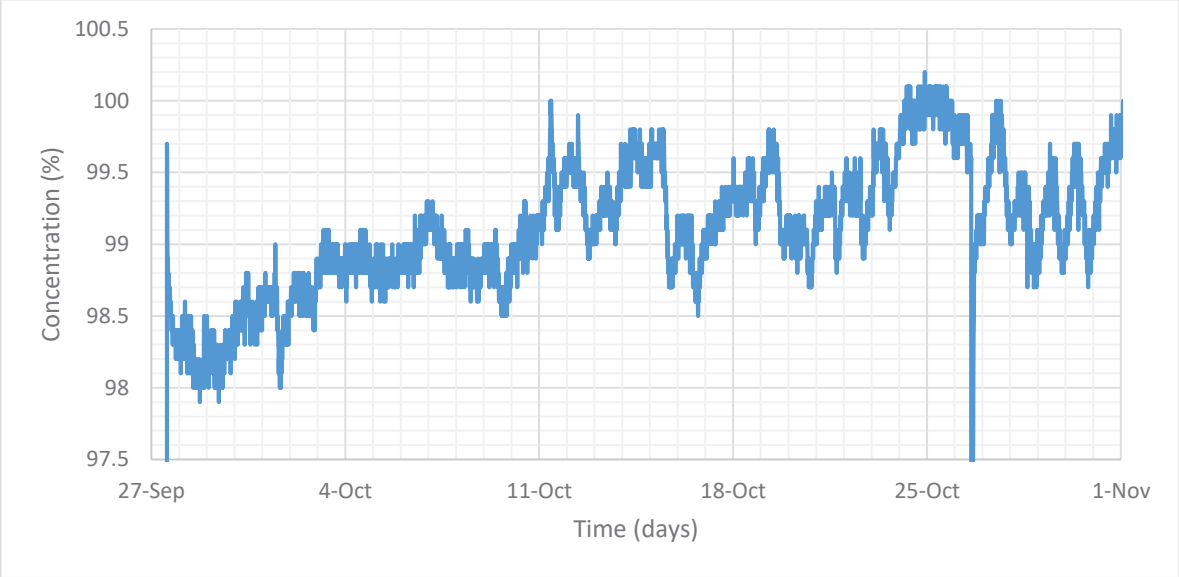

Figure 51 – Methane-carbon dioxide combined concentration between September 27th and November 1st.

6.3.5. Six-days feed regime

The period considered in this section also includes week 19 due to also being part of the HRT analysis. Therefore, period average and comparisons to other periods were done considering week 19 in both ends, if it is applicable. Week 19 data is under-discussed in this section to avoid redundancy, but it is cited when convenient to show effects of a reduced HRT or to explain any meaningful lingering effect later in sections 7.3.2 and 7.2.2.

After a period of daily feed, feeding stopped to be conducted on Sundays, leading to a weekly 6-days feeding. In addition, the total volume fed increased over time, from 10 L/day to 60 L/day, but the increase in volume was only by the addition of water and a slight increase in PS, as shown by Table 10. With that, TDM, ODM, and COD in the input were all lower than in previous weeks due to the dilution of PS.

Table 10 – Total dry matter, Organic dry matter, Chemical oxygen demand in the input and output during weeks 19 through 22.

Week	Input			Output		
	TDM (%)	ODM (%)	COD (mg/L)	TDM (%)	ODM (%)	COD (mg/L)
19	4,16 ± 2,53	3,61 ± 2,15	57567 ± 37213	0,44 ± 0,35	0,22 ± 0,21	1997 ± 854
20	1,05 ± 0,63	0,91 ± 0,56	14265 ± 7974	0,37 ± 0,25	0,22 ± 0,17	3178 ± 2974
21	0,98 ± 0,37	0,75 ± 0,21	11718 ± 3207	0,16 ± 0,02	0,10 ± 0,01	1265 ± 85
22	0,70 ± 0,19	0,62 ± 0,19	9209 ± 1732	0,19 ± 0,11	0,13 ± 0,11	1067 ± 271
Period	1,72 ± 1,87	1,47 ± 1,61	23190 ± 26637	0,29 ± 0,24	0,17 ± 0,14	1877 ± 1650

The input composition also showed certain variability besides ones related to dilution effects. TDM and ODM had similar behavior to weeks 16-19, values were kept similar only for a maximum of two days, changing afterward, as shown by Figure 52 and Figure 53. On October 22nd and 23rdPS quality was low, showing a TDM below 0,4% in the period. For that reason, 20 L of PS was fed on October 23rd each day without the addition of water, after the low quality had been confirmed by the TDM analysis. On October 14th, a higher quality sludge was obtained, allowing the return to the planned feeding mixture. Besides these days on week 20, a low concentrate PS was fetched only on the 20th of October, having high concentrations during all other days.

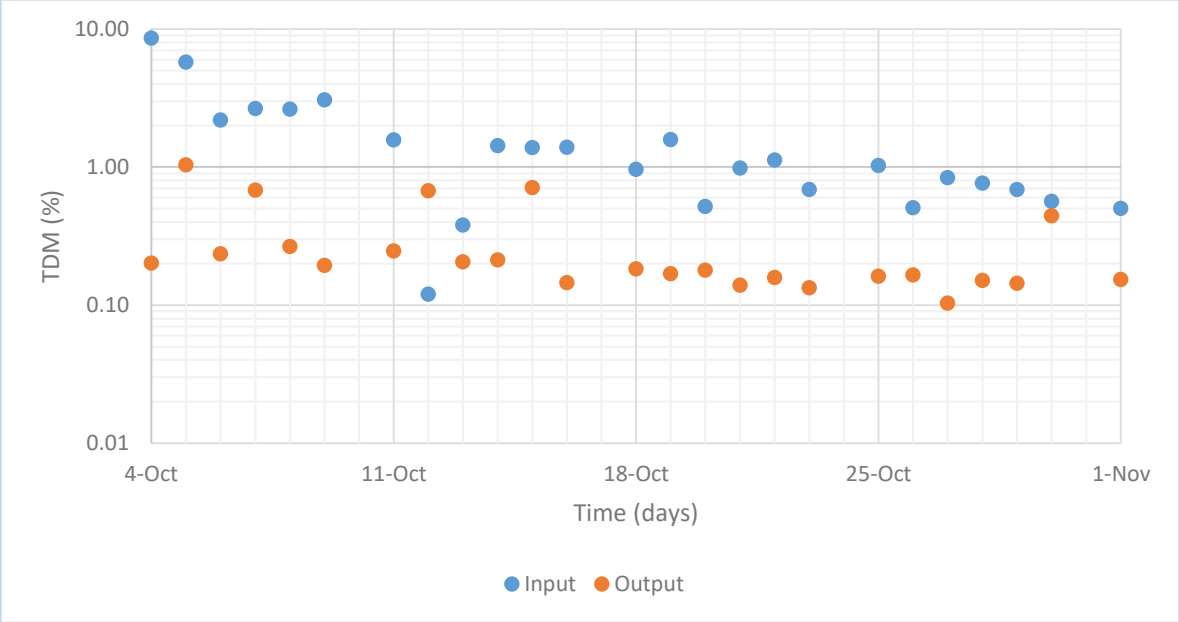

Figure 52 – Total dry matter in the input and output between October 4th and November 1st.

With that, ODM in the input was kept between 0,7-1,5% during most of the period, as shown by Figure 53. Due to dilution, ODM decrease over the weeks, but the reduction was controlled to not feed the digester with a too diluted mixture. Therefore, on weeks 21 and 22, an additional 2L of PS was added with the commonly used 10 L. However, ODM in the input range between 0,50% and 1,6% during week 21 and were below 1% during week 22, lowering along the week. But with this change, extremely low values as the ones observed on October 12th and 14th were not verified in the feeding mixture anymore

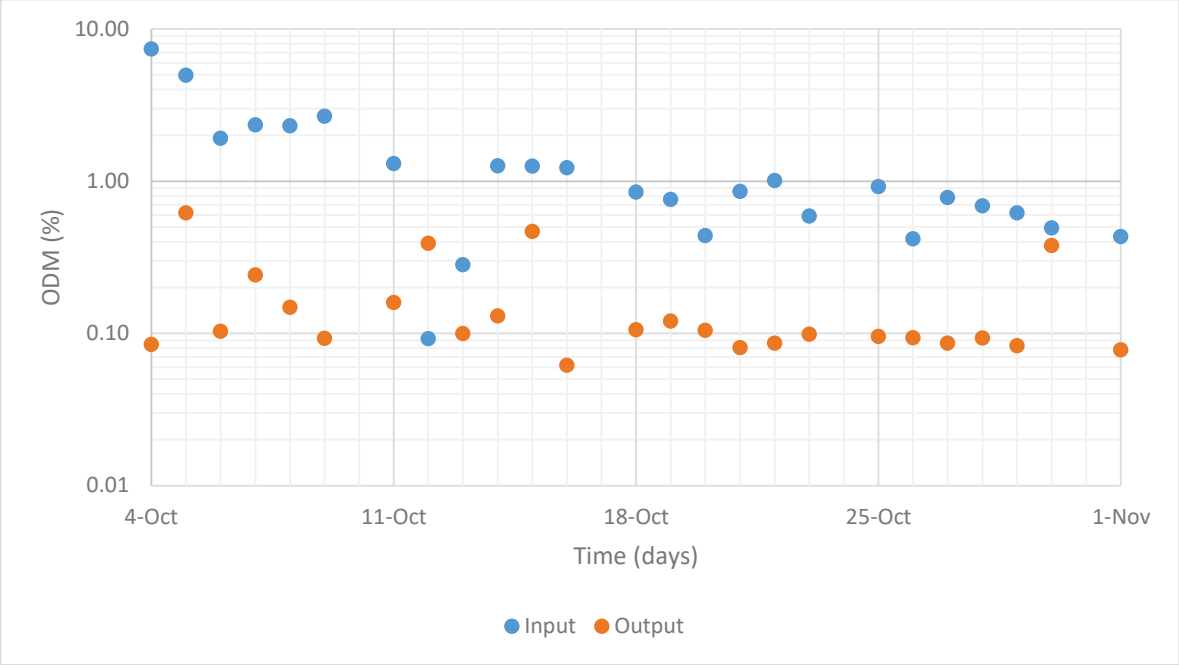

Figure 53 – Organic dry matter in the input and output between October 4th and November 1st.

COD in the input followed the profile observed for TD and ODM. Besides drops when only a low concentrate PS was available, COD was kept above 10000 mg/L even in high diluted mixtures in week 22, dropping below this mark only three times. Moreover, week 21 had the lowest ratio between ODM and COD, 0,59, which was considerably lower than adjacent weeks. Variations in COD showed also to be slightly smoother than what was observed for TDM and ODM, as shown in Figure 54.

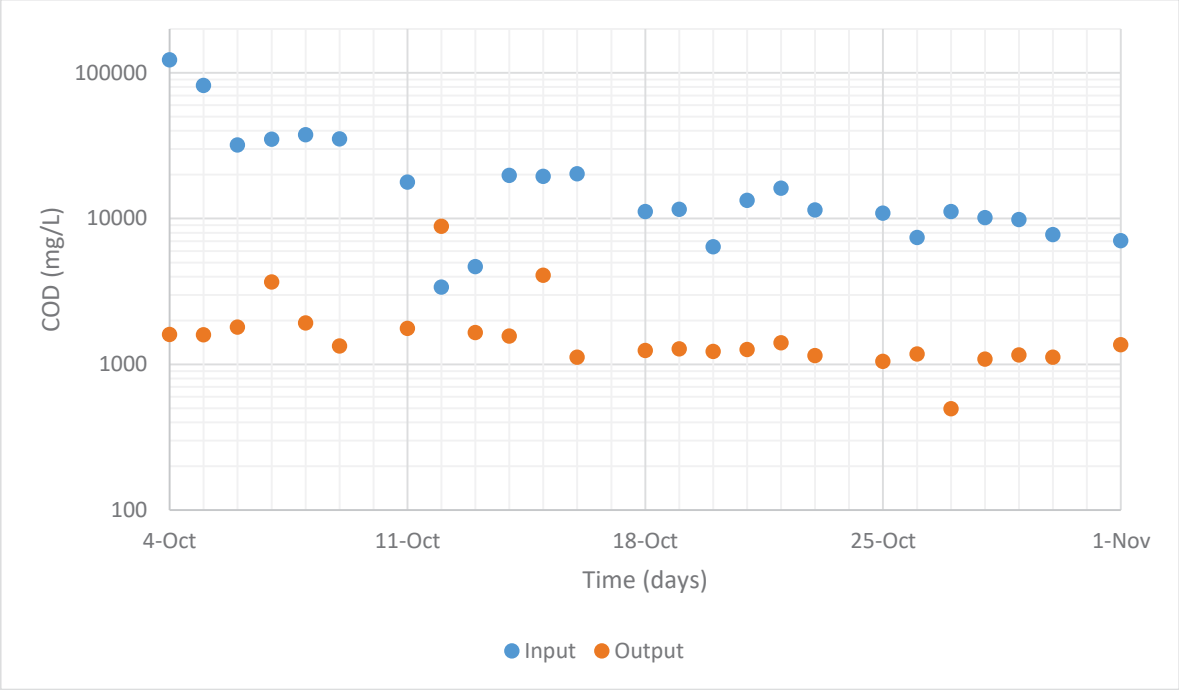

Figure 54 – Chemical oxygen demand in the input and output between October 4th and November 1st.

With that, the average quality of PS was 25,19 g/L of ODM and 39,11 g/L of COD between weeks 19 and 22. This was slightly lower on average of what was obtained between weeks 16 and 19, lowering which was more expressive in week 20, when the reactor was fed with a total of 775 g/m³d. This was reflected in the low-quality PS on October 22nd and 23rd, which reduced the overall quality of the sludge to an average of 15,53 g VS/L of PS. However, the low OL during week 20 was compensated during weeks 21 and 22, when the PS quality was better. OL, COD, HRT, and PS quality are shown in Table 11.

Table 11 – Average organic and chemical oxygen demand loads, primary sludge quality, and hydraulic retention time during weeks 19 through 22.

Week	HRT (days)	OL (kg/m³d)	COD load (kg/m³d)	PS (L)	ODM/PS (g/L)	COD/PS (g/L)
19	23,37	1,440	2,463	10	33,66	57,57
20	11,69	0,775	1,225	10	15,53	24,54
21	7,79	0,965	1,504	12	18,80	29,30
22	3,90	1,682	2,449	12	32,76	47,83
Period	11,69	1,215	1,910	11,4	25,19	39,11

In addition, OL and COD load followed the behavior of the mixtures TDM, ODM, and COD during the weeks. As shown by Figure 57, the load was kept constant in intervals of up to 4 days, with some days of slightly lower values in-between. After week 19, OL was above 200 g/day on most days, being lower only on 3, October 12th, 13th, and 20th. During all weeks, OL and COD loads were kept high through the end of the week.

About the output during this period, it had an overall higher instability in TDM, ODM, and COD than previously. Two new spikes were observed in week 20 in addition to the ones from week 19 with similar intensity, as shown in Figure 52, Figure 53, and Figure 54. High values were observed on the 12th and 15th of October, with a TDM of 0,67% and 0,71% respectively. ODM and COD were also high on these days, cracking an ODM 0,40% and 0,48% and a COD of 8860 mg/L and 4090 g/L, respectively for October 12th and 14th. Due to the low quality of PS on October 12th, output values were higher than input ones.

Besides problems with foam in the output, TDM and ODM in the output were below 0,20% and 0,10% respectively during the days which foam was avoided during sampling collection after week 20. However, between October 18th and 20th, ODM was slightly above 0,10%, reaching the maximum at 0,12% on October 19th. As shown by Figure 54, between October 11th and 23rd, TDM was within the range of 0,13% and 0,18%, with an average of 0,15%. This same trend was verified on week 22 as TDM values were below the 0,20% mark on five days, being higher only

on October 30th when it was verified a TDM of 0,45%. ODM had similar behavior, ranging from 0,07% and 0,09% with October 30th showing a higher value at 0,38%.

On the other hand, COD was below 1500 mg/L after October 15th, not showing the spike verified for TDM and ODM on October 30th. In addition, on October 27th, the COD in the output was 498 mg/L, the lowest value verified since August 26th when 452 mg/L was verified. However, TDM and ODM values for that point did follow the drop, being 0,10% and 0,08% respectively, as values verified for both on August 26th were 0,06% and 0,03%. These features are displayed in Figure 35 and Figure 54.

With that, reduction/retention of TDM and COD inside the reactor widely ranged in the period. Besides October 12th and 15th[3], TDM and COD removal were above 80% and 90%, topping at 89,52% on October 16th and 94,85% on October 14th respectively. As shown by Figure 55, week 20 had an overall lower retention of TDM at 65,84%, with an expressive drop on October 20th, when the value in the input was lower than adjacent days at 0,52%. COD had a similar drop during this day, but retention did not go under 80%, diminishing only to 80,81%. Besides that, COD retention ranged from 88,36% to 90,36 between October 18th and 25th.

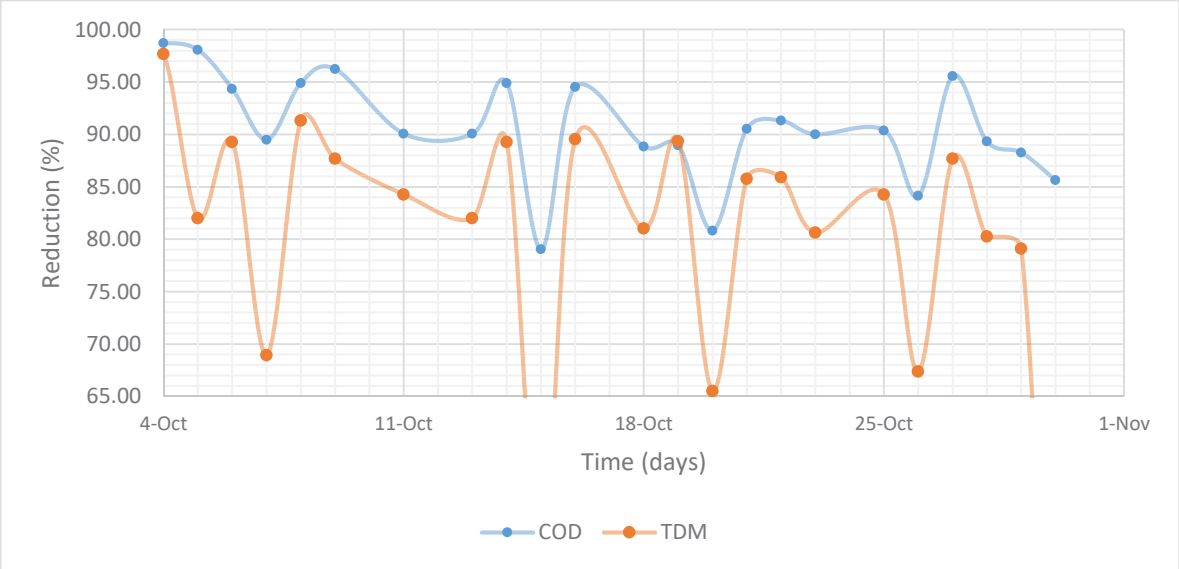

Figure 55 – Chemical oxygen demand and total dry matter reduction between October 11th and November 1st.

[3] Retention for October 12th was removed from Figure 55 due to having a negative value.

Week 22 showed retention of ODM below 85%, with an exception of October 27th when a value of 87,56% was verified. In addition, on October 26th and 30th, retention had lower values than what was observed previously, being 67,36% and 21,36¨% respectively. COD retention, however, showed a lesser drop on October 26th, as the value of 90,37% on October 25th decreased to 84,11% on the following day. After this first loss of efficiency, retention of TDM and COD increased up to 87,67% and 95,53% respectively, as shown in Figure 56. The two following days had similar values, but the last day of measurements showed a steep decrease only in TDM retention and not in COD.

Besides the two spikes in week 20, it was noticed that the aspect and color of the output changed during the feeding procedure. After some observations on the 16th of October, it was noticed that the output turned black when the feeding velocity was sustained above 200 L/h, gradually losing this color as the velocity was reduced. In addition, “chunks” of black solids were often observed with the flow during the start of the feeding procedure. They were avoided during sample collection and were collected only when no more “chunks” were verified.

Table 12 – Total dry matter and organic dry matter in the output for three different feeding flow rates.

Flow Rate (L/h)	TDM (%)	ODM (%)
150	0,15	0,08
200	0,11	0,05
300	2,15	1,35

At the end of the project, an experiment, which measured TDM and ODM of the output collected at flow rates of 150, 200, and 300 L/h, was conducted on November 1st. Values showed an increase between 200 and 300 L/h, but a decrease between 150 and 200 L/h, as shown in Table 12. The variation between 150 and 200 L/h samples was in contradiction of what was verified visually, as shown by the color of the liquid collected. This difference in aspect is shown in Figure 56, in which samples were disposed of from the left to the right: 150, 200, 300 L/h.

Figure 56 – Output samples for feeding flow rates of 300, 200, and 150 L/h on November 1st.

In addition, total dissolved solids analyses were conducted between October 18th and 30th to verify if changes of TDM and ODM were reflected on it. Results for such analyses showed an overall dissolved solids value under 0,15% during the period, being overshadowed by the one obtained on the 30th of October. On this day, the material retained in the filter (solids in suspension) showed similar values to others, however, the difference to TDM (which gives values of dissolved solids) was way higher, as seen in Table 13. This confirmed the fact that the sampling procedure was inadequate on that day because samples used for TDM and dissolved solids were collected at different times.

Table 13 – Solids in suspension and dissolved solids in the output between October 18th and 30th.

Date	Solids in suspension	Dissolved Solids
18/10/2021	0,06%	0,12%
19/10/2021	0,07%	0,10%
20/10/2021	0,04%	0,13%
21/10/2021	0,09%	0,05%
22/10/2021	0,06%	0,10%
25/10/2021	0,05%	0,08%

26/10/2021	0,09%	0,07%
28/10/2021	0,03%	0,13%
27/10/2021	0,03%	0,08%
29/10/2021	0,07%	0,08%
30/10/2021	0,06%	0,38%

Moreover, the inorganic matter content in the input ranged between 0,03% and 1,21% and the output 0,02% to 0,801%. The average for the period was calculated to be 0,24% in the input and 0,14% in the output, which consists of a dry content of 14,40% and 41,14%. This led to an average reduction of 40,42% from the input and output. This value was the lowest obtained by the period due to two days during that time having a low-quality sludge, bringing the removal of solids to the same levels at the output, even with a constant content in the output.

Regarding gas production, weekly production was overall 12% higher than the period between weeks 16 to 19, with a total production of 2396,94 L. Despite the lower OL, weeks had a weekly production above 600 L, with week 21 having the overall highest at 629,36 L/week. In addition, higher production was observed even though the reactor was not being fed during Sundays in the period. Total gas production and production per kilogram of OL and COD as well as per liter of PS can be seen in Table 14.

Table 14 – Total biogas production and yields for the amount of feed during weeks 19 through 22.

Week	Biogas (L)	Biogas /OL (L/kg)	Biogas/COD (L/kg)	Biogas/PS (L/L)
19	592,85	293,53	172,52	9,881
20	616,11	566,76	358,62	8,802
21	629,36	465,02	298,37	8,741
22	560,68	237,70	162,83	7,790
Period	2396,94	351,52	224,00	8,755

This reflected into values of production relative to the amount of OL, COD, and PS. Overall, values were higher in comparison to the period between weeks 16 and 19. Yields were at their highest in week 20, when 566,76 L/kg VS were produced, representing 358,62 L/kg COD. This higher production efficiency is partially explained by not feeding the reactor on Sundays, adding more time to gas being produced for the same amount of feed. However, the average from the period was even higher than the maximum observed between weeks 10 and 15, 474,33 L/kg VS in week 14. Production for the amount of PS was 28% higher than the combined average of the previous 9 weeks.

Production profile during week 20 had a distinct shape than observed in week 19, as shown by Figure 57. On October 11th, production rates increased after the feeding procedure from a baseline of 2739 mL/h to a local maximum at 3804 mL/h within 5 h. This was followed by a reduction towards a local minimum of 3541 mL/h six hours later, increasing once again up to the maximum of 4029 mL/h afterward. Top production was achieved 4 hours before the feeding started to be conducted on October 12th.

On the following two days, the profile showed a similar shape to week 19, which a well-defined maximum of 2-3 hours followed by a deceleration in production. However, the decrease in production on October 12th was slower than October 13th, as the second day had a fast decay and slow decay phase, as shown by Figure 57. A decreasing trend was observed during these days, baseline production and top production reduced from 3031 mL/h and 3904 mL/h to 2484 mL/h and 3472 mL/h, respectively. It is important to note that the feed-to-feed interval between 12th and 13th was 5 hours smaller than 13th and 14th in addition to OL during these days being the lowest during the 6-days feed regime.

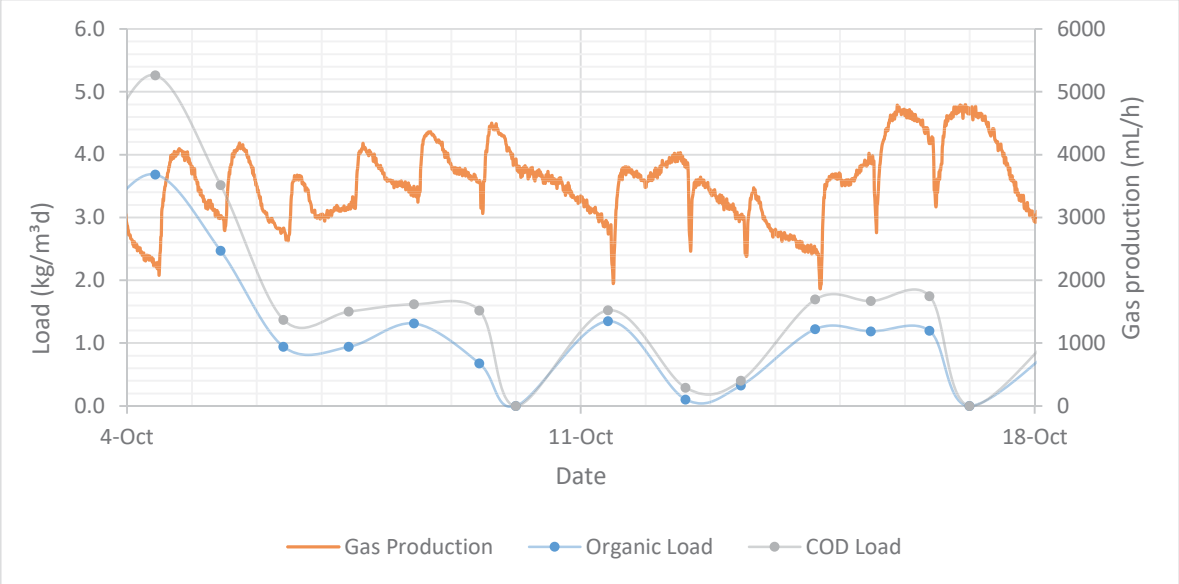

Figure 57 – Gas production (mL/h), organic load (kg/m³d), and chemical oxygen demand load (kg/m³d) between October 4th and 18th.

On October 14th, production had a similar profile as observed on October 11th. After feeding, production increased reaching a local maximum at 3703 mL/h within 5 hours of feeding, decreasing to a local minimum at 3512 mL/h three hours after. Following this, production slowly increase towards the maximum at 4017 mL/h, when started to drop once again until the next feeding on October 15th. During both 11th and 15th, top production was not well-defined, as values oscillate around the maximum instead of quickly decreasing.

October 15th and 16th had a similar profile to what was observed on weeks 14 and 15 but with a longer closure of the gas collection valves, as shown by comparing Figure 39 and Figure 57. On October 15th, production reached a well-defined maximum of 4787 mL/h 9h after the feeding, decreasing until the next feeding with a parabolic shape. This behavior happened similarly on October 16th, regarding the shape, time to the maximum being reached, 8h, and the maximum itself at 4795 mL/h. In both cases, production decrease did not lead to a baseline production, as the production profile shape did not change to a more stable one within 24 h of feeding.

Week 21 showed a similar production rate profile as the last four days of week 20. On October 18th, production increased to a local maximum at 3521 mL/h 3

h after feeding, decreasing to a local minimum at 3153 mL/h 4 hours later. Afterward, production increase over 12h until reaching the top production at 4088,94 mL/h, as shown in Figure 58. The following two days had a similar shape, increasing towards a well-defined maximum above 5000 mL/h after 8 h of feeding and decreasing until the next feed. On both days, no end baseline could be verified, but rates just before the feeding procedure were approximately 1000 mL/h higher on October 20th than October 21st.

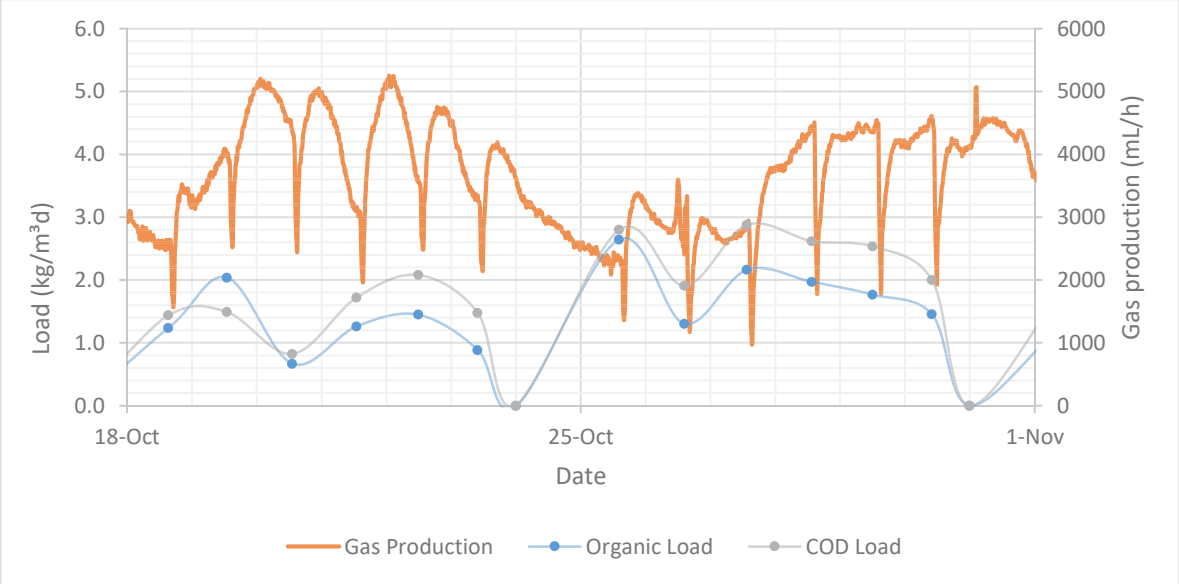

Figure 58 – Gas production (mL/h), organic load (kg/m³d), and chemical oxygen demand load (kg/m³d) between and October 18th and November 1st.

Between October 21st and 25th, the production profile kept a similar shape to the previous days, but time for the maximum production to be achieved and the maximum production itself reduced over the week. Time for reaching top production went from 8 hours with top values going from 5251 mL/h to 4188 mL/h on October 21st to 4 on October 23rd, respectively. In addition, an initial formation of production baseline could be identified on October 22nd and 23rd, being close to the 3200 mL/h' mark, as illustrated in Figure 58.

On the other hand, the profile on week 22 was not similar to what was observed during the 6- and 7-days feed regime. Four hours after feeding the reactor on October 25th, production rates increased towards a maximum of 3381 mL/h,

starting to decrease to 3051 mL/h until the next feed. The spikes in production during the feeding procedure on October 26th were caused by the necessity to manipulate the gas collection valves. These variations can be observed in Figure 58.

Profile on October 26th was similar to what was observed on October 14th, but the secondary increase did not surpass the local maximum reached after feeding. Maximum rates were achieved 4 hours after the feed at a level of 2980 mL/h, decreasing towards a local minimum at 2588 mL/h afterward. Rates started to increase after this point, reaching a value of 2943 mL/h just before the next feeding started, as shown by Figure 58 and Figure 60.

The following three days, October 27th through 29th, had a higher overall production with a different profile than previous days, as shown by Figure 58. During the three days, production first increases to a local maximum of 4h after the feeding, staying at the value for approximately 5 hours. Afterward, the rate continuously increased towards the next feeding, achieving a well-defined maximum on October 27th and 29th, but oscillating around a virtual maximum on October 28th. Differences between local and true maximum were higher on October 27th and 29th, as the increase was from 3701 mL/h and 4118 mL/h to 4498 mL/h and 4610 mL/h. The production rate increment of October 28th was between production oscillations, as the global maximum cannot be defined, having a difference of 195 mL/h.

Overall, the average profile of the first 24h after feeding was different between weeks 19 to 22, as shown by Figure 59. Comparing the profiles, it was observed that week 19 reached peak production fasters than other weeks and this time increased with the decrease of overall HRT in the following weeks. This meant a difference from 6 hours in week 19 to 20 hours in week 22, which showed small increases of production rates over the hours, decreasing only close to the next feed.

In addition, the decay of the production rate was also slower for lower HRT, with week 22 not showing a reduction in production rates. Variations at the end of the 24h cannot be confirmed due to intervals between feed-in weeks 21 and 22 being lower than 24 on Thursdays to Fridays. Even with this problem, the production baseline can be visualized in Figure 59, showing higher values for lower HRT. However, the difference between them is all within the 3000-3500 mL/h range.

Moreover, the greater reduction of production on the first hours after feeding was due to the increasing time of the feeding procedure over the weeks. To achieve lower HRT, a greater amount of volume had to be fed, which increased the amount of time require to complete de procedure. On week 22, when the largest daily volume was used, the procedure lasted up to 40 min, which ultimately led to a longer recovery time for the gas production.

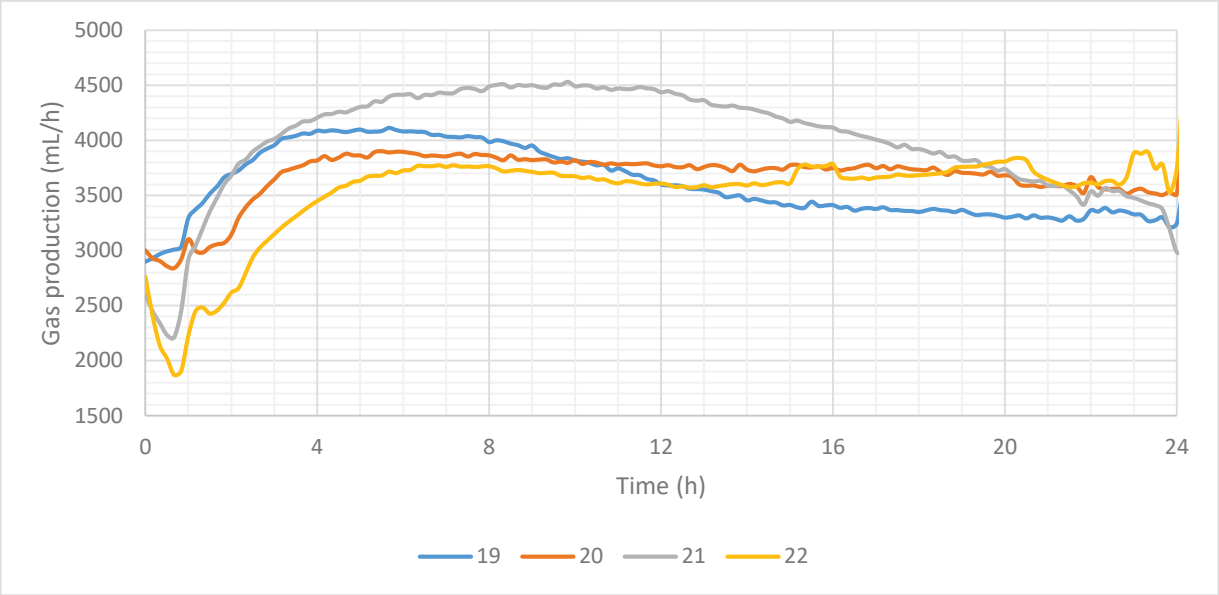

Figure 59 – 24h average gas production profile during weeks 19 through 22.

As shown in Figure 60, the production profile during the first 24 h after the last feeding in each week was similar to what was observed on average during normal operating days. However, during week 22, production increased for 24h until reaching a plateau and finally started decreasing in steps. This was different from other weeks which decreased smoothly during the weekend. Except for week 21, weeks topped at values above 4500 mL/h decreasing to a production of 2500 mL/h after 48 hours. Even with the highest maximum production at 4709 mL/h, the final production of week 20 was only higher than week 21 at 2580 mL/h.

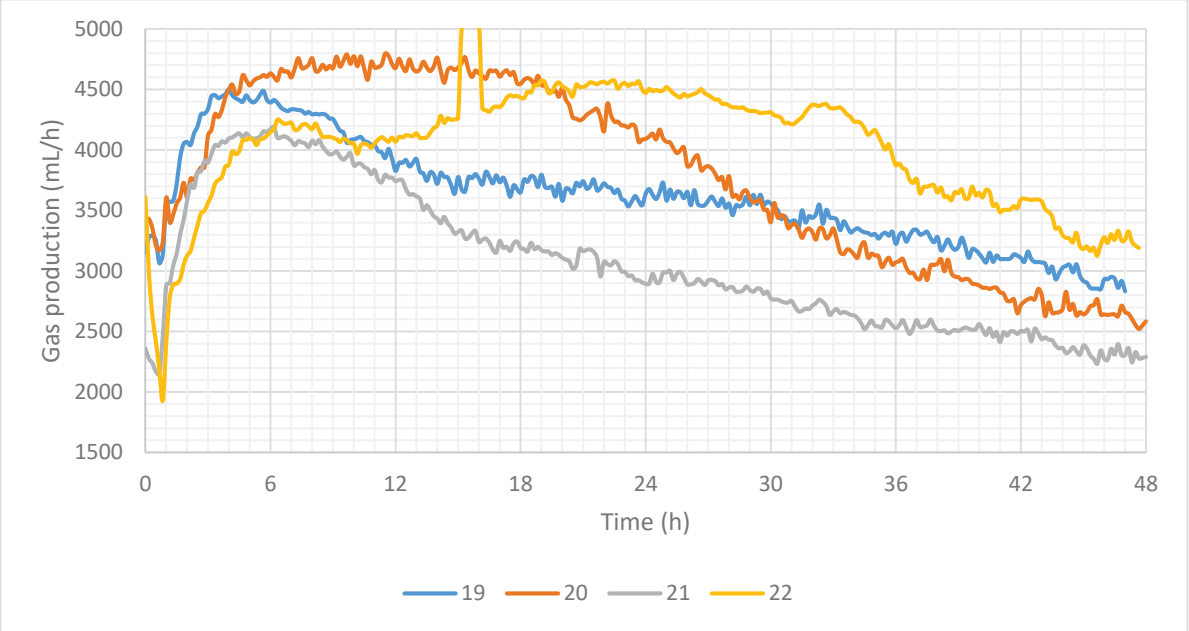

Figure 60 – 48h gas production profile after feeding on weekends during weeks 19 through 22.

In addition, weeks 19 and 21 had the shortest time to reach top production, 4 and 6 hours respectively, as weeks 20 and 22 only reached maximums after 12h and 22h. This was in concordance with maximum productions during weeks 20 and 22 being higher than the other two. The unusual peak observed in week 22 on the 31st of October cannot be considered top value, because it happened due to failure in the gas clock related to unknown reasons.

Even with a long period without feeding analyzed, the period for the production to reach half of the maximum production could not be observed for all four weeks. As shown by Figure 60, production rates for all weeks did not reach values below 2250 mL/h. This was in contradiction of what was observed during weeks 12 to 15, which required 22h after the maximum was achieved to reach half production. Moreover, end values obtained after 48h were twice as high, with week 22 cracking 3191 mL/g after 48h.

With that, the accumulated gas production feed-to-feed ranged from 60,92 to 110,49 L between weeks 19 and 22, excluding weekends. During week 20, accumulated productions were 104,35 L and 96,7 L on Monday and Friday, respectively, with the days in between having similar production around 75 L, as shown by Figure 61. On the other hand, week 21 had its lowest values on Monday

and Friday, being respectively at 75,04 and 87,81 L, as days between October 19th and 23rd ranged from 87,01 kg/m³d and 110,49 kg/m³d.

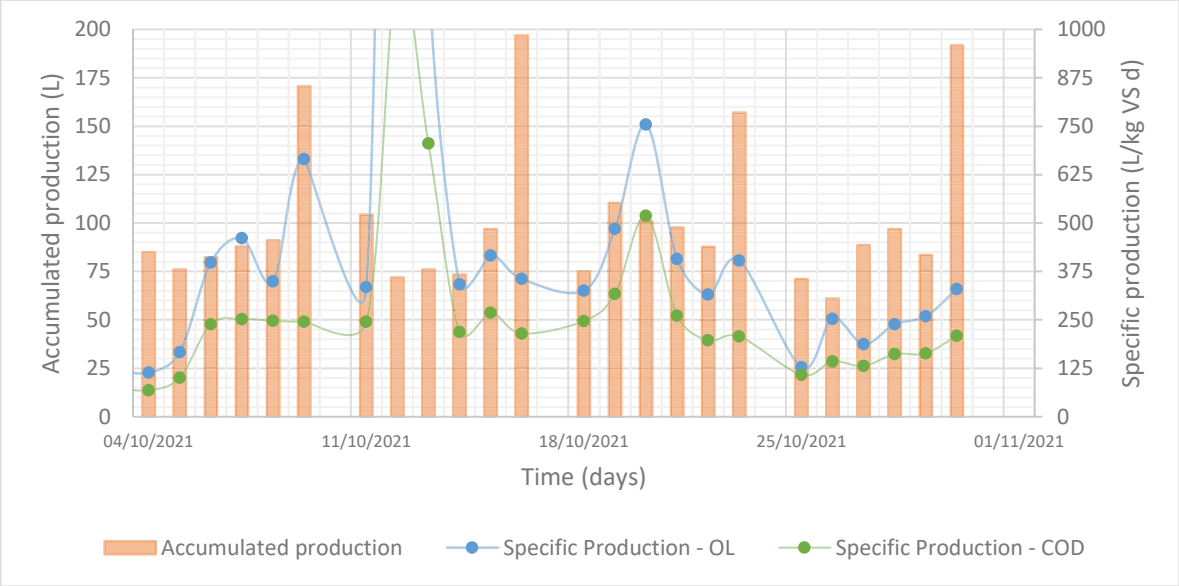

Figure 61 – Accumulated production (L), specific gas production based on the organic load (L/kg VS d), and specific gas production based on the chemical oxygen demand (L/kg COD d) between October 4th and November 1st.

During week 22, accumulated feed-to-feed production was below 75 L on the first two days, which a total production for the two days of 131,92 L. The accumulated production on October 27th and 28th were higher than the previous two days, with a total of 88,63 L and 96,83 L respectively, decreasing on October 29th, as only 83,41 L of gas were produced. As shown by Figure 61, production over the weekends was higher on weeks 20 and 22, with values of 196,84 L and 191,82 L respectively, in comparison with weeks 19 and 21, which had 170,63 L and 157,06 L respectively.

The accumulated production in combination with the OL is reflected in the specific production shown in Figure 61. After a specific production of 334,39 L/kg VS d on October 11th, values exploded on October 12th and 13th, reaching 4244,22 L/kg VS d and 1172,42 L/kg VS d respectively, as OL during this period were below 0,4 kg/m³d. Yields dropped to 342 L/kg VS d on October 15th, being around this value until October 18th when specific production was 325,31 L/kg VS d. An increase of specific products on a low feed day was observed also in week 21, where values of 754,34 L/kg VS d were observed on October 20th when OL was 0,668 kg/m³d.

Yields at the end of week 21 ranged between 407,70 L/kg VS d and 315,27 L/kg VS d, oscillating down and upwards until decreasing to lower values during week 22, as shown by Figure 61. Specific production on October 25th was 128,32 L/kg VS d, being as low as what was calculated for the period between October 1st and 5th when OL was above 3,5 kg/m³d. Specific production increase over the following days, reaching 253,54 L/kg VS d on October 26th up to 329,83 L/kg VS d on October 30th. However, values during weekdays were lower than what was observed during the other three previous weeks.

In addition, specific production regarding COD peaked on October 12th and 13th above 700 L/ kg COD d, reaching 1156,34 L/ kg COD d, before dropping to range between 215,45 and 268,92 L/ kg COD d on the following three days. During week 21, yields increased during the first three days of feeding, from 247,21 L/ kg COD d on October 18th to 519,13 L/ kg COD d on October 20th, but values decreased towards the end of the week, down to 207,49 L/ kg COD d. As shown by Figure 61, specific production regarding COD increased over the week, from 108,34 L/ kg COD d on October 25th to 209,42 L/ kg COD d on October 30th, oscillating down on October 27th before climbing once again.

Moreover, methane content in the period ranged between 62,3% and 72,1%, with an average of 66,1%±2,4%, as shown in Figure 62. Concentration oscillated between weeks as well as within a week, but with similar timings. Values were above 68% on Mondays during weeks 20 to 22, steadily dropping to 64% afterward on weeks 20 and 21 and 66% on week 22. After, concentrations showed a recovery over the week, dropping once again as the PS quality changed on Thursdays during weeks 20 and 21.

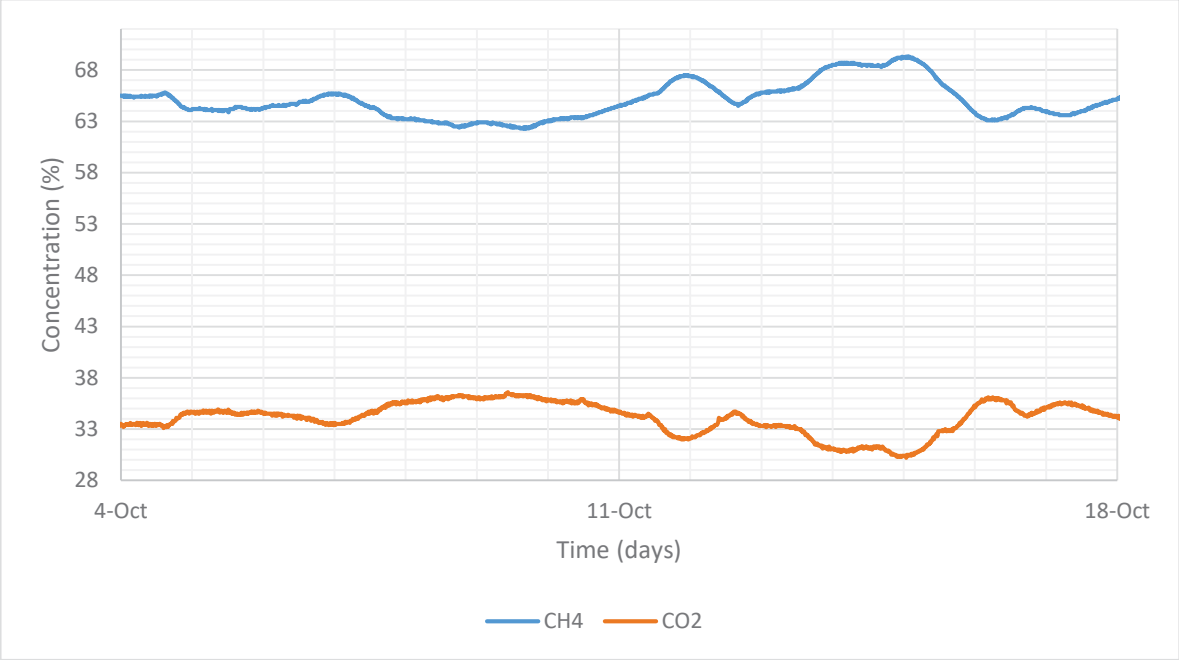

Figure 62 – Methane and carbon dioxide concentration in the biogas between October 4th and 18th.

Besides the drop observed on the 26th of October, no other drop could be identified through weeks 20 to 22, as seen in Figure 62 and Figure 63. In addition, drops did not happen immediately after feeding, concentrations increased for on average 8 hours after feeding before starting to crumble. Moreover, it was observed during weeks 20 and 22, that recovery in concentration happened immediately after feeding, which was not verified in week 19.

As shown by Figure 62, between October 24th and 26th, concentrations were above 68%, showing a smaller decay in comparison to other weekends during the period. As a similar quality PS was fed after Wednesday during the previous days, the concentration drop on Thursday was smaller, leading to a higher value on the last feeding day. With that, the system sustained a gas quality close to the maximum over the weekend until being fed once again.

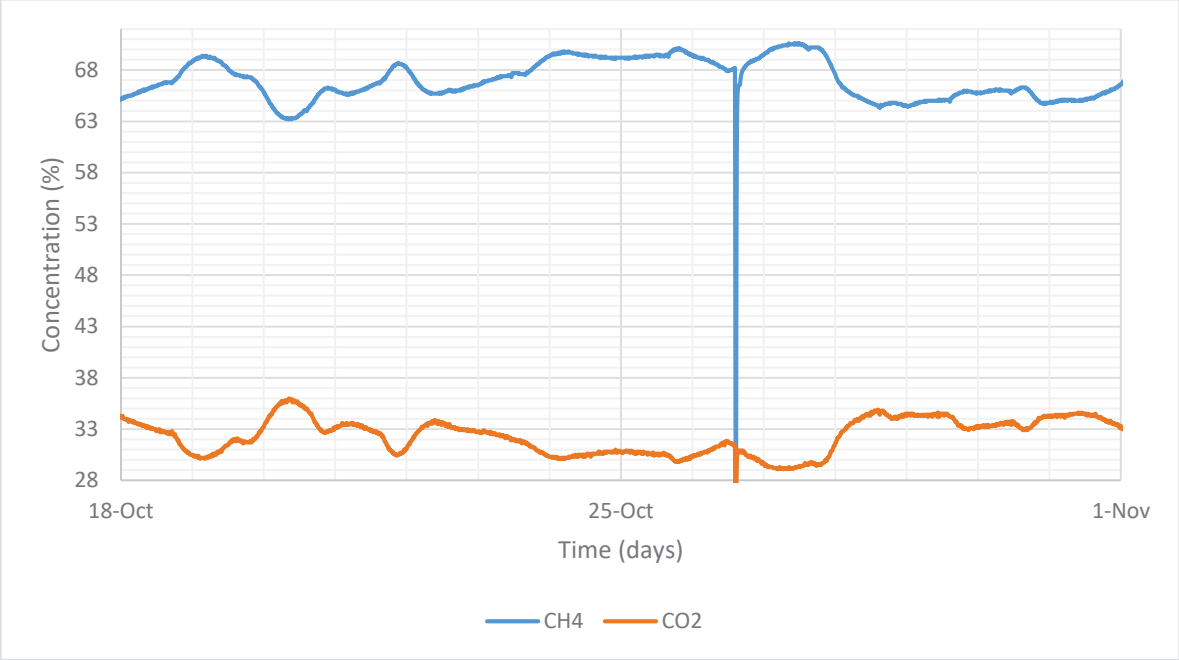

Figure 63 – Methane and carbon dioxide concentration in the biogas between October 18th and November 1st.

Moreover, after the air infiltration on the 26th of October, methane concentration did not only increase but switched from a clear decreasing trend to a clear increasing one. Even with this problem, feeding was conducted normally with PS with similar quality as the one used on the previous day. With that, methane concentration showed the same behavior as observed on Mondays and Tuesdays of the weeks 20 and 21, but with a higher top concentration, 70,4%. After this decay, methane content did not recover back to 70% during the week, it only oscillated between 64 and 66%. However, after the weekend content showed an increasing trend, reaching 72,1% at midnight of the 1st of November (normal feeding did happen during this day).

With methane and carbon dioxide measurements, methane production for the period could be determined, as shown in Figure 64. The shape and variation of the production profile were very similar to the total gas production. Methane production was between 3500 mL/h during top production and 1500 mL/h just before the first weekly feed. The accumulated production for the period was 1598,7 L

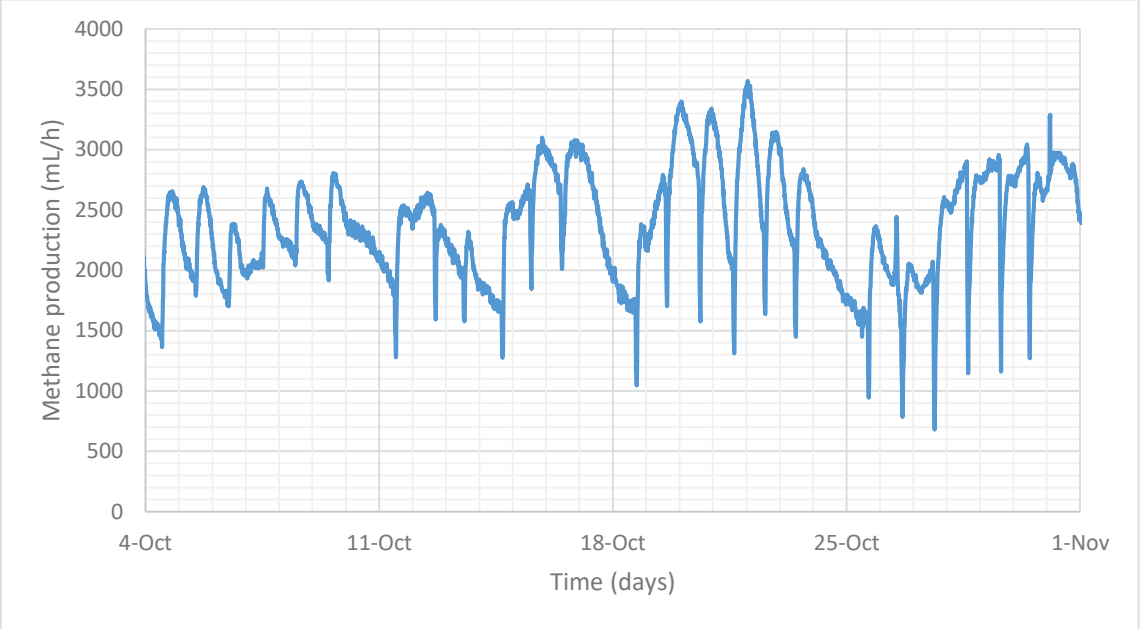

Figure 64 – Methane production between October 4th and November 1st.

6.4. Mass balances

For the mass balances, the initial load used during the startup was neglected, hence calculation only refers to differences from an initial state set on August 2nd. With this, and considering that the gas produced was only due to the ODM and water conversion to gas is null, accumulation of solids could be determined and it is plotted in Figure 65, Figure 66, and Figure 67. For days which the gas quality was unknown (all days until September 27th), the average methane and carbon dioxide concentrations of 65,6% and 34,3% respectively were considered.

With these considerations, it was calculated that the total accumulation between August 2nd and September 13th was 2,909 kg. The following three weeks had a faster accumulation, increasing the mass retained in the reactor by 2,351 kg, a rate 126% faster. Due to extremely high concentrate PS, weeks 18 and 19 had the greater accumulation rate registered with a total of 4,056 kg in two weeks. The following week only a small accumulation of 294 g was registered, with a reduction between October 13th and 14th. The last two weeks of experiments showed slightly lesser retention of matter than weeks 16 and 17, with a total of 2,314 kg. A summary

of the mass balances for volatile and total solids from weeks 10 through 22 is displayed in Table 15.

Table 15 – Weekly summary of mass balances from weeks 10 through 22.

Week	Input		Output			Accumulation	
	ODM (kg)	TDM (kg)	ODM (kg)	TDM (kg)	Gas Production (kg)	ODM (kg)	TDM (kg)
10	0,470	0,547	0,027	0,059	0,111	0,332	0,377
11	0,648	0,755	0,022	0,048	0,141	0,484	0,566
12	0,522	0,609	0,023	0,050	0,170	0,329	0,388
13	0,707	0,833	0,020	0,042	0,203	0,485	0,588
14	0,682	0,759	0,039	0,081	0,276	0,368	0,402
15	0,859	0,943	0,023	0,075	0,280	0,556	0,588
16	1,864	2,202	0,051	0,100	0,464	1,349	1,639
17	1,066	1,256	0,049	0,115	0,439	0,577	0,702
18	2,575	3,052	0,074	0,122	0,442	2,059	2,488
19	2,020	2,342	0,133	0,262	0,512	1,375	1,568
20	1,087	1,258	0,177	0,440	0,524	0,386	0,294
21	1,353	1,763	0,110	0,290	0,530	0,714	0,944
22	2,359	2,641	0,204	0,704	0,566	1,589	1,372
Total	16,212	18,959	0,954	2,386	4,658	10,601	11,915

At the end of the experiments period, it was estimated that accumulation between August 2nd and November 1st was in TDM 11,915 kg and ODM 10,601 kg. This represented an accumulation rate of on average 917 g/week in TDM and 816 g/week in ODM. Weekly ODM ranged between 329 g to 2,059 kg during the period, being higher than TDM's in weeks 20 and 22. Overall, ODM corresponded to 88,9% of the matter accumulated during the period, being never below 75% weekly. It is important to point that problems with sampling during week 22 might have caused the ratio ODM/TDM to be unreliable.

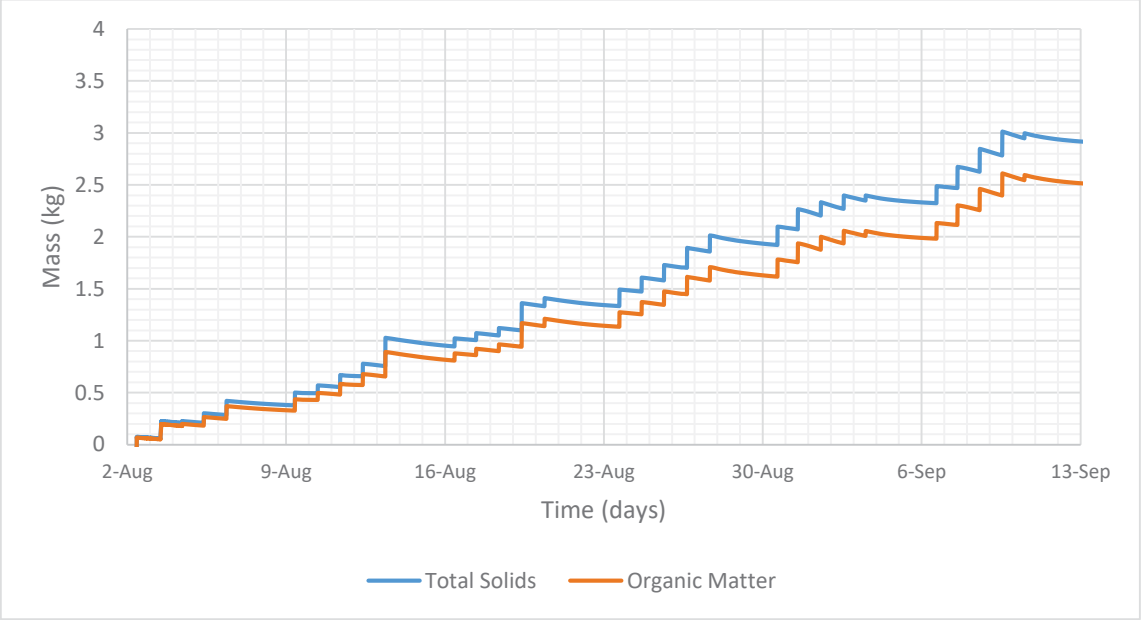

Figure 65 – Solid matter and organic matter accumulation into the reactor between August 2nd and September 13th.

If one considers the concentration of the whole substrate the average values measured at 12 to 16 (see Figure 10) after August 9th, 2,75%, one can estimate the accumulated volume to be 433,7 L. This represented an increment in volume of the concentrated phase of 33,4 L a week, which would have made the concentrated phase level reach the output in 9 weeks if the reactor was empty. With that, as the total amount of solid matter in the reactor is estimated to be at a minimum of 11,915 kg, the total volume of the dense phase should have been at least 433,7 L.

Moreover, the accumulation of inorganic matter was calculated to be 1,315 between August 2nd and November 1st, with represent 47,9% of the total fed during the period. This represented an accumulation rate of on average 102 g a week, being at highest in week 18 and at lowest in week 22, with values of 429 g and -217 g. It was estimated that the inorganic matter accumulation during the 5-days feeding period was 357 g, being lower than what was calculated for the following two weeks, 415 g, but higher than the combined four last weeks, 114 g.

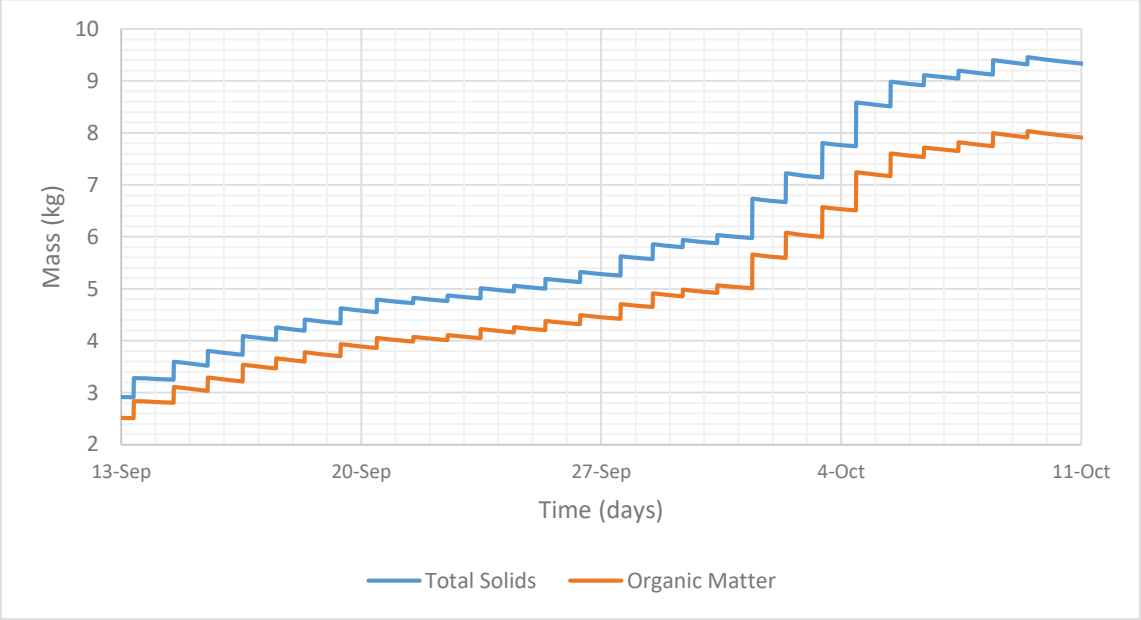

Figure 66 – Solid matter and organic matter accumulation into the reactor between September 13th and October 11th.

As seen by Figure 65, after the normal operation started, accumulation increased by 1 kg after 12 days of feeding, on August 18th. After this point, the accumulation rate increased, being 2 kg being reached on August 31st, with a more expressive inorganic fraction. After this period, approximately 700 g of solids were retained before the 7-days feed regime started.

With the increase in periodicity of feeding and input, the rate of matter being retained in the reactor increased, as accumulation during week 16 was 1,639 kg. As shown by Figure 66, accumulation reached 4 kg of TDM on 16th, but it took 10 days to surpass the 5 kg mark, as retention decelerated over week 17. This pace was maintained until October 1st when the high OL period started, which led to an increase from a total of 5,85 kg accumulated to 8,46 kg on October 5th. After this period, only 721 g of TDM were retained until October 11th.

As shown by Figure 67 and Table 15, accumulation during week 20 was at its lowest, leading to an increase up to a total of 9,600 kg on October 18th. However, as shown by mass balances, this increase was only related to organic matter, as inorganic matter reduced 92 g over the period. In the following weeks, a total of 2,315 kg accumulated in the reactor, being 0,944 kg during week 21 and 1,372 kg during week 22. It is important to note that depletion of the inorganic matter was greater

during week 22 than week 20, as 217 g of TDM were lost during week 22 instead of 92 of week 20. This was not observed during any of the other weeks.

Considering the average recycle concentration between September 23rd and October 20th of 1,84%, the recirculation for the solid matter in the reactor increased 3,24 h for a flow rate of 200 L/h since the normal operation had been started. This value is only valid if one also considered that the transport of particles is dependent on only flow rate, and the concentration of TDM in the recirculation is constant.

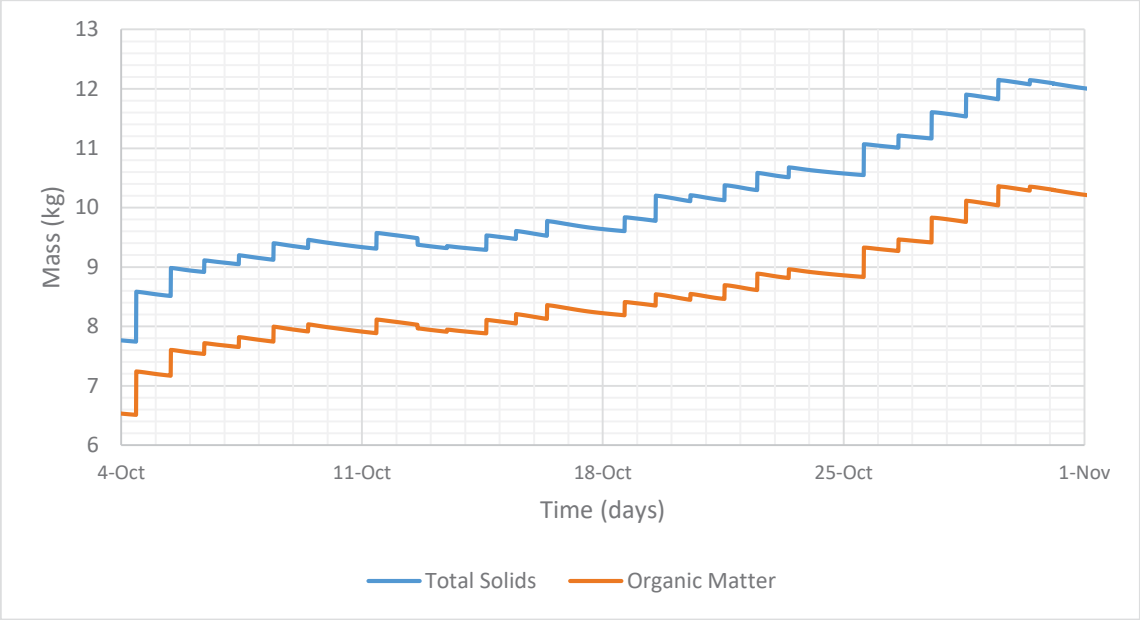

Figure 67 – Solid matter and organic matter accumulation into the reactor between October 4th and November 1st.

In addition, the accumulated degradation and organic load from the 2nd of August to the 1st of November were calculated and are plotted in Figure 68. As shown, the degradation rate increased with an exponential shape, but it later develops to a linear shape. Organic matter digestion during the normal operation period reached 4,658 kg, which represented 33,5% of the total OL of the period. Moreover, the degradation rate did not increase significantly in response to the increasing OL.

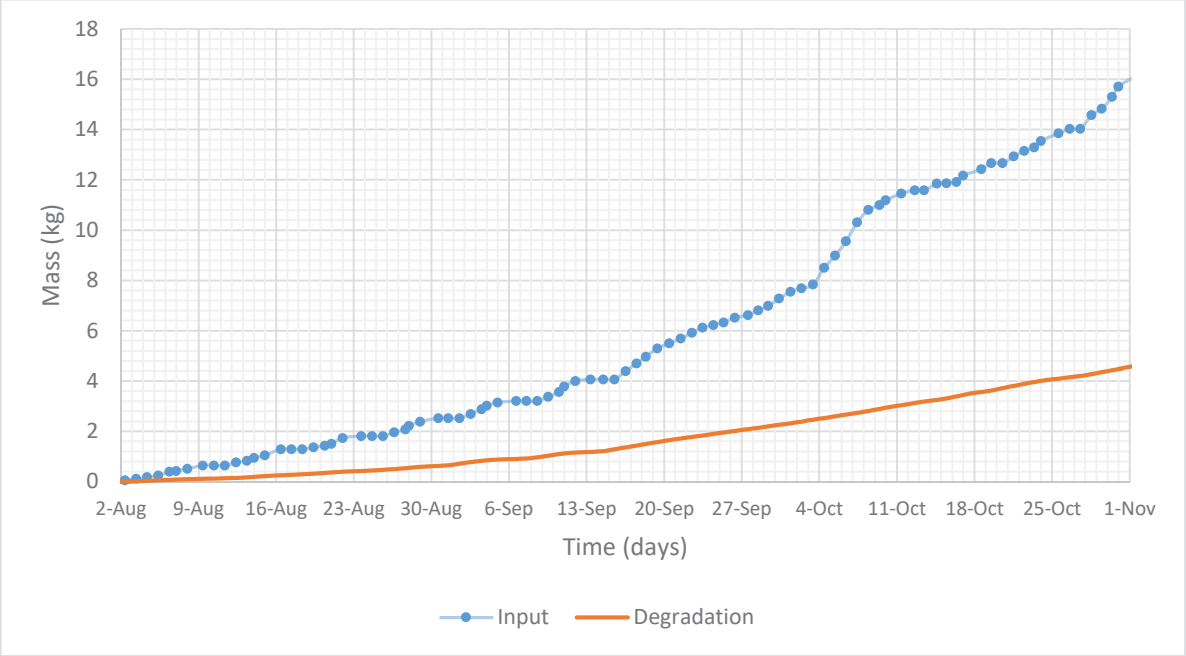

Figure 68 – Accumulated volatile solids in the input and estimated degradation between August 2nd and November 1st.

After the accumulation had been determined in the system, sludge age was calculated for the period and the graph of Figure 69 was plotted with the 7-days moving average. Sludge age had an increasing trend during the 5-days feed regime, reaching a daily value of 106,6 days on September 6th with values above 60 days on the following days, which keep the increasing trend of the moving average. After this date, values oscillated around 60 days until the end of week 18 with the moving average oscillating between 48 and 65 days. During weeks 19 and 20, daily values greatly oscillated around 52 days, with a range of 90,31 days on October 9th and 16,75 days on October 12th. Values had an increasing trend during week 21 until week 22, when values average 75 days, as daily values spiked two times above 130 days. Besides these spikes, the daily sludge age was stable around 38 days.

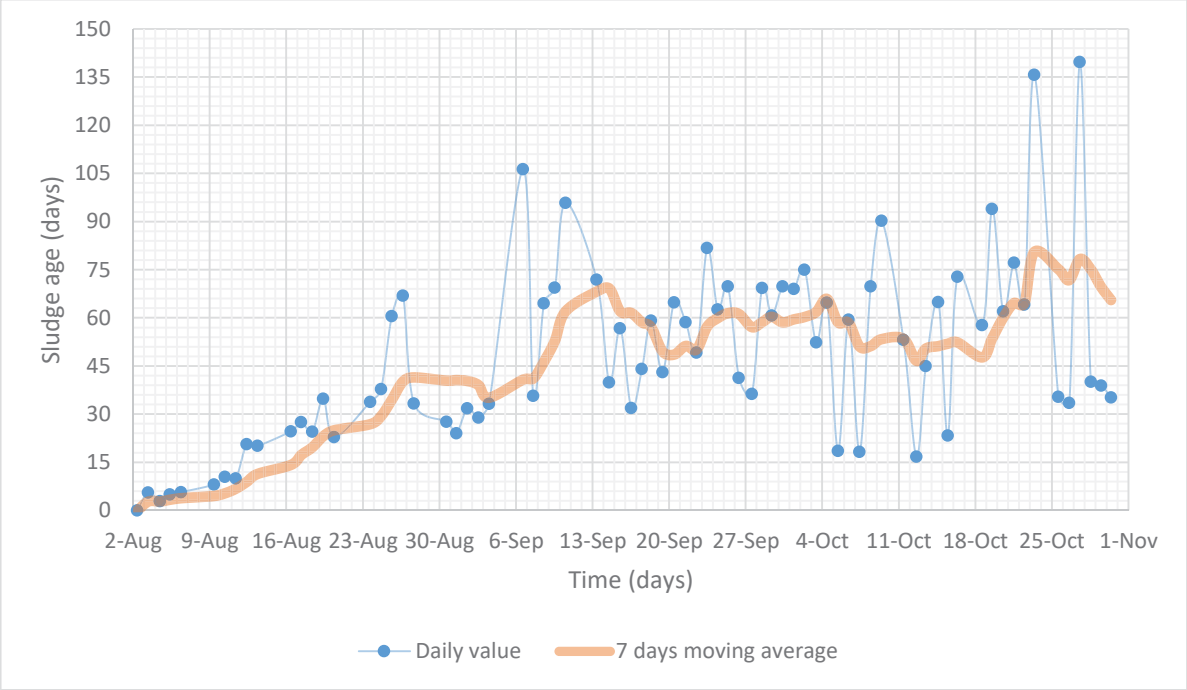

Figure 69 – Sludge age daily and 7-days moving averages between August 2nd and November 1st.

Overall a total of 5,361 m³ of biogas was produced during normal operation, it is estimated to be composed of 3,589 m³ of methane and 1,833 m³ of carbon dioxide. With that, biogas yields for the period were 330,22 L/kg VS, 220,69 L/kg COD, and 7,66 L/LPS; in terms of methane production 216,07 L/kg VS, 144,40 L/kg COD, and 5,01 L/LPS.

In terms of liquid input and output, a total of 16,560 kg of TDM was retained/degraded of a total of 19,461 kg fed. This represented an overall reduction of 85,07% of TDM, which was in alignment with the 84,48% reduction of ODM. At last, from a total of 25,184 kgO_2 of COD fed, only an amount of 1,724 kgO_2 left the system, resulting in a total reduction of 93,11%.

7. Discussion

In this section, the discussion is divided into three subsections to better analyze the yields and efficiencies of this system. The first subsection, Operation, discusses the effects and outcomes of non-intended changes in operation during the experiments. The second one, Solids retention and digestion discuss effects that could have affected solid matter internally or at the output. The third and last subsection, Gas quality and production, analyze the response of the gas quality and production upon changes in the input parameters.

7.1. Operation

7.1.1. Temperature

As shown by Figure 18, temperatures could not be kept equally distributed along the reactor nor maintained constant in all sections during normal operation. The only period that the heating system was capable to maintain a similar temperature was between June 1st and 21st (see Figure 16) when the reactor operated only with water. Differences in measurements between points observed during this time can be associated with equipment uncertainty and interferences due to thermometer installation, as temperatures were measured by the electrical resistance.

Comparing Figure 17 and Figure 18, one can observe a relationship between flow rate and temperature. During pump failure episodes, temperatures in all sections increased to a level above 38°C, dropping to normal levels after 2h on average after the pumping was reestablished. This relationship is further exemplified in Figure 71, in which an increase in flow velocity quickly decreases the overall temperature. Even with variations being expected, the levels were not, heating and cooling rates were too fast, which indicates great heat losses in the non-isolated external hoses.

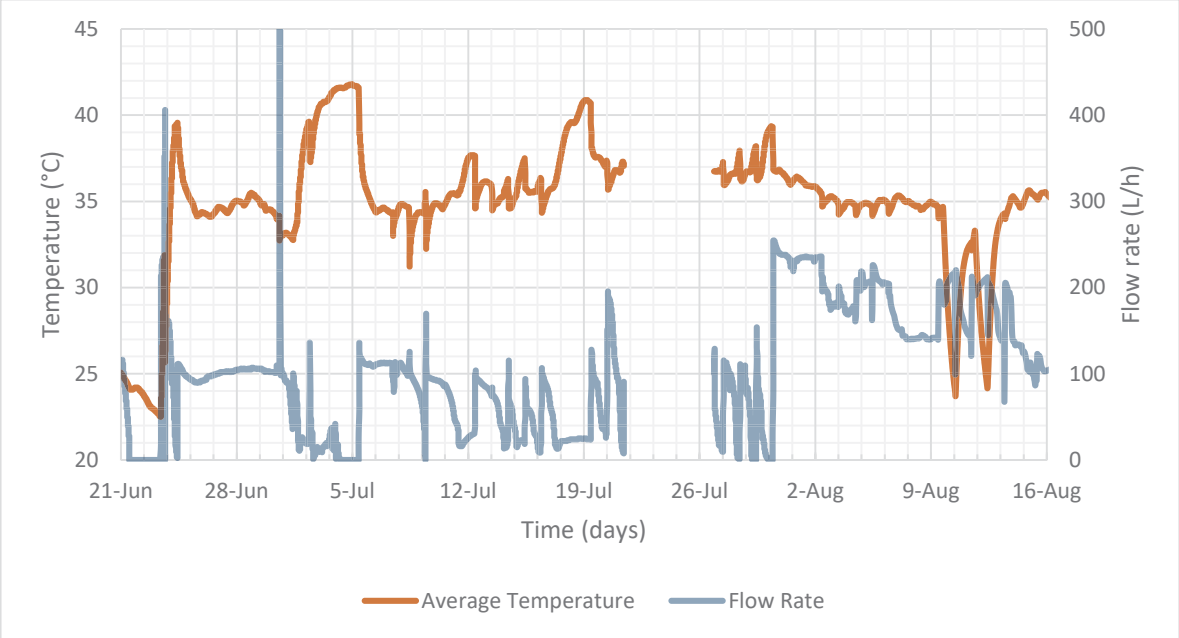

Figure 70 – Average reactor temperature (°C) and recirculation flow rate (L/h) between June 21st and August 16th.

In addition, during pump failures, temperatures increased up to 43°C in all sections, as shown in Figure 18. This happened due to great heat losses in hoses connecting the pump to the reactor, which reduced overall temperatures while the operation was conducted normally. Hence, when the pump was stopped, no cooled liquid was mixed back in the reactor, leading to higher temperatures. However, drops in temperatures did not occur when the flow rate was reduced to around 100 L/h, which indicates that the temperature of the liquid entering the reactor is already at ambient temperature when the flow rate is at 200 L/h.

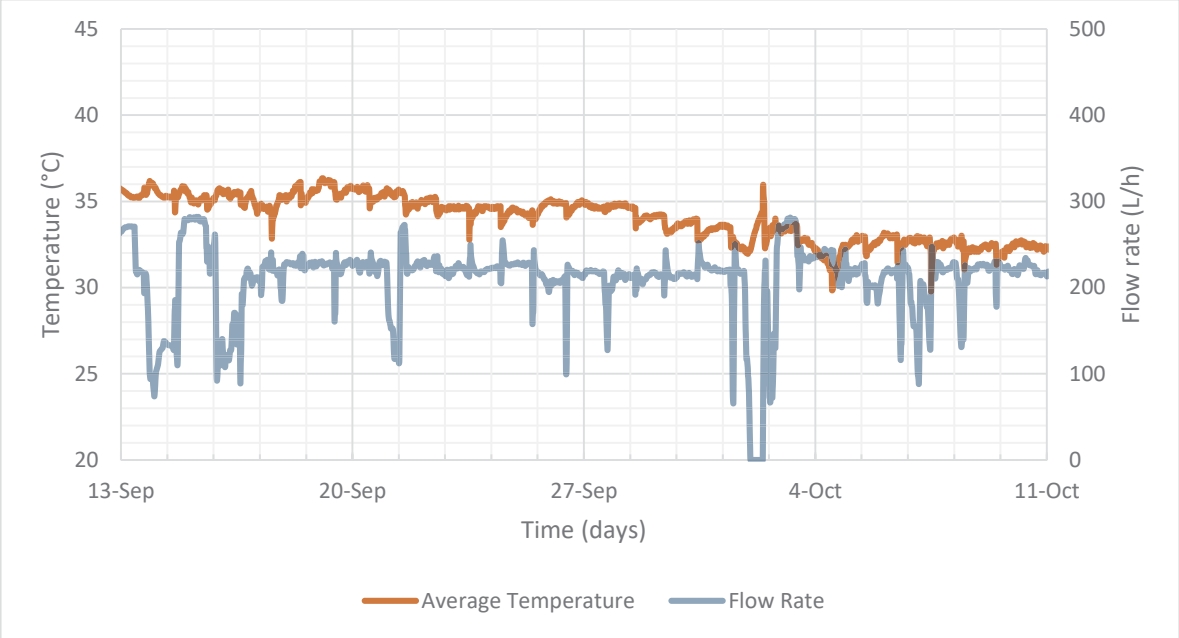

Figure 71 – Average reactor temperature (°C) and recirculation flow rate (L/h) between September 13th and August 11th.

With the start-up of the digester, temperatures could be maintained, but as experiments progressed, this scenario changed. As shown by Figure 23, the average temperature dropped over time as a result of drops at sections D and E after September 13th, reducing from a solid average of 35°C to 31°C in October. The deterioration of temperatures after September 13th at E and D showed that the system has started to wear out. This happened because temperatures in the heating circulator had to be kept at 70°C. In addition, the flow rate in the heating system operated at maximum capacity (160 mL/min) to maintain temperatures levels. These factors in combination with the maximum temperatures that the hoses could handle (80°C) led to great stresses in the heating system.

As time went on, the fatigue increased pressure drops at several points in the heating system, reducing the passage of hot fluid in some sections. Due to its design, hot water arrived first at A and last at E, hence a problem of this kind would affect first sections D and E than sections A through C. The profile after September corroborates this hypothesis, as temperatures at D and E decreased until the end of experiments, as shown in Figure 22. In addition, temperatures at A and B slightly increased in September, as expected.

Moreover, at some locations in the heating system, particles and colored matter were verified inside the hoses, indicating also incrustation. This was in combination with the fact that a change in the arrangement of control valves did not lead to higher temperatures at D and E. This showed an inefficiency in controlling system fatigue with the tools available, as only sections A and B responded to it. At the end of the experiments, temperatures at C started to drop, indicating the fatigue started to affect other sections.

Another evidence of the deterioration of the heating system can be seen in Figure 72. On the night between October 1st and 2nd, the recirculation system failed, leading to the flow rate being zero for approximately 9 hours. As shown in Figure 72, after the flow interruption, only temperatures at A and B increased over time, reaching over 40°C after 9 hours, which was similar to what was observed on June 30th (see Figure 70). However, temperatures at C and E decreased from 32°C to below 30°C, instead of rising like what was observed in previous failures events. This confirms the loss of heat transfer efficiency in sections C through E over time.

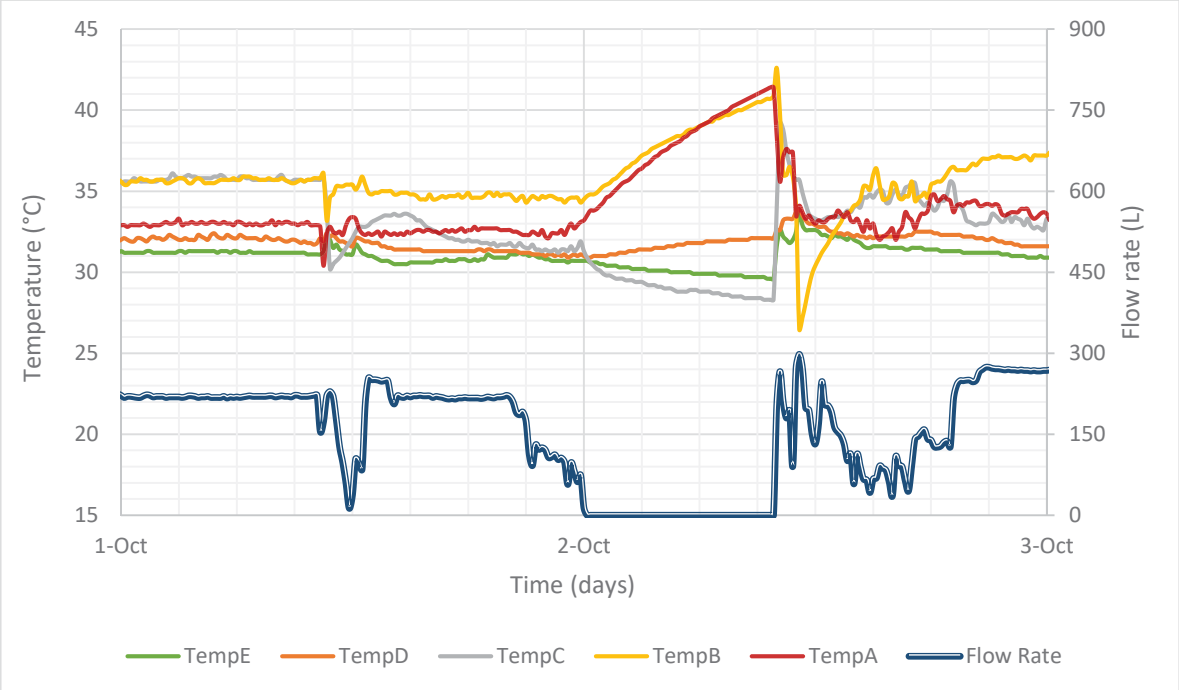

Figure 72 – Temperature profile (°C) and recirculation flow rate between October 1st and 3rd.

At last, the system showed a small drop in temperature after being fed with cold sludge, as shown by Figure 24. Even with the feed having between 5-7°C,

temperatures dropped at a maximum of only 1,5°C at A, which indicates that the heating system was robust enough to absorb these disturbances for the load used. Even with higher volumes of feed during October, temperatures in A and B did not drop more than 2°C after feeding, confirming the resilience of the system regarding input temperature. This resulted in averages drop in overall reactor temperature during the feeding at only 0,5°C, creating the oscillatory profile in Figure 71.

However, the recovery of those losses took over 10h to be achieved, indicating that in case of bigger disturbances, the recovery would take more than 24h. As observed in Figure 22, temperatures took 30h to be reestablished on August 12th, when a failure in the heating system happened, confirming this theory.

Temperature effects on gas production could not be identified during the experiments. This happens since there were no two periods when the temperature difference was greater than 4°C and OL and HRT were similar. The best two periods which come close to fit these criteria are the periods between September 15th and 20th (1) and October 11th and 16th, which had an average reactor temperature of 35,6°C and 31,5°C and an average OL of 1,286 and 1,221 kg VS/m³d. For this case, it was verified a higher specific production on 3 of 6 days during the second period, with two of these being due to extremely low OL on October 12th and 13th (2 and 3). This comparison is made in Figure 73.

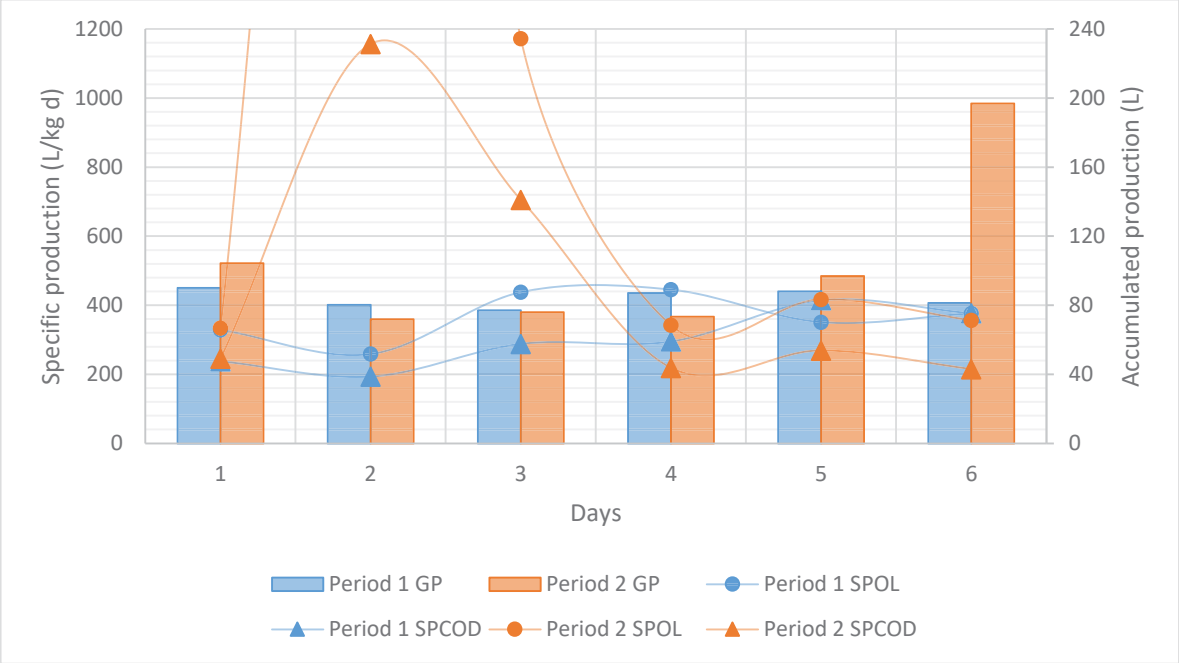

Figure 73 – Accumulate feed-to-feed production (GP, L), gas production regarding organic load (SPOL, L/kg VS d), and gas production regarding chemical oxygen demand (SPCOD, L/kg COD d) comparison between periods 1 (September 15th and 20th) and 2 (October 11th and 16th).

Even with the similarity between these two periods, it is important to note that HRT during period 2 was half that what was used during period 1. In addition, during ay 2 and 3, values for period 2 of specific gas production were above 1000 L/kg VS d due to the low OL used during these days, on average 0,3462 kg VS/m³d. Other periods showed lesser similarity, which made it impossible to confirm if the decay of temperature was sufficient to impact production in the system. However, studies showed that temperature drops from 37°C to 30°C were found to reduce methane yields in AD of sewage sludge up to 20% (BLASIUS et al., 2020; ZÁBRANSKÁ et al., 2000)., which indicates that this drop might have had some negative impact.

Therefore, it is concluded that the heating system could not sustain operation for a long time and heat losses in external hoses greatly contribute to reduced overall temperature in the reactor. In addition, the system could handle disturbances due to feeding without any manual adjustments in the system while feeding. In addition, even with a reduction of 4°C at D and E since the reactor has

started, temperatures could be still controlled above 30°C in all sections during normal operation.

A possible solution for the poor temperature control is an installation of a secondary thermal recirculation in addition to adjustments in the isolation and replacement of the heating hoses. The secondary bath would be connected to sections C to E, being centered at D. With that, the primary bath should be connected only to sections A and B. Hoses should be replaced with larger ones with a material that can resist at least 100 °C. At last, hoses connecting the reactor to the pump and flowmeter must be isolated with similar material to the one used for the reactor body. With these changes, it is believed that digester can be maintained stably at mesophilic and thermophilic conditions if need it.

7.1.2. Flow rate

Similar to what was observed regarding the temperature, the flow rate was stable during the water recirculation period and early start-up, as shown by Figure 15. Failures observed in July happened solo due to problems with the pump stator, which could not handle the change of pump material from water to sludge. Before this replacement, the set operation of 100 L/h could not be maintained reliably.

After repairing the pump, the flow rate did not drop after the feeding. This was achieved consistently during the whole period, only showing problems when exception episodes happened. With that, the flow rate could be sustained around the set point of 200 L/h for most of the operation, as shown by the examples in Figure 26. However, due to the presence of large particles and, during October especially, leaves in the substrate, oscillations and slow drops in flow rate were often observed. This led to pumping failures only when the amount of these particles in the recycle reached high levels, a fact that happened only twice during operation (on October 3rd and 26th).

Regarding the replacement of the hose connecting valve 4 to the pump (see Figure 10), there was not enough time to evaluate changes in performance. However, after the replacement, no failures were observed. In addition, the pump

could operate for a week in reverse without any failure and major differences in profile to when normal flow direction was applied.

Moreover, the pumping system did not have an acceptable performance when pumping high concentrate feed (TDM>7%). Between October 1st and 5th, when PS had the highest TDM content, the pump had to be stopped and reverse multiple times to flush in the material. However, this was related not to the pump type, but with the diameter of the feeding hose and the suction port. Due to high concentration, particles formed “blobs” with a bigger size than their diameter, blocking the hose and suction port. Therefore, the mixture was sucked in only after these conglomerates were broken, which was only possible after increasing set power.

In addition, the air was constantly fed into the digester unintentionally, as shown by gas production spikes in Figure 21 and combined content methane-carbon dioxide content in Figure 51. This happened because the feeding hose was not connected to any other device besides the pump itself, which allowed air to be present inside of it before the feeding had started. Even pumping in reverse before starting the procedure did not make all the air escape, being some pumped into the digester with the feed. In addition, when this air was pumped out of the hose, trapped oxygen mixed into the cold sludge, due to a higher solubility of oxygen in water at low temperatures. This combination allowed a certain level of oxidation to take place inside the reactor.

Comparing the flow rates with gas production rates, it was found that the flow velocity used was too fast for the reactor to be considered a typical plug flow reactor. The time scale observed for the methane production was observed to be in days, as the HRT for the circulation operates on the scale of hours. This led to any reaction effects on the substrate happening too slow in comparison to the flow movement, which make it impossible to evaluate properties changes with the length. Therefore, analyses for recirculation rates equivalent to what was used during experiments can be only analyzed on time, but not on position.

Overall, the pumping system was capable to maintain a reliable flow rate around the setpoint without any automated control. However, the characteristics of the substrate made that the flow rate ranged 50 L/h on average during a day of

operation. Besides that, the screw pump used only showed failures due to the presence of leaves or random high-density particles in the current. At last, the pumping system did not show a good performance and efficiency during the feeding procedure.

With that, improvements to the pumping system can be done to allow more stable and continuous operation. Firstly, a secondary smaller pump should be installed, as the pump used during the experiment did not allow feeding to be conducted whilst recirculating. Moreover, an installation of a T-connection at the input could be also done, allowing the pump to be connected to the reactor separately. In addition, it is prudent to replace the screw pump in operation for others with cutting blades to avoid pump damages by leaves or larger particles.

In addition to a new pump, the filling level control arm (see Figure 11) should be connected to a tank filled with water up to the operating height. The flow resistance of the gas valves should also be increased, as the reactor could not operate with vales 6 to 10 open (see Figure 10). For that, it is necessary to enlarge the blockers between the section and decrease the useful volume of the reactor to allow a large space for the gas to be stored. At last, the equipment should be automated to operate at a chosen set point and avoid great oscillations during operation.

7.1.3. Solids recirculation and transport

After the reactor received the first load of sludge, TDM in further sections (15 and 16, see Figure 10) had smaller values (<50%) than what was obtained in other ones, as shown by Figure 19. This behavior was also verified in the recirculation, where TDM started to climb after week 10. This indicates that the time for dense solids to reach the output/recirculation point must be a minimum of 6 weeks since the reactor had been first fed in week 4.

The fact that solids took 6 weeks is in contradiction to the minimum time calculated from the mass balances at the end of the run, 3,23 h. This difference indicates that the transport of solid matter inside the reactor was not equal between particles. This can be explained by only lighter particles and ones on higher layers of the substrate being transported directly by the recirculation, but not the ones

located on lower layers. This is supported by the fact that, on average, TDM in the recirculation was 50% of the value found in the substrate.

Mass balances also showed that the volume required to fit all the accumulated solids was much higher than the reactor volume if the average concentration of the substrate was considered. This indicates that most of the substrate had a higher TDM than what was obtained, which suggests that a fraction of the bed could have settled.

Even though total solids measurements are not able to provide any information on the total quantity of solids being transported, it does give information about their presence in a given place. As suggested by the fact that values of TDM varied less than 15% between measurement points after the 11th of August, as shown by Figure 19, particles did not reach the later section of the reactor during an HRT. Considering the time to verify similar TDM in all sampling points, one can estimate that the time for volumes of concentrate solids to be transported along the reactor should be between 6-7 weeks during the startup. This is also supported by the sludge age, which stabilized around 60 days between weeks 16 and 19, slowly increasing during weeks 10 through 15 (see Figure 69).

One could explain these observations with the hypothesis that the solid transport inside the reactor develops likewise a riverbed. The entrance point of the input is located at the upper part of the reactor with an upper interface with gas and a moving bed at the bottom. With this analogy, as samples were collected, instead of the substrate coming out of the digester, water from upper layers infiltrated through the substrate, dragging some solids with it. This explains why TDM in the bed did not lead to a possible volume at the mass balances.

If one explores the riverbed analogy in more detail, one will verify that this also explains why the solids have transport velocities of different magnitudes. As the reactor was being filled, solids were accumulating at the first section, slowly building up while upper layers were transported and settling forward. During this process, layers on the bottom started to be compressed, sticking to the reactor's floor, which reduced its velocity. As this process develops, it behaved more and more similar to a riverbed, until it reached the location close to the recycle output, valve 4 (see Figure

10). This hypothesis is supported by the PS fast sedimentation speed and it explains why TDM was only similar after 6 weeks of operation.

Moreover, this hypothesis also demonstrates why the lower solids HRT calculated by the mass balances were higher than the HRT of the liquid. Due to the gas/liquid interface, the flow inside the reactor behaved as a free-surface type of flow, which properties refer more to a shallow river than a flow inside a pipeline. Therefore, the velocity profile in the liquid phase was at its highest close to the interface instead of close to the center of the pipe. This divided the flow pattern into three sections: Free surface, intermediate, and near-bed, as shown by Figure 74. Because most solids are concentrated in the near-bed region, they move slower than the upper layers, as the velocity of this region is smaller. Hence, the liquid was diluted by a less concentrated mixture from upper layers, reducing the TDM in the recirculation current.

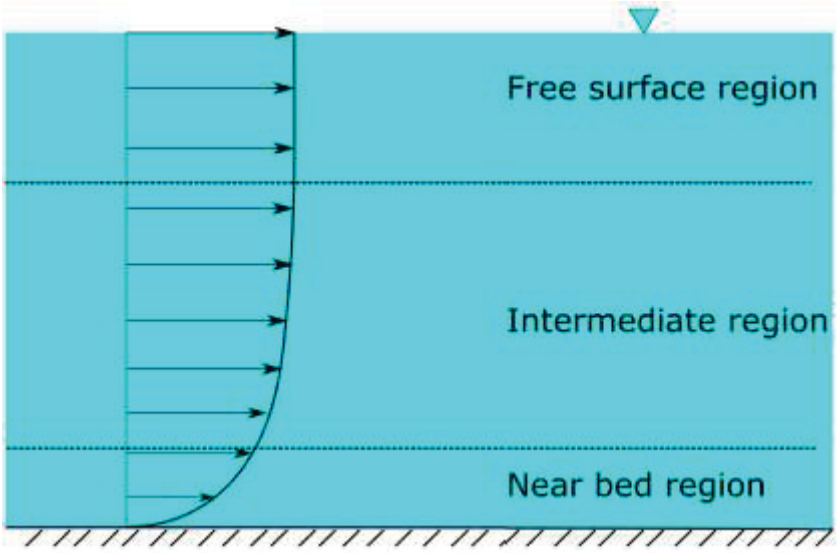

Figure 74 – Free surface flow velocity profile scheme (adapted from Maji et al., 2020).

In addition, this hypothesis also helps to explain why high concentrate volumes were observed during the feeding procedure at the output. As the PS were fed, free organic particles would have started to agglomerate due to their cohesive properties, increasing their particle size and overall density. This would have made particles with smaller specific masses sink with other ones and, as time passes by, the flow at the near-bed region would erode the bed surface, slowly releasing

particles into the upper layers. This would have allowed greater volumes to be released at once, as greater portions of low-density particles could have been entrapped by a layer of dense cohesive matter which was eroded.

This process would have accelerated as the velocity in the near-bed region increased. However, it did not happen because of an increase in flow rate, but because of an increase in height of the bed, reducing the distance between its surface and the gas/liquid interface. With this, the velocity gradient in the near-bed region increased, leading to higher velocity in smaller heights (BOUTOUNET; MONNIER; VILA, 2016). This helps explain why the periodicity of high concentrate being observed at the output increased.

Due to reactor design, the recirculation was conducted from the bottom of the reactor to the top, as shown by Figure 10. With that, lesser dense particles released from the sediment bed floated close to the gas/liquid interface, which made it difficult for them to be flush into the recirculation system. Therefore, floating matter accumulated close to the output valve, being flushed out during the beginning of the feeding procedure. This phenomenon is regardless of the transport mechanisms involved in the bed, but its frequent occurrence indicates that erosion and entrainment could have been occurring.

In addition, the inorganic fraction in the TDM did not increase during spikes in ODM at the input, which indicates that the portion of inorganics was being retained in the sediment bed with the organic matter is not very high. However, this can be misleading as organic matter present in the output floated, meaning that the bed composition might be different. Even with mass balances showing an accumulation between August 2nd and November 1st of 2,09 kg of inorganic matter, it is not possible to determine if this matter is directly bound to biological matter or just mixed in the bed.

At last, if the bed formation did happen as described by the analogy to a riverbed, solids on deeper layers did not recirculate effectively during normal operation nor were in direct contact with new material. Even then, the amount of particles present in the recirculation indicates that particles on the upper layers were being carried by the flow. In addition, this also suggested that the feed could be

transported along the reactor regardless of its high sedimentation speed, as even if reached the substrate bed shortly after being fed, it could be carried forward by the flow.

Nevertheless, even if the riverbed hypothesis is found not to be correct, evidence showed that particles could be transported by the pumping system. However, it is not completely clear how the transport developed along the reactor, but experiments suggested that transport occurred differently depending on particle size. To better understand the transport mechanics, it is necessary to develop computational models and adapt sample points aiming at the necessity to measure flow velocity with good precision at different heights.

Even if not fully understood, the particle transport acted differently from what was observed in an equivalent tank reactor. In that case, recirculation takes place by pumping high concentrate solid currents from the bottom of the reactors, flushing the bed as a whole. This process is capable to recirculate most of the particles inside the reactors, which is different from what was observed in the PFR.

7.1.4. Input and primary sludge control

As shown by Table 4, Table 7, and Table 11, PS had a great variability in quality over the days. Even with constant quantities in the input, values of OL and COD load could not be controlled in a range below 40% of the average. This happens because PS availability was strongly dependent on external conditions, such as weather conditions, which can make properties vary randomly within a wide range along a week. As a result, precise control of organic load was found to be unfeasible.

With that, sludge started to be collected in large quantities and stored for later use. However, due to practical limitations regarding storage and cooling, PS and ES were fetched at least twice a week, which allowed sludge to be collected for a total of four days of feeding. This resulted in the pattern of organic and COD loads verified along with the experiments, but variability over these days could be verified as PS quality was not enough for experiments.

Nevertheless, it was found that storage at cooled conditions (6°C) allowed a constant feed quality, with only small decays being verified. The greatest variations were observed between October 1st and 5th when OL was above 2,5 kg VS/m³d. But

in these cases, the difference in feeding mixture quality was not caused by changes in the sludge while stored, but by the uncontrolled amount of water used to flush the PS out of the storage vessels.

Besides that, sludge properties had a good relationship in the input. As shown by Figure 29 and Figure 31, ODM and COD showed a good linear correlation with TDM, with values of R^2 above 0,95 for both cases. This indicates that these parameters can be accurately estimated by measuring on TDM when other analyses would be not possible. For both cases, the relationship was valid for the range of TDM used during the experiments. However, only ODM showed a good correlation with TDM at the output, COD did not show an R^2 above 0,6 for a linear and polynomial adjustment.

7.2. Solids retention and digestion

7.2.1. Organic Load and operation schedule

Organic load greatly varied along with the experiments, but it was not controlled directly. The control was done by the amount of PS fed in a day, regardless of its quality, hence OL could only be kept similar if PS was collected and stored. However, due to storage limitations, it was not possible to store more than 50 L of sludge (PS and ES) at the same time, which allowed the feeding procedure to be conducted up to four times. Therefore, it was possible to keep sludge quality and OL similar for a period of four consecutive feeding batches.

Moreover, besides the pre-operation and startup phases, the operation schedule was divided into three steps regarding the number of days in a week that the reactor was fed: 5, 6, and 7 days. Even with changes in the agenda, the daily feeding volume was kept constant at 10 L/d. Therefore, analyses regarding feeding periodicity discuss factors only related to starvation periods and reactor stress, all for an HRT of 23,37 days.

As seen in Figure 75, TDM behaved around 0,20% in the output after September 13th, only on five days, measurements were considerable above this

trash hole. Of these spikes, however, only two happened when operating at a residence time of 23,34 days, on the 5th and 7th of October. ODM followed a similar behavior to TDM, being around an average of 0,10%. On the other hand, COD showed a steady increase between weeks 10 and 16, but it kept itself around 1500 mg/L for the rest of the experiments, if one does not consider spikes.

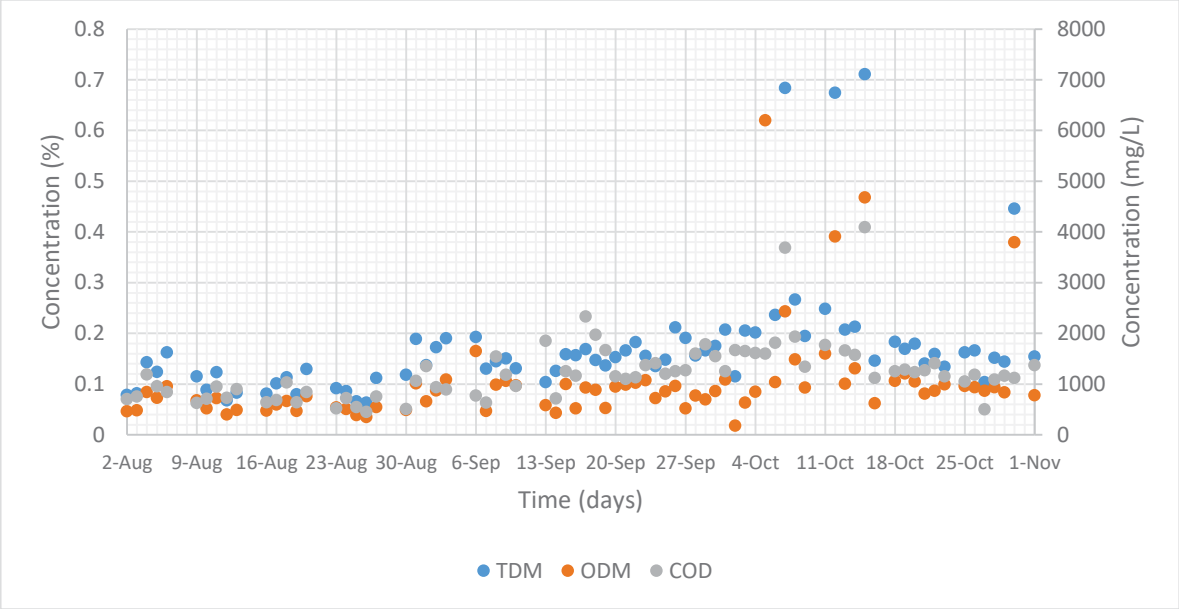

Figure 75 – Total dry matter (%), organic dry matter (%), and chemical oxygen demand (mg/L) in the output between August 2nd and November 1st.

This consistency in values in the output was observed both when OL increased and after changing the number of days being fed in a week. Comparing Figure 34 and Figure 38, one can observe that ODM in the output did not change when a larger volume of PS was fed in weeks 14 and 15 in comparison to weeks 10 through 13. This indicates that the increase in OL was not sufficient to impact ODM in the output during the 5-days feed regime.

Stability in ODM values was also observed during the 6 and 7-days feeding period. As shown by Figure 76, ODM stayed between 0,07% and 0,15% during most of the days during both periods, being comparable to the first one. In Figure 76, week 19 is overlapped between the 6 and 7-days feed regime, hence seven spikes are shown instead of 5. Moreover, it is possible to conclude that differences in feeding schedule did not show an impact on solids retention.

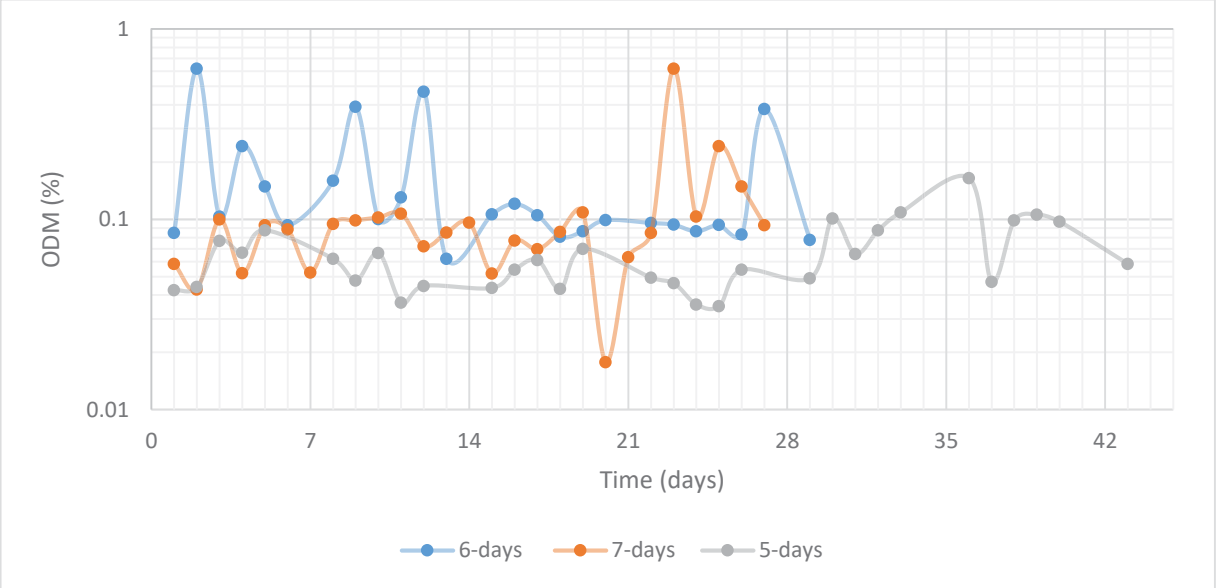

Figure 76 – ODM comparison between different feeding schedules in the output.

If one analyzes COD behavior, one will verify that the average value increased over time. Between weeks 10 and 14, the average weekly COD in the output was below the 1000 mg/L mark, increasing from 850 mg/L to 1016 mg/L in week 15 and a maximum of 3178 mg/L in week 20. If peaks above 3000 mg/L are not considered, COD values were very similar when 6 and 7-days weekly feed was conducted, as shown by Figure 77. This indicates a higher presence of degradable substances in the output for the same ODM, as its values did not increase during the period.

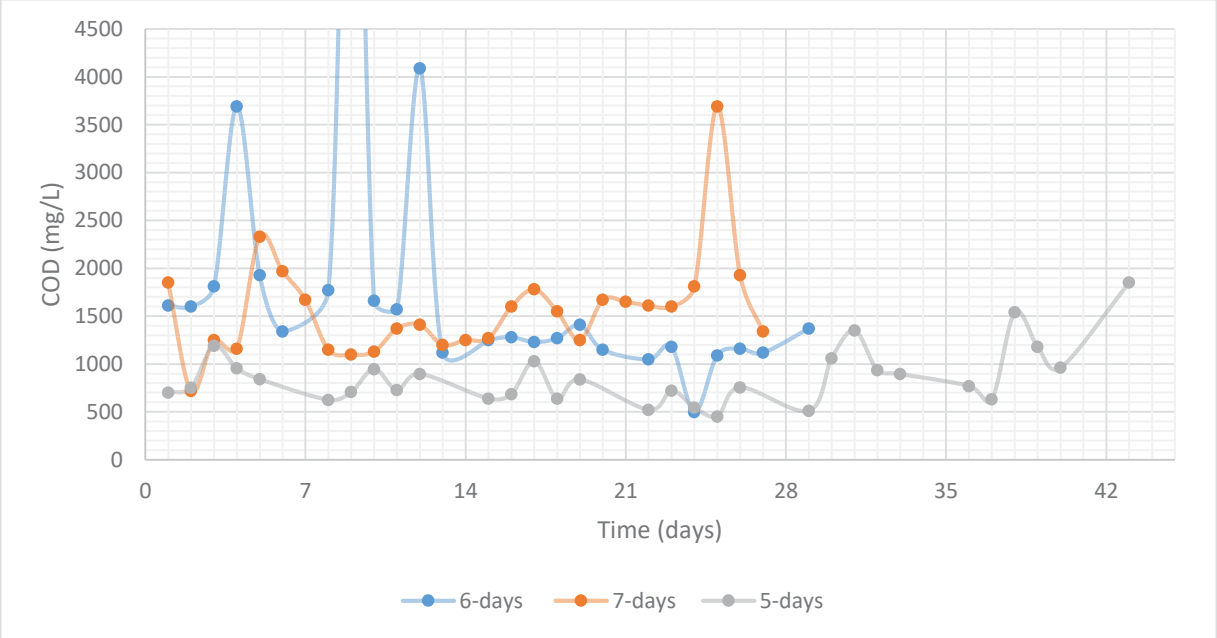

Figure 77 – COD comparison between different feeding schedules in the output.

This phenomenon can be explained by increments in the overall quantity of PS and the interruption of the usage of ES, which could have modified the liquid phase composition. From week 14 and forward, ES stopped being used in feed mixture, being replaced by water when it was necessary to dilute PS. During all weeks when ES was used, COD was below 1000 mg/L, surpassing this value twice on August 4th and 18th. Therefore, the ES influence could have reduced the degradable fraction in the output.

Another explanation is the increase of volatile fatty acids which are produced during the digestion process, as explained in section 2.1. Volatile fatty acids with low carbon count are water-soluble, such as acetic and propionic acid. With that, these acids can be transported by diffusion or convection to the upper layer of the flow and are found in the output. The increase in volatile fatty acids concentration is often associated with overloading the reactor when the OL is greater than its capacity (BRAZ et al., 2019; MAGDALENA; GRESES; GONZÁLEZ-FERNÁNDEZ, 2019).

A global overload is very unlikely, as biogas yields did not drop after the COD had decreased. In addition, an increase in OL would also increase even further the presence of VFAs and, as a result, degradable fraction, which was not verified. Between October 1st and 5th, OL was at its highest, with an average feed of 2,97 kg

VS/m³d twice as high as the week 16 average, however, it showed a considerable increase in COD in the output. COD values for the same period and the following 5 measured days were on average 1556 mg/L and 1712 mg/L, in comparison to 1461 mg/L observed in week 16.

The 12% COD increment observed between October 1st and 10th cannot confirm that the increase in the degradable fraction was due to overloading. As observed in measurements during experiments, output did vary randomly as the feeding and sampling procedure was done, adding one more uncertainty. In addition, the standard variation for the period was 692 mg/L (42%), which is four times greater than the overall increase. Therefore, it is not possible to confirm that a proper increase in COD occurred during the period, which is different from weeks 10 through 15. Between weeks 10 and 13, the weekly standard deviation was below 200 mg/L, being higher in weeks 14 and 15, as shown by Table 3. These values were small enough to reliably show that a COD increment did happen.

Therefore, an increase of COD due to widespread overloading is very unlikely, but a localized one could be possible, see more in the section Gas quality and production. On the other hand, leading to the hypothesis of ES influence to be more likely for the period. To verify this assumption, it is necessary to evaluate gas production and output regarding VFA content and quality in addition to analyses already done in this work. In addition, filtration analysis results cannot confirm this theory, as values shown in Table 13 do not support the hypothesis.

Besides this small increase in COD, the output also suffered from black volumes being flushed out randomly during operation. It was observed that the increase in periodicity was not related to variation in OL itself, even with spikes being observed in the week following the highest OL. The high presence of float matter in the output during this is attached to the PS characteristics and not the OL itself. Between October 1st and 5th, the OL was on average 2,97 kg VS/m³d, which was high enough to introduce foam in the system, as studies have shown that foam can form already in a concentration above 2,5 kg VS/m³d (GANIDI; TYRREL; CARTMELL, 2011). With that, lesser denser particles present in the foam would be

dragged out by the flow during sample collection. Because the quantity of foam was too big to be avoided, samples showed an unusually high TDM, ODM, and COD.

The random presence of floating solids in the output made the sampling method used not reliable. Samples were collected by directly fetching a volume from the output in a vessel and then transferring whilst agitating to sample vials. This had to be done in a short time window, as the output was only available for sampling during the feeding, which usually took less than 5 minutes until October 11th. Due to being not possible to properly control the feed and collect the complete output at the same time, a full compost sample could not be obtained. Therefore, it was decided to avoid floating solids during collection, which was done visually, carrying out human-related errors during the process. This and the fact that on some days floating material could not be avoided increased the uncertainty and reliability of ODM, TDM, and COD in the output.

Regardless of problems with measurements, the system showed resilience to changes in the OL concerning particle's presence in the output. In addition, ODM and TDM were not connected to the digestion process, but only with particle transport mechanics and their size and weight. The combination of a low average velocity (0,114 cm/s) and an output located at the same height as the input (12,5 cm above the reactor floor), made heavy particles sink, retaining them. As seen by the rate of reduction in Figure 36, this design showed to be capable to keep a reduction of TDM above 80% and COD above 90% during most days.

Regarding reduction values, it is possible to notice several steep drops. A part of them is associated with the PS quality used to make the feeding mixture. A bad quality sludge would push down the reduction value as one at the output were constant, such as the examples on August 4th and October 26th, when mixture TDM was below 0,50%. Another group of drops is related to TDM and ODM spikes in the output due to the presence of floating matter, on October 12th and 15th, the first showed negative values and was removed from the plot of Figure 36.

Compared to the literature, the removal was way above what was observed for tank reactors due to different principles of removal. When one compares to the literature, one must consider that the output in-tank reactors contain the solid phase,

which was not separated inside the digester. As explained previously, solids are retained in the digester by sedimentation, being separated from the liquid phase before being degraded. With that, direct comparisons related to solids removal at the output are meaningless, because the removal principles are different between them.

As a result of those differences, comparison to the literature must be concerning the degradation of solid matter, due to lack of reliable literature related to digesters of this kind. Examples in the literature showed that digestion of high concentrated PS (TDM>7%) had removal of ODM between 30-35% in tank reactors at mesophilic conditions on a laboratory scale (AN et al., 2017; BRAGUGLIA et al., 2015). This range was observed in batch operations with an evaluation period above 30 days or in semi-batch operation. However, other instances found a reduction of up 50% in thickened PS digestion in semi-continuous tank reactors (LEE; PARAMESWARAN; RITTMANN, 2011).

It is important to notice that degradation was calculated directly by the gas production, which assumed that degradation is conducted only by methanogens. Therefore, degradation values are underestimated to real ones, as the organic matter was also degraded by other processes, such as fermentation. Moreover, secondary reactions could have converted part of the ODM to water, which would increase degradation, this phenomenon was not considered in the calculation, however.

As shown by Figure 78, mass balances estimated that the relative removal increased from 24,5% in the first half of August to an average of 31,8% in September. This rate was maintained until the end of the experiments, only dropping below 30% after high concentrated PS was used between October 1st and 5th. Increases in TDM to values above 8% result in a reduction in overall efficiency in degradation in continuous and semi-continuous systems (AN et al., 2017), which can be further reduced if the increase happens suddenly (BRAZ et al., 2018a).

This reduction could also indicate that the reactor could have been locally overloaded with a maximum OL between 0,741 and 2,467 kg VS/m³d. However, this cannot be confirmed due to the short period with a high OL. The duration of the high OL implemented was not larger enough to exclude statistical, as the sample days

are not significant in comparison to the total days fed and the HRT at the time. This in combination with the large OL difference between September 30th and October 1st could have caused an OL shock to the microorganisms, which would be mitigated over time. Therefore, a larger observation time is necessary to differentiate those effects.

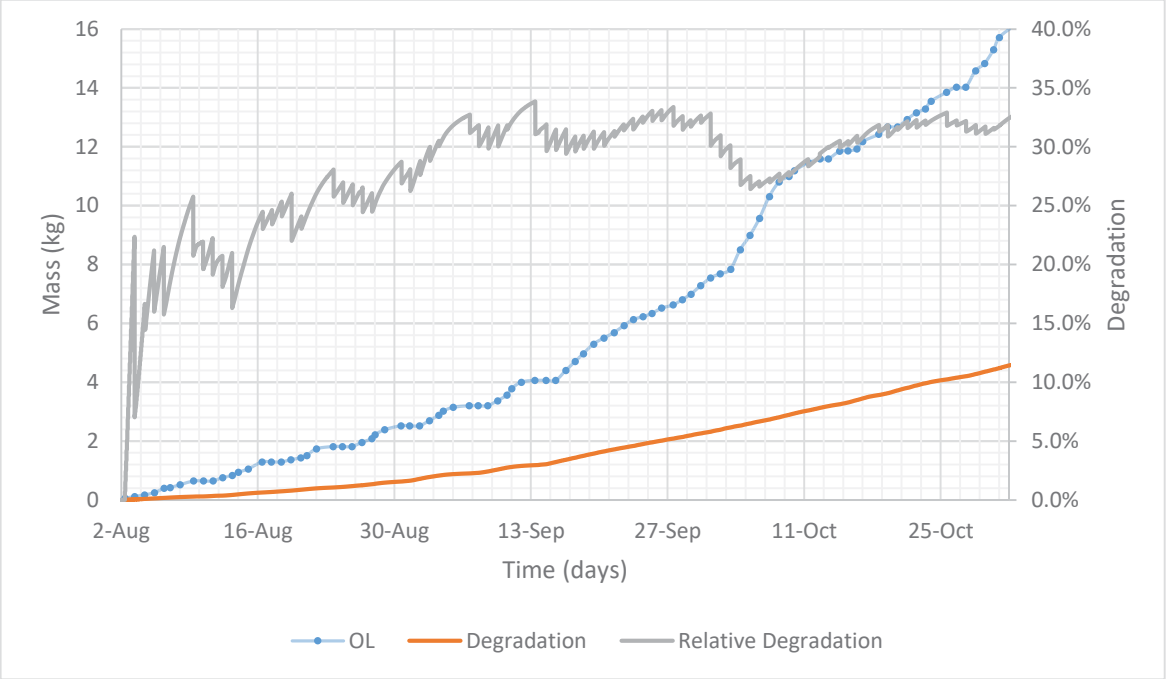

Figure 78 – Volatile solids in the input (kg), estimated degradation (kg), and calculated relative degradation (%) between August 2nd and November 1st.

Removal between August 2nd and 7th showed unusual low values due to the calculation method, which was done by dividing the accumulated degradation by the accumulated OL. Hence, a reduced number of days would have resulted in great oscillations and an overall lower value than the real one. However, subsequent days showed a relative degradation below 25% as well, which can be related to the presence of ES. This happens because ES has a high concentration of ammonium, which can inhibit anaerobic digestion and, therefore, reduce overall ODM degradation (DAI et al., 2017; LI et al., 2020).

Examples of plug flow reactors using PS as the main feeding material could not be found, but examples of its utilization for other feed types showed a higher degradation. Studies regarding digestion of beef cattle and pork manure found values between 25-51% of overall ODM reduction in PFRs with an HRT within 25 to

30 days (CHEN et al., 2015; GÓMEZ et al., 2019). Other feed types showed higher reduction when operated in a PFR with similar residence time (20-30 days), such as agricultural waste (>40%) and food waste (EFTAXIAS et al., 2021; VELUCHAMY; GILROYED; KALAMDHAD, 2019). Even with higher overall values, drops with increases of OL were often observed, but the reduction of overall degradation was above 5%. This showed a similar response for what of observed in experiments, even though absolute values were not comparable due to different feed types.

In addition to the estimated degradation of ODM of 33,2%, the system offered a reduction of solids at the effluent comparable to usual clarifiers. Primary clarifiers often operate within a TDM removal range between 85-95% (SALIBA, 2016), which englobes what was observed both regarding COD and TDM. In addition, the digester performance was within this range even in different levels of concentration in the input, showing a similar resilience to OL than clarifiers.

Overall, the reactor showed performance regarding TDM, ODM, and COD reduction in agreement with what was shown by the literature, with an overall degradation of 29,4%. Reduction in TDM of 87,4% and 92,9% in COD were within the range of what was observed in clarifiers in wastewater treatment plants. Moreover, values at the output did not vary in response to changes in OL and feeding schedule, even with the overall degradation being smaller due to the increase in OL. At last, a small increase in COD at the output was verified, which was not significant to reduce the performance.

7.2.2. Hydraulic retention time

Hydraulic retention time (HRT) was maintained at 23,37 days between August 2nd and October 11th, when it was reduced to 11,69, 7,79, and 3,90 days in the following weeks. Due to being verified that the OL did not have great influences on the output, a too low concentration in the input was avoided regardless of the increase of the input. Therefore, during the two last weeks, two additional liters were added with the original 10.

As HRT was reduced, TDM and ODM at the output showed an overall decrease in weeks 21 and 22, as shown by Table 10. However, as seen in Figure 79, averages from weeks 19 and 20 were increased by the presence of spikes due

to the presence of foam in the output, leading to relative standard deviations above 75%. Not considering these deviations, values for TDM and ODM showed no increasing or decreasing trend with the variation of HRT, resulting in an average and standard deviation of 0,17%±0,04% and 0,10%±0,03%, respectively.

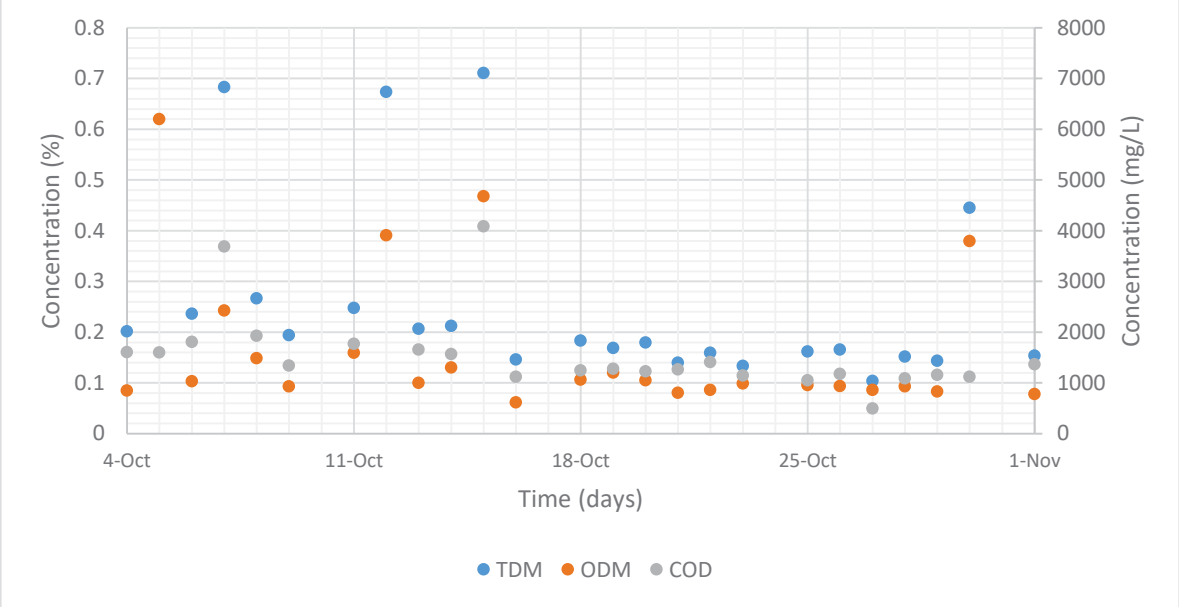

Figure 79 – Total dry matter (%), organic dry matter (%), and chemical oxygen demand (mg/L) in the output between October 4th and November 1st.

Even with a stable ODM and TDM in the output, weeks with lower retention time showed more instability regarding foam. Besides the increasing erosion effects due to the increase in velocity at the near-bed region and lingering foam from the high concentrate PS, a third could have also occurred. To reduce the HRT, it was necessary to increase the total volume fed. Consequently, the liquid volume removed increased, as the reactor was operated at a constant volume. With a greater volume being moved, a higher length of the reactor was covered during each feeding procedure, from 4,3% of the total length for 10 L/d to 25,6% to 60 L/d. With a larger area covered, the probability of flushing out a wandering foam piece during the feeding procedure increased, as its periodicity in the output.

Similarly, COD showed a stable behavior at the output as TDM and ODM. However, the number of spikes between October 4th and November 1st did not match what was observed for other parameters. On October 5th and 30th, TDM and ODM were approximately three times higher than the average of adjacent days, as COD

was slightly lower (see Figure 54). This can indicate that foam collected on these days had a small degradable fraction than usual or that a sampling error had happened. Due to spikes in TDM and ODM as well COD being observed on October 7th, a sample error was seen to be more likely to have happened.

Even with a reduction in HRT from 23,37 to 3,9 days, HRT was not comparable to clarifiers, which operate around at a maximum HRT of 6h (PIVELI, 2004). Therefore, HRT cannot be compared to what was used in clarifiers, but the stability in concentration at the output with its decrease indicates that HRT can be reduced even further. This is supported by the fact that retention of solids is not associated with the digestion process itself, but by a particle transport mechanism, as explained in section Solids recirculation and transport. Therefore, if one maintained flow conditions and accumulation rate, TDM and ODM at the output should not be affected.

A reduction in overall efficiency in retention of particles during the period of lower HRT shown in Figure 36 was not related to the reduction of HRT itself. Due to PS volume used increasing on 2 L and total volume fed increasing 50 L, input had an inherent lower TDM and COD due to dilution effect, as the water was used to complete the volume. With that, the ratio between the input and output increased as TDM and COD at the output has stayed constant and in the input decreased.

On the other hand, degradation increased between weeks 19 and 22, from a minimum of 26,4% on October 7th to a maximum of 32,9% on October 26th, when an HRT of 23,37 and 3,9 days was used respectively. This behavior, however, was not related to HRT reduction, but it was a recovery from the high concentrated PS feeding period. With that, between October 1st and 19th, HRT changing effects were overshadowed by the recovering from the high OL period.

After a reduction in the recovering rate, degradation achieved a plateau, ranging between 31,1% and 32,9%, which lasted from October 20th until November 1st, as shown by Figure 78. An increased tendency was observed on November 1st, but this can be related to the fact that no feed was conducted on October 31st. As a result, no notable changes in degradation could be observed between weeks 21 and

22. This was in contradiction to examples from the literature, which suggested a drop in degradation with the reduction of HRT.

Studies regarding AD of thickened WWTP sludge found a reduction in degradation of ODM from 50% to 35% with a reduction in HRT from 20 to 4 days in semi-continuous tank reactors (LEE; PARAMESWARAN; RITTMANN, 2011). Reduction of this magnitude was also observed during AD in semi-continuous two-stage digesters, where HRT reduction from 40 days to 10 would result in a 30% reduction in efficiency (JANG et al., 2014). Other examples showed even greater efficiency drops when even with pre-treatment, degradation rates could not reach 20% for an HRT of five days in semi-continuous operation (TORECI; KENNEDY; DROSTE, 2009).

The contradiction between experimental results and what was found in the literature is in alignment with what was discussed in section Solids recirculation and transport. Due to the separation of liquid and solids phase, particles were trapped inside the reactor and were not flushed out with the output. With that, their retention time could not be defined as during operation, leading to mostly foam and dissolved matter being flushed out of the reactor. This indicates that most of the microbial community is not present in the lesser dense liquid phase.

Microorganisms that participate in the AD have a doubling time from less than 24h up to 15 days, in the case of methanogen bacteria (BAUER; LEBUHN; GRONAUER, 2009). With that, if microorganisms were concentrated in the liquid phase, a reduction in HRT would cripple the AD bacteria population due to the removal being higher than the replenishment rate. This would result in a reduction in the degradation rate in the reactor, as the microbial community would not be numerous enough the keep with the degradation. As no such effect was observed, it is indicated that the presence of organisms in the liquid phase was negligible in comparison to the quantity observed in the sediment bed.

Even with this evidence, experiments conducted in October were not sufficient to fully confirm this hypothesis. Experiments at a given HRT lasted for six days only, which was way less than the 3 HRT that was observed in the literature for HRT impact analyses (GOSSETT; BELSER, 1982; KIM et al., 2006). In addition, one

week was not sufficient to verify any sustained effect due to a long period of operation and, in the case of weeks 19 and 20, to allow the system to recover from a high OL period. With that, a longer analysis period is required to confirm the low microorganism presence in the less dense liquid phase hypothesis.

Overall, a short period of operation at lower HRT showed results contrariwise what was found in the literature. A stable degradation rate and output average ODM, TDM, and COD were different than the drops expected from a digester in response to a shrinking HRT. Moreover, degradation values were comparable to high concentration PS AD even when operated at a 4 day HRT. Comparisons to clarifiers cannot be made, because the HRT was not small enough to be comparable to normal uses of this equipment. Solids retention efficiency had lower values than previous periods due to PS dilution in the input.

7.3. Gas quality and production

Gas production was measured starting from the 30th of June, before the normal operation period. However, as shown in Figure 21, the combination of production rate being below the quantification limit of equipment and a data log problem between July 21st and 27th provide low reliability of the gas production measured in the period. Therefore, no discussion concerning gas production is made for this period.

In addition, due to a delay in the gas analyzers installation, gas quality measurements started after the 27th of September, as shown by Figure 50. Therefore, the gas quality between August 2nd and September 27th is uncertain, making it not possible to measure the total methane production for the period. However, this parameter could be estimated by the average behavior of this parameter after September 27th. Therefore, methane production was not used for comparisons with the literature, but only gas production.

7.3.1. Organic load and feeding schedule

Different from what was observed regarding TDM, ODM, and COD at the output, gas production was sensitive to changes in the feeding schedule. As shown by Figure 80, production had very different profiles over the weeks. The 5-days feed regime showed a weekly profile, in which the same days of the week had similar

production rates, increasing during Monday and Tuesdays and dropping after Saturday until the next week. Following periods had this same profile, but daily, with a lesser final drop until the following feed.

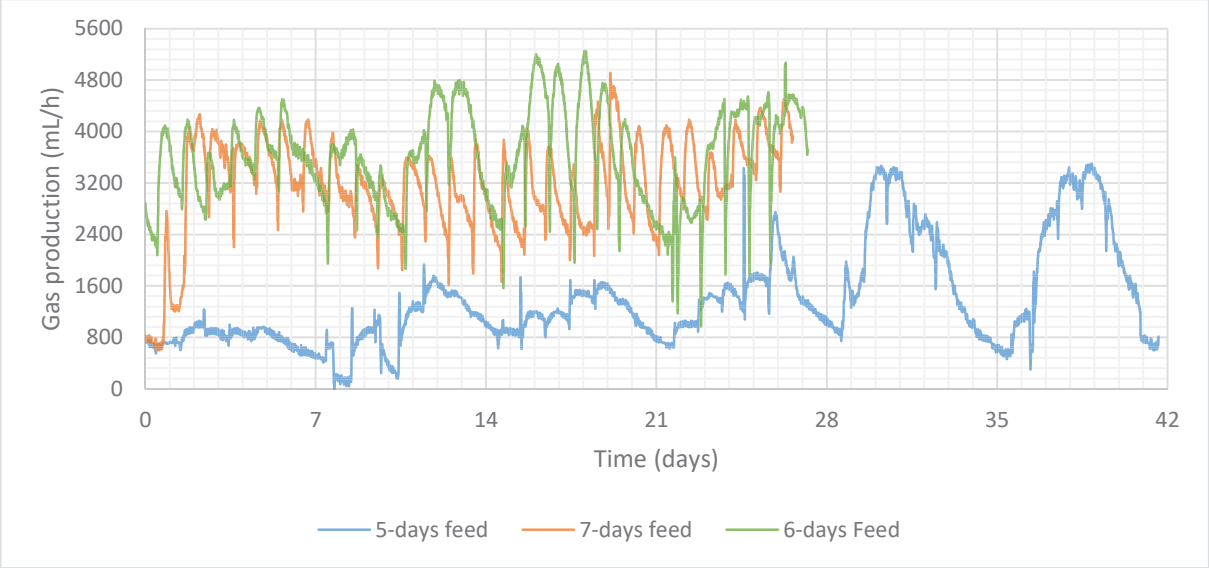

Figure 80 – Gas production profile comparison between different feeding schedules.

This behavior showed that production did not start immediately after feeding when it was done after two days without feed, as shown by Figure 81 and Figure 82. This was observed more clearly during weeks 14 and 15, where gas production rates achieved 2500 mL/h only on Tuesday afternoons despite an OL of 0,967 and 1,041 kg VS/m³d having been used on Mondays during weeks 14 and 15 respectively. This can be associated with the time necessary for the microorganism population to recovery from a starvation period and to products of fermentation being again available in the medium. The starvation was intensified by the fact that the OL during both Fridays was very low, < 0,300 kg VS/m³d, reducing overall available nutrients for the no-feed period and accelerating the gas production drop.

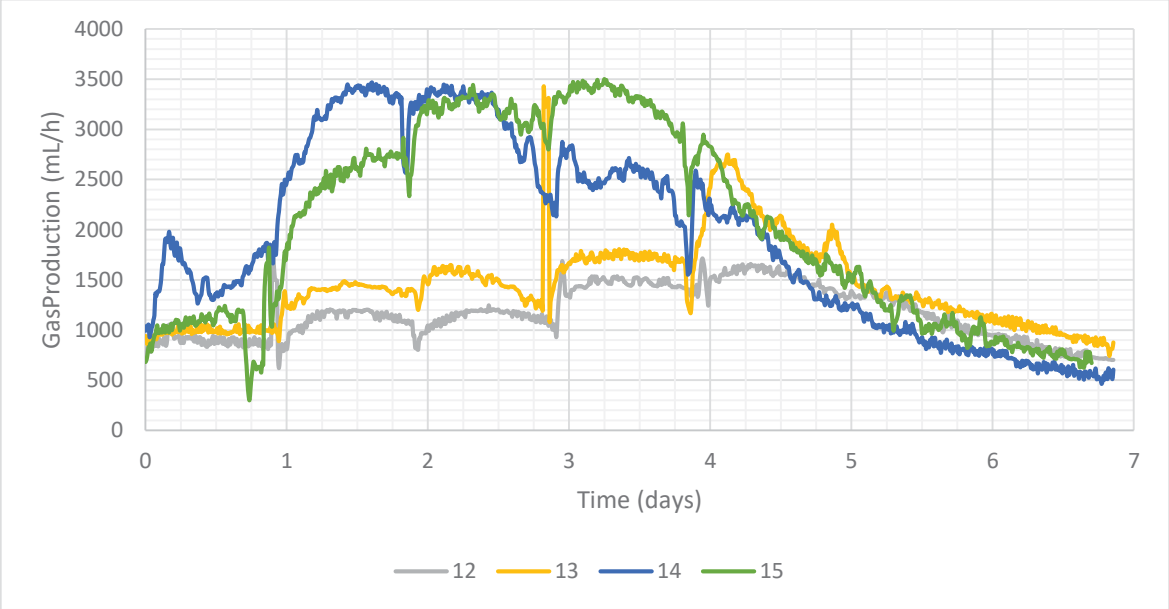

Figure 81 – Gas production profile comparison between weeks 12, 13, 14, and 15.

As shown by the gas production, after two days without feeding, rates dropped to levels that could not be reliably quantified by the measurement device. This was also reflected in the accumulated and specific gas production for the day, which was the lowest during each week (see Figure 41). This indicates that most of the easy degradable matter had been consumed, leading to a reduction of the number of organisms that were responsible for the primary hydrolysis and fermentation. This is confirmed by the fact that specific production on both weekends was high, indicating that most of the easier degradable had been already consumed.

Therefore, to reestablish the degradation rate, a waiting time was required to replenish this population. With this time, OL that was not degraded during the first day of feeding was degraded along the following day, which explains why the maximum weekly production rate was sustained for 48h. This same effect was not observed when only one day of feeding was skipped during the 6-days feed regime as shown by Figure 82. This can be further verified by the specific production and the accumulated feed-to-feed production, as values for Mondays were similar in comparison to other weekdays (see Figure 61).

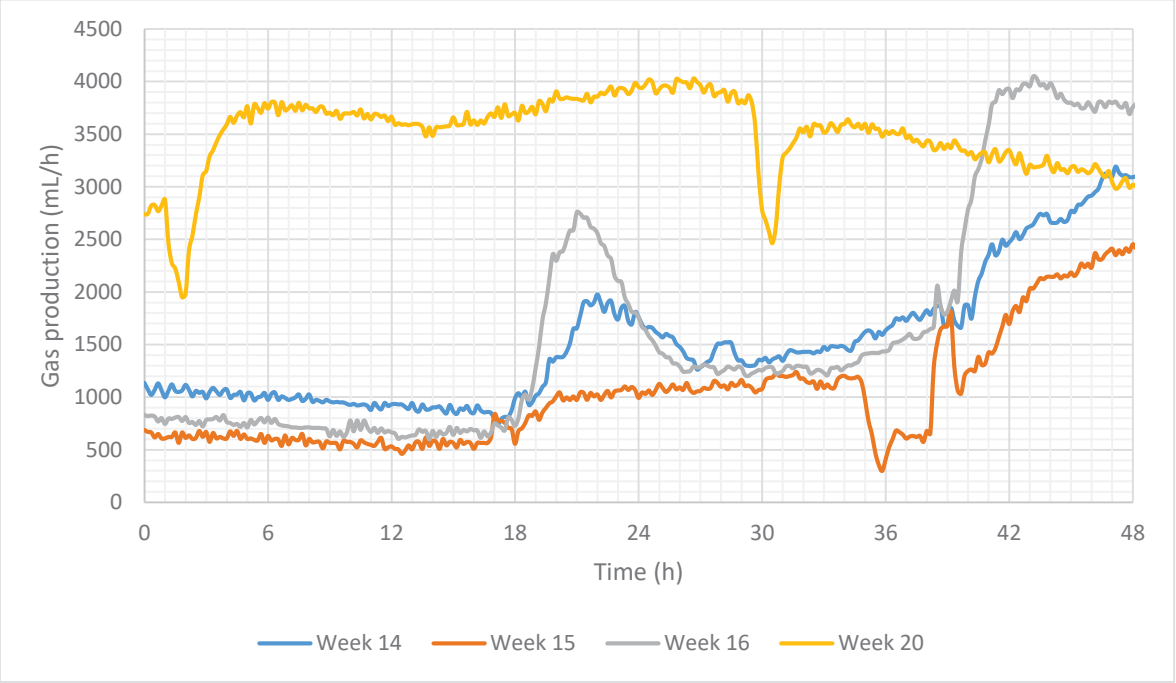

Figure 82 – Gas production profile comparison of the first 48h after the first feeding of weeks 14, 15, 16, and 20.

The production delay was similar to what was expected for the doubling time for the bacteria responsible for hydrolysis, 15-20h (LEBUHN; GRONAUER, 2009). Moreover, this effect is not likely to be associated with a change from a mixture that contained ES to one that did not. This happens, because this delay was observed both in weeks 15 and 16, which showed a very similar behavior even though no ES had been used in the week preceding them. ES effects, however, can be seen between weeks 10 and 13, as specific gas production for the period was below the average observed for weeks when only PS was used in the feeding mixture (see Figure 41).

Weeks 10 through 12 showed a lower gas production due to lower OL during these weeks, however, 13 a slightly lower production despite an equivalent load if it is compared to weeks 14 and 15. As shown by Table 5, yields during 13 were 17% lower than the average of weeks 14 and 15. In addition, production was below 1800 mg/L between Monday and Thursday, only surpassing this mark on Friday and Saturday, when it dropped to levels below 1000 mL/h (see Figure 38). Production during the week increased in steps with each maximum production being at least

15% higher than the previous days. As the OL during these days did not increase similarly, this behavior indicates recovery from a possible inhibition followed by a shrinking of the microbial population during previous weeks.

The inhibition hypothesis can be associated with to use of ES in the feeding mixture between weeks 10 and 13. Due to ES having a higher concentration of ammonia, a possible ammonia inhibition might have occurred, being more intense during weeks 10, 11, and 13 when 5 L were used. With that, the overall production would be reduced. The reduction during weeks 10 to 11 cannot be taken into account as the products were often below the equipment quantification limit (1000 mL/h).

Moreover, starting from week 13, sludge was not collected daily anymore, being collected once each four days and stored. This can explain why the production during week 13 increased over time with a step-like profile and a constant production of the day, as highlighted in Figure 83. Due to the cooling of ES, ammonia solubility in water increased, leading to a higher concentration of NH_4^+ in solution due to ammonia dissociation in water (ASTDR, 1997). This increased the inhibition potential of the ES (GUO et al., 2021b), which could have killed the inactive microbial population in the PS during the feeding mixture preparation. In addition, this mixture would have also an increased inhibitory effect while it has heated to the reactor temperature and a new equilibrium has reached. With that, fermentation would have been undermined, resulting in a slower degradation rate of organic matter and, as a result, a more constant gas production.

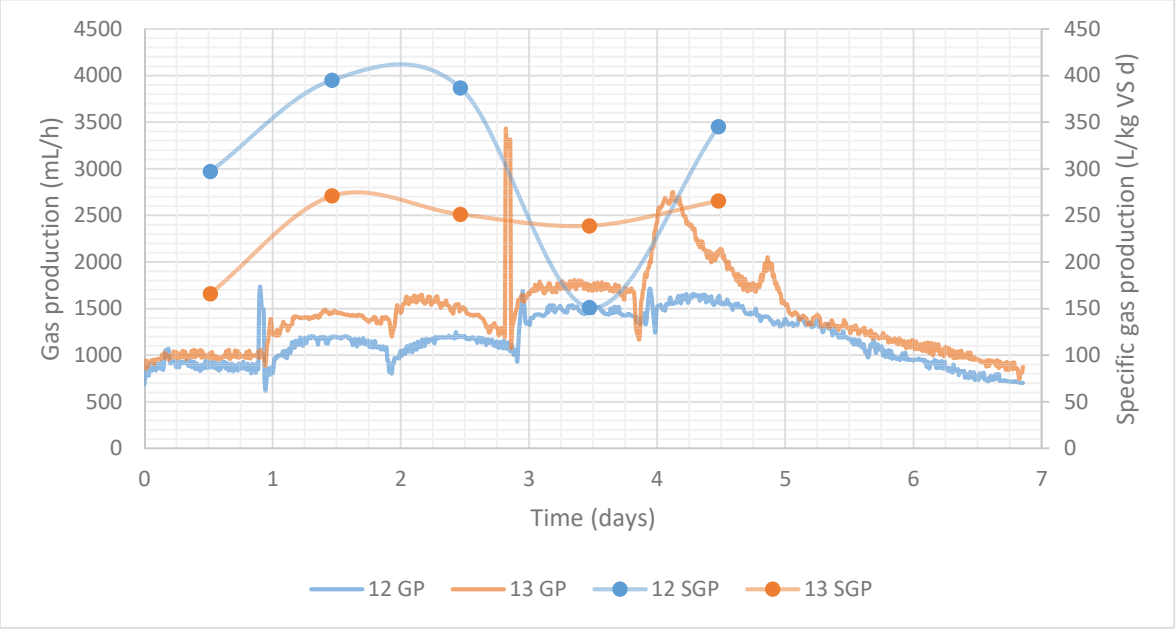

Figure 83 – Gas production profile (GP, mL/h) and specific production (SGP, L/kg VS d) comparison between weeks 12 and 13.

The strengthening of the ammonia inhibition hypothesis is further supported by the gas production profile after the feeding on August 28th, as shown by Figure 83. PS and ES used for the feeding mixture on that day were collected on the same day, therefore the temperature was ambient. This goes in concordance with why yields on week 12 were considerably higher than 13, despite a lower quantity of ES being feed but no cooling was involved.

With that, inhibitory effects were dwindled, speeding up the fermentation processes and increasing the gas production during the first hours after feeding. This led to a similar production profile observed on weekends during the 6-days feed period, but with a lesser overall production, (see Figure 60). It is important to note that on Monday, sludge was collected during the morning and fed during the afternoon, being stored under cooling conditions meanwhile.

However, the enhanced ammonium inhibition effect cannot be fully proved with the data available. To achieve this, it is necessary to evaluate a longer time with a cooled feeding mixture and an ambient temperature one. In addition, measurements of ammonium content of the input and output must be conducted as well as VFA concentration. A better understanding of different sediment beds would be also ideal to better analyze the impacts of mixing ES with PS in the input.

Gas production profile after week 16 had similar daily variation shapes until the end of experiments, as described in sections 6.3.4 and 6.3.5. This similar shape resulted in a similar feed-to-feed production independent of the OL used in a day at an HRT of 23,37 days, as highlighted by Figure 84. Except for September 13th, the first day of feed of the 7-days regime during week 16, accumulated production was above 65 L, but even with the highest OL on Monday during week 19, production did surpass the 90 L mark, as shown in Figure 84. This same performance pattern for lower OL days, as exemplified by Friday and Tuesday of week 18.

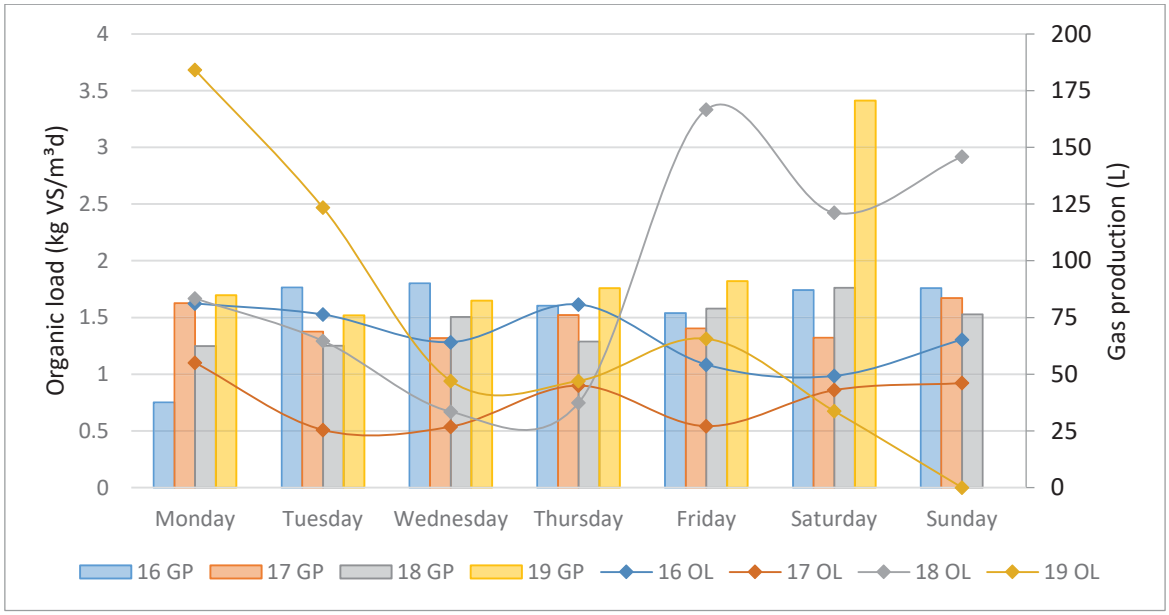

Figure 84 – Organic load (OL, kg VS/m³d) and accumulated feed-to-feed gas production (GP, L) comparison between weeks 16, 17, 18, and 19.

Explanations for that can be seen in Figure 85 which compares two periods with both methane concentration and gas production measurements available during the 7-days feeding regime. The high OL period (HOL) is between October 1st and 4th when an average of 3,092 kg VS/m³d was fed, and the low OL period (LOL) is between September 27th and 30th, when an average of 1,095 kg VS/m³d was fed. It is important to note that between October 6th and 10th, OL was lower than between September 27th and 30th, but to avoid possible lingering effects of the HOL, the second period was chosen.

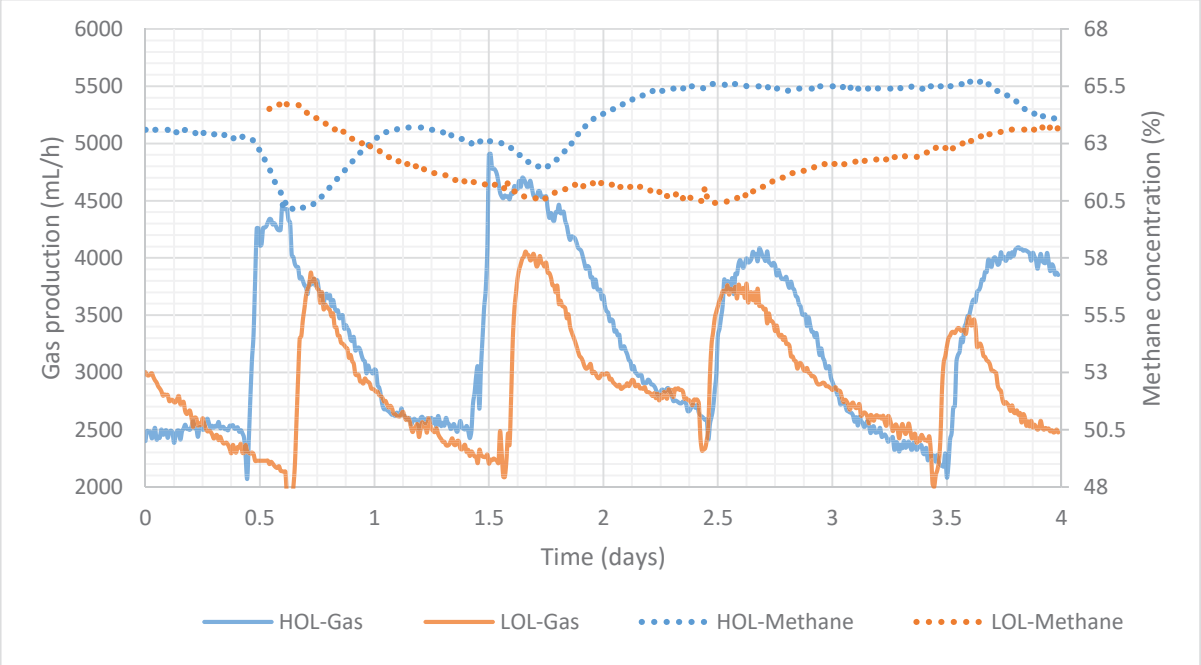

Figure 85 – Gas production (mL/h) and methane concentration (%) comparison between high (HOL) and low organic load (LOL) during the 7-days feeding period.

Comparing the HOL and LOL, one can observe that the production profile shape was similar, but peak production was higher during HOL. However, the production baseline was very similar on all days, but during HOL, rates dropped faster than in LOL, taking the same amount of time to reach the baseline. This behavior was only not observed on the last day in the HOL when top production took 4 extra hours to be reached. This resulted in an average feed-to-feed production during HOL of 82,06 L, which was only 24% higher than the 66,08 L during the LOL, despite three times higher OL (see Figure 49).

This small increase in response to a huge increase in OL indicates that the reactor reached maximum production rates and started to suffer from overloading. This is also supported by mass balances, with indicate that the degradation rate between October 1st and 5th dropped from 32,5% to 26,7%. Methane concentration did not indicate otherwise due to oxygen infiltration on September 28th during the LOL, which reduced the methane content as carbon dioxide was being produced by oxidation instead. Therefore, there is more evidence that supports the hypothesis that the maximum OL capacity of the reactor at operating conditions should be less

than 2,468 kg VS/m³d, which covers the value found for the same value in a reactor with equal volume in previous works (LIENER, 2020).

Furthermore, as displayed in Figure 49, specific production crumble between October 1st and 5th, being below 180 L/kg VS d. In addition, the average production feed-to-feed was slightly lower than what was observed between September 14th and 20th, 84,52 L, and the higher specific production at a maximum of 445,37 L/kg VS on September 18th. Considering only days in which interval in between feeding was around 24 h, the highest feed-to-feed production was verified on October 8th, at 90,98 L with a specific production of 349,95 L/kg VS d, for an HRT of 23,27 days. This further supports that at 2,468 kg VS/m³d, overload effects can be felt, but reduced the estimation for the maximum load to be at least 1,361 kg VS/m³d at these operations conditions, a value which the maximum production was achieved.

Nevertheless, as shown in Figure 85, OL shock effects were less intense than what was observed in-tank reactors. Braz *et al.*, 2018, showed that methane content can decrease to concentration under 30% after a 3 times OL shock. Other studies showed similar drops in methane concentration, in addition, to a drop in biogas yields in response to doubling OL during the first 24 hours (SCHOEN et al., 2009). With that, it is possible to conclude that the digester had a higher resistance to OL shocks, as it could endure a tripling in OL without showing any gas production drops and a small methane content reduction.

Moreover, overloading can be associated with the gas production during days following the HOL, which suggested a lingering effect related to the high load used between October 1st and 5th. As highlighted in Figure 86, the baseline production rate increased from 2200 mL/h on October 4th to more than 3000 mL/h after October 7th, reaching 3600 mL/h on October 9th. In addition, production was kept constant or increased slightly until the next feed after reaching a minimum. This indicates that the methanogens continued even after most of the organic matter had been hydrolyzed.

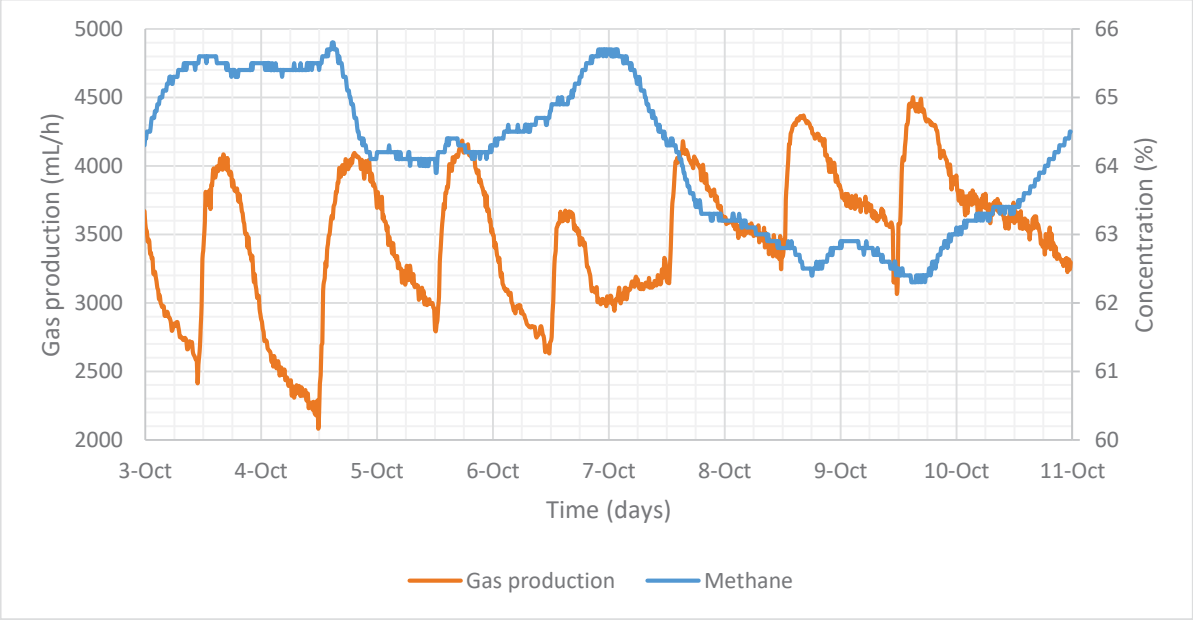

Figure 86 – Gas production (mL/h) and methane content (%) between October 3rd and 11th.

In addition, the methane concentration profile between October 6th and 10th indicates VFA had been being accumulated in the reactor. This can be assumed because CO_2 concentration has increased during the period, which was a result of methanogens being conducted mainly via the acetate pathway (ANUKAM et al., 2019). With that carbon dioxide would be produced faster than it is consumed during the hydrogen pathway, pulling the methane concentration closer to 50%. This indicates overloading effects in the reactor, as VFA accumulation is an indicator of such phenomenon (FERRER; VÁZQUEZ; FONT, 2010). As a secondary consequence, an increase in carbon dioxide concentration suggests that the difference between the sum of methane and carbon dioxide and 100%, as shown by Figure 51, can be related to the presence of hydrogen.

The overloading effect hypothesis is also supported by the increase of methane on October 10th. This pattern was also seen on Sundays during the 6-days feed regime. Methane content had increased over the weekend and the beginning of the week to a concentration above 70% before it started to drop to values around 64% (see Figure 62). This showed that as the reactor was fed, VFA accumulated, decreasing methane content. However, after the feeding ceased, VFAs were consumed, allowing CO_2 to be consumed faster than it was produced, hence

methane content increased. Data indicates that if more days were skipped, production would diminish, as shown by the gas production profile of the 5-days feed regime in Figure 38.

These effects can be also verified during week 20, when despite low OLs on October 14th and 15th, showed similar values of total gas production in the week, leading to a yield of 566,76 L /kg VS, as (see Table 14 and Figure 57). As the OL was reduced, methane content increased up to 69% as the production slowly decreased, as shown by Figure 87. After the OL was reestablished to a high standard, methane content decreased to 63,8%, until increasing once again on Sunday, when feeding was skipped. Differences to 100% of the combined methane and carbon dioxide content, suggested also the presence of hydrogen in the system, which further supports the overloading hypothesis.

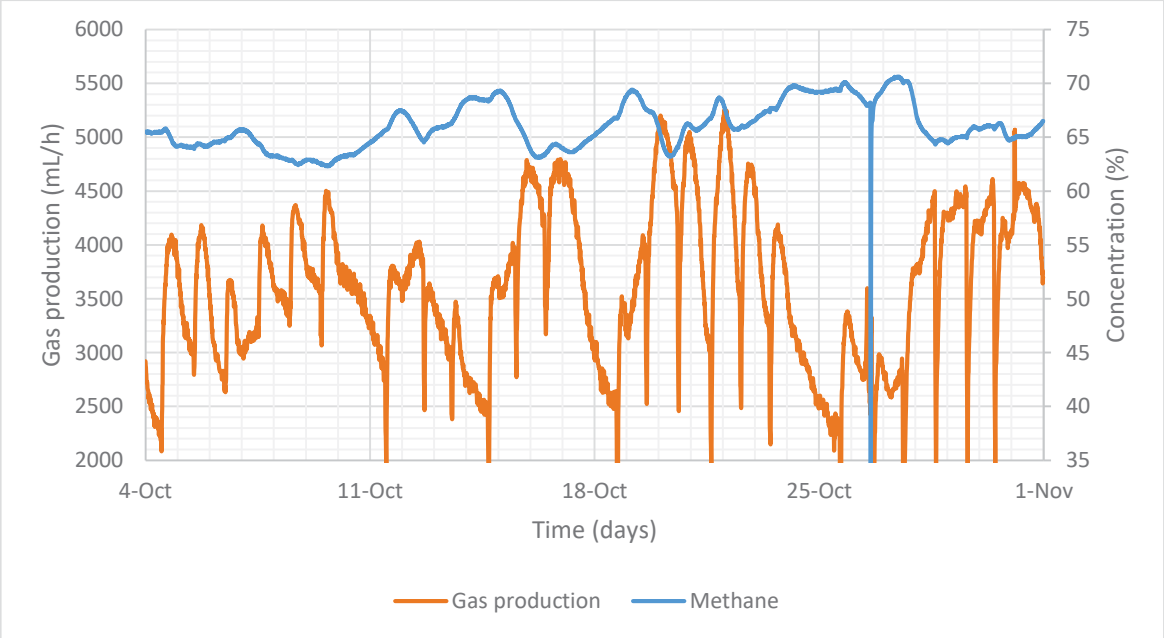

Figure 87 – Gas production (mL/h) and methane content (%) between October 4th and November 1st.

It is important to note that overload and OL shock act differently in a PFR in comparison to a tank reactor. Overload happens when in a given volume amount of organic matter is above what that volume can handle. In a perfectly stirred tank, if a fraction of the reactor is overloaded, the whole reactor is also overloaded due to perfect mixing assumption, the concept that can be carried over to a well-mixed real

reactor. However, in a PFR, mixed in the length direction is very limited, overload effects can happen locally and not widespread like in-tank reactors, as the volume is not perfectly mixed.

In the case of the digester and the operation conducted, overloads effects could have been felt in isolated sections, due to particle transport mechanisms. As high concentrated PS is fed, particles tended to sediment while they were being carried by the flow. With that, the distribution of matter was strongly related to sedimentation parameters, such as flow velocity, particle size, and concentration. The maximum capacity before the reactor is overload is not a value that only depends on the digestion process, but also particle dynamics. Therefore, particle distribution in the reactor might have caused these effects instead of the OL itself.

Even with overloading problems, methane content on most days was within the usual range for wastewater treatment plant sludge standards of 63-67% (BACHMANN, 2015). However, if compared to cases when overloading effects had happened, methane content was significantly higher. As an example, Braz *et al.*, 2019, observed methane concentration below 40% when studying the effects of overloading during AD of primary sludge at mesophilic conditions. However, methane values were lower if compared to thermophilic conditions, which can reach content up to 72% on small scales (JANG et al., 2014).

In addition, Figure 88 shows that the specific gas production increased greatly upon a reduction of OL and COD load. This is a result of a stable accumulated feed-to-feed production during the 7-days feed regime (see Figure 49). This indicates that organic matter could not be fully degraded throughout approximately 24h, creating a buffer that supported production during the following days. This effect made specific production extremely higher on days with low production, such as September 21st and 22nd, giving a false impression that the system has higher efficiency.

As a consequence, it is necessary to use a period that is long enough to make these lingering effects negligible. For an HRT of 23,37 days and continuous feeding, the period between September 14th and 30th is the most suited to be used as the true efficiency of the reactor. This avoids any overloading effects from the

high load period between October 1st and 5th and their lingering potential on the following days. This also avoid the first day of feeding, which had a period with lower gas production and a distinct production profile. With that, the average reactor performance for a daily feed at 23,37 days HRT is 373,60 L/kg VS and 260,04 L/kg COD. If one considers the average methane content between September 27th and 30th, 62,2%, as the average content for the period, specific methane production can be estimated as 232,41 L/kg VS and 161,79 L/kg COD.

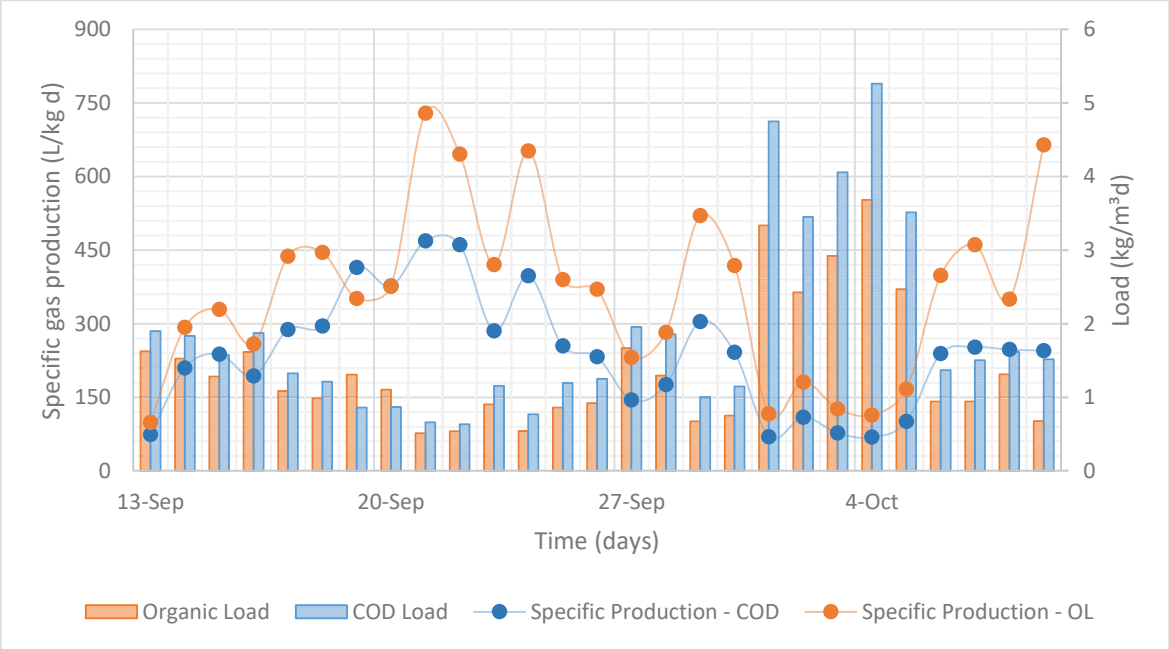

Figure 88 – Organic load (kg VS/m³d), chemical oxygen demand load (kg COD/m³d), specific gas production regarding COD (L/kg COD d), and specific production regarding organic load (L/kg VS d) between September 13th and October 9th.

This problem did not happen during the 5- and 6-days feed regime, to an extent. Production during the 5-days feeding regime, gas production rates reached levels below 1000 mL/h before the next cycle had started, as illustrated in Figure 81. Therefore, even if lingering effects would have occurred within the week, specific gas production for the week itself would not be affected. Therefore, the weekly specific gas production was not significantly affected by lingering effects from previous weeks.

During the 6-days feed regime, time in-between cycle was insufficient to allow the production drop below 1000 mL/h, if the end production rate is above 2500 mL/h (see Figure 60). However, it was observed that the first day of specific gas

production during weeks 20 and 21 had similar values to others, besides the spikes on October 12th, 13th, and 20th (see Figure 61). Week 22 showed an increasing trend over the week regarding both specific gas production and production rates, of which both had the lowest values on Monday (see Figure 58). Therefore, one can neglect influences from the previous cycles in the weekly specific gas production for weeks 20, 21, and 22.

With that, yields were on average lower than the range expected for sludge, 450-500 L/kg VS at mesophilic conditions (BACHMANN, 2015), during the7-days feed, this rage could be only achieved during 14. However, yields are comparable to other sources which suggest a wider range for the expected production for mesophilic conditions, 300-750 L/ kg VS, being closer to the lower end as OL increased (APPELS et al., 2008; TORECI; KENNEDY; DROSTE, 2009; WELLINGER; MURPHY; BAXTER, 2013). If compared to overload regimes, gas yields are twice as higher as what was observed in tank reactors (BRAZ et al., 2019; SCHOEN et al., 2009).

On the other hand, specific gas production was close to being within the range observed in conventional and high loads anaerobic digesters in WWTP in the region of Stuttgart. As studied by Wealkens (2020), the performance of anaerobic digesters ranged from 395 L/kg VS and 614 L/kg VS for both conventional and high load reactors, with an average load range of 0,3-2,0 kg VS/m³d and 3,7-6,9 kg VS/m³d. However, the small difference to what was observed can be justified by the presence of fat in the input, which can decrease the ODM values in analysis, thus overestimating the specific gas production (YAN, 2017).

Compared to previous works in the institute, which analyzed the operation of a tank reactor with an equivalent volume, results showed that the PFR had a better performance. Overall the production per added COD (183,28 L/kg COD 20h) was 12% higher than what was observed in the tank reactor for PS at mesophilic conditions (LIENER, 2020). The increase was even more substantial if one compares to the value between September 14th and 30th, (216,71 L/kg COD 20h), being this 32,4% higher. Methane content was also higher on average, but maximum values were lower than what was observed both for PS and co-digestion with other

substrates (LIENER, 2020; YAN, 2017). However, methane content cannot be properly compared due to the high presence of air inside the tank reactor during previous works.

The most noticeable difference was in the gas production profile. As seen in Figure 60, 48h after the feeding production rates were all above 2500 mL/h after peaking at on average 4200 mL/h. Compared to previous works, all showed that, after a period of 48h, production rates were below the 1000 mL/h quantification limit, reaching this low-end production after on average 30h (LIENER, 2020; WEI, 2020). This showed a more stable gas production than other works and, as the same gas counter was used, more reliable measurements during operation.

Overall, the reactor showed great resilience to changes in OL and high concentrations shocks, as the gas production followed the same pattern during the 6- and 7-days feed regimes. It was found that the reactor could have suffered from overloading effects after the HOL between October 1st and 5th, but effects were not as harsh as showed by the literature. Moreover, it was observed that overloading effects were related to solids dynamics and flow pattern in addition to the OL itself.

In addition, data showed that production could be maintained above a baseline production of 2500 mL/h during 6- and 7-days feed regime with a methane content above 60% consistently. It was also observed that skipping a feeding day improved methane content significantly during subsequent days, being possible to achieve concentration above 70%. At last, data indicate that ES could have had an inhibitory effect between weeks 10 to 13, being intensified when a cooled feeding mixture was used.

7.3.2. Hydraulic retention time

The reduction of HRT did not have a degenerative impact on the gas production and methane content. As seen in Figure 57, the production profile had a similar shape as the HRT reduced from 23,37 to 11,69 days between October 4th and October 25th. This resulted in a similar gas production between weeks 19 and 22, being weeks 19 and 22 the lowest, as shown by Table 14.

If one compares it to the previous period, besides an apparent increase in capacity, the reactor performance improved at a lower residence time. Week 20 had the highest weekly specific gas production at 566,76 L/kg VS, being 51,7% higher than what was verified between September 14th and 30th. Even not considering the gas production the 24h prior to the start of week 21, specific gas production was 34,5% higher at 506,13 L/kg VS. The increase is substantial enough to be related to possible interferences of the high load during previous periods. Therefore, this indicates that the reactor had a better performance at an HRT of 11,69 days.

An improvement was also verified for an HRT of 7,90, but with a smaller increase. Yields were 23,4% higher than the period between September 14th and 30th at 465,02 L/kg VS, but only 11,3% at 418,08 L/kg VS if the gas production 24h prior to the first feeding is not considered. This is not enough to confirm a better performance, but it is enough to confirm that the performance was equivalent or slightly better than an HRT of 23,37 days. A similar improvement was not observed for an HRT of 3,90 days.

Figure 89 compares two periods with both methane concentration and gas production measurements available during the 6-days feed regime. The high HRT period (HHRT) selected is between October 18th and 25th when the HRT was 7,79 days, and the low HRT period (LHRT) is between October 25th and November 1st, when the HRT was 3,90 days. It is important to note that between October 4th and 18th, OL could not be kept similar during the week due to extremely high concentrate sludge on October 4th and 5th and bad quality PS on October 14th and 15th. Week 22 was chosen despite the air infiltration on October 26th, because its production profile shape in addition to during this week HRT was at a minimum.

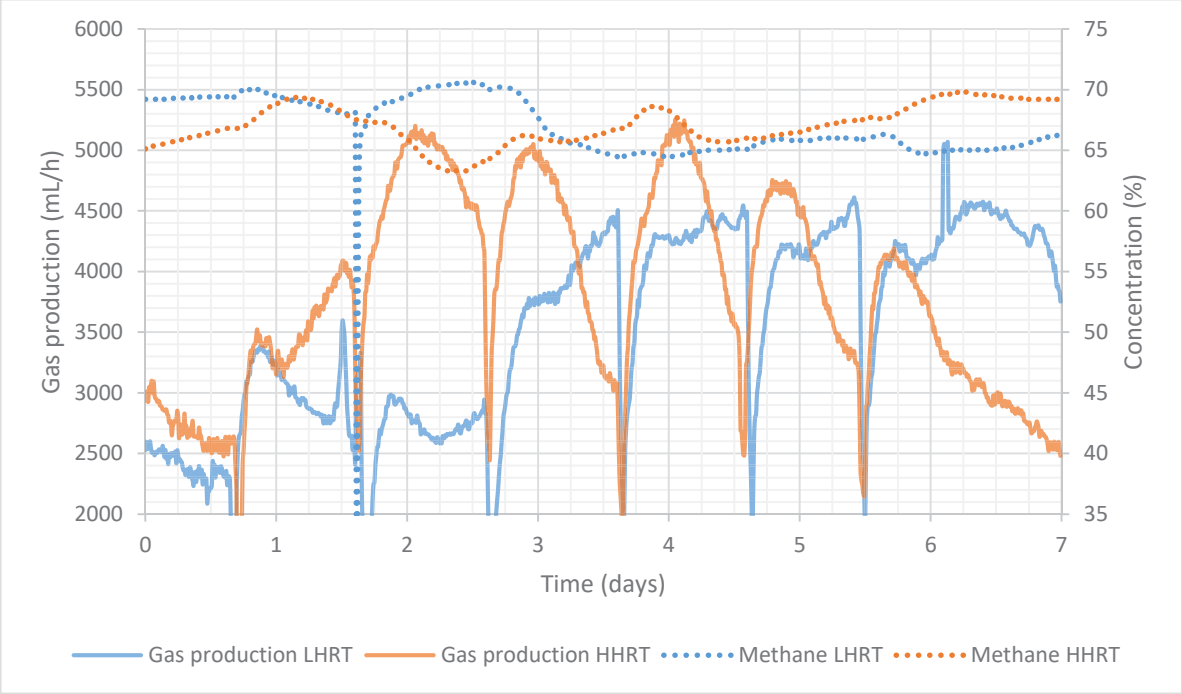

Figure 89 – Gas production (mL/h) and methane content (%) comparison between the high (HHRT) and low hydraulic retention periods (LHRT) during the 6-days feed regime.

As highlighted by Figure 89, gas production profiles during the HHRT and LHRT developed differently during the week. HHRT has a similar development as what was observed during lower HRT during the 7-days regime, as one can see if comparing Figure 89 to Figure 46. Intense drops were associated not with HRT itself, but with the feeding procedure. As explained in section 7.1.3, the feeding procedure took longer to be conducted than in previous weeks, forcing the valves to remain close for a longer time, which intensified the daily production drop. This indicates that a reduction from 23,67 days to 7,79 days was not sufficient to disturb gas production during one week of operation.

However, accumulated feed-to-feed production during week 21 supports the hypothesis that a change in flow pattern or feeding can change the reactor capacity. On October 19th, the production feed-to-feed was the highest for an in-between interval of 24h during experiments at 110,49 L, being the production also above 100 L on October 20th. This was achieved at an OL of 2,038 kg VS/m³d reflecting in a specific production of 485,24 L/kg VS d. This suggested that overloading effects

were lesser during this period, hence the capacity of the reactor should have increased.

In addition to indicating a capacity increase, the profile during week 21 also supports the hypothesis that high OL contributes to gas production on several days. Production on the weekend preceding week 21 had the highest feed-to-feed production registered, with 196,84 L, which was followed by the two highest production of weekdays (see Figure 61). Despite that, October 20th showed an OL of 0,668 kg VS/m³d. This suggested that organic matter cannot be degraded up to a point that it would not interfere on following days, which creates a buffer of nutrients and keeps the gas production high for a longer period.

On the other hand, the further HRT reduction to 3,90 days did result in a different production profile, as highlighted by Figure 89. Even producing taking a similar time to reach their maxima, top production during the first half of the LHRT was lower than what was observed during HHRT, despite OL being two times higher (see Figure 57). In addition, during the second half time for top production to be achieved increased from 5-8 hours to up to 20 hours, with an increasing trend until the following feeding. This indicated that fermentation could have been slower than in previous weeks.

The stagnation and the slow increase of gas production after the feed indicate that methanogens had been limited by hydrolysis. Due to methanogens relying on fermentation products to happen, a reduction in hydrolysis kinetics results in a reduction in gas production rate (DEEPANRAJ; SIVASUBRAMANIAN; JAYARAJ, 2015), which could have the production profile seen in Figure 89 as an outcome. This suggested that VFA did not accumulate over time after the feeding procedure had been finished. However, the methane content drop on Wednesday indicates that VFA concentrations should have reached high values before they had stopped increasing.

The lower hydrolysis kinetics is further supported by the production profile on the weekend after the last feed, which is shown in Figure 60. After the last feed, production rates had reached a local maximum after 6 hours at 4215 mL/h before

reaching the global maximum 18h later at 4570 mL/h[4]. This kept production above 3000 mL/h for the whole weekend with a smooth increasing trend in methane content.

As a post experiments observation, methane content reached 72,1% on November 2nd, which aligns with what was observed on other weeks regarding methane concentration. It is important to notice that reactor was also fed on November 1st, keeping the same regime like the one used between weeks 19 and 22. Even with this evidence, it is necessary to measure VFA and hydrogen over time to confirm the slower hydrolysis kinetics hypothesis.

Causes for these effects, however, may not have been caused by the reduction of HRT itself, but by changes in the feeding procedure and input ODM and OL relationship. As previously discussed, overloading and overfeeding depend on the distribution of organic matter in the reactor bed, following mechanisms discussed in the section Solids recirculation and transport. Therefore, changes in the feeding procedure in combination with changes in input concentration could have had a greater impact on the gas production than the HRT itself.

During the LHRT period, OL was higher than in previous weeks, however, TDM and ODM in the feeding mixture were below what was used during other weeks in October. This was a result of the increasing volume of feed required to reduce the HRT to 3,90 days in a combination of using water to dilute a similar amount of PS for it. In addition, feeding velocity had to be reduced to due problems with the pump, as leaves were found in the PS, requiring a lower flower rate to avoid any pump damages. This could have increased the range of which particles were deposited on the sediment bed, changing the distribution of particles along with the digester. This would change the local initial availability of nutrients and, consequently, change the gas production profile as a result of a change in kinetics due to concentration.

Due to what was discussed in section 7.3.1, one can assume that effects related to modifications of the matter distribution in the bed may have had a greater impact than the HRT. As shown by Figure 53 and Figure 54, ODM and COD

[4] The sudden spike between hour 15 and 17 were shown to be an outlier, therefore it was excluded during the discussion. Causes for this problems are unknown.

concentration at the output did not change much with HRT reduction. Despite the presence of foam, retention of ODM stayed above 80% and 85% for COD between October 25th and November 1st. In combination with what was discussed in the section Solids recirculation and transport, one can conclude that the solids retention time did not change despite a reduction of 75% in HRT. Therefore, due to shreds of evidence showing that the AD takes places majority in the solid phase, only changes in the solids retention time would have noticeable effects.

Nevertheless, more investigation is required to evaluate and individualize HRT and particles distribution effect. For that, it is necessary to measure flow velocity at different heights and lengths in addition to measurements of the height of the sediment bed. Free-surface flow model development and a longer feeding period are also required to better understand particle distribution and then prepare an experimental schedule to validate hypotheses. In addition, it is necessary to evaluate the reactor performance at a low HRT for a longer period in order to run at a stable profile, as an increasing trend was observed until the end of week 22.

The lack of impact upon a reduction of HRT can be also seen when one compares with effects in the literature. A reduction in HRT from 20 to 5 days can create instability in the gas production, which can reduce gas production up to 50% in addition to dwindle its methane content in tank reactors (TORECI; KENNEDY; DROSTE, 2009). This was only observed during the first day of week 22 when specific production dropped to 128,32 L/kg VS d, which can be associated with the reestablishment of the feeding and changes in the flow pattern. This can be assumed because specific production increase towards the end of the week reaching 329,10 L/kg VS d on October 30th, as shown by Figure 61.

Even with these variables, overall, the reactor showed an improvement of performance at lower HRT, being at best at 11,69 days in week 20. During this time, gas production was within the range of 353-659 L/kg VS in conventional anaerobic digesters installed in WWTP in the region of Stuttgart (WEALKENS, 2020). Gas production was comparable even for an HRT of 7,79 at 456,02 L/kg VS, indicating that the system can yield similar results at an HRT 25% lower than conventional high load anaerobic digesters, which operate at a minimum HRT of 10 days (WEALKENS,

2020). However, performance at an HRT of 3,9 days did not show good performance, but an increasing trend observed in Figure 61 suggests that a longer period is required to evaluate the reactor performance at this regime.

At last, HRT had a low impact on gas production, with evidence suggesting that changes in profile were due to changes in particles dynamics inside the reactor. Overfeeding effects could be seen during both HHRT and LHRT periods. Data also indicate that during the LHRT period hydrolysis proceeded slower than previous weeks, its cause was rooted in particle dynamics and not on HRT itself. Week 21 profile suggests that the reactor capacity can be changed with changes in the flow pattern and HRT. Nevertheless, more experiments are required to confirm the hypothesis discussed in this section

8. Conclusion

A plug flow reactor could be operated for a total of 140 days. After operational data and TDM analysis, it was concluded that a screw pump could successfully maintain the recirculation of particles with a concentration of an average TDM of 1,84%. Experiments showed that the current system cannot operate continuously with the current setup, being a secondary pump is strongly recommended for that. It was also found that for dealing with higher concentrate sludge, the current screw pump should be replaced with one equipped with a cutting blade.

Operational data showed that temperature could be safely kept above 30°C in the whole reactor during normal operation, but the heating system showed evidence to be worn out at the end of experiments. In addition, evidence showed that the thermal isolation of the system and the utilization of only one thermal recirculation cannot provide a reliable control at higher temperatures. After comparing gas production with the literature and evaluating the temperature profile, it was found that temperature could have reduced gas production rates.

Overall a total of 5,353 m³ of biogas was produced during normal operation, it is estimated to be composed of 3,503 m³ of methane and 1,833 m³ of carbon dioxide. Biogas yields for the period were 330,23 L/kg VS, 220,70 L/kg COD, and 7,66 L/LPS; in terms of methane production 216,06 L/kg VS, 144,40 L/kg COD, and 5,01 L/LPS. In terms of liquid input and output, an overall reduction of 85,07% of TDM and 84,48% of ODM was obtained, being 93,11% of COD reduced.

Moreover, after comparing mass balances results and experimental observations, it was concluded that solids matter had a higher retention time than the HRT. Evidence indicates that particles within different layers of the flow have a different velocity. In addition, after observation of the output behavior and foam formation pattern, it was concluded that the particle transport can be described in analogy to a riverbed.

TDM, ODM, and COD analyses showed that the digester could operate at the stable output through a wide range of OL and HRT. After literature comparison, one can conclude that the system can operate with a removal rate close to what was

obtained in clarifiers, with similar degradation rates to those observed in tank reactors. Moreover, evidence suggested that particles retention does not depend on degradation rate.

Overall, gas production data indicated a great resilience to changes in OL and high concentrations shocks. Production could be maintained above a baseline production of 2500 mL/h during 6- and 7-days feed regime with a methane content above 60% consistently. Literature comparison showed that yields at an HRT of 23,37 days were at the lower end of what is expected for AD of PS at mesophilic conditions. However, methane concentration was above what was expected for WWTP sludge.

In addition, variations in methane content and gas production profile indicate that the reactor could have suffered from overloading effects. Due to differences with what was found in the literature, one can conclude that these effects were related to solids dynamics and flow pattern in addition to the OL itself, suggesting that overload occurred locally. In addition, data operation data analyses suggested that the maximum reactor capacity should be around 1,350 kg VS/m³d. However, the evidence collected is not conclusive, being necessary further investigations to prove or dismiss this hypothesis.

Comparing the weekly gas production profile, it was also concluded that skipping a feeding day improved methane content significantly during subsequent days. At last, data indicate that ES could have had an inhibitory effect between weeks 10 to 13, being intensified when a cooled feeding mixture was used. At last, by analyzing consecutive days with high and low OL, it was found that a high concentrate feed increased the gas production on the following days if they had a low OL.

At last, analyses of the gas production data showed that the performance of the reactor improved at lower HRT, with an optimal at 11,69 days. In addition, yields at these conditions were close to the higher limit of what is expected for anaerobic digestion of WWTP sludge. Performance at an HRT of 7,79 days was also better than what was observed during operation at 23,37 days of HRT, being within the range of what was observed in the literature.

9. References

ACHINAS, S.; ACHINAS, V.; EUVERINK, G. J. W. A Technological Overview of Biogas Production from Biowaste. **Engineering**, 2017.

AN, D. et al. Effects of total solids content on performance of sludge mesophilic anaerobic digestion and dewaterability of digested sludge. **Waste Management**, v. 62, p. 188–193, 1 abr. 2017.

ANUKAM, A. et al. Methods of accelerating and optimizing process efficiency. **Processes**, v. 7, n. 8, p. 1–19, 2019.

APPELS, L. et al. Principles and potential of the anaerobic digestion of waste-activated sludge. **Progress in Energy and Combustion Science**, v. 34, n. 6, p. 755–781, 1 dez. 2008.

ASTDR. 3 . CHEMICAL AND PHYSICAL INFORMATION Table 3-1 . Chemical Identity of Endosulfan. **Identity**, n. Windholz 1983, p. 3–7, 1997.

BACHMANN, N. Sustainable biogas production in municipal wastewater treatment plants. **IEA Bioenergy**, p. 20, 2015.

BAUER, C.; LEBUHN, M.; GRONAUER, A. Mikrobiologische Prozesse in landwirtschaftlichen Biogasanlagen. **Bayerische Landesanstalt für Landwirtschaft**, v. 1. Auflage, p. 38, 2009.

BERGHUIS, B. A. et al. Hydrogenotrophic methanogenesis in archaeal phylum Verstraetearchaeota reveals the shared ancestry of all methanogens. **Proceedings of the National Academy of Sciences of the United States of America**, v. 116, n. 11, p. 5037–5044, 2019.

BLASIUS, J. P. et al. Effects of temperature, proportion and organic loading rate on the performance of anaerobic digestion of food waste. **Biotechnology Reports**, v. 27, p. e00503, 1 set. 2020.

BOUTOUNET, M.; MONNIER, J.; VILA, J. P. Multi-regime shallow free surface laminar flow models for quasi-Newtonian fluids. **European Journal of Mechanics - B/Fluids**, v. 55, p. 182–206, 1 jan. 2016.

BRAGUGLIA, C. M. et al. The impact of sludge pre-treatments on mesophilic and thermophilic anaerobic digestion efficiency: Role of the organic load. **Chemical Engineering Journal**, v. 270, p. 362–371, 2015.

BRAZ, G. H. R. et al. The time response of anaerobic digestion microbiome during an organic loading rate shock. **Applied Microbiology and Biotechnology**, v. 102, n. 23, p. 10285–10297, 2018a.

BRAZ, G. H. R. et al. The time response of anaerobic digestion microbiome during an organic loading rate shock. **Applied Microbiology and Biotechnology**, v. 102, n. 23, p. 10285–10297, 1 dez. 2018b.

BRAZ, G. H. R. et al. Organic overloading affects the microbial interactions during anaerobic digestion in sewage sludge reactors. **Chemosphere**, v. 222, p. 323–332, 1 maio 2019.

BUNDESAMT, S. **Dry matter of sewage sludge disposed of directly from waste water treatment plants: Länder, years, types of sewage sludge disposal**. Disponível em: <https://www-

genesis.destatis.de/genesis/online?operation=abruftabelleBearbeiten&levelindex=1&levelid=1638391296832&auswahloperation=abruftabelleAuspraegungAuswaehlen&auswahlverzeichnis=ordnungsstruktur&auswahlziel=werteabruf&code=32214-0001&auswahltext=&w>. Acesso em: 1 dez. 2021.

CHEN, C. et al. Continuous dry fermentation of swine manure for biogas production. **Waste Management**, v. 38, n. 1, p. 436–442, 1 abr. 2015.

CONRAD, R. The global methane cycle: Recent advances in understanding the microbial processes involved. **Environmental Microbiology Reports**, v. 1, n. 5, p. 285–292, 2009.

CÓRDOVA, O.; CHAMY, R. Microalgae to Biogas: Microbiological Communities Involved. **Microalgae Cultivation for Biofuels Production**, p. 227–249, 1 jan. 2020.

DAI, X. et al. Impact of a high ammonia-ammonium-pH system on methane-producing archaea and sulfate-reducing bacteria in mesophilic anaerobic digestion. **Bioresource Technology**, v. 245, n. August, p. 598–605, 2017.

DEEPANRAJ, B.; SIVASUBRAMANIAN, V.; JAYARAJ, S. Kinetic study on the effect of temperature on biogas production using a lab scale batch reactor. **Ecotoxicology and Environmental Safety**, v. 121, p. 100–104, 1 nov. 2015.

DU, W.; PARKER, W. Modeling volatile organic sulfur compounds in mesophilic and thermophilic anaerobic digestion of methionine. **Water Research**, v. 46, n. 2, p. 539–546, 1 fev. 2012.

ECUWW. **UWWTD Treatment Plants- Treatment map**. Disponível em: <https://uwwtd.eu/Germany/uwwtps/treatment>. Acesso em: 30 nov. 2021.

EFTAXIAS, A. et al. Performance of an anaerobic plug-flow reactor treating agro-industrial wastes supplemented with lipids at high organic loading rate. **Waste Management and Research**, v. 39, n. 3, p. 508–515, 2021.

FERRER, I.; VÁZQUEZ, F.; FONT, X. Long term operation of a thermophilic anaerobic reactor: Process stability and efficiency at decreasing sludge retention time. **Bioresource Technology**, v. 101, n. 9, p. 2972–2980, 1 maio 2010.

FRANKE-WHITTLE, I. H. et al. Investigation into the effect of high concentrations of volatile fatty acids in anaerobic digestion on methanogenic communities. **Waste Management**, v. 34, n. 11, p. 2080–2089, 2014.

GANIDI, N.; TYRREL, S.; CARTMELL, E. The effect of organic loading rate on foam initiation during mesophilic anaerobic digestion of municipal wastewater sludge. **Bioresource Technology**, v. 102, n. 12, p. 6637–6643, 1 jun. 2011.

GERARDI, M. H. The Microbiology of Anaerobic Digesters. **The Microbiology of Anaerobic Digesters**, 8 ago. 2003.

GÓMEZ, D. et al. Development of a modified plug-flow anaerobic digester for biogas production from animal manures. **Energies**, v. 12, n. 13, p. 1–17, 2019.

GOSSETT, J. M.; BELSER, R. L. Anaerobic digestion of waste activated sludge. **Journal - Environmental Engineering Division, ASCE**, v. 108, n. EE6, p. 1101–1120, 1982.

GROBELAK, A.; CZERWIŃSKA, K.; MURTAŚ, A. General considerations on sludge disposal, industrial and municipal sludge. **Industrial and Municipal Sludge: Emerging Concerns and Scope for Resource Recovery**, p. 135–153, 1 jan. 2019.

GUO, H. et al. Reconsidering hydrolysis kinetics for anaerobic digestion of waste activated sludge applying cascade reactors with ultra-short residence times. **Water Research**, v. 202, p. 117398, 1 set. 2021a.

GUO, Z. et al. Synergistic ammonia and fatty acids inhibition of microbial communities during slaughterhouse waste digestion for biogas production. **Bioresource Technology**, v. 337, 1 out. 2021b.

HAMILTON, D. W. **Anaerobic Digestion of Animal Manures: Understanding the Basic Processes**. Disponível em: <https://extension.okstate.edu/fact-sheets/anaerobic-digestion-of-animal-manures-understanding-the-basic-processes.html>. Acesso em: 2 dez. 2021.

HENDRIKS, A. T. W. M.; VAN LIER, J. B.; DE KREUK, M. K. Growth media in anaerobic fermentative processes: The underestimated potential of thermophilic fermentation and anaerobic digestion. **Biotechnology Advances**, v. 36, n. 1, p. 1–13, 1 jan. 2018.

JANG, H. M. et al. Influence of thermophilic aerobic digestion as a sludge pre-treatment and solids retention time ofmesophilic anaerobic digestion on the methane production, sludge digestion and microbial communities in a sequential digestion process. **Water Research**, v. 48, n. 1, p. 1–14, 2014.

KIM, J. K. et al. Effects of temperature and hydraulic retention time on anaerobic digestion of food waste. **Journal of Bioscience and Bioengineering**, v. 102, n. 4, p. 328–332, out. 2006.

LEBUHN, M.; GRONAUER, A. Microorganisms in the biogas-process-the unknown beings. **Landtechnik**, v. 64, p. 127–130, 2009.

LEE, I. S.; PARAMESWARAN, P.; RITTMANN, B. E. Effects of solids retention time on methanogenesis in anaerobic digestion of thickened mixed sludge. **Bioresource Technology**, v. 102, n. 22, p. 10266–10272, 1 nov. 2011.

LI, L. et al. Early warning indicators for monitoring the process failure of anaerobic digestion system of food waste. **Bioresource Technology**, v. 171, p. 491–494, 1 nov. 2014.

LI, X. et al. New insight into volatile sulfur compounds conversion in anaerobic digestion of excess sludge: Influence of free ammonia nitrogen and thermal hydrolysis pretreatment. **Journal of Cleaner Production**, v. 277, p. 123366, 20 dez. 2020.

LIENER, S. **Untersuchung der Auswirkung von feststoffarmen Co-Substrat auf den Faulbehälterbetrieb**. [s.l.] Universität Stuttgart, 2020.

LOSSIE, U.; PÜTZ, P. Gezielte Steuerung von Biogas- anlagen mittels FOS / TAC FOS / TAC : Einfache Bestimmung für eine sichere Beurteilung des Gärprozesses. **Hach- Lange**, 2019.

LUQUE, R. et al. Handbook of Biofuels Production. **Handbook of Biofuels Production**, 2016.

MA, S. JIA et al. Effect of mixing intensity on hydrolysis and acidification of sewage sludge in two-stage anaerobic digestion: Characteristics of dissolved organic matter and the key microorganisms. **Water Research**, v. 148, p. 359–367, 2019.

MAGDALENA, J. A.; GRESES, S.; GONZÁLEZ-FERNÁNDEZ, C. Impact of Organic Loading Rate in Volatile Fatty Acids Production and Population Dynamics Using Microalgae Biomass as Substrate. **Scientific Reports**, v. 9, n. 1, p. 1–11, 2019.

MAJI, S. et al. A Review on Hydrodynamics of Free Surface Flows in. p. 1–17, 2020.

MOELLER, L. et al. Foam formation in biogas plants caused by anaerobic digestion of sugar beet. **Bioresource Technology**, v. 178, p. 270–277, 1 fev. 2015.

MOSET, V. et al. Mesophilic versus thermophilic anaerobic digestion of cattle manure: methane productivity and microbial ecology. **Microbial Biotechnology**, v. 8, n. 5, p. 787, 1 set. 2015.

NATHANSON, J. A.; AMBULKAR, . . ARCHIS. **Wastewater treatment**. Disponível em: <https://www.britannica.com/technology/wastewater-treatment>. Acesso em: 30 nov. 2021.

PIVELI, R. P. Tratamento De Esgotos Sanitários. **Ufal**, p. 71, 2004.

PRAMANIK, S. K. et al. Performance and kinetic model of a single-stage anaerobic digestion system operated at different successive operating stages for the treatment of food waste. **Processes**, v. 7, n. 9, 2019.

R. BENGELSDORF, F. et al. Syntrophic microbial communities on straw as biofilm carrier increase the methane yield of a biowaste-digesting biogas reactor. **AIMS Bioengineering**, v. 2, n. 3, p. 264–276, 2015.

SALIBA, P. D. Avaliação de Desempenho do Sistema de Tratamento de Esgoto Sanitário composto de Reator UASB seguido de lodo ativado : Estudo De Caso Da Ete Betim Central-Mg. p. 143, 2016.

SCHOEN, M. A. et al. Population dynamics at digester overload conditions. **Bioresource Technology**, v. 100, n. 23, p. 5648–5655, 2009.

SCHOLZ, M. Sludge Treatment and Disposal. **Wetlands for Water Pollution Control**, p. 157–168, 1 jan. 2016.

SCOTT FOGLER, H. Elements of chemical reaction engineering. **Chemical Engineering Science**, v. 42, n. 10, p. 2493, 1 jan. 1987.

SEBOLA, R.; TESFAGIORGIS, H.; MUZENDA, E. Production of Biogas through Anaerobic Digestion of various Wastes: Review Value addition of waste biomass View project Waste to Energy Technologies View project. n. October 2015, 2014.

SONG, Y.-J. et al. Characteristics of Biogas Production from Organic Wastes Mixed at Optimal Ratios in an Anaerobic Co-Digestion Reactor. **Energies**, v. 14, n. 20, p. 6812, 18 out. 2021.

TELLIARD, W. A. Method 1684: Total, Fixed, and Volatile Solids in Water, Solids, and Biosolids. **U. S. Environmental Protection Agency**, n. January, p. 13, 2001.

THAUER, R. Biochemistry of methanogenesis : a tribute to Marjory Stephenson. p. 2377–2406, 1998.

TORECI, I.; KENNEDY, K. J.; DROSTE, R. L. Evaluation of continuous mesophilic anaerobic sludge digestion after high temperature microwave pretreatment. **Water Research**, v. 43, n. 5, p. 1273–1284, 2009.

VELUCHAMY, C.; GILROYED, B. H.; KALAMDHAD, A. S. Process performance and biogas production optimizing of mesophilic plug flow anaerobic digestion of corn silage. **Fuel**, v. 253, p. 1097–1103, 1 out. 2019.

WAHONO, S. K.; MARYANA, R.; KISMURTONO, M. Biogas purification process to increase gen - Set efficiency. **AIP Conference Proceedings**, v. 1169, n. November, p. 185–

189, 2009.

WEALKENS, B. E. **Investigation of High Load Anaerobic Digester Design Parameters: Effect of Reaction Kinetics on Digester Design Recommendations**. [s.l.] Universität Stuttgart, 2020.

WEI, S. **Untersuchung zum Einsatz von Abpresswasser aus Biomüllsammlung für eine stromautarken Betrieb des Lehr und Forschungsklärwerk**. [s.l.] Universität Stuttgart, 2020.

WELLINGER, A.; MURPHY, J.; BAXTER, D. **The Biogas Handbook: Science, Production and Applications**. [s.l: s.n.].

WIECHMANN, B. et al. Sewage Sludge Management. **Journal of Hydrology**, v. 200, p. 198–221, 2013.

YAN, S. **Untersuchung zur anaerober Biogasvergärung in Abhängigkeit von unterschiedlichen Substraten Vorgelegt von : Shengtao Yan Prüfer : Dipl . Ing . Peter Maurer Erklärung :** [s.l.] Universität Stuttgart, 2017.

ZÁBRANSKÁ, J. et al. The activity of anaerobic biomass in thermophilic and mesophilic digesters at different loading rates. **Water Science and Technology**, v. 42, n. 9, p. 49–56, 2000.

ZEIG, C. Stoffströme der Co-Vergärung in der Abwasserwirtschaft. 2014.

ZHAI, X.; KARIYAMA, I. D.; WU, B. Investigation of the effect of intermittent minimal mixing intensity on methane production during anaerobic digestion of dairy manure. **Computers and Electronics in Agriculture**, v. 155, n. July, p. 121–129, 2018.

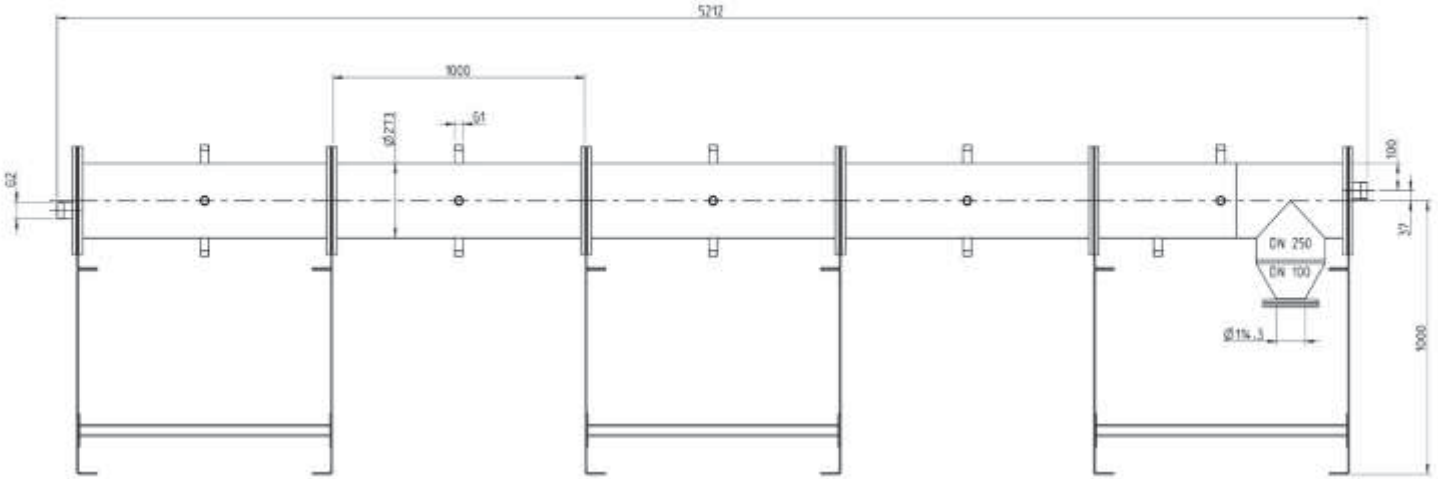

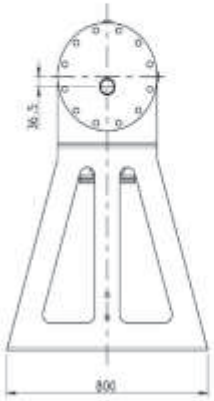

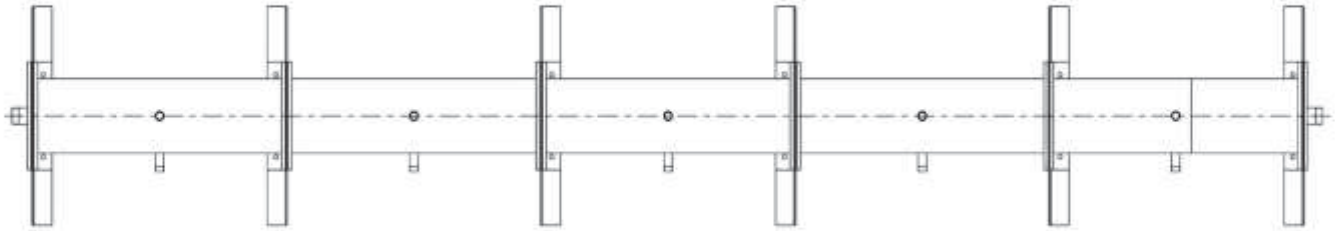

Gasschorl

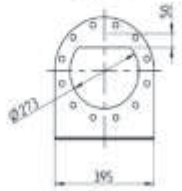

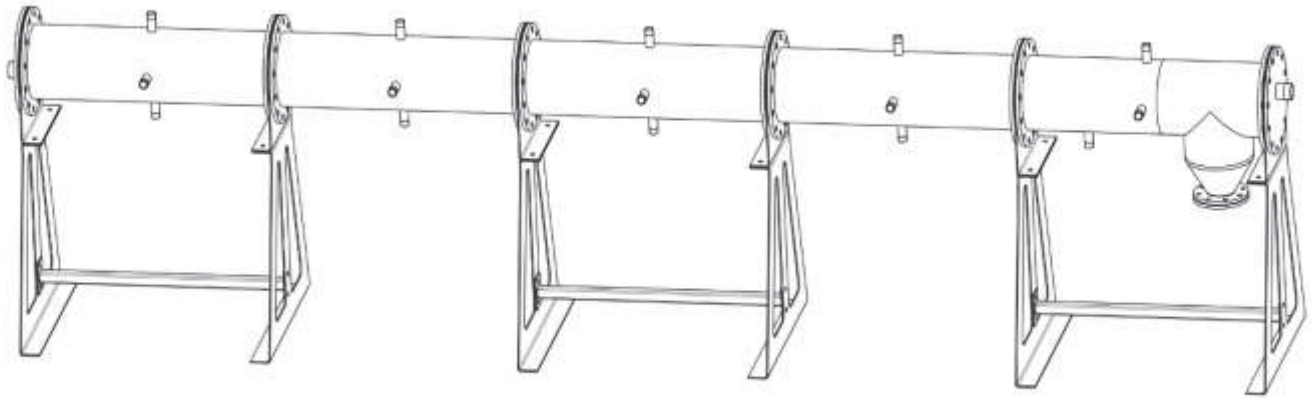

Material:
1.4571 für medienberührte Teile
1.0038 für Unterbau

EISENBAU HEILBRONN

Versuchsreaktor

0193/40